Shape-Persistent Multimetallic Cartwheel Complexes

Design, Catalysis and Recycling

Starre Radvormige Multimetaal-Complexen

Ontwerp, Katalyse en Recycling

(met een samenvatting in het Nederlands)

Proefschrift ter verkrijging van de graad van doctor
aan de Universiteit Utrecht
op gezag van Rector Magnificus, Prof. dr. W. H. Gispen
ingevolge het besluit van het College van Promoties
in het openbaar te verdedigen
op 9 september 2002 des middags te 14.30 uur

door

Harmen Pieter Dijkstra

Geboren op 26 oktober 1973 te Nes

Promotor: Prof. dr. G. van Koten
verbonden aan het Debye Instituut van de Universiteit Utrecht

Co-Promotor: Dr. G. P. M. van Klink
verbonden aan het Debye Instituut van de Universiteit Utrecht

CIP-GEGEVENS KONINKLIJKE BIBLIOTHEEK, DEN HAAG

Dijkstra, Harmen Pieter.

Shape-Persistent Multimetallic Cartwheel Complexes: Design, Catalysis and Recycling
Utrecht, Universiteit Utrecht, Faculteit Scheikunde
Thesis Universiteit Utrecht – with ref. – with summary in Dutch.
ISBN 90-393-3078-6

Subject headings: macromolecular pincer complexes, nanofiltration, homogeneous catalysis, catalyst recycling, pincer protecting group

The work described in this thesis was carried out at the Debye Institute, Department of Metal-Mediated Synthesis, Utrecht University, The Netherlands.

This investigation was financially supported by the Council for Chemical Sciences (CW) of the Netherlands Organization for Scientific Research (NWO).

– *Table of Contents* –

– Chapter 1 –

The Use of Ultra- and Nanofiltration Techniques in Homogeneous Catalyst Recycling

Abstract: In recent years, the application of membrane technology in homogeneous catalyst recycling has received wide-spread attention. This technology offers a solution for the major drawback of homogeneous catalysis, *i.e.* recycling of the catalyst. Both from an environmental and industrial point of view this technology is very interesting, since it allows the future application of homogeneous catalysts in the synthesis of commercial products, leading to faster, cleaner and highly selective *green* industrial processes. In this chapter an overview is given of the promising results obtained in the field of homogeneous catalyst recycling using ultra- and nanofiltration membrane technology.

H. P. Dijkstra, G. P. M. van Klink, G. van Koten, *Acc. Chem. Res.*, in press.

1.1. Introduction

Homogeneous catalysts are frequently used in highly selective organic transformations. Numerous reactions are now easily accessible which would not have been the case without the use of homogeneous catalysts. Especially in asymmetric syntheses, the contribution of homogeneous catalysts is significant.[1] Where kinetic resolution used to be the only possibility to separate two enantiomers, enantiomerically pure products can now be obtained by using chiral homogeneous catalysts in asymmetric transformations. Nevertheless, in industry most catalytic processes are still performed by heterogeneous catalysts because of the facile separation of these catalysts from the product stream. In the field of homogeneous catalysis, separation of the catalyst from the product mixture is rather complicated, preventing large scale industrial processes. Nevertheless, a number of important large scale industrial processes are catalyzed by homogeneous catalysts, such as the production of adiponitrile by Dupont, acetic acid by Monsanto and butanal by Ruhr Chemie, pointing at the importance of homogeneous catalysis.[2] Mainly homogeneous catalysts which can be used in very low concentrations find commercial application, since the catalyst quantity in the product stream is at the ppm-level and thus separation of the catalyst is not necessary.[3] In Table 1, the features of homogeneous *versus* heterogeneous catalysis are summarized. Homogeneous catalysts are superior in terms of activity and selectivity and possess a high atom-efficiency. Furthermore, the reaction conditions are relatively mild and the actual catalytic species are well-defined, allowing an easy fine-tuning of the catalytic properties, an aspect which is not easily achieved with heterogeneous catalysts. Heterogeneous catalysts on the other hand, are very easy to separate from the product-stream and can be recycled efficiently. As a consequence, the quantity of catalyst needed is rather low and high total turnover numbers are obtained, making the catalysts relatively cheap. Therefore, finding a way to integrate the advantages of homogeneous and heterogeneous

Table 1. Homogeneous *vs.* heterogeneous catalysis.

	Homogeneous	**Heterogeneous**
Activity	+++	-
Selectivity	+++	-
Catalyst description	+++	-
Reaction conditions	+++	+
Catalyst recycling	-	+++
Quantity of catalyst	++	+++
Total Turnover Number	+	+++

catalysis into one chemical process would be extremely interesting, both from an environmental and commercial point of view.

An attractive approach to achieve this goal, is the development of recyclable homogeneous catalysts.[4] This approach will create catalytic processes which possess a high selectivity and activity, leading to high product yields and minimal amounts of side-products and waste materials. In particular, the need for processing of the product-stream (work-up and purification) can also be minimized. Furthermore, catalyst recycling allows an efficient use of the generally expensive homogeneous catalysts (increased total turnover number), making such a process commercially feasible. In addition, it also allows catalytic processes in which higher catalyst loadings are required. Ultimately, development of such systems and applying them industrially will lead to *green* commercial processes.

An interesting and promising development in the area of homogeneous catalyst recycling is the attachment of homogeneous catalysts to soluble organic supports. In this way, macromolecular homogeneous catalysts are created which can be recovered from the product-stream by ultra- or nanofiltration techniques and reused again. This Chapter will discuss the achievements of membrane technology in the field of homogeneous catalyst recycling, as well as review a number of representative examples of recyclable soluble-enzymes using enzyme membrane reactors.

1.2. Membrane Technology

Since the 1950s membrane technology has been growing steadily. Nowadays in some fields, membrane technology is a *proven technology* and is incorporated in various production lines or purification processes.[5] The main fields of application are the food and dairy industries, water purification[6] and treatment of liquid effluent streams.[7] For medicinal applications smaller membrane modules are also common, whereas large units are still rare in the medicinal process industry.

In the field of membrane filtration, a distinction is made between different kinds of membrane processes based on the size and geometry of the particles to be retained, *i.e.* microfiltration, ultrafiltration, nanofiltration,[8] and reverse osmosis. Ultra- (UF) and nanofiltration (NF), the two types of filtration techniques discussed in this Chapter, are defined to retain macromolecules with dimensions between 8–800 nm and 0.5–8 nm, respectively.

The demand on industry for better environmental solutions and cleaner technologies has been pushing membrane technology into the forefront.[5] End-of-pipe solutions for purification of effluent streams will to a larger extent be substituted by closed systems with integrated process solutions in the future, resulting in simpler and cleaner industrial processes. Recently, solvent-stable UF- and NF-membranes were introduced which show high retentions for medium-sized soluble molecules. This development allows the application of homogeneous catalysts which can be recycled by using membrane technology (in particular important when higher catalyst loadings are required). This will widen the scope of *green* homogeneous catalytic systems for commercial processes.

The applicability of membrane technology in the field of homogeneous catalyst recycling depends on a number of important features of the membranes used. Most UF- and NF-membranes are asymmetric membranes; the pore-sizes on the solute-side of the membrane are smaller than those on the permeate-side, thereby preventing clogging of the membranes. Furthermore, the stability of the membranes under various conditions is very important, as it determines the number of potential catalytic applications using this technology. Also, the interactions of the various compounds and intermediates in the catalytic process with the membrane surface have to be considered. In general, the latter aspects are still a matter of trial and error since for most membranes data concerning these aspects are often not available.

Usually, the molecular weight cut-off (MWCO) is used as the quantitative criterion for the retention characteristics of a membrane. The MWCO is defined as the molecular weight at which 90% of the solutes are retained by the membrane. It should be kept in mind, however, that pore-size distribution (which exists in all UF- and NF-membranes), charge-effects and hydrophilicity, hydrophobicity and polarity (of the solvent) can also greatly influence the permeability of the membrane. Furthermore, in case of macromolecules, the molecular shape is an important factor too. For example, globular proteins are more efficiently retained by membranes in comparison to flexible polymers with elongated chains.

$$R = 1 + \left(\frac{1}{\theta}\right) \ln\left(\frac{[A_R]}{[A_R] + [A_P]}\right) \qquad \text{(eq. 1)}$$

R = Retention

$[A_R]$ = Concentration A in retentate

$[A_P]$ = Concentration A in permeate

θ = Number of exchanged reactor volumes

For separation processes using membranes, an additional important feature is the *retention* (R) of the material to be separated from the product mixture. The retention of a material is defined by the ratio of the concentration of a component A in the permeate and the retentate and is expressed in equation 1.

The suitability of membrane technology in a chemical process roughly depends on the features described above. However, in order to describe the physical processes which take place in membrane-filtration processes, various other features, such as pressure, polarity, permeability of the membrane, etc., have to be taken into account as well.

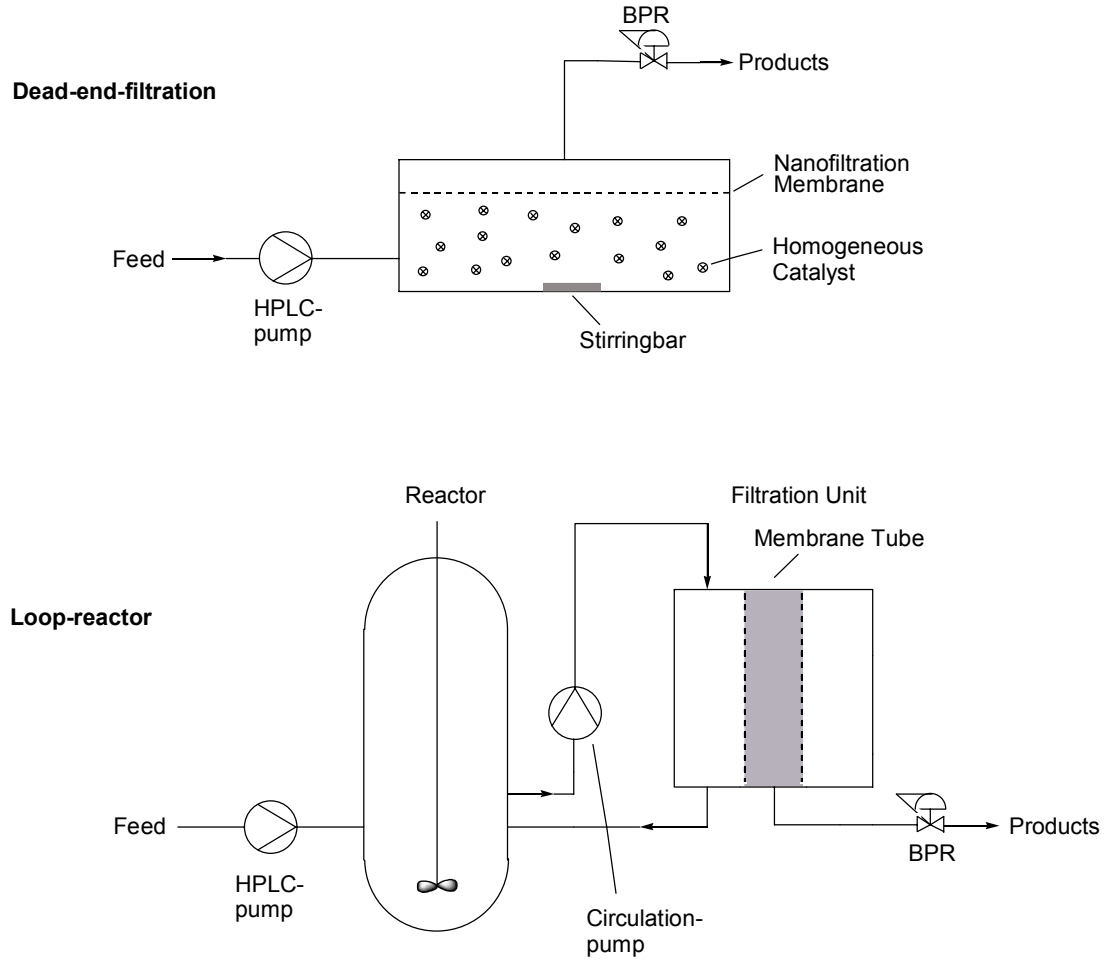

Figure 1. Continuous membrane reactors.

1.2.1. Continuous Membrane Reactors

Two types of continuous membrane reactors are mainly used in this research field (Figure 1). In a collaborative project with the group of Vogt,[9] we make use of the *dead-end-filtration* to recycle our homogeneous catalysts (see Figure 2). With this

technique, the catalyst is compartmentalized in the reactor and is retained by the nanofiltration membrane. Reactants are continuously pumped into the reactor, while products (and unreacted materials) cross the membrane and can be further processed. Concentration polarization of the catalyst, that is accumulation of the catalyst near the membrane, can occur using this technique. In contrast, when a *loop-reactor* is used, such behavior is prevented, since the solution is continuously circulated through the reactor, while only small particles (products and unreacted materials) can cross the membrane lateral.

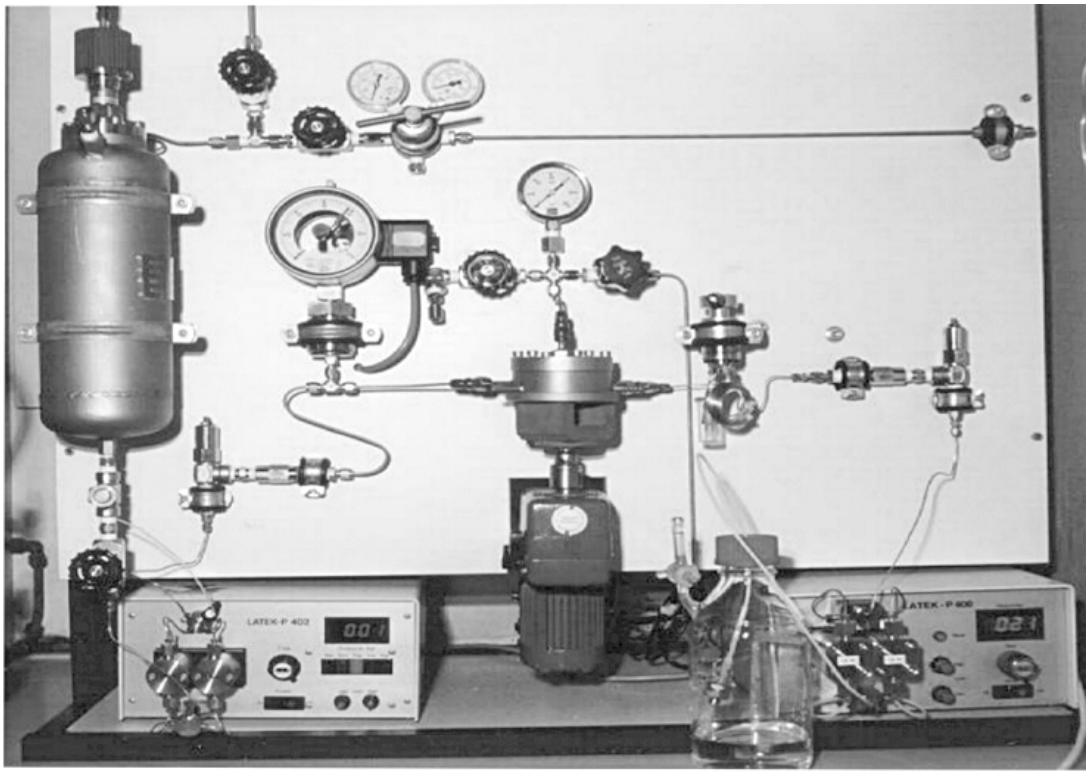

Figure 2. Set-up of a nanofiltration membrane reactor (Prof. D. Vogt, Eindhoven University of Technology).

1.3. Biotechnology: (Co)-Enzyme Recycling

Often enzymes are regarded as the ideal catalysts, since they possess extremely high activities and selectivities, which are often impossible to obtain with synthetic homogeneous catalysts. Nevertheless, enzymes as such are hardly applied as catalysts in industry mainly due to their high costs. Therefore, recycling of the biocatalyst, in order to reduce costs, is a major goal in applied biocatalysis. An

interesting approach to achieve this is by applying membrane ultrafiltration, *e.g.* in an enzyme membrane reactor.[10] This method has to be distinguished from systems where the enzyme is immobilized on or in a membrane. Membrane-immobilized enzymes have an improved stability as compared to the soluble enzyme systems and it is also an *established technology*. On the other hand, these membrane-immobilized enzymes also have to deal with mass-transfer limitations, immobilization costs and loss of activity during immobilization. Obviously, soluble enzyme systems have no immobilization costs and no mass-transfer limitations. However, they also possess a lower stability and have higher investment costs since it is a *new technology*. Soluble enzyme systems have the major advantage that almost every enzyme is retained by the same membrane, whereas for the immobilized enzymes every immobilization protocol can be different. In this section, representative examples are discussed of soluble enzyme systems which are recycled by applying membrane filtration technology.[11]

Amino acylase I is used for the resolution of racemic amino acids in an enzyme membrane reactor, *e.g.* represented by the formation of L-methionine as depicted in Scheme 1.[12] By this method, Degussa AG produces proteinogenic and non-proteinogenic amino acids, such as norvaline, aminobutyric acid and S-benzylcysteine, in a continuously operated enzyme membrane reactor on an annual multi-ton scale.

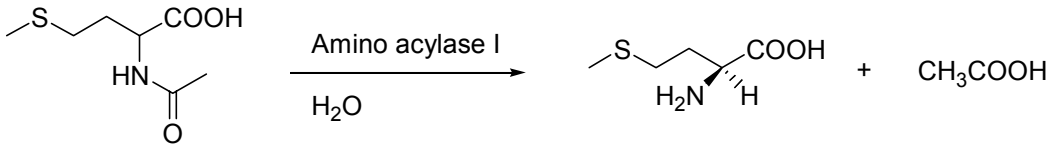

Scheme 1. Enzymatic synthesis of L-methionine.

In a second example, optically pure α-amino acids are synthesized via reductive amination of α-keto acids using recyclable L-amino acid dehydrogenases (Scheme 2).[10,12,13] Degussa uses this system on a multi-kg scale using an enzyme membrane reactor. To avoid the stoichiometric use of the expensive co-factor NADH, this co-factor is regenerated using FDH,[14] a fairly cheap enzyme. This increases the cycle numbers (ttn) of the co-factor, defined as mol product formed per mol co-factor, and considerably reduces the high costs of co-factors, rendering such a process economically feasible. Later, it was found that co-factors NADH and NADPH used in the same catalytic system could also be recycled by means of nanofiltration in a continuous enzyme membrane reactor.[15] For these systems, retentions between

0.86–0.98 were found, leading to a constant conversion rate of >95% for 10 days. With more prolonged reaction times, the concentration of NAD^+ dropped below a critical value as a substantial decrease in conversion was observed. Furthermore, the enzyme and FDH also had to be re-supplied after 120 h to compensate for enzyme deactivation. With this (co-)enzyme recycling using membrane technology, a total turnover number of this enzymatic system was reached which was considerably higher (up to 3.4 times) than the same system without recycling.

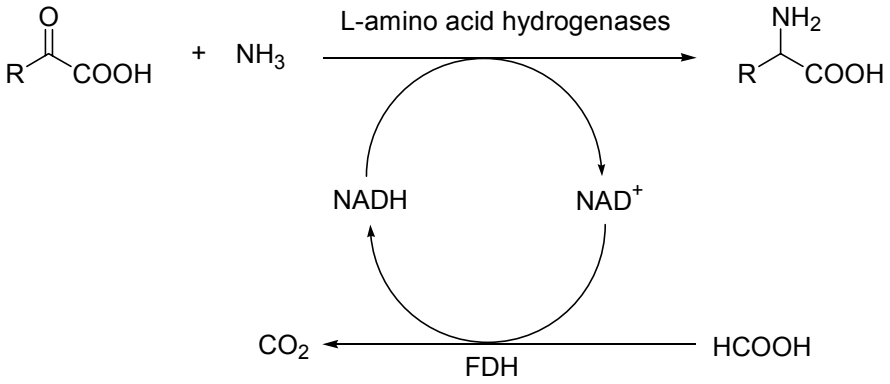

Scheme 2. Synthesis of chiral α-amino acids. FDH = formate dehydrogenases.

Attachment of co-factors to homogeneously soluble polymers, *e.g.* water-soluble polyethylene glycol, which can be retained by ultrafiltration membranes and reused in batch or continuous processes, is another method to improve the cycle numbers of co-factors.[16] It is also possible to use charged UF-membranes to recycle the native co-factor, however, this method is limited to the production of non-charged products only.[17]

In a final example, 5-azido-neuraminic acid ($Neu5N_3$) is prepared using an aldolase in a bench-scale experiment applying a repetitive batch technique in a UF-cell (Scheme 3).[13] This system has a constant conversion for 25 h with a conversion rate >80%.

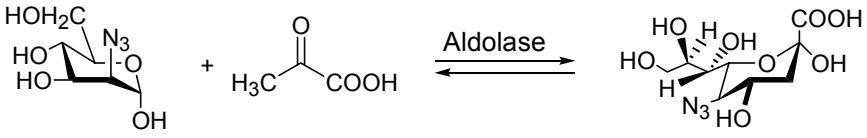

Scheme 3. Synthesis of Neu5Ac using enzymatic synthesis.

In conclusion, these illustrative examples nicely show the potential of membrane technology in enzymatic synthesis. Efficient recycling of the bio-catalysts decrease their high costs and enhance their performance, making these systems industrially applicable on multi-ton scale. One always has to keep in mind, however, that enzymes usually are very sensitive to reaction conditions. Examples are known in which enzyme deactivation occurs by interaction with the reactor material or even destabilization by interaction with the membranes.[10] Finally, the availability of the soluble enzymes can also be a limited factor, since many manufacturers of enzymes only sell bulk-quantities of immobilized enzymes.

1.4. Recycling of Homogeneous Catalysts

Homogeneous catalysis is nowadays a valuable tool in the selective construction of diverse organic compounds. Especially in asymmetric syntheses, chiral catalysts show their extreme value.[1] Nevertheless, only a few of these processes made the step from an academically promising method to industrial application,[3] mainly due to the generally low total turnover numbers (especially in comparison with enzyme systems) and the poor recycling behavior of homogeneous catalysts. Therefore, developing efficient recycling techniques for homogeneous catalysts, makes homogeneous catalysis more attractive for industry, since the total turnover number of the catalysts is increased and the costs are thus decreased, also allowing catalytic processes which need higher catalyst loadings.

Currently, considerable attention is given to the development of homogeneous catalysts anchored on soluble supports such as polymers and dendrimers. Such an approach allows the recovery (and reuse) of homogeneous catalysts from product-streams by means of UF- and NF-membranes in continuously operating catalytic processes. In this section, an overview is given on the state-of-the-art of homogeneous catalyst recycling using membrane systems.[18]

1.4.1. Polymer-enlarged Homogeneous Catalysts

Kragl and Wandrey and coworkers described the use of polymer-enlarged homogeneous catalysts in continuously operating membrane reactors. In 1996, Kragl reported the first example of a polymer-enlarged chiral homogeneous catalyst (**1**) which was used in the enantioselective addition of diethylzinc to benzaldehyde

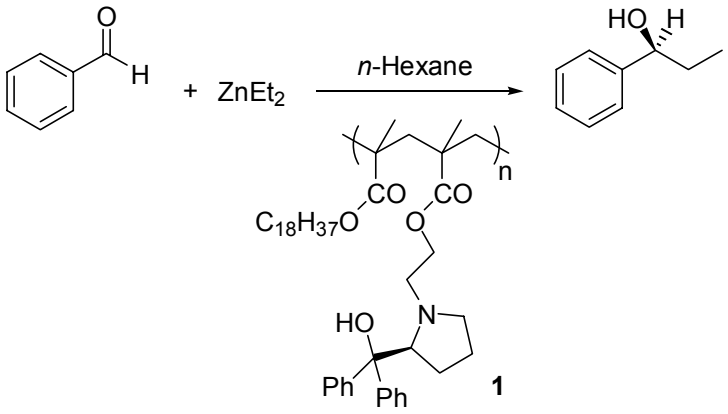

Scheme 4. Enantioselective addition using a recyclable polymer-enlarged catalyst.

(Scheme 4).[19] α,α-Diphenyl-L-prolinol coupled to a copolymer made from 2-hydroxyethyl methacrylate and octadecyl was used as the chiral ligand and could be retained from the reaction mixture by UF-membranes. It was found that >99.8% of the polymer-enlarged system was retained by the membrane (Hoechst Nadir UF PAH20). Under optimized conditions, the total turnover number of this system under continuous conditions was raised by a factor of 10 up to 500. For a system without catalyst recycling, a ttn of 500 corresponds to an effective chiral catalyst concentration of 0.2 mol%, which is still exceptional in asymmetric syntheses.[3] Furthermore, the system did not show any signs of deactivation for a period of 7 days, implying the possibility of longer operating times in the reactor. The enantiomeric excess of this reaction using the polymer-enlarged system was considerably lower than the ee achieved with the non-coupled ligand (80 *vs.* 97%). It has been suggested that this lower selectivity can be improved by higher catalyst concentrations.[19]

Polymer-enlarged oxazaborolidines **2a** and **2b** were also applied as homogeneous catalysts in enantioselective reductions of several ketones in a membrane reactor (Scheme 5, R > 0.98).[20] A solvent stable NF-membrane (SelRo MPF-50 NF-membrane, Koch Int.) was used for this setup. In comparison with the batch process in which the ketone was added in one portion, higher enantioselectivities were found. This is in agreement with additional reported data, according to which slow addition of the ketone to a solution of the other reagents resulted in higher ee's. Under the reaction conditions, the catalyst showed a slight deactivation (1.8% / h) and the reactor seemed to operate under stable conditions until the concentration of the active catalyst dropped below a critical value. Nevertheless, the total turnover numbers of these systems could be enhanced from 10 up to 560.

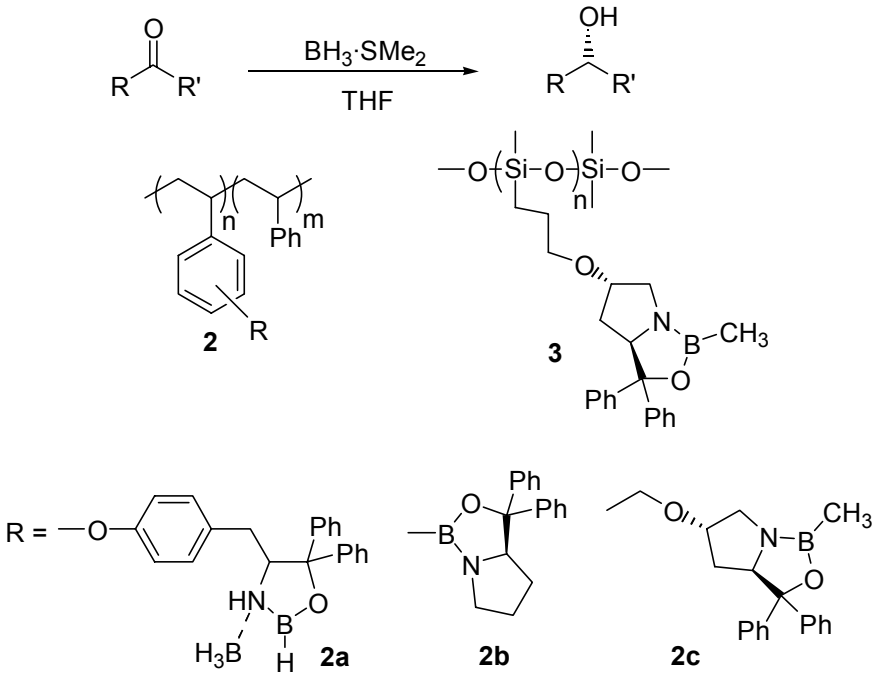

Scheme 5. Enantioselective reduction using recyclable polymer-enlarged catalysts.

Immobilized oxazaborolidine catalysts **2c** and **3**, which are based on the Corey-diphenylprolinol, were also tested under similar catalytic reaction conditions (Scheme 5).[21] Polysiloxane-bound catalyst **3** (R = 0.985) could be used for 200 residence times at almost quantitative conversion and 96.8% ee, while polystyrene-bound catalyst **2c** (R = 0.9994) even showed a constant conversion (>99%) and enantioselectivity (96.8%) for > 400 residence times. The average ee with both catalysts was somewhat lower as compared to the original Corey-catalyst (>99% ee), however the total turnover number was increased from 100 (batch) to 1374.

In another example, micellar rhodium catalyst **4** was used in the asymmetric hydrogenation of α-acetamidoacrylic acid methyl ester in aqueous media in a repetitive batch experiment (Scheme 6).[22] The triblock copolymer P105 was used as surfactant in which the rhodium catalyst was embedded. Using a UF-membrane (YC05, Amicon), this micellar enlarged catalyst was found to have a retention of 0.991, causing slow leaching of the catalyst. Conversions and ee's were found to be constant for at least 6 runs. Traces of oxygen had to be avoided in this process, since this rapidly decreased the activity of the system. Furthermore, since the rhodium is not covalently attached to the ligand system, a slightly higher rhodium leaching,

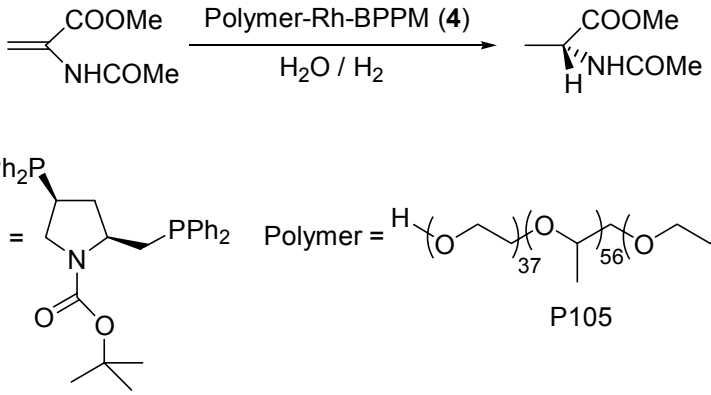

Scheme 6. Asymmetric hydrogenation using a recyclable micellar catalyst.

which is determined by the complex stability between the metal and the phosphine ligand, than that found for the embedded system (R = 0.991) was observed. Nevertheless, by applying this system the ttn was doubled up to 194.

Recently, a continuous Sharpless dihydroxylation of homocinnamic acid using an osmate catalyst immobilized on a soluble polymer support (**5**) was reported (Scheme 7).[23] It was found that after six residence times, the conversion dropped from 80 to 18%. As there was no change in ee, this deactivation was due to osmate

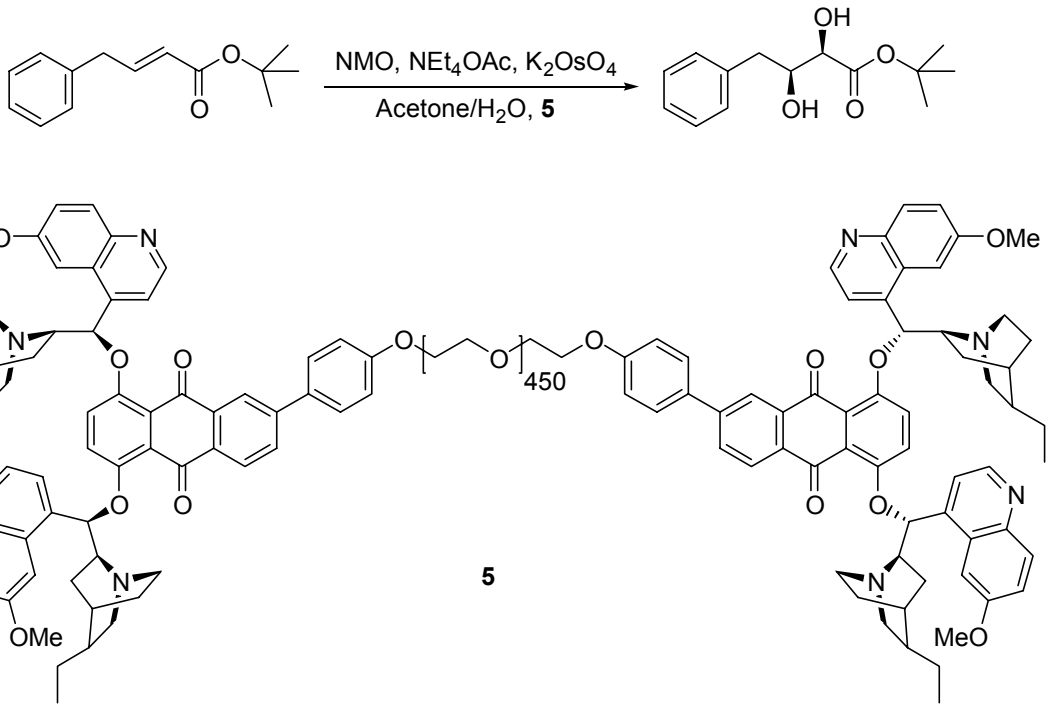

Scheme 7. Continuous Sharpless dihydroxylation using a polymer enlarged osmate catalyst.

leaching. Apparently, the osmate binds very weakly to the support, resulting in fast leaching of the active metal. A constant osmate concentration in the reactor was obtained by continuous dosing of potassium osmate to the feed stream, allowing a continuous catalytic process for prolonged reaction times.

In a final example, a rhodium catalyst immobilized by electrostatic interactions of multiply charged phosphine ligands on a soluble polyelectrolyte (**6**) was used in the hydroformylation of 1-hexene (Scheme 8).[24] The catalytically active material was prepared by mixing PDADMA-B(Ar_F)$_4$ (PDADMA = poly(diallyldimethylammonium)) with a rhodium precursor containing sulfonated phosphine ligands, resulting in partial replacement of the borate anions for the phosphine-Rh catalyst. The catalytic system could be recovered by ultrafiltration membranes (R = 0.998, PES membranes, Sartorius) and reused again, applying a repetitive batch procedure. In every cycle small amounts of rhodium (2–7%) leached through the membrane, probably caused by oxidation of the phosphine ligands.

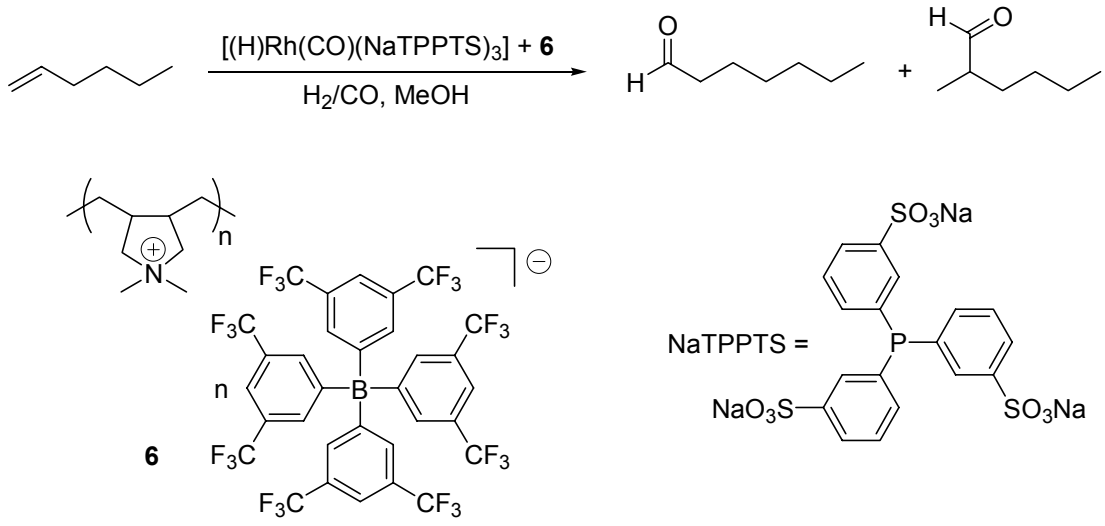

Scheme 8. An electrostatically immobilized rhodium catalyst in a hydroformylation reaction.

As shown in this section, anchoring homogeneous catalysts to soluble polymer supports and applying membrane-filtration technology greatly enhances their performance in catalytic processes (increased ttn). Also, the selectivities of the catalytic reactions were in most cases found to be similar to that of the non-supported catalysts.

1.4.2. Dendrimer-enlarged Homogeneous Catalysts

The use of dendrimers as soluble supports for homogeneous catalysts in membrane separation experiments has received considerable attention in recent years. Several groups focused on the incorporation or complexation of (transition) metal

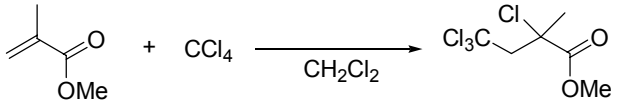

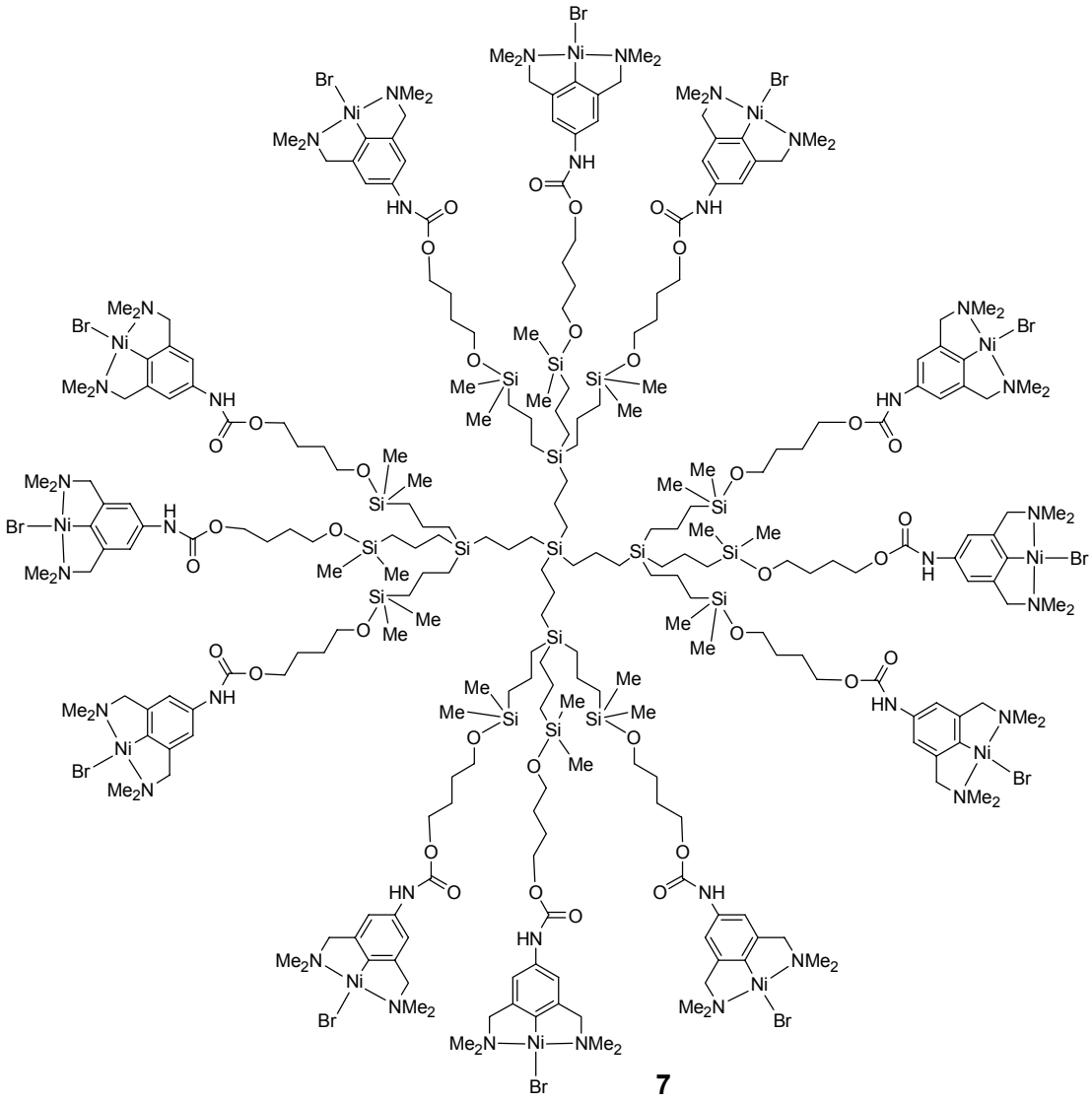

Scheme 9. Kharasch addition catalyzed by a metallodendrimer.

fragments onto dendrimers and nowadays a broad spectrum of so-called *metallodendrimers* are known which are active as homogeneous catalysts.[25] In contrast to polymers, dendrimers are tree-like molecules with well-defined macrostructures. The dimensions of a dendrimer can be altered quite easily by varying the generation of the dendrimer. In membrane separation technology, this is an important feature allowing fine-tuning of the retention rate of these dendritic catalysts. Because dendrimers are well-defined pseudo-spherical structures, the catalyst loading can be exactly determined, rendering a direct comparison with non-supported mononuclear catalysts. Such a comparison is less straightforward with the less well-defined polymeric systems described in section 1.4.1., since in these systems it is very difficult to accurately control the number and location of the catalytic sites. In this section, the use of dendrimers as support materials for homogeneous catalysts which can be retained and reused by applying NF-membrane technology is discussed.

The groups of Van Koten, Van Leeuwen and Vogt have developed different types of *carbosilane dendrimers* which were used as supports for homogeneous catalysts and could be retained by means of NF-membrane technology. In 1994, the first examples of *metallodendrimers* were reported which were used as homogeneous catalysts and were, in principle, suitable for retainment by NF-membranes.[26] In this report, nickelated carbosilane dendrimers were used in a regioselective Kharasch addition of polyhalogenoalkanes to carbon-carbon double bonds (Scheme 9, example of dodecanickel carbosilane dendrimer **7**). The catalytic data suggested that each catalytic site acted as an independent unit, and even more important, the regioselective 1:1 addition without telomerization/polymerization of the alkene was similar to the mononuclear catalyst. No retention data of the enlarged homogeneous catalysts were provided. This report started a complete new research area in the field of dendrimer chemistry, *i.e.* the development of catalytically active metallodendrimers.[25]

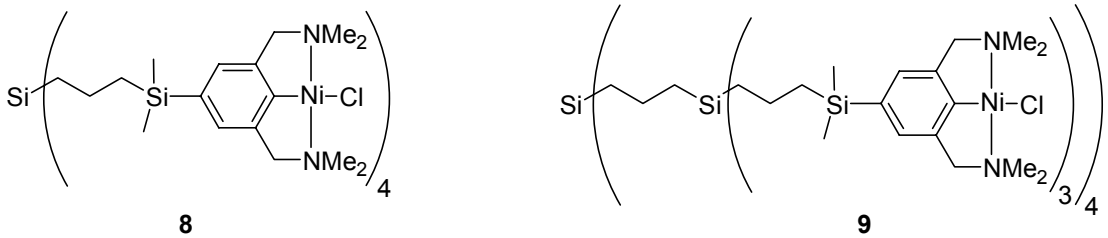

8 **9**

Figure 3. Nickelated carbosilane dendrimers used in the Kharasch addition.

Recently, other examples of soluble nickelated carbosilane dendrimers (**8** and **9,** Figure 3) as homogeneous catalysts in the Kharasch addition were reported by Van Koten *et al.*[27] Tests with catalysts **8** and **9** in a NF-membrane reactor (MPF-50 NF membrane, Koch Int.) showed retentions of 0.974 and 0.998 for **8** and **9**, respectively. Unfortunately, applying the dendrimer with the highest retention (**9**) in the Kharasch addition (see Scheme 9) in a membrane reactor, resulted in a fast deactivation of the catalyst. This deactivation is caused by the "proximity effect" (or dendritic effect) between peripheral Ni^{II} sites, which translates into lower catalytic efficiencies and irreversible formation of insoluble, inactive Ni^{III} sites.[28] This proximity effect was solved by introducing longer spacers between the catalytic site and the dendrimer branching points, thus creating a situation in which the Ni-centers are further away from each other. No experiments in a NF-membrane reactor have been performed with this material yet.

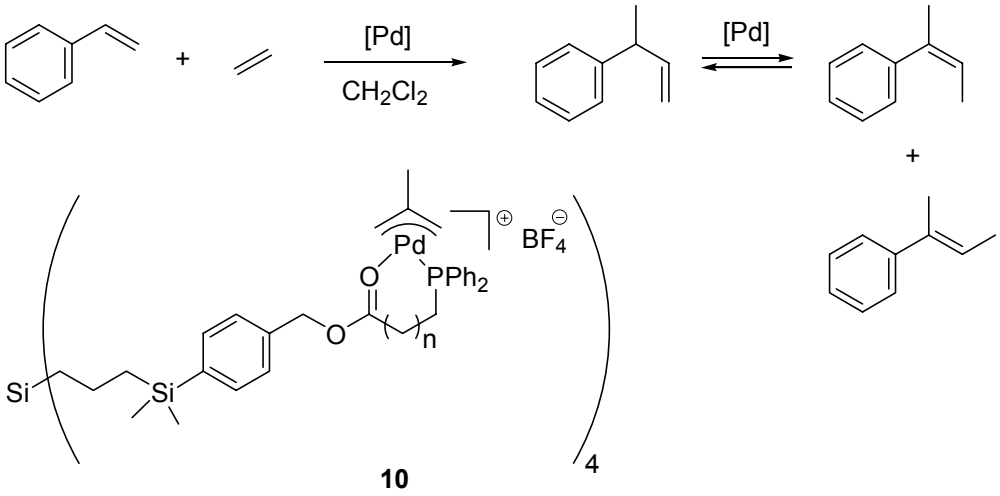

Scheme 10. Hydrovinylation of styrene using palladated dendrimers.

Palladated carbosilane dendrimers with hemilabile P,O-ligands were shown to be applicable as homogeneous catalysts in the selective hydrovinylation of styrene in a membrane reactor (MPF-60 NF membrane, Koch Int.) (Scheme 10).[29] In a continuous setup using G0-dendrimer **10**, a considerable decrease in activity was observed, which was partly explained by wash-out of the catalyst (R = 0.85 for a model compound) and partly by decomposition of the catalytic unit (formation of Pd (black) was observed). A first generation dendrimer with a higher retention showed

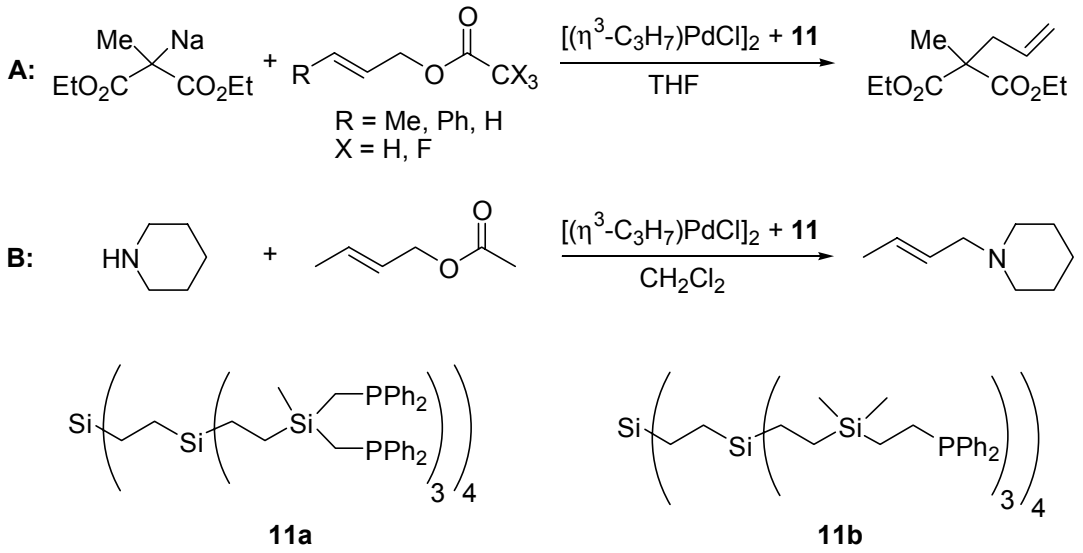

Scheme 11. Allylic alkylation and amination reaction using phosphine functionalized dendrimers.

almost the same deactivation behavior.[29b] Thus, catalyst decomposition is most probably the main reason for the observed deactivation. Nevertheless, the G0-catalyst **10** was able to produce product for a period of 80 h.

Van Leeuwen and coworkers reported palladated phosphine functionalized carbosilane dendrimers as catalysts in the reaction between sodium diethyl methylmalonate and allyltrifluoroacetate in a continuous flow membrane reactor (Reaction A, Scheme 11).[30] In batch processes, the activity per palladium center of different generations Pd(allyl) dendrimer complexes was constant, indicating that all active sites act as independent catalysts. Under continuous reaction conditions, however, using the largest dendrimer (**11a**) (Scheme 11, R > 0.981, MPF-60 NF membrane, Koch Int.) an unexpected rapid decrease in activity was found, which could not solely be ascribed to wash-out of the homogeneous catalyst. It was proposed that the catalyst decomposed during the process. When the same catalyst was applied in the continuous allylic amination reaction of crotyl acetate and piperidine (Reaction B, Scheme 11), again a fast deactivation of the catalyst was observed.[30b] However, when catalyst **11b** was applied under the same conditions in the allylic amination reaction, only a minor decrease in yield was observed. After 10 reactor volumes the system still possessed 70% of the initial activity. This number could even be increased by increasing the P/Pd ratio from 2 to 4. It was proposed that introducing a longer spacer between the silicon branching point and the phosphorous atom and increasing the P/Pd ratio results in more stable catalysts, allowing the application in continuous

processes. The same dendritic ligands but in combination with rhodium were used in hydroformylation reactions.[31] Preliminary experiments with this catalytic system in a NF-membrane reactor, however, showed that the NF-membrane setup used (MPF-60 NF, Koch Int.) is not compatible with the standard hydroformylation conditions due to its temperature and solvent restrictions.

Different generations carbosilane dendrimers functionalized with ruthenium metathesis catalysts were also reported (Scheme 12).[32] The activity per metal center of the dendritic catalysts was found to be comparable to that of the corresponding mononuclear catalyst. Unfortunately, the metathesis reaction conditions were not compatible with the NF-membrane setup as was found with G0-catalyst **12** (Scheme 12); after 20% conversion the reaction stopped. This phenomenon was proposed to be due to interaction of the catalyst with the membrane surface (MPF-60 NF, Koch Int.).

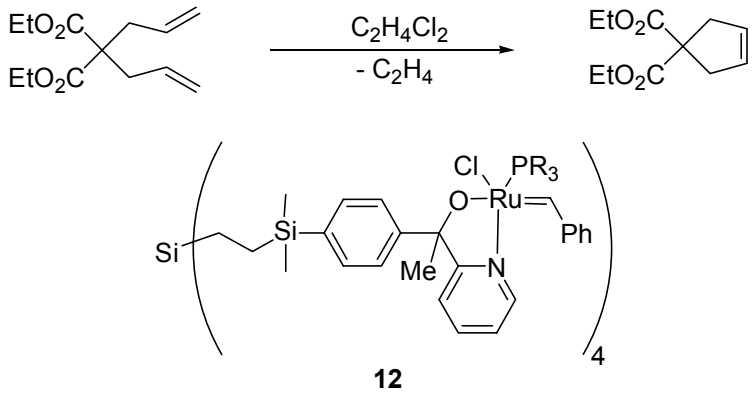

12

Scheme 12. Ru-functionalized dendritic catalyst in metathesis.

The first examples of metalated phosphine functionalized dendrimers which were suitable as homogeneous catalysts were reported by Kragl, Reetz and coworkers.[33,34] When a DAB based (DAB = 1,4-diaminobutane) phosphino dendrimer was loaded with Pd^{II}-centers, the resulting system (**13**) was active in the allylic substitution of 3-phenyl-2-propenylcarbonic acid methyl ester (Scheme 13). The application of catalyst **13** in a NF-membrane reactor (MPF-50 NF, Koch Int.) for a period of 100 residence times, resulted in a conversion decrease to *ca.* 80%, which would be equivalent to a palladium leaching of about 0.07 to 0.14% per residence time. However, the retention of the catalyst was determined independently and was found to be 0.999. Therefore, the drop in conversion must partly be due to catalyst deactivation and/or decomposition.

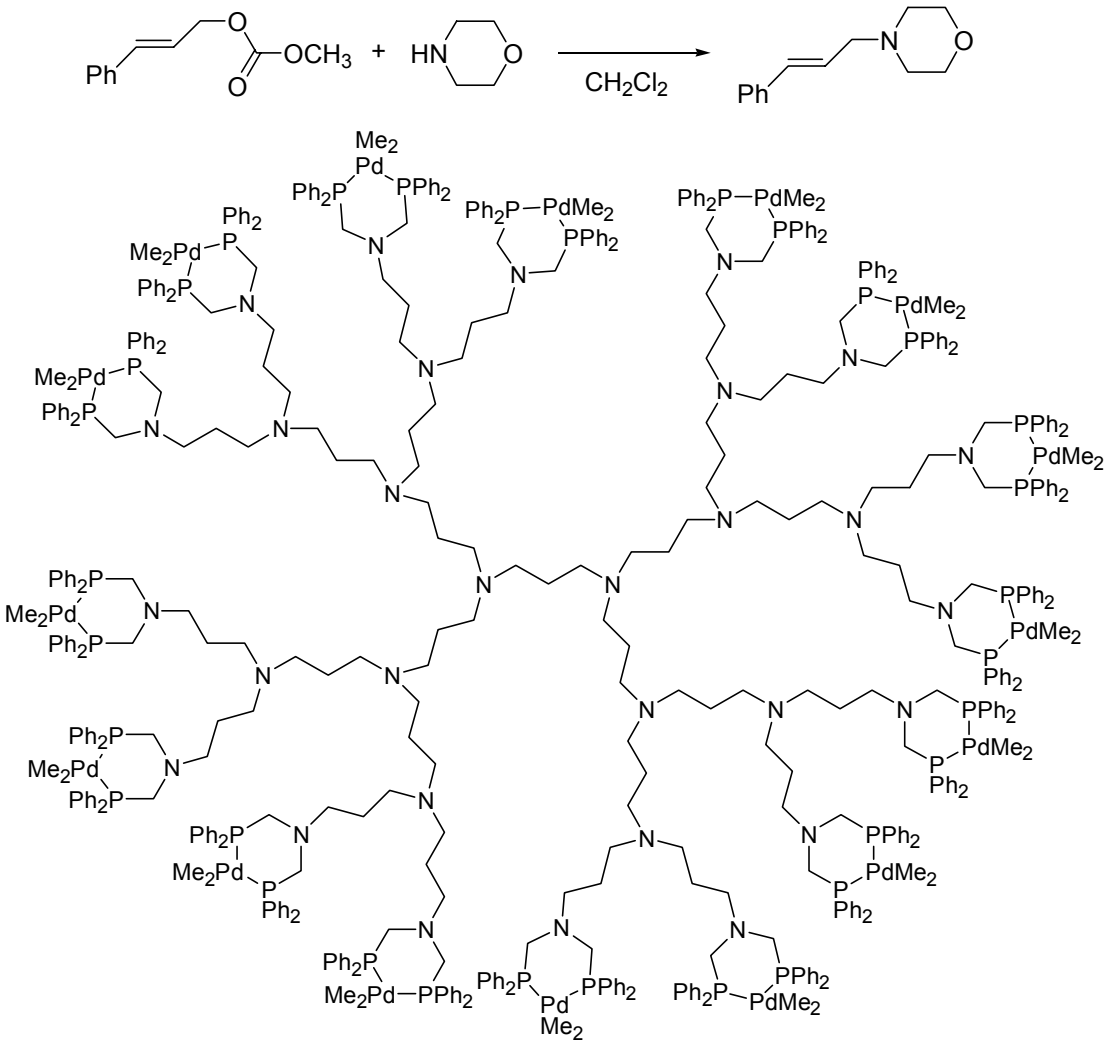

Scheme 13. Phosphine functionalized dendrimer in allylic substitution.

Togni and coworkers reported the use of asymmetric dendritic catalysts derived from ferrocenyl bisphosphine ligands loaded with rhodium (**14**) for the asymmetric hydrogenation reaction of dimethyl itoconate (Scheme 14).[35] In this paper, the authors claimed that dendritic catalyst **14** is completely retained by NF membranes, however, no data of the filtration experiments were provided.

A nickel(II) catalyst anchored to a G3-Fréchet-type dendritic wedge (**15**, M = Ni) was also prepared and applied in a Kharasch addition reaction (Scheme 15).[36] In the setup that was used, third-generation dendritic catalyst **15** was compartmentalized in a NF-membrane-capped vial which was placed into the reaction mixture where catalysis took place. After the reaction was completed, the vial, still containing the

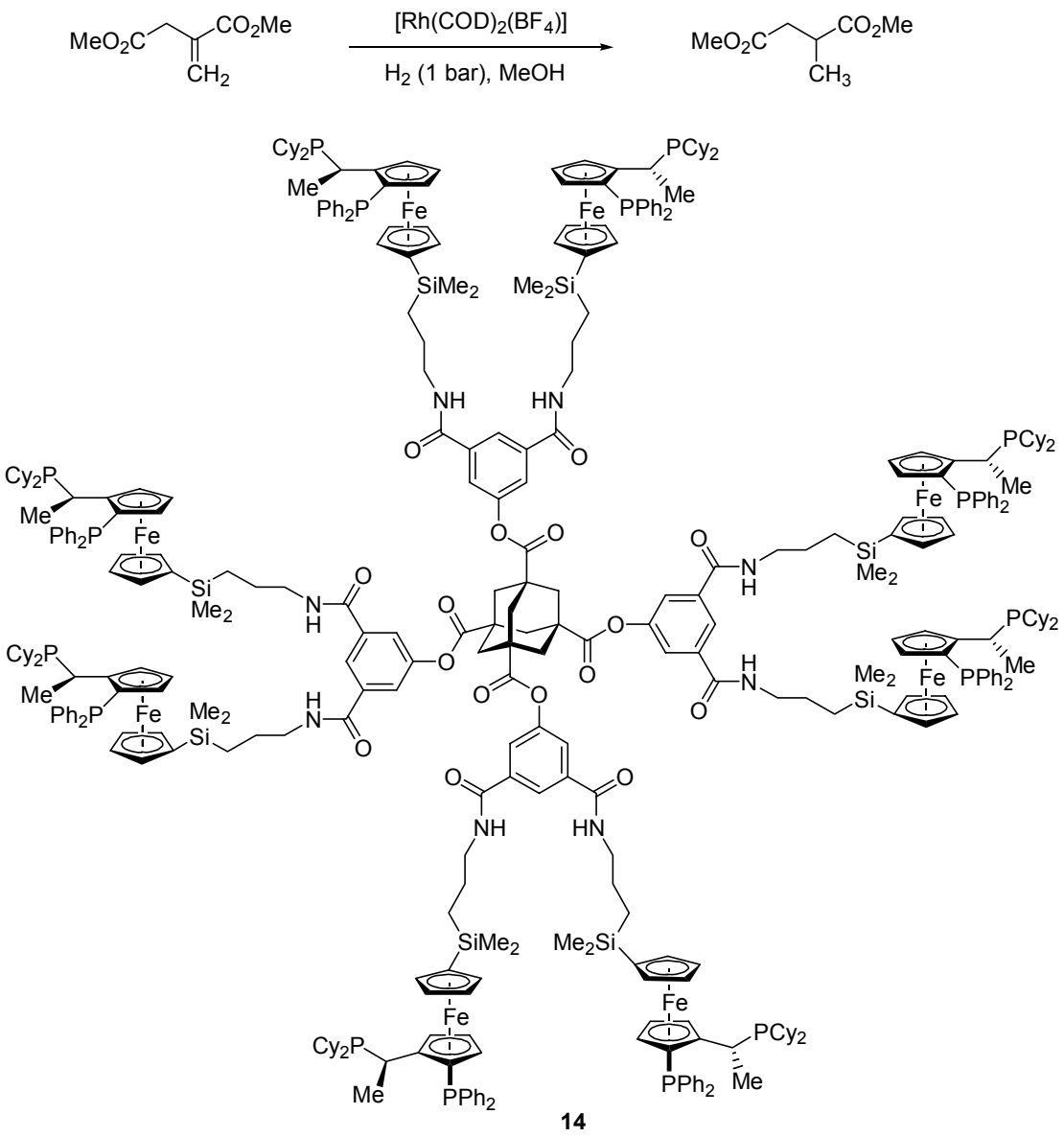

Scheme 14. Asymmetric hydrogenation using a dendritic-rhodium catalyst.

catalyst, could easily be removed and reused. In this case, no pressure was applied during the filtration experiments, which resulted in a catalytic process that is rate-limited by spontaneous diffusion of the substrates through the membrane and by mass transfer limitation due to the relatively small membrane surface area. This idea was supported by a control experiment in which the catalyst was not compartmentalized, resulting in complete conversion within 4 h, while the compartmentalized catalyst gave complete conversion after 36 h only. Most interestingly, the vial containing the

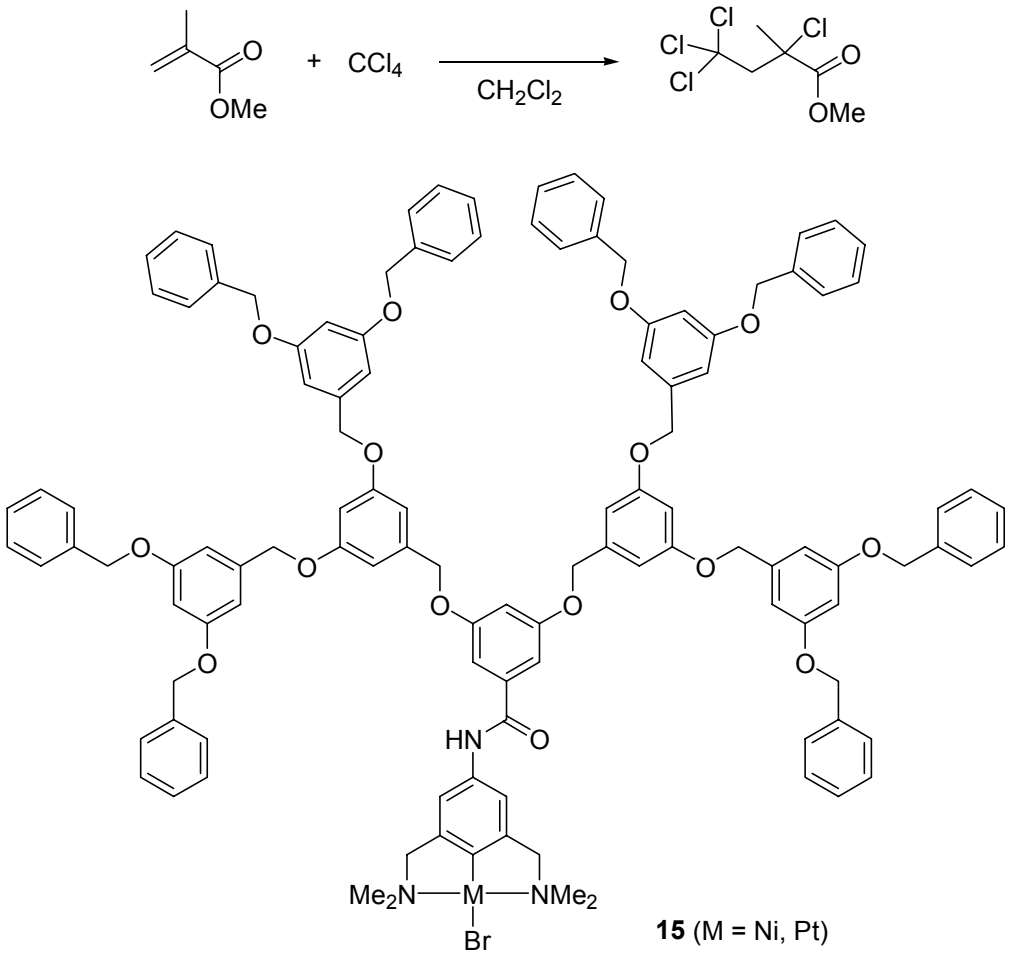

Scheme 15. Nickel functionalized dendrimer in Kharasch addition reaction.

catalyst could be removed and stored for prolonged times, without loss in catalytic activity. This result is now used for the development of one-pot cascade reactions, catalyzed by various compartmentalized homogeneous catalysts.

Another very interesting aspect of this work is the elegant way in which the retention rate of the G3 dendrimer was determined. The G3 dendrimer **15** in which Ni was replaced by Pt (thus keeping the overall properties for membrane retention measurements the same) was used for this purpose, since this material strongly colorizes upon exposure to sulfur dioxide.[37] This allows the detection of very low concentrations of **15** by means of UV/Vis spectroscopy. Obviously, using such a sensitive analysis technique for determining retention rates is preferred over the generally used but less accurate weighing methods, since the analysis is performed *in situ* and does not require additional work-up. Applying this procedure revealed that

<20% of the G3 dendrimer **15** (M = Pt) was washed out of the membrane-capped vial in 280 h.

The latest example of a dendritic enlarged homogeneous catalyst which was recycled by means of nanofiltration technology was reported by Van Leeuwen and coworkers.[38] In an alternative approach, the catalytically active part was anchored to the soluble dendritic support via noncovalent linkages. The resulting system (**16**) was used as a homogeneous catalyst in the allylic amination of crotyl acetate in a continuous flow membrane reactor (MPF-60 NF, Koch Int.) (Scheme 16). The catalyst precursor was prepared by mixing the dendritic ligand with a suitable palladium precursor and the catalytic activity and selectivity of this supramolecular catalyst in a batch process was found to be similar to a mononuclear model compound. The retention of the palladated dendritic catalyst precursor **16** was found to be dependent on the P/Pd ratio. With a P/Pd ratio of 1, a retention of 0.994 was found, while a P/Pd ratio of 2 resulted in a retention of 0.999. Furthermore, a slow decrease in conversion was observed when the dendritic catalyst was applied in a continuous flow membrane reactor. This decrease could not completely be explained by wash-out of the catalysts, thus most probably deactivation of the catalyst occurred as well.

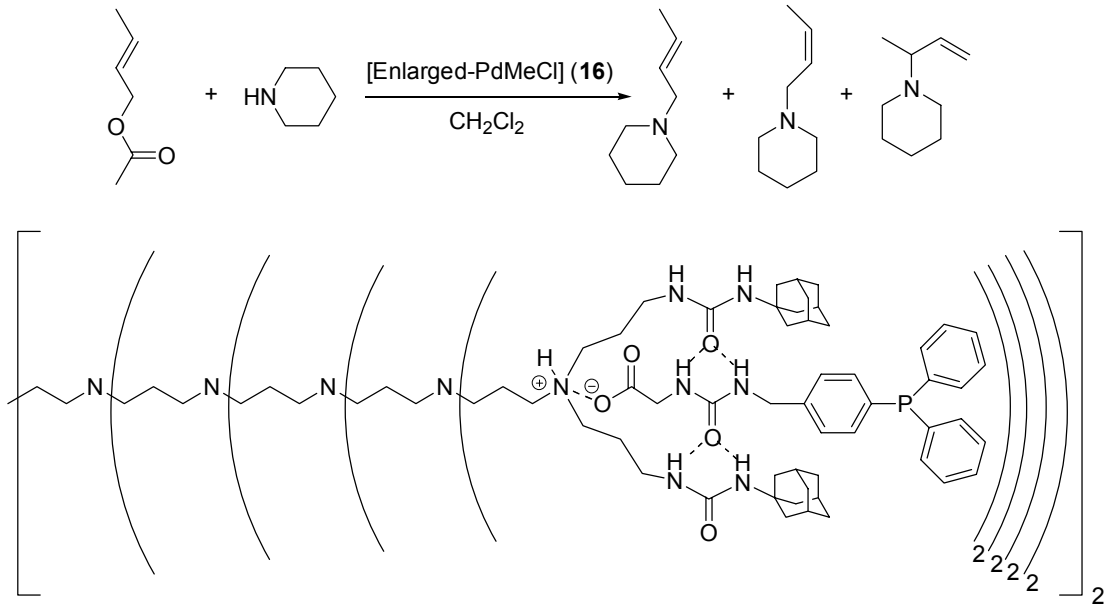

Scheme 16. Non-covalently bound catalyst in allylic amination.

1.5. Non-enlarged Systems

The group of Jacobs reported the use of non-enlarged mononuclear ruthenium and rhodium bisphosphine systems in asymmetric hydrogenation reactions (Scheme 17).[39] In a first example, Rh-EtDUPHOS **17** was applied in the chemo- and enantioselective hydrogenation of methyl-2-acetamidoacrylate (MMA) (reaction A, Scheme 17) in a NF-membrane reactor (MPF-60 NF membrane, Koch Int.) under continuous conditions. During 10 cycles a decrease in conversion was observed, which could not solely be ascribed to incomplete rejection of the catalyst by the membrane (R = 0.97). Therefore, it was proposed that a slow deactivation of the catalyst, probably due to oxidation of the phosphines, took place. In a second reaction, the Ru-BINAP system **18** was used in the continuous hydrogenation of dimethyl

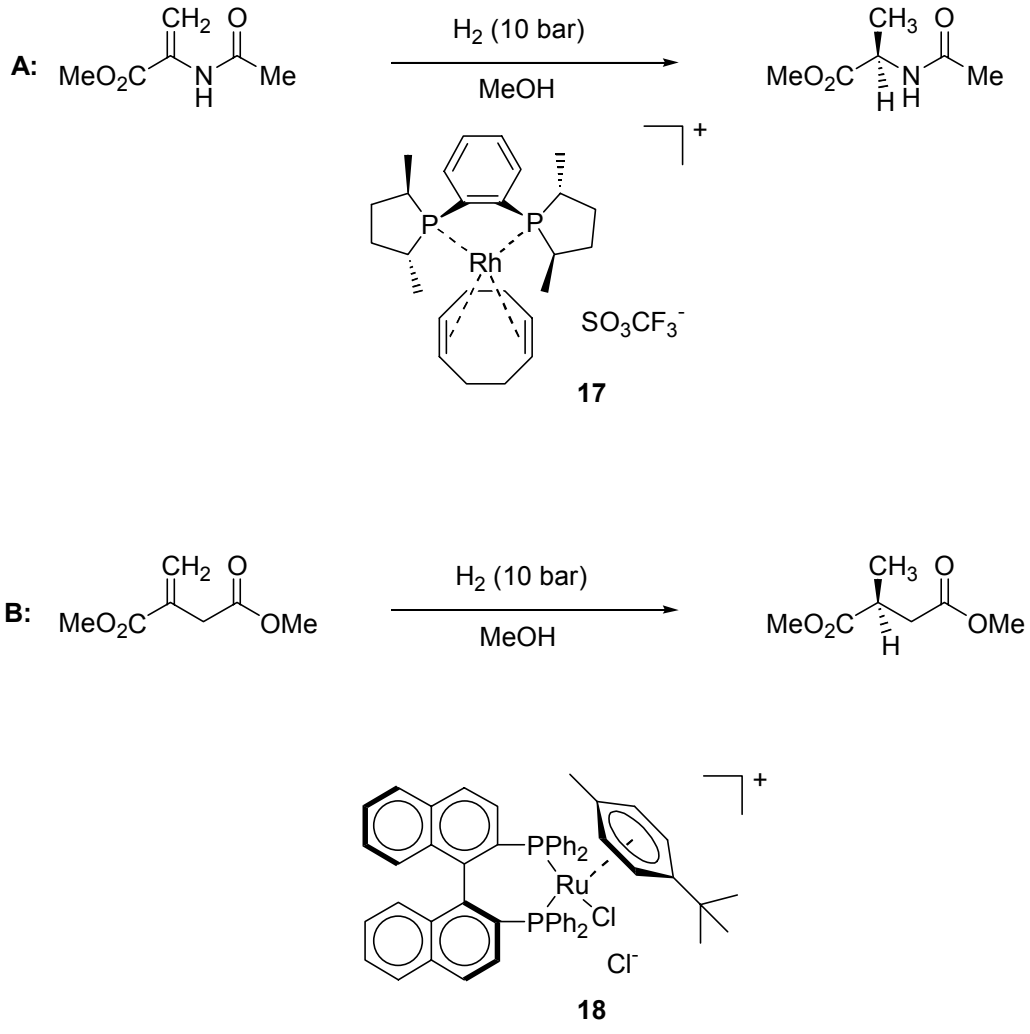

Scheme 17. Non-enlarged catalysts in NF-membrane recycling setup.

itaconate (reaction B, Scheme 17). In this reaction, a small decrease of conversion was also observed, however, this could completely be ascribed to minor wash-out of the catalyst (R = 0.98). No deactivation or decomposition of the catalyst was observed.

Recently, an example was reported in which a fluorous catalyst was used for the hydrogenation of 1-butene in supercritical CO_2 ($scCO_2$) in a continuous membrane reactor (Scheme 18).[40] A fluorous derivative of Wilkinson's catalyst (**19**) was used in combination with a microporous silica membrane with an average pore size of 0.6 nm, which completely retained the catalyst. This system was operated under continuous conditions for 75 hours (32 reactor volumes), only showing a slow decrease of the activity in time (conversion dropped from 40 to 33%). Since this minor deactivation behavior could not be ascribed to catalyst leaching, it was proposed to be due to slow oxidation of **19** by oxygen. This example shows an interesting development, in which homogeneous catalyst recycling is combined with the use of environmentally friendly solvents, *i.e.* high-density gases ($scCO_2$).

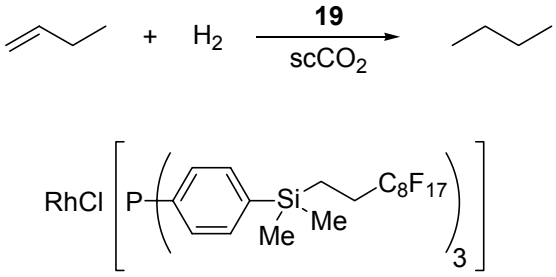

19

Scheme 18. Fluorous catalyst in continuous hydrogenation reaction.

These three examples nicely show that when the appropriate conditions (solvent, pressure, membrane, temperature, etc) are chosen, anchoring of the homogeneous catalyst to a soluble support is not always necessary in order to get high retention of the catalytic system by NF-membranes.

1.6. Conclusions and Outlook

With the development of membrane technology for purification of water-streams, this technology gained growing attention in other research fields as well. Nowadays, membrane technology can also be applied in the recycling of

homogeneous catalysts. This interesting development creates a way to combine the advantages of homogeneous and heterogeneous catalysis. The high selectivity and activity and the well-defined catalyst description of homogeneous catalysts can now

Table 2. Summary of achievements in the field of homogeneous catalyst recycling by applying membrane filtration technology.

Cat.	Catalyzed Reaction Type	M_w (g/mol)	Solvent[a]	Membrane[b]	Retention	Ref
1	$ZnEt_2$ addition	9600	n-Hexane	PAH-20	0.998	19
2a,b	Reduction of ketones	13800	THF	MPF-50	> 0.98	20
2c, 3	"		THF	MPF-50	> 0.985	21
4	Asymm. hydrogenation	> 7460	H_2O	YC05	0.991	22
5	Dihydroxylation	> 20000	Acetone/H_2O	unknown	n.d.	23
6	Hydroformylation	$>3 \times 10^5$	MeOH	PES	0.998	24
8	Kharasch addition	1570	CH_2Cl_2	MPF-50	0.974	27
9	Kharasch addition	4940	CH_2Cl_2	MPF-50	0.998	27
10	Hydrovinylation	2800	CH_2Cl_2	MPF-60	> 0.85	29
11a	Allylic alkylation	8252	THF	MPF-60	0.981	30a
11b	Allylic amination	>5000	CH_2Cl_2	MPF-60	> 0.985	30b
12	Olefin metathesis	3230	$C_2H_4Cl_2$	MPF-60	n.d.	32
13	Allylic substitution	10200	CH_2Cl_2	PAH-5	0.992	33, 34
	"	"	"	MPF-50	0.999	"
14	Asymm. hydrogenation	7550	MeOH	Centricon-3	n.d.	35
15	Kharasch addition	2060	CH_2Cl_2	MPF-60	n.d.[c]	36
16	Allylic amination	> 40000	CH_2Cl_2	MPF-60	> 0.994[d]	38
17	Asymm. hydrogenation	929	MeOH	MPF-60	0.97	39
18	Asymm. hydrogenation	723	MeOH	MPF-60	0.98	39
19	Hydrogenation	5295	$scCO_2$	SiO-membr.	> 0.999	40

a) Solvent in which the retention is determined. This solvent is not necessarily also the solvent in which catalysis was performed.

b) PAH-20 and PAH-5, MWCO = unknown, Hoechst Nadir. MPF-50, MWCO = 700 and MPF-60, MWCO = 400, Koch Int (www.kochmembrane.com). YC05: MWCO = 500, Amicon (www.millipore.com). Centricon-3, MWCO = 3000, Amicon (www.millipore.com). PES membranes: MWCO = 50 kD, Sartorius (www.sartorius.com).

c) Only system in which no pressure was applied; <20% of catalyst leached through the membrane in 380 h.

d) Retention depends on the P/Pd ratio: P/Pd = 1, R = 0.994; P/Pd = 2, R = 0.999

be integrated with the easy recycling, low catalyst quantities and high ttn of heterogeneous systems, ultimately leading to *Green Industrial Processes*. This whole process started in biotechnology, where UF- and NF-membrane systems were used for the recycling of expensive enzymes and co-enzymes. This made these systems feasible for application in commercial production processes. With the development of more resistant membranes, it is also possible to perform such processes in organic solvents using polymer and/or dendrimer-enlarged homogeneous catalysts. To date, a number of very promising results have been obtained in this area (Table 2), showing the high potential of homogeneous catalysts in this research field.

A number of important points have to be considered, however, before applying membrane technology in continuous processes using recyclable homogeneous catalysts. First of all, since most homogeneous catalysts contain transition metals coordinated to appropriate ligands, catalyst stability becomes an important factor. In particular, the switch from batch-like processes to continuous processes is often accompanied by a higher deactivation/decomposition rate of the catalysts, meaning that optimization of the conditions is required in order to obtain a suitable process. Interaction of the catalysts with the membrane or the reactor material has to be considered as well, since these interactions can also lead to deactivation of the catalysts. Finally, the solvent is very important, since the pore-sizes of the membranes depend on the hydrophilicity/hydrophobicity/polarity of the solvent. Therefore, making a real comparison between all systems discussed in this chapter is not feasible, since in most membrane setups the conditions were different.

In conclusion, contrary to enzyme-catalyzed reactions which are normally performed under very mild conditions, homogeneous catalysts often need more severe reaction conditions, making application of homogeneous catalysts in membrane technology more difficult. Therefore, developing more resistant membranes and improving the reactor technology is desirable, since these factors largely determine the applicability of membrane technology in homogeneous catalyst recycling. Nevertheless, membrane technology is a very promising technique for the development of selective and fast commercial catalytic processes using homogeneous catalysts. Further development of this technology in the future is important, since it will lead to energy saving and cleaner industrial catalytic processes, *i.e. green* processes.

1.7. Aim and Scope of this Thesis

In recent years, the development of efficient methods to recycle homogeneous catalysts has gained a lot of attention. Both from an environmental and economical point of view, homogeneous catalyst recycling is important, as was already outlined in Chapter 1.1. A very promising method to separate the homogeneous catalyst from product-containing solutions is via nano- (NF) or ultrafiltration (UF) using solvent resistent UF- and NF-membranes. One approach is to adjust the reaction conditions in such a way that the low-molecular-weight catalysts do not pass the membrane. A disadvantage of this approach is that most catalytic reactions do not fulfill these requirements, making this approach only suitable for a limited number of catalytic reactions. A second approach is to increase the size of the homogeneous catalysts to nanosize dimensions, resulting in an efficient separation of the macromolecular catalysts by UF- and NF-techniques. The advantage of such a setup is that high retentions of the macromolecular catalysts are obtained in various reaction media, allowing application in many catalytic reactions. This latter approach is the subject of this thesis. So far, mainly so-called *metallodendrimers* were used in this field, since these materials have well-defined compositions, making direct comparison with the mononuclear analogs possible. Another important feature of most metallodendrimers, however, is their highly flexible backbone, making them susceptible to shape-changes in solution which can have a negative influence on their retention by nano- or ultrafiltration membranes.

The aim of this research has been to develop synthetic routes to *shape-persistent* nanosize homogeneous catalysts and to investigate the influence of shape-persistence on the retention behavior of these materials by nanofiltration membranes. In addition, suitable catalytic homogeneous reactions had to be developed for application of these macromolecular catalysts in continuous processes in a nanofiltration membrane reactor. Finally, as some of the novel complexes described in this thesis consist of symmetric, rigid, two-dimensional aromatic backbones connected to metalated, terdendate coordinating YCY-pincer ligands, also their use as supramolecular templates for the construction of large heterocyclic structures has been studied.

In *Chapter One*, an overview is given of the application of ultra- and nanofiltration techniques in the field of homogeneous catalyst recycling. Various synthetic catalytic systems, mainly enlarged homogeneous catalysts, are discussed, as

well as a few illustrative examples in which soluble enzymes are recycled using these filtration techniques.

Chapter Two describes the synthesis of palladated and platinated hexakis(YCY-pincer) and tris(NCN-pincer) ligands. These ligand systems containing six and three potential metal-binding sites, respectively, were prepared prior to metalation.

In *Chapter Three*, procedures to prepare palladated and platinated dodecakis- and octakis(NCN-pincer) complexes are discussed. In this modular approach, the multimetallic materials are assembled by coupling pre-prepared mono(palladated- or platinated-NCN-pincer) building blocks to dodecakis- or octakis(benzylic bromides), respectively.

The synthesis and catalytic application of a series of YCY-Pd^{II} complexes and *para*-substituted NCN-Pd^{II} complexes as Lewis acidic catalysts are described in *Chapter Four*. The influence of both the donor substituent Y and the *para*-substituents on the catalytic activity of the cationic Pd^{II}-center in the double Michael reaction between methyl vinyl ketone and ethyl-α-cyanoacetate was studied. Also the electronic influence of the various *para*-substituents on the Lewis-acidic Pd^{II}-centers was investigated by DFT-calculations. In addition, the catalytic behavior of various shape-persistent multi(NCN-Pd^{II}) catalysts in the double Michael reaction is discussed.

The retention behavior of the various shape-persistent multi(NCN-Pt^{II}) species by nanofiltration membranes is presented in *Chapter Five*. In this study, the sensor properties of the NCN-Pt^{II} unit, *i.e.* strong orange coloring upon treatment with sulfur dioxide, was used to determine accurately the retentions of the various complexes by NF-membranes. The molecular structures of the various NCN-pincer systems were calculated by molecular modeling, allowing the comparison between the size and dimension of these systems and their retention rates by NF-membranes. Finally, the application of a homogeneous dodecakis(NCN-Pd^{II}) catalyst in a double Michael reaction under continuously operating conditions in a nanofiltration membrane reactor has been investigated. The selection of this homogeneous catalyst was based on the excellent retention properties of the corresponding isostructural platinum-containing material.

The work in *Chapter Six* concerns the development of transcyclometalation procedures to prepare platinated and ruthenated hexakis(PCP-pincer) complexes. The transcyclometalation reaction turned out to be superior over the classical direct metalation procedures in constructing these hexakis(PCP-Pt^{II} and –Ru^{II}) complexes.

Furthermore, the application of the hexakis(PCP-Ru^{II}) complex as a homogeneous catalyst in the hydrogen transfer reactions of several ketones to the corresponding alcohols was studied.

Chapter Seven shows the use of pincer-metal-complexes as protecting groups for the pyridine-*N*-atom of diolefin-substituted pyridines, allowing selective intramolecular ring closing by olefin metathesis (RCM). The results obtained with the monometallic pincer systems have been used as a model study for the construction of macrocyclic structures in which the shape-persistent multimetallic species developed in *Chapter Two* were used as templates. Pyridines substituted at either the 3,5- or 2,6-positions with olefinic tails of different lengths were used. The selectivity of the RCM reaction depended on the type of pincer-system used (NCN, SCS) as well as on the nature of the metal-center (palladium or platinum). Attempts to use the highly symmetric hexakis(SCS-Pd^{II}) complex, bound at each Pd^{II}-center to a diolefin-substituted pyridine, as a template for the construction of large heterocycles containing six pyridines connected by α,ω-alkanediyl chains using RCM will also be discussed.

1.8. References and Notes

[1] Noyori, R. *Asymmetric Catalysis in Organic Synthesis*, Wiley, New York, **1994**.

[2] a) Parshall, G. W.; Ittel, S. D. *The Applications and Chemistry of Catalysis by Soluble Transition Metal Complexes*, Wiley, New York, **1992**. b) Cornils, B.; Herrmann, W. A. *Applied Homogeneous Catalysis with Organometallic Compounds*, VCH, Weinheim, Germany, **1996**.

[3] For representative examples of homogeneous catalysts which are commercial applied see: a) Noyori, R. *CHEMTECH* **1992**, *22*, 360. b) Noyori, R.; Ikeda, T.; Ohkuma, T.; Widhalm, M.; Kitamura, M.; Takaya, H.; Akutagawa, S.; Sayo, N.; Saito, T.; Taketomi, T.; Kumobayashi, H. *J. Am. Chem. Soc.* **1989**, *111*, 9134. c) Kitamura, M.; Ohkuma, T.; Inoue, S.; Sayo, N.; Kumobayashi, H.; Akutagawa, S.; Ohta, T.; Takaya, H.; Noyori, R. *J. Am. Chem. Soc.* **1988**, *110*, 629. d) Spindler, F.; Pugin, B.; Jalett, H. -P.; Buser, H. -P.; Pittelkow, U.; Blaser, H. -U. *Catalysis of Organic Reactions*; Maltz, R. E., Jr., Ed.; Chem. Ind.; Dekker: New York, **1996**, *68*, 153.

[4] Baker, R. T.; Tumas, W. *Science* **1999**, *284*, 1477.

[5] a) Hägg, M. -B. *Separation and Purification Methods* **1998**, *27*, 51, and references therein. b) Singh, R. *Ultrapure Water* **1997**, *14*, 21. c) *Membrane Handbook* (Eds. Ho, W. S. W.; Sirkar, K. K.) Chapman & Hall, New York, **1992**. d) Reidy, R. *Profile of the International Filtration and separation Industry* **1993**, Elsevier, Oxford.

[6] a) Cassano, A.; Molinaari, R.; Romano, M.; Drioli, E. *J. Membr. Science* **2001**, *181*, 111. b) Smith, B. F.; Robinson, T. W.; Cournoyer, M. E.; Wilson, K.; Sauer, N. N.; Lu, M. T. *52nd Purdue Industrial Waste Conference Proceedings*, Ann Arbor Press, Chelsea, Michigan, USA, **1997**, 559.

[7] Thompson, J. A.; Jarvinen, G. *Filtration & Separation* **1999**, *36*, 28, and references therein

[8] Rautenbach, R.; Gröschl, A. *Desalination* **1990**, *7*, 73.

[9] Prof. dr. D. Vogt, N. Ronde, Eindhoven University of Technology, The Netherlands. For more information see: www.catalysis.nl/homogeneous_catalysis.

[10] Kragl, U. *Industrial Enzymology*, 2nd ed (Eds.: Godfrey, T., West, S.), Macmillan, Hampshire, **1996**, 275, and references therein.

[11] Bommarius, A. S. *Biotechnology: Vol. 3: Biotechnology* (Eds.: Rehm, H. -J.; Reed, G.; Puhler, A.; Stadler, P; Stephanopoulos), VCH, Weinheim, **1993**, 427.

[12] Draus, K. *Proceeding of chiral '93 USA*, **1993**.

[13] Kragl, U.; Gödde, A.; Wandrey, C.; Kinzy, W.; Cappon, J. J.; Lugtenburg, J. *Tetrahedron: Asymm.* **1993**, *4*, 1193.

[14] a) Kragl, U.; Vasic-Racki, D.; Wandrey, C. *Chem. Ing. Tech.* **1992**, 499. b) Schütte, H.; Florsdorf, J.; Sahm, H.; Kula, M. -R. *Eur. J. Biochem.* **1976**, 151. c) Bommarius, A. S.; Drauz, K.; Groeger, U.; Wandrey, C. *Chirality in Industry*, Collins, A. N.; Sheldrake, G. N.; Crosby, J. (Eds.); John Wiley & Sons Ltd, **1992**, 371.

[15] Seelbach, K.; Kragl, U. *Enzyme Microb. Technol.* **1997**, *20*, 389.

[16] Kula, M. -R.; Wandrey, C. *Meth. Enzymol.* **1987**, *136*, 9.

[17] a) Ikemi, M.; Ishimatsu, Y. *J. Biotechnol.* **1990**, *14*, 211. b) Röthig, T. R.; Kulbe, K. D.; Bückmann, F.; Carrea, G. *Biotechnol. Lett.* **1990**, *12*, 353. c) Nidetzky, B.; Schmidt, K.; Neuhauser, W.; Haltrich, D.; Kulbe, K. D. *Spec. Publ. - R. Soc. Chem.* **1994**, *158* (*Separations for Biotechnology III*), 351. d) Kulbe, K. D.; Schmidt, H.; Schmidt, K.; Scholtze, H. D. *Prog. Biotechnol.* **1992**, *7*, 565.

[18] See for the latest review in this research field: Kragl, U.; Dreisbach, C.; Wandrey, C. *Appl. Homogeneous Catal. Organometal. Comp.* **1996**, *2*, 832.

[19] Kragl, U.; Dreisbach, C. *Angew. Chem. Int. Ed. Engl.* **1996**, *35*, 642.

[20] a) Giffels, G.; Beliczey, J.; Felder, M.; Kragl, U. *Tetrahedron: Asym.* **1998**, *9*, 691. b) Rissom, S.; Beliczey, J.; Giffels, G.; Kragl, U.; Wandrey, C. *Tetrahedron: Asym.* **1999**, *10*, 923.

[21] a) Wöltinger, J.; Bommarius, A. S.; Drauz, K.; Wandrey, C. *Organic Process Research & Development* **2001**, *5*, 241. b) Wöltinger, J.; Drauz, K.; Bommarius, A. S. *Appl. Catal. A* **2001**, *221*, 171.

[22] Dwars, T.; Haberland, J.; Grassert, I.; Oehme, G.; Kragl, U. *J. Mol. Cat. A: Chem* **2001**, *168*, 81.

[23] Wöltinger, J.; Henniges, H.; Krimmer, H. –P.; Bommarius, A. S.; Drauz, K. *Tetrahedron: Asym.* **2001**, 2095.

[24] Schwab, E.; Mecking, S. *Organometallics* **2001**, *20*, 5504.

[25] For reviews on dendritic catalysts see: a) Kreiter, R.; Kleij, A. W.; Klein Gebbink, R. J. M.; van Koten, G. *Topics in Current Chemistry, Dendrimers IV*; Vögtle, F., Ed.; Springer-Verlag Berlin Heidelberg, **2001**, *217*, 163. b) Kleij, A. W.; Klein Gebbink, R. J. M.; van Koten, G. *Dendrimers and other Dendritic Polymers*; Frechet, J., Tomalia, D., Eds.; Wiley, New York, **2002**. c) Oosterom, G. E.; Reek, J. N. H.; Kamer, P. C. J.; van Leeuwen, P. W. N. M. *Angew. Chem. Int. Ed.* **2001**, *40*, 1828.

[26] Knapen, J. W. J.; van der Made, A. W.; de Wilde, J. C.; van Leeuwen, P. W. N. M.; Wijkens, P.; Grove, D. M.; van Koten, G. *Nature* **1994**, *372*, 659.

[27] Kleij, A. W.; Gossage, R. A.; Klein Gebbink, R. J. M.; Brinkmann, N.; Reijerse, E. J.; Kragl, U.; Lutz, M.; Spek, A. L.; van Koten, G. *J. Am. Chem. Soc.* **2000**, *122*, 12112.

[28] Kleij, A. W.; Gossage, R. A.; Jastrzebski, J. T. B. H.; Boersma, J.; van Koten, G. *Angew. Chem. Int. Ed.* **2000**, *39*, 176.

[29] a) Hovestad, N. J.; Eggeling, E. B.; Heidbüchel, H. J.; Jastrzebski, J. T. B. H.; Kragl, U.; Keim, W.; Vogt, D.; van Koten, G. *Angew. Chem. Int. Ed.* **1999**, *38*, 1655. b) Eggeling, E. B.; Hovestad, N. J.; Jastrzebski, J. T. B. H.; Vogt, D.; van Koten, G. *J. Org. Chem.* **2000**, *65*, 8857.

[30] a) De Groot, D.; Eggeling, E. B.; de Wilde, J. C.; Kooijman, H.; van Haaren, R. J.; van der Made, A. W.; Spek, A. L.; Vogt, D.; Reek, J. N. H.; Kamer, P. C. J.; van Leeuwen, P. W. N. M. *Chem. Comm.* **1999**, 1623. b) De Groot, D.; Reek, J. N. H.; Kamer, P. C. J.; van Leeuwen, P. W. N. M. *Eur. J. Org. Chem.* **2002**, 1085.

[31] De Groot, D.; Emmerink, P. G.; Coucke, C.; Reek, J. N. H.; Kamer, P. C. J.; van Leeuwen, P. W. N. M. *Inorg. Chem. Comm.* **2000**, *3*, 711.

[32] Wijkens, P.; Jastrzebski, J. T. B. H.; van der Schaaf, P. A.; Kolly, R.; Hafner, A.; van Koten, G. *Org. Lett.* **2000**, *2*, 1621.

[33] Reetz, M. T.; Lohmer, G.; Schwickardi, R. *Angew. Chem. Int. Ed. Engl.* **1997**, *36*, 1526.

[34] Brinkmann, N.; Giebel, D.; Lohmer, G.; Reetz, M. T.; Kragl, U. *J. Cat.* **1999**, *183*, 163.

[35] Köllner, C.; Pugin, B.; Togni, A. *J. Am. Chem. Soc.* **1998**, *120*, 10274.

[36] Albrecht, M.; Hovestad, N. J.; Boersma, J.; van Koten, G. *Chem. Eur. J.* **2001**, *7*, 1289.

[37] a) Albrecht, M.; Gossage, R. A.; Spek, A. L.; van Koten, G. *Chem. Comm.* **1998**, 1003. b) Albrecht, M.; van Koten, G. *Adv. Mater.* **1999**, *11*, 171. c) Albrecht, M.; Lutz, M.; Spek, A. L.; van Koten, G. *Nature* **2000**, *406*, 970.

[38] de Groot, D.; de Waal, B. F. M.; Reek, J. N. H.; Schenning, A. P. H. J.; Kamer, P. C. J.; Meijer, E. W.; van Leeuwen, P. W. N. M. *J. Am. Chem. Soc.* **2001**, *123*, 8453.

[39] De Smet, K.; Aerts, S.; Ceulemans, E.; Vankelecom, I. F. J.; Jacobs, P. A. *Chem. Comm.* **2001**, 597.

[40] van den Broecke, L. P. J.; Goetheer, E. L. V.; Verkerk, A. W.; de Wolf, E.; Deelman, B. –J.; van Koten, G.; Keurentjes, J. T. F. *Angew. Chem. Int. Ed.* **2001**, *40*, 4473.

– *Chapter 2* –

Synthesis of Shape-Persistent Nanosize Palladium(II) and Platinum(II) Cartwheel Complexes based on Terdentate Coordinating YCY-Ligands connected to an Aromatic Core

Abstract. Synthetic procedures for the synthesis of hexakis(pincer) ligands $C_6[C_6H_3(CH_2Y)_2\text{-}3,5]_6$ (Y = NMe_2, SPh, PPh_2, pz (= pyrazol-1-yl)), the tris(pincer) ligand $C_6H_3[Br\text{-}4\text{-}C_6H_2(CH_2NMe_2)_2\text{-}3,5]_3\text{-}1,3,5$, the extended tris(pincer) ligand $C_6H_3[C_6H_4\text{-}4\text{-}(Br\text{-}4\text{-}C_6H_2(CH_2NMe_2)_2\text{-}3,5)]_3\text{-}1,3,5$ and the bis(pincer) ligand $C_6H_4[I\text{-}4\text{-}C_6H_2(CH_2NMe_2)_2\text{-}3,5]_2\text{-}1,4$ were developed. These multisite-ligand systems were selectively palladated and/or platinated. The X-ray crystal structures of a hexakis(SCS-Pd^{II})- and a tris(NCN-Pd^{II})-species, respectively, were determined and showed the symmetric propeller-like structures of these, so-called, *cartwheel*-type multimetallic structures.

H. P. Dijkstra, P. Steenwinkel, D. M. Grove, M. Lutz, A. L. Spek, G. van Koten, *Angew. Chem. Int. Ed.* **1999**, *38*, 2186

H. P. Dijkstra, M. D. Meijer, J. Patel, R. Kreiter, G. P. M. van Klink, M. Lutz, A. L. Spek, A. J. Canty, G. van Koten, *Organometallics* **2001**, *20*, 3159.

H. P. Dijkstra, C. A. Kruithof, N. Ronde, R. van de Coevering, D. J. Ramón, D. Vogt, G. P. M. van Klink, G. van Koten, *J. Org. Chem.*, *in press*.

2.1. Introduction

A recent, promising development in the area of homogeneous catalyst recovery and reuse (recycling) is the incorporation of homogeneous catalysts on large organic frameworks. In this way, homogeneous catalysts of nanosize-dimensions are created which can be separated from product-containing solutions by ultra- (UF) or nanofiltration (NF) techniques.[1] By this method, several advantages of homogeneous (high selectivity, activity, good catalyst description and reproducibility) and heterogeneous catalysis (easy catalyst recovery, high total turnover numbers (ttn) and small amounts of catalyst needed) can be combined. For this purpose, homogeneous catalysts bound to the periphery or the core of carbosilane- and Fréchet-type dendrimers were investigated extensively in recent years.[2] For most of the dendritic systems used in this research field, it was found that even the higher generation dendrimers are still not fully retained by NF-membranes, while based on their molecular weights complete retention was expected. This behavior most likely arises from the flexible backbone of these dendritic catalysts; for example, going up one generation not necessarily results in a significant increase of the size of the dendrimers, but rather results in back folding of the dendritic branches, affording more dense molecules.[3] Furthermore, the dendrimer-size in solution is not well-defined and can vary upon altering the polarity of the solvent-system or when pressure is applied. A detailed investigation on the influences of flexibility, size and geometry of nanosize catalysts on their retention rates by NF-membranes has never been performed. Therefore, to investigate this important aspect in ultra- and nanofiltration, we set out to synthesize various rigid (shape-persistent) nanosize homogeneous catalysts.

In this chapter, the synthesis of shape-persistent bis-, tris- and hexakis(pincer-metal) complexes is described. These compounds are based on monoanionic, terdentate coordinating YCY-pincer ligands (Figure 1), directly connected to a rigid

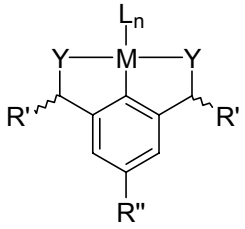

Y = NR_2, PR_2, SR, pz
M = Pd, Pt, Ni, Ru, Ir, Rh
R' = hydrogen, alkyl
R'' = hydrogen, alkyl, alkoxy, amide, dendrimer, fullerene, silica, peptide

Figure 1. Metalated pincer complexes; a versatile catalyst.

aromatic backbone. In the pincer moiety various functionalities can be altered rather easily allowing fine-tuning of these compounds for the desired application.[4] In addition, these complexes generally possess relatively high kinetic and thermal stabilities, preventing fast deactivation and/or decomposition of the organometallic moiety. This last aspect is an absolute prerequisite when the nanosize multimetallic pincer-complexes are applied as homogeneous catalysts under continuous reaction conditions.

2.2. Results and Discussion

Synthesis of hexakis(YCY) ligands. The various hexakis(pincer) ligands $C_6[C_6H_3(CH_2Y)_2\text{-}3,5]_6$ **7–10**, were prepared using dodecabromide $C_6[C_6H_3(CH_2Br)_2\text{-}3,5]_6$, **6**, as the key synthetic intermediate (Scheme 1). The synthesis of **6** was first reported by Duchêne and Vögtle,[5] but this route involved a number of time-consuming and expensive column chromatography techniques. Therefore, we developed an improved route to **6**, as outlined in Scheme 1.

Diazotization of 3,5-dimethylaniline gave iodoarene **1**, which was subsequently converted into bis(bromomethyl)arene **2** using *N*-bromosuccinimide. Treatment of **2** with sodium methoxide in methanol, afforded bis(methoxymethyl)arene **3**. Bisaryl acetylene **4** was prepared in a one-pot Pd/Cu catalyzed Sonogashira coupling starting from iodoarene **3** and gaseous acetylene.[6] This procedure afforded **4** in 90% overall yield, which is a significant improvement over the four-step procedure reported earlier (22% overall yield for **4**).[5] Trimerization of bis(pincer)acetylene **4** to persubstituted benzene **5** and subsequent treatment with acetyl bromide, afforded key intermediate **6** (Scheme 1).

The dodecamine $C_6[C_6H_3(CH_2NMe_2)_2\text{-}3,5]_6$, **7**, was obtained by direct nucleophilic amination of **6** with $HNMe_2$ (Scheme 1). For the synthesis of the dodecaphosphine **8**, a two-step procedure was used. Treatment of **6** with *in situ* prepared lithium-diphenylphosphine·BH_3 and subsequent deprotection of the dodecaphophine·$12BH_3$ with $HBF_4{\cdot}OEt_2$, yielded dodecaphosphine **8** as a white air-sensitive compound. The reaction of **6** with thiophenol under basic conditions (DMF in the presence of K_2CO_3), afforded the corresponding dodecasulfide $C_6[C_6H_3(CH_2SPh)_2\text{-}3,5]_6$, **9**, in 83% yield. Finally, dodecapyrazole ligand **10** was obtained by reaction of **6** with the *in situ* prepared potassium salt of pyrazole.

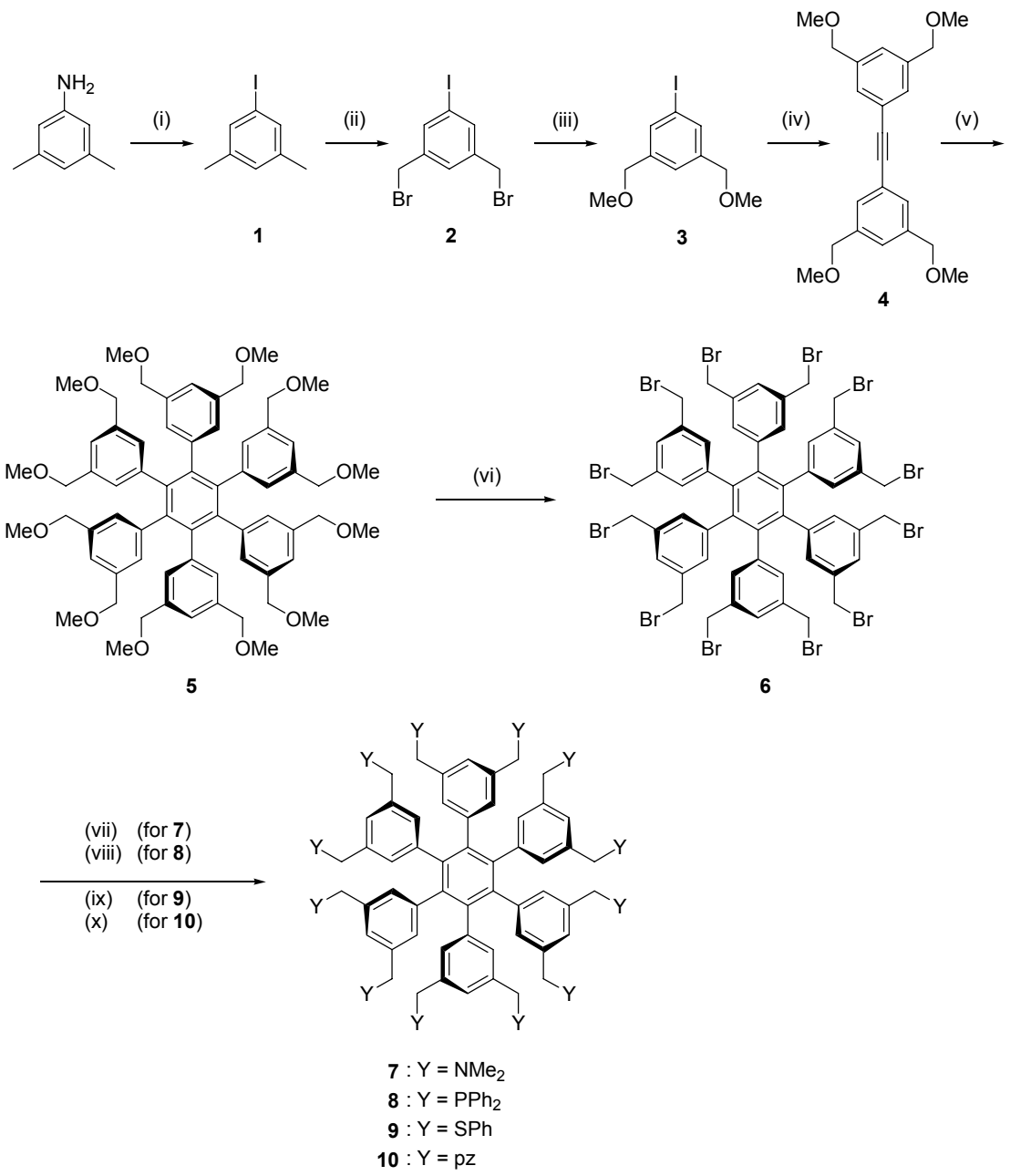

Scheme 1. (i) 25% H_2SO_4 (aq), $NaNO_2$ (aq), –10 °C, 15 min, followed by KI (aq), –10 → 90 °C, 2 h; (ii) *N*-Bromosuccinimide, AIBN, MeOAc, reflux, hν, 12 h; (iii) NaOMe, MeOH, reflux, 18 h; (iv) HC≡CH, $[PdCl_2(PPh_3)_2]$, CuI, Et_2NH, rt, 16 h; (v) $[PdCl_2(NCPh)_2]$, benzene, reflux, 6 h; (vi) AcBr, $BF_3{\cdot}OEt_2$, CH_2Cl_2, reflux, 24 h. (vii) $HNMe_2$, CH_2Cl_2, rt, 3 h; (viii) $HPPh_2{\cdot}BH_3$, *n*-BuLi, THF, –40 ˚C → rt, 18 h, followed by $HBF_4{\cdot}OEt_2$, Et_2O, rt, 2 h; (ix) PhSH, K_2CO_3, DMF, 50 ˚C , 18 h; (x) Pyrazole, K, THF, reflux, 1 h, followed by addition of **6**, THF, reflux, 15 h.

Metalation of hexakis(pincer) ligands. Complete palladation of hexakis(NCN-pincer) ligand **7** was not feasible via direct electrophilic palladation. Therefore, a lithiation-transpalladation method was used, using *t*-BuLi as the lithiation agent and $[PdCl_2(SEt_2)_2]$ as the palladium source (Scheme 2), a method previously developed for the mono(NCN-pincer) complex.[7] Although complete lithiation of **7** was feasible, as shown by a deuteration reaction with D_2O and subsequent analysis by ^1H and ^{13}C NMR spectroscopy, complete palladation, affording **11**, via this route could not be achieved. On average, four to five pincer groups were palladated by this method.

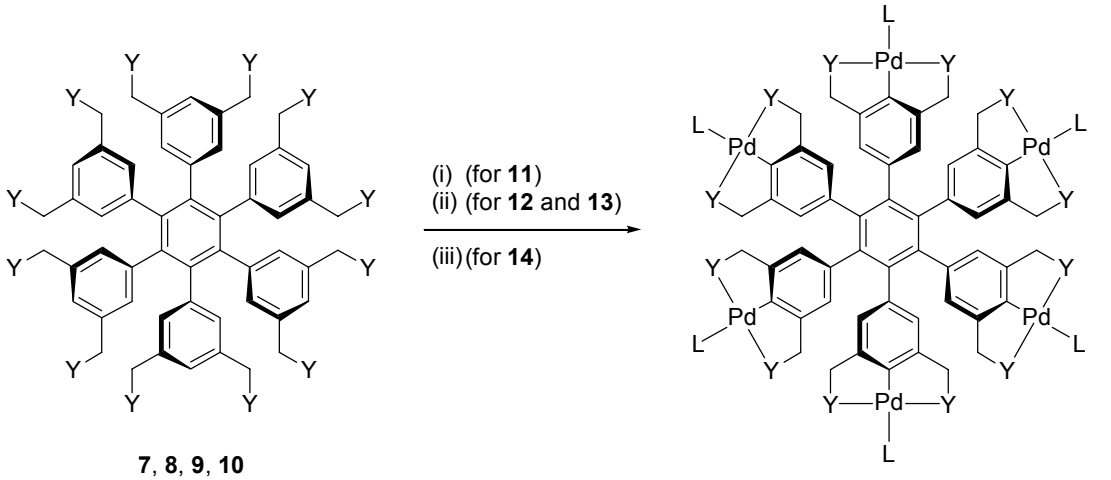

Scheme 2. (i) *t*-BuLi, hexanes, −80 °C → rt, 18 h followed by $[PdCl_2(SEt_2)_2]$, Et_2O, rt, 4 h; (ii) $[Pd(NCMe)_4](BF_4)_2$, MeCN, reflux, followed by LiCl, acetone, rt, 1 h; (iii) $Pd(OAc)_2$, AcOH, reflux, 15 h; (iv) LiCl, acetone, rt, 15 h. (v) $AgBF_4$, acetone, rt, 3 h.

Direct electrophilic palladation of dodecaphosphine **8** and dodecasulfide **9** with a small excess of $[Pd(MeCN)_4](BF_4)_2$ in acetonitrile,[8] followed by addition of LiCl gave the hexakis(chloropalladium) complexes **12** and **13** in 89 and 90% yield, respectively (Scheme 2). The reaction time needed for complete metalation of **9** (3 h), however, was considerably shorter than the time needed for **8 (**110 h). Thus far, the hexapalladium(II) complex **12** has been analyzed by ^1H, ^{13}C and ^{31}P NMR spectroscopy only, no elemental analysis indicating the isolation of the pure product

has yet been obtained.

Treatment of dodecapyrazole **10** with $Pd(OAc)_2$ in acetic acid resulted in the formation of $C_6[(PdOAc)\text{-}4\text{-}C_6H_2(CH_2pz)_2\text{-}3,5]_6$, **14**, which was isolated in 53% yield. Reaction of **14** with LiCl gave the corresponding hexakis(chloropalladium) complex **15**, which upon reaction with $AgBF_4$ in wet acetone afforded the hexakis(aquapalladium) complex $C_6[\{Pd(OH_2)\}\text{-}4\text{-}C_6H_2(CH_2pz)_2\text{-}3,5]_6$, **16**, in 70% yield (Scheme 2).

Dodecasulfide **13** has been characterized by X-ray crystallography. The molecular geometry of **13** shows a central benzene ring substituted with six

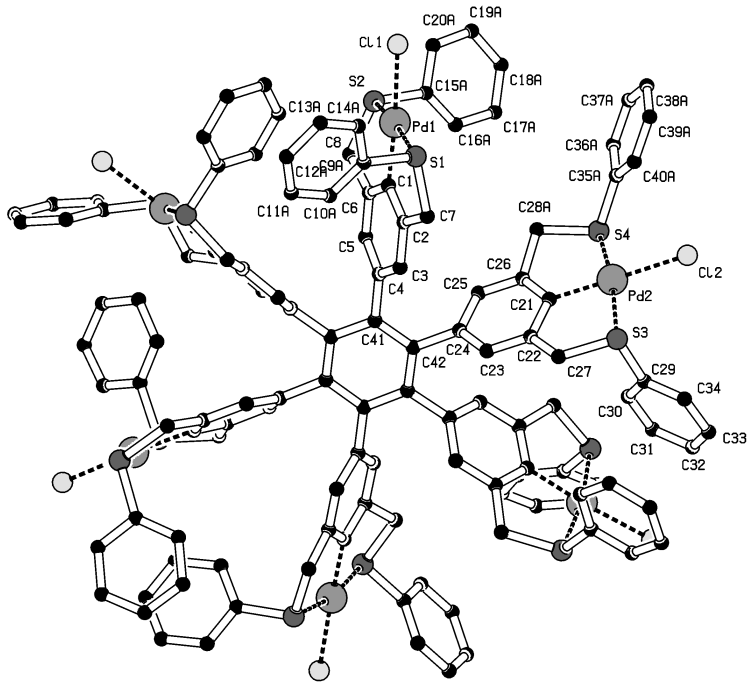

Figure 2. Molecular plot of **13**. Hydrogen atoms and solvent molecules are omitted for clarity. Only one conformation of the disordered S-Ph groups is shown. Selected bond lengths, angles and torsion angles: Pd1-C1 1.978(12), Pd1-S2 2.283(3), Pd1-S1 2.300(4), Pd1-Cl1 2.403(4), Pd2-C21 1.964(11), Pd2-S4 2.277(4), Pd2-S3 2.285(4), Pd2-Cl2 2.367(4) Å; C1-Pd1-S2 85.5(4), C1-Pd1-S1 84.5(4), S2-Pd1-S1 169.96(14), C1-Pd1-Cl1 175.9(4), S2-Pd1-Cl1 91.61(13), S1-Pd1-Cl1 98.42(15), C21-Pd2-S4 84.5(4), C21-Pd2-S3 85.8(4), S4-Pd2-S3 167.69(12), C21-Pd2-Cl2 176.5(5), S4-Pd2-Cl2 7.66(18), S3-Pd2-Cl2 92.41(18)°; C25-C24-C42-C41 -67(2), C23-C24-C42-C41 113.5(15), C5-C4-C41-C42' -63.5(16), C3-C4-C41-C42' 120.6(14)°. (Symmetry operations: ' -x+y, -x+1; " -y+1, x-y+1,z).

diorganosulfide moieties each of which is cyclopalladated at the position between the CH_2SPh groups (Figure 2). This affords square planar Pd^{II}-centers with a ligand environment that comprises tridentate SCS-coordination by the organic moiety with a chloro ligand *trans* to the metal-bonded aromatic carbon atom. An interesting aspect of the molecular structure of **13** is that there are three molecules in the unit cell; in each molecule all six Pd^{II}-centers adopted the same relative orientation with respect to the central C6 ring (twist angle 63.5 - 67°) resulting in a chiral cartwheel-like structure with a C_3 symmetry. The spatial arrangement of the metal atoms in **13** led to adjacent radial Pd-Pd separations of 7.339(2) and 8.006(2) Å, and a diametrically opposed Pd-Pd separation of 15.340(2) Å, while the distance between diametrically opposed chlorine atoms is 20.089(11) Å. Although this molecule has a fairly low molecular weight of 2846 Dalton its six-spoked cartwheel structure gives the true nanoparticle size dimensions and thus possesses appropriate properties for retainment by nanofiltration membranes.

Synthesis of tris(NCN-metal) complexes. The synthesis of the tris(pincer) ligand $C_6H_3[Br\text{-}4\text{-}C_6H_3(CH_2NMe_2)_2\text{-}3,5]_3\text{-}1,3,5$, **18**, started from substituted acetophenone **17** (Scheme 3), which was prepared according to a previous literature procedure.[9] A triple condensation reaction of **17** with tetrachlorosilane in ethanol afforded multisite ligand **18** in 70% yield.[10] Palladation of this tris(pincer) ligand was achieved via an oxidative addition reaction with $Pd(dba)_2$, resulting in the formation of palladated trispincer complex **19** in 70% yield. The corresponding trisplatinum(II) compound **20** was obtained in 73% yield by reaction of **18** with $[Pt(p\text{-tol})_2SEt_2]_2$, a method previously reported.[11] The neutral trispalladium complex **19** can easily be converted to the corresponding tri-ionic aqua complex **21** by treatment with silver tetrafluoroborate in wet acetone (76% yield) (Scheme 3).

Light-brown crystals of **19** suitable for crystal structure determination were obtained by slow diffusion of Et_2O into a concentrated solution of **19** in CH_2Cl_2. The molecular geometry of **19** shows a central benzene ring substituted at the 1-, 3-, and 5-positions with diorganoamine moieties each cyclopalladated at the intra-annular position between the CH_2NMe_2 groups (Figure 3). This affords square planar Pd^{II} centers with a ligand environment comprised of tridentate NCN-coordination by the organic moiety with a bromo ligand *trans* to the metal-bonded aromatic carbon. Compound **19** crystallizes in the trigonal space group $R\,\overline{3}\,c$ with the molecule on a special position with crystallographic 32 symmetry. This leads to an exact molecular

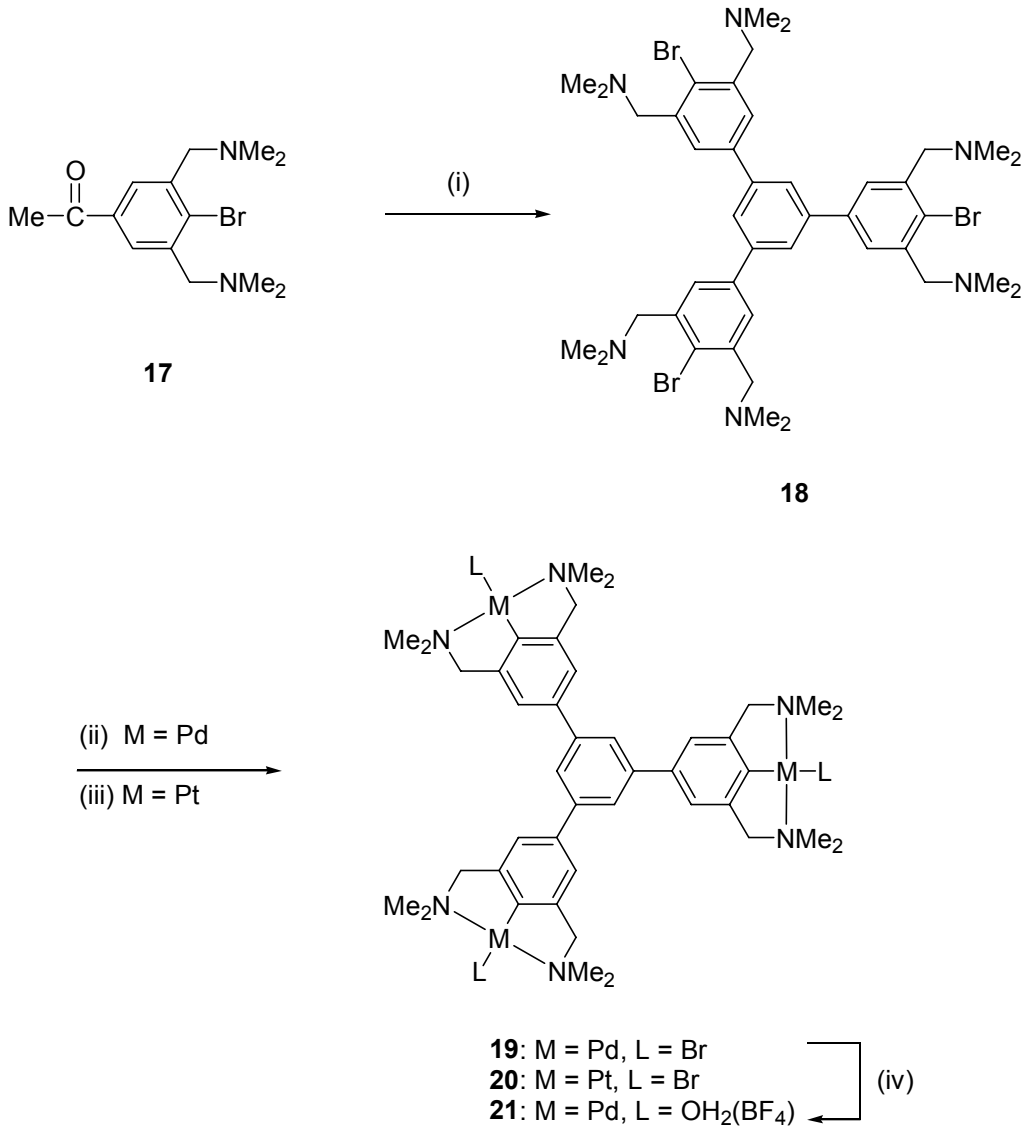

Scheme 3. (i) $SiCl_4$, EtOH, reflux, 18 h; (ii) $Pd(dba)_2$, benzene, rt, 18 h; (iii) $[Pt(p\text{-}tol)_2SEt_2]_2$, benzene, reflux, 3 h; (iv) $AgBF_4$, wet acetone, rt, 30 min.

symmetry of D_3. The 'pincer'-systems are therefore tilted in the same direction with respect to the central benzene ring (twist angle 47.31°). The size of the molecule is probably best defined by the fixed bromine-bromine distance of 17.4573(4) Å. If the molecular shape is approximated by a triangle, the height of the triangle would be 15.2 Å. The molecules are stacked on top of each other in the direction of the crystallographic c axis with six molecules in one unit cell. Thus, the thickness of the molecule in the crystal is roughly approximated by c/6 = 5.9 Å.

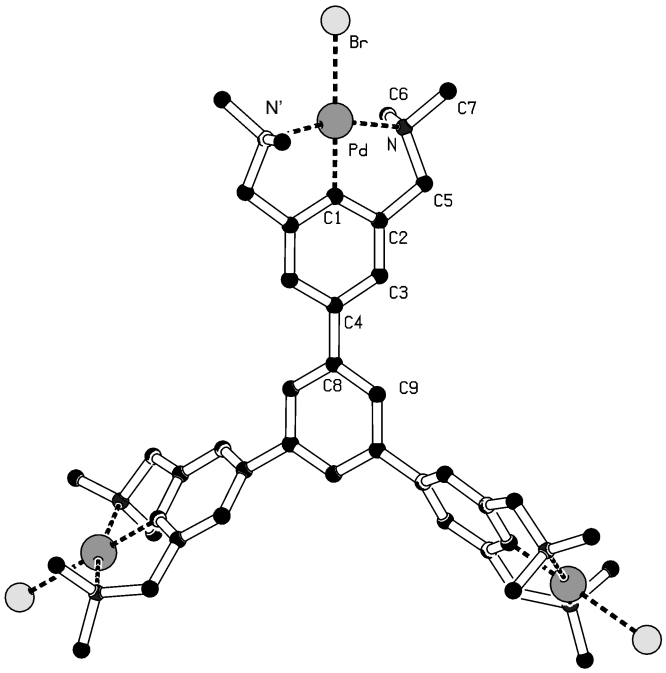

Figure 3. Molecular plot of **19**. Hydrogen atoms and solvent molecules are omitted for clarity. Selected bond lengths, angles and torsion angles: Pd-Br 2.5477(4), Pd-N 2.1053 (22), Pd-C1 1.9195 (31) Å; Br-Pd-N 98.70 (7), Br-Pd-C1 180.0 (2), Br-Pd-N' (98.70(11), N-Pd-C1 81.30(7), N-Pd-N' (162.59(13), C1-Pd-N' (11)°; C3-C4-C8-C9 46.61 (11)°; (Symmetry operations: i 1-y, x-y, z; ii 1-x+y, 1-x, z; iii 1/3+y, -1/3+x, 1/6z; iv 4/3-x, 2/3-x+y, 1/6-z; v 1/3+x-y, 2/3-y, 1/6-z).

The synthesis of the phenylene extended tris(pincer) ligand **25** is outlined in Scheme 4. The synthesis commences with the palladium-catalyzed Suzuki coupling of boronic acid **22** to iodo-pincer **23**,[12] affording substituted acetophenone **24** in 53% yield. In this reaction, the carbon-iodine bond is selectively converted without affecting the carbon-bromine bond.[12] In the next step, a triple condensation reaction of **24** using tetrachlorosilane in dry ethanol resulted in the formation of tris(NCN)-benzene **25** in 70% yield.[10] Palladation of this tris(pincer) ligand is achieved via a three-fold oxidative addition reaction with $Pd(dba)_2$, affording palladated tris(pincer) complex **26** in 72% yield. The trisplatinum(II) compound **27** was obtained in 66% yield by reaction of **25** with $[Pt(p\text{-tol})_2SEt_2]_2$.[11] The neutral trispalladium(II) complex **26** could readily be converted into the corresponding tri-ionic complex **28** by treatment with silver tetrafluoroborate in wet acetone.

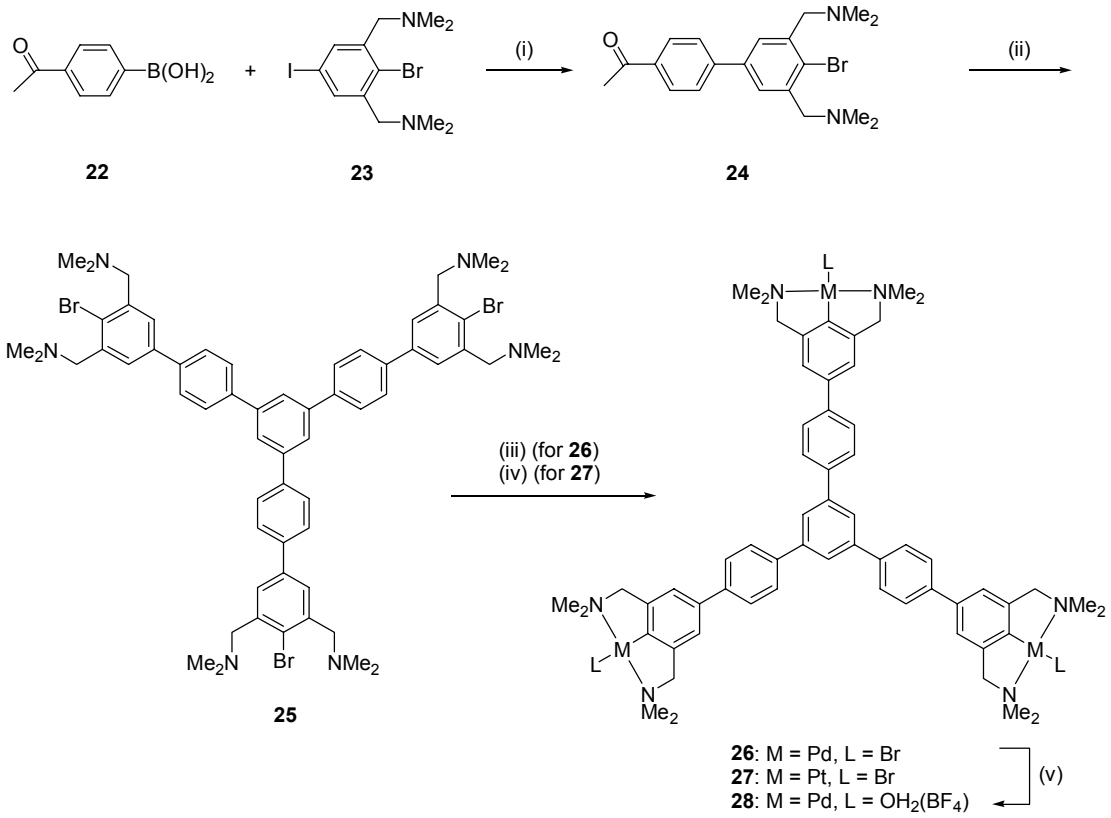

Scheme 4. (i) $Pd(PPh_3)_4$, DME, 2 M Na_2CO_3 (aq), reflux, 18 h; (ii) $SiCl_4$, dry EtOH, reflux, 18 h; (iii) $Pd(dba)_2$, C_6H_6, rt, 18 h; (iv) $[Pt(p\text{-tol})_2SEt_2]_2$, C_6H_6, reflux, 3 h; (v) $AgBF_4$, wet acetone, rt, 1 h.

Synthesis of a bis(NCN-pincer) complex. The bis(NCN-Pt^{II}) complex **33** was prepared in four steps as depicted in Scheme 5. In the first step, bromopincer ligand **29** was, via a lithiation / boronation step, converted into boronic acid **30**, which was subsequently reacted with 1,4-diiodobenzene under Suzuki-coupling conditions to yield bis(pincer)benzene **31**. Via a double lithiation / iodination step, iodine was introduced resulting in the formation of ligand precursor **32** in 63% yield. Treatment of **32** with 2 equivalents of $[Pt(p\text{-tol})_2SEt_2]_2$ gave the corresponding bis(pincer-platinum(II)) complex **33** in 60% yield.

The shape-persistent multimetallic complexes synthesized in this Chapter have been further explored in the field of homogeneous catalysis and were used to study the influence of shape-persistence and geometry of macromolecular catalysts on their retention rates by nanofiltration membranes.

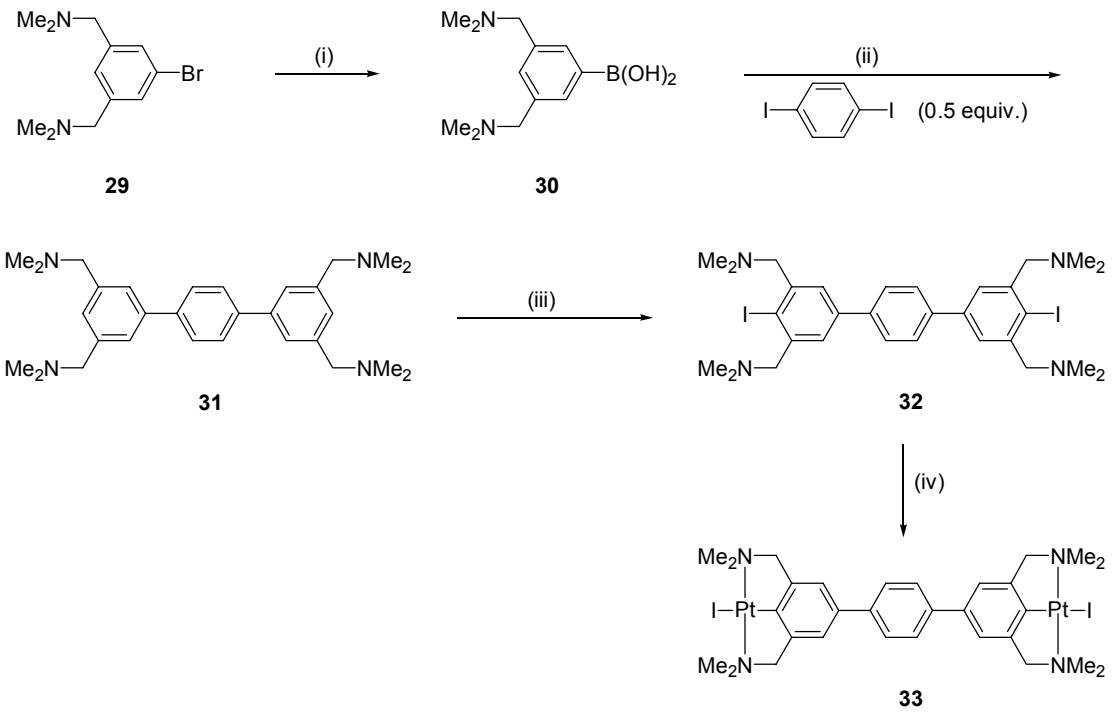

Scheme 5. (i) *t*-BuLi (2 equiv), Et_2O, −78 °C, 10 min followed by $B(O\textit{i}Pr)_3$, −78 °C → rt, 18 h followed by NH_4OH (aq), rt, 15 min; (ii) $Pd(PPh_3)_4$, Na_2CO_3, DME, 90 ºC, 48 h; (iii) *n*-BuLi (2 equiv), hexanes, rt, 18 h, followed by I_2, THF, rt, 1 h; (iv) $[Pt(p\text{-}tol)_2SEt_2]_2$, C_6H_6, 55 °C, 3 h.

2.3. Concluding Remarks

Convenient synthetic routes have been developed for the synthesis of novel, shape-persistent, nanosize organometallic materials based on an aromatic backbone. The aromatic backbone of these materials assures a high rigidity, which is considered to be important for obtaining a high retention when these multimetallic nanosize complexes are applied as homogeneous catalysts in a nanofiltration membrane reactor. Hexakis(pincer) complexes **11**–**16**, tris(NCN-pincer) complexes **19**–**21**, extended tris(NCN-pincer) complexes **26**–**28** and bis(NCN-pincer) complex **33** were prepared in good yields and were, except for **11** and **12**, analytically fully characterized. According to NMR spectroscopy, pure hexakis(PCP-Pd^{II}) complex **12** was prepared and isolated, however, no exact elemental analysis could be obtained. In attempts to prepare hexakis(NCN-Pd^{II}) complex **11** using a lithiation/transmetalation procedure, unfortunately only incomplete metalation (~70%) could be achieved as was indicated by ^{1}H NMR spectroscopy. Important to note is that all multisite ligands

discussed in this chapter were prepared prior to the final palladation/platination reaction step. This approach has the advantage that a limited number of reactions has to be performed with the multimetallic material, thereby minimalizing the chance of destruction of individual organometallic moieties. On the other hand, it also means that in the final step a relatively large number of metal centers has to be introduced into the multisite ligand in a one-pot reaction, which can lead to incomplete metalation, as was observed for the preparation of **11**.

The molecular structure of **13** shows a cartwheel-like structure with a C_3 molecular symmetry and a diametrically opposed Cl-Cl distance of 20.089(11) Å. The X-ray crystal structure of **19** represents a propeller-like structure with a D_3 molecular symmetry and with a Br-Br distance of 17.4573(4) Å. These structures nicely illustrate the nanosize dimensions of these materials, which, due to their shape-persistent backbones, are retained in solution, making these systems very promising for recycling procedures using nanofiltration membranes.

2.4. Experimental Section

General: All reactions were carried out using standard Schlenk techniques under an inert nitrogen atmosphere unless stated otherwise. Et_2O, THF and hexanes were carefully dried and distilled from Na/benzophenone prior to use. CH_2Cl_2 was distilled from CaH_2. All standard reagents were purchased. Compounds **17**,[9] **23**,[12] **29**,[13] $Pd(dba)_2$[14] and $[Pt(p\text{-tol})_2SEt_2]_2$[11] were prepared according to literature procedures. ^1H (200 or 300 MHz) and ^{13}C (50 or 75 MHz) NMR spectra were recorded on a Varian AC200 or Varian 300 MHz spectrometer at 25 °C, chemical shifts are in ppm referenced to residual solvent resonances. MALDI-TOF-MS spectra were acquired using a Voyager-DE Bio-Spectrometry Workstation mass spectrometer equipped with a nitrogen laser emitting at 337 nm. The matrix (3,5-dihydroxybenzoic acid) and the sample were dissolved in THF or CH_2Cl_2 (~30 mg/ml) and 0.2 µl of both solutions were mixed and placed on a gold MALDI target and analyzed after evaporation of the solvent. Elemental microanalyses were performed by Dornis und Kolbe, Mikroanalytisches Laboratorium, Müllheim a.d. Ruhr, Germany.

Synthesis of 3,5-dimethyliodobenzene (1): A solution of $NaNO_2$ (30.0 g, 435 mmol) in H_2O (100 mL) was added dropwise over a period of 15 min to a solution of 3,5-dimethylaniline (50.0 g, 413 mmol) in aqueous H_2SO_4 (650 mL, 4.5 M) at –10 ˚C. The resulting reaction mixture was stirred at –10 ˚C for an additional 15 min, after

which a solution of KI (80 g, 482 mmol) in H_2O (100 mL) was slowly added over a period of 5 min, while maintaining the temperature at –10 ˚C. The mixture was warmed and allowed to stir for two hours each at 0 ˚C, 20 ˚C and 90 ˚C. The resulting dark-brown reaction mixture was cooled to room temperature and subsequently extracted with Et_2O (3 × 200 mL). The combined organic extracts were washed successively with aqueous Na_2SO_3 (100 mL, 1 M), aqueous NaOH (100 mL, 4 M) and brine (100 mL) and were then dried with K_2CO_3. After filtration, the filtrate was reduced *in vacuo* to leave a brown oily residue. This residue was flame-distilled from solid KOH (10 g) to afford $C_6H_3I(Me)_2$-3,5, **1**, as a light orange oil. Yield: 67.1 g (70%). ^{1}H NMR (C_6D_6, 200 MHz): δ 7.18 (s, 2H, Ar*H*), 6.57 (s, 1H, Ar*H*), 1.90 (s, 6H, C*H*$_3$). ^{13}C NMR (C_6D_6, 50 MHz): δ 140.0, 135.4, 129.6, 94.9, 21.0.

Synthesis of 3,5-bis(bromomethyl)iodobenzene (2): $C_6H_3IMe_2$-3,5, **1** (55.0 g, 237 mmol), *N*-bromosuccinimide (95.0 g, 534 mmol) and AIBN (azo-bisisobutyronitrile) (2.63 g, 16 mmol) were mixed in methyl acetate (400 mL). This mixture was photolytically heated by irradiation of the flask with a 100 W IR bulb to reflux for 12 h (no additional heating source was used). The reaction mixture was then allowed to cool to room temperature, followed by evaporation of the volatiles. This resulted in the formation of a solid residue which was washed with cold hexanes (0 ˚C, 2 × 200 mL) and subsequently extracted with boiling hexanes (4 × 400 mL). The combined hexanes extract was heated to reflux to redissolve all solids, and the solution was allowed to cool to room temperature over a period of 4 h. Crystals of pure **2** that had formed during this time were collected by filtration, washed with cold hexanes (0 ˚C, 2 × 200 mL) and dried *in vacuo*. Yield: 43.5 g (47%), mp 110–113 ˚C (Lit:[5] 112–114 ˚C). ^{1}H NMR ($CDCl_3$, 200 MHz): δ 7.67 (s, 2H, Ar*H*), 7.38 (s, 1H, Ar*H*), 4.38 (s, 4H, C*H*$_2$). ^{13}C NMR ($CDCl_3$, 50 MHz): δ 140.3, 137.8, 129.0, 94.4, 31.4.

Synthesis of 3,5-bis(methoxymethyl)iodobenzene (3): Synthesis as described by Duchêne and Vögtle[5] using **2** (75.9 g, 194 mmol) as the starting material. Yield: 54.0 g (95%). ^{1}H NMR ($CDCl_3$, 200 MHz): δ 7.58 (s, 2H, Ar*H*), 7.22 (s, 1H, Ar*H*), 4.35 (s, 4H, C*H*$_2$), 3.35 (s, 6H, OC*H*$_3$). ^{13}C NMR ($CDCl_3$, 50 MHz): δ 140.7, 135.6, 125.8, 94.5, 73.6, 58.4.

Synthesis of bis[3,5-bis(methoxymethyl)phenyl]acetylene (4): Solid $[PdCl_2(PPh_3)_2]$ (2.60 g, 3.7 mmol) and CuI (0.35 g, 1.85 mmol) were added to a stirring solution of 3,5-bis(methoxymethyl)iodobenzene (**3**) (54.0 g, 185 mmol) in Et_2NH (500 mL) at room temperature in a 1 L round bottomed Schlenk tube. After stirring of the reagents, a slow stream of acetylene was passed through the stirred solution for 16 h at room temperature. The color of the reaction mixture gradually turned to dark red and after 16 h a two-phase system had formed. After *in vacuo* evaporation of the volatiles, the residue was extracted with hexanes (2 × 200 mL) and the combined organic extracts were stored at –25 ˚C for 24 h. The precipitated white solid which formed during this time was filtered off, washed with cold hexanes (–25 ˚C, 100 mL) and dried *in vacuo* to afford **4** as a white solid. Yield: 29.5 g (90%), mp 37–39 ˚C (Lit. 38 - 41 ˚C)[5]. ^{1}H NMR ($CDCl_3$, 200 MHz): δ 7.42 (s, 4H, Ar*H*), 7.28 (s, 2H, Ar*H*), 4.44 (s, 8H, CH_2), 3.39 (s, 12H, OCH_3). ^{13}C NMR ($CDCl_3$, 50 MHz): δ 136.6, 129.9, 126.7, 123.4, 89.3, 74.1, 58.3.

Synthesis of hexakis[3,5-bis(methoxymethyl)phenyl]benzene (5): Synthesis as described by Duchêne and Vögtle[5] using **4** (27.3 g, 77.0 mmol) and $[PdCl_2(NCPh)_2]$ (12.1 g, 47.3 mmol) in benzene (150 mL). The work-up was performed as follows: after evaporation of the volatiles, the solid residue was extracted with boiling hexanes (3 × 250 mL). The combined hexane extract was allowed to cool to room temperature over a period of 4 h after which pure **5** had separated from the solution as colorless crystals, which were collected by filtration, washed with hexanes (2 × 100 mL) and dried *in vacuo*. Yield: 16.4 g (60%). ^{1}H NMR ($CDCl_3$, 200 MHz): δ 6.70 (s, 12H, Ar*H*), 6.61 (s, 6H, Ar*H*), 3.99 (s, 24H, CH_2), 2.83 (s, 36H, OCH_3). ^{13}C NMR ($CDCl_3$, 50 MHz): δ 140.4, 139.6, 136.6, 130.0, 124.3, 73.8, 56.8.

Synthesis of hexakis[3,5-bis(bromomethyl)phenyl]benzene (6): Synthesis as described by Duchêne and Vögtle[5] using **5** (16.4 g, 15.4 mmol), $BF_3{\cdot}Et_2O$ (80 mL, 635 mmol) and acetyl bromide (55 mL, 740 mmol) in CH_2Cl_2 (1200 mL). The work-up was performed as follows: the reaction mixture was cooled with an ice bath and aqueous Na_2CO_3 (25%, 400 mL) was slowly added. After complete addition the mixture was stirred for 15 min at room temperature. The CH_2Cl_2 layer was then collected, dried with $MgSO_4$, filtered and concentrated to *ca.* 300 mL. Hexane was slowly added to the resulting solution, resulting in the separation of pure hexasubstituted benzene **6** as white crystals. The crystals were collected by filtration,

washed with hexanes (2 × 100 mL) and dried *in vacuo*. Yield: 23.5 g (93%). ^{1}H NMR ($CDCl_3$, 200 MHz): δ 6.90 (s, 6H, Ar*H*), 6.83 (s, 12H, Ar*H*), 4.17 (s, 24H, CH_2). ^{13}C NMR ($CDCl_3$, 50 MHz): δ 140.4, 139.4, 137.6, 131.9, 127.1, 32.9.

Synthesis of hexakis{3,5-bis[(dimethylamino)methyl]phenyl}benzene (7): Neat $HNMe_2$ (10 mL, 150 mmol) was added in one portion to a solution of **6** (1.65 g, 1.00 mmol) in CH_2Cl_2 (100 mL) at 0 ˚C. The reaction mixture was allowed to warm to room temperature over a period of 1 h and was stirred for an additional 3 h. Aqueous NaOH (40 mL, 4 M, 160 mmol) was then added, the CH_2Cl_2 layer was collected and the water layer was extracted with Et_2O (4 × 50 mL). The combined organic fraction was washed with saturated aqueous NaCl (50 mL), dried with $MgSO_4$ and filtered. Evaporation of the filtrate *in vacuo* afforded crude **7** as a pale yellow solid, mp 51–54 ºC. Pure **7** was obtained by recrystallization of the corresponding HBF_4 salt, $[C_6\{C_6H_3(CH_2N(H)Me_2)_2\text{-}3,5\}_6](BF_4)_{12}$, **7'**, which was prepared by addition of aqueous HBF_4 (35%, excess) to a solution of crude **7** in H_2O (20 mL). Addition of MeOH (150 mL) followed by warming of the mixture to *ca.* 60 ˚C afforded a clear solution, from which upon cooling to room temperature analytically pure white crystals (mp 161–163 ˚C) of the dodecakis(tetrafluoroborate) salt **7'** separated. The crystals were filtered off, washed with MeOH (2 × 30 mL) and dried *in vacuo*. Dissolving crystalline **7'** in H_2O afforded a clear solution which was neutralized with aqueous NaOH (2 M, excess), followed by extraction of the desired product **7** with CH_2Cl_2 (3 × 60 mL). The combined CH_2Cl_2 extracts were dried with $MgSO_4$, filtered and evaporated *in vacuo* to afford pure **7**. Yield: 0.96 g (79%). Analytical data for **7:** ^{1}H NMR (C_6D_6, 200 MHz): δ 6.97 (s, 6H, Ar*H*), 6.94 (s, 12H, Ar*H*), 3.10 (s, 24H, CH_2), 1.98 (s, 72H, CH_3). ^{13}C NMR (C_6D_6, 50 MHz): δ 141.3, 140.5, 137.9, 131.5, 126.9, 64.5, 45.4. Analytical data for **7'**: ^{1}H NMR (D_2O, 300 MHz): δ 7.37 (s, 12H, Ar*H*), 7.17 (s, 6H, Ar*H*), 4.05 (s, 24H, CH_2), 2.46 (s, 72H, NCH_3). ^{13}C NMR (D_2O, 75 MHz): δ 141.8, 138.7, 134.9, 130.9, 130.6, 59.1, 41.9. Anal. Calcd for $C_{78}H_{126}B_{12}F_{48}N_{12}$, **7'**: C, 41.21; H, 5.59; N, 7.39. Found: C, 41.19; H, 5.55; N, 7.35.

Synthesis of hexakis{3,5-bis[(diphenylphosphino)methyl]phenyl}benzene (8): *n*-BuLi (3.62 mL, 5.79 mmol) was added to $HPPh_2{\cdot}BH_3$ (1.08 g, 5.40 mmol) in THF (30 mL) at −70 °C. The temperature was allowed to rise to room temperature and stirring was continued for 2 h. Next, this solution was added to a solution of **6** (0.50 g, 0.30 mmol) in THF (30 mL) at –40 °C. The temperature was allowed to rise to room

temperature and was stirred for another 18 h. All volatiles were evaporated, CH_2Cl_2 (75 mL) was added and this mixture was washed with H_2O (3 × 50 mL) and dried over $MgSO_4$. The CH_2Cl_2 was evaporated and the white solid was washed with hot EtOH (2 × 50 mL), and hexanes (3 × 50 mL), and dried *in vacuo*, to give **8**·$(BH_3)_{12}$ as a white air-stable powder. Yield: 0.87 g (94%). ^{1}H NMR (toluene-d_8, 300 MHz): δ 8.17 (pseudo t, $^3J_{H,H}$ and $^3J_{P,H}$ = 9 Hz, 24H, PAr*H*-*o*), 7.87 (pseudo t, $^3J_{H,H}$ and $^3J_{P,H}$ = 9 Hz, 24H, PArH-*o*), 7.42–7.15 (m, 72H, Ar*H*), 6.55 (s, 12H, Ar*H*), 6.21 (s, 6H, Ar*H*), 4.07 and 3.39 (pseudo t, ABX, $^2J_{H,H}$ and $^2J_{P,H}$ = 12.5 Hz, 24H, CH_2), 1.61 (br s, 36H, BH_3). ^{13}C NMR ($CDCl_3$, 75 MHz): δ 32.38 (d, $^1J_{P,C}$ = 34.0 Hz), 128.4–140.5 (9 different Ar-C). ^{31}P NMR ($CDCl_3$, 121 MHz): δ 17.78. Anal. Calcd for $C_{198}H_{198}P_{12}B_{12}$: C, 77.23; H, 6.48; P, 12.07; B, 4.21. Found: C, 77.17; H, 6.64; P, 11.95; B, 4.16.

Removal of BH_3: HBF_4·OEt_2 (1.98 mL, 6.60 mmol) was added dropwise to a solution of **8**·$(BH_3)_{12}$ (0.31 g, 0.10 mmol) in CH_2Cl_2 (25 mL) at 0–5 °C. The temperature was allowed to rise to room temperature and stirring was continued for 2 h. Next, a saturated $NaHCO_3$ (aq) solution (50 mL) was added dropwise at 0 °C, resulting in considerable gas evolution. After complete addition the reaction mixture was stirred for 1 h at room temperature. The organic layer was collected and the water layer was washed with CH_2Cl_2 (2 × 25 mL) and the combined organic layer was dried ($MgSO_4$). After evaporation of all volatiles, **8** was obtained as a white solid in quantitative yield. This product was used without further purification. ^{1}H NMR (C_6D_6, 200 MHz): δ 7.29–6.94 (m, 72H), 6.13 (s, 6H), 3.21 (br s, 24H). ^{13}C NMR (C_6D_6, 50 MHz): δ 139.6 (d, $^1J_{P,C}$ = 11.3 Hz), 136.4, 133.2 (d, $^2J_{P,C}$ = 12.1 Hz), 128.4, 128.3, 128.2, 127.9, 127.6, 36.3. ^{31}P NMR (C_6D_6, 54 MHz): δ = –7.95 (s).

Synthesis of hexakis{3,5-bis[(phenylsulfido)methyl]phenyl}benzene (9): Thiophenol (2.5 mL, 24.4 mmol) was added in one portion to a solution of **6** (1.65 g, 1.00 mmol) in degassed DMF (50 mL) under nitrogen at room temperature. Solid K_2CO_3 (7.9 g, 50 mmol) was added and the resulting mixture was stirred for 18 h at 50 ˚C. The volatiles were evaporated *in vacuo* and the residue was extracted with CH_2Cl_2 (3 × 50 mL). The combined organic fraction was washed with brine (50 mL), dried with $MgSO_4$ and filtered. Evaporation of the filtrate *in vacuo* afforded crude **9** as a pale yellow waxy solid. The hexasubstituted benzene **9** was purified by slow diffusion of pentane into a concentrated solution of crude **9** in CH_2Cl_2. This resulted in the formation of off-white crystals which were collected by filtration, washed with

pentane (50 mL) and dried *in vacuo*. Yield: 1.66 g (83%). ^{1}H NMR ($CDCl_3$, 300 MHz): δ 7.22–7.10 (m, 60H, Ar-H), 6.96 (s, 12H, Ar-H), 6.64 (s, 6H, Ar-H), 3.67 (s, 24H, CH_2). ^{13}C NMR ($CDCl_3$, 75 MHz): δ 146.1, 140.9, 139.8, 137.2, 136.0, 130.8, 128.8, 126.9, 125.9, 38.4. MALDI-TOF-MS *m/z*: 1999.78 ($[M]^+$, Calcd 2000.97), 1891.49 ($[M\text{-}SPh]^+$, calcd 1891.80), 1781.47 ($[M\text{-}2{\cdot}SPh]^+$, calcd 1782.63). Anal. Calcd for $C_{126}H_{102}S_{12}$: C, 75.63; H, 5.14; S, 19.23. Found: C, 75.85; H, 5.29; S, 19.23.

Synthesis of hexakis{3,5-bis[(pyrazol-1-yl)methyl]phenyl}benzene (10): To a stirred suspension of finely cut potassium (0.16 g, 4.18 mmol) in dry THF (40 mL) was added pyrazole (0.30 g, 4.36 mmol). The mixture was heated to reflux and maintained at this temperature until the beads of molten potassium were no longer evident (± 1 h). The resulting white suspension was cooled to ambient temperature and **6** (0.50 g, 0.30 mmol) was added in one portion. The reaction mixture was heated at reflux for 15 h, then quenched by addition of H_2O (0.1 mL), filtered and the solvent was removed *in vacuo*. The product was dissolved in CH_2Cl_2 (20 mL), the mixture was filtered, and the filtrate reduced to ~ 1 mL. The product precipitated as a white solid on addition of Et_2O and was finally crystallized from CH_2Cl_2 / Et_2O, giving **10** as small white crystals. Yield: 0.40 g (89%). ^{1}H NMR ($CDCl_3$, 300 MHz): δ 7.46 (d, 12H, $^{3}J_{H,H}$ = 1.80 Hz, pz*H*3), 6.80 (d, 12H, $^{3}J_{H,H}$ = 2.10, pz*H*5), 6.65 (s, 6H, Ar*H*), 6.38 (s, 12H, Ar*H*), 6.15 (t, 12H, pz*H*4), 4.84 (s, 24H, CH_2). ^{13}C NMR ($CDCl_3$, 75 MHz): δ 140.46, 139.28, 135.97, 130.05, 128.95, 125.20, 105 78, 55.09. Anal. Calcd for $C_{90}H_{78}N_{24}$: C, 72.27; H, 5.26; N, 22.47. Found: C, 72.35, H, 5.82; N, 22.36.

Synthesis of hexakis{4-(chloropalladio)-3,5-bis[(diphenylphosphino)methyl]-phenyl}benzene (12): $[Pd(NCMe)_4](BF_4)_2$ (0.16 g, 0.38 mmol) dissolved in degassed MeCN (5 mL) was added to a suspension of **8** (0.18 g, 63 μmol) in degassed MeCN (15 mL), immediately resulting in a yellow solution. This mixture was heated at reflux for 110 h and then cooled to room temperature. The mixture was filtered over Celite, washed with MeCN (20 mL), and the filtrate was concentrated to ~5 mL. Subsequently, Et_2O (10 mL) was added, resulting in a yellow precipitate, which was collected, washed with Et_2O (2 × 15 mL) and dried *in vacuo*. Yield: 0.25 g. The yellow solid was dissolved in acetone (15 mL) and LiCl (54 mg, 1.26 mmol) dissolved in H_2O (1 mL) was added. This mixture was stirred for 1 h at room temperature, resulting in the precipitation of a yellow solid. This solid was collected, washed with H_2O (2 × 15 mL), with acetone (3 × 20 mL), with Et_2O (3 × 20 mL) and

dried *in vacuo*, affording a brownish solid. Yield: 0.21 g (89%). ^{1}H NMR ($CDCl_3$, 200 MHz): δ 7.90–6.97 (br m, 120H, Ar*H*), 6.45 (br s, 12H, Ar*H*), 3.16 (br s, 24H, C*H*$_2$). ^{13}C NMR ($CDCl_3$, 75 MHz): δ 146.1–128.5 (9 different Ar-C), 41.7. ^{31}P NMR ($CDCl_3$, 81 MHz): δ 34.29.

Synthesis of hexakis{4-(chloropalladio)-3,5-bis[(phenylsulfido)methyl]phenyl}-benzene (13): A solution of $[Pd(NCMe)_4](BF_4)_2$ (1.41 g, 3.2 mmol) in degassed MeCN (10 mL) was added over a period of 2 min to a solution of the hexasubstituted benzene $C_6\{C_6H_3(CH_2SPh)_2\text{-}3,5\}_6$, **9**, (1.0 g, 0.50 mmol) in degassed MeCN (40 mL). A red/brown solution formed immediately and was heated at reflux for 3 h. The resulting solution was evaporated to ~ 15 mL and Et_2O (50 mL) was slowly added. This resulted in the precipitation of $[C_6(\{Pd(NCMe)\}C_6H_2(CH_2SPh)_2\text{-}3,5)_6](BF_4)_6$ as a pale yellow solid which was collected, washed with Et_2O and dried *in vacuo*. Yield: 1.56 g. Subsequently, this solid was dissolved in MeCN (80 mL) and LiCl (large excess) was added in one portion. This resulted in a suspension which was stirred for an additional 1 h. Subsequently, the solid material was filtered off and washed with H_2O (100 mL) and Et_2O (2 × 100 mL), giving a yellow solid. This solid was dissolved in DMSO (80 mL), and THF (140 mL) was added, resulting in a white precipitate. This procedure was repeated three times, the solid was collected, and dried *in vacuo*, affording **13** as a light yellow solid. Yield: 1.28 g (90%). Yellow crystals suitable for X-ray analysis were obtained by suspension of **13** in toluene, addition of CH_2Cl_2 until all solids were dissolved, followed by slow evaporation of the solvent in air. ^{1}H NMR (DMSO-d_6, 200 MHz): δ 7.60-7.56 (m, 24H, Ar*H*), 7.44–7.31 (m, 36H, Ar*H*), 6.33 (s, 12H, Ar*H*), 4.20 (br s, 24H, C*H*$_2$). ^{13}C NMR (DMSO-d_6, 50 MHz): δ 161.06, 148.22, 139.38, 136.80, 132.09, 130.60, 130.28, 130.20, 125.65, 49.76. MALDI-TOF-MS *m/z* 2811.52 ($[M–Cl]^+$, calcd 2810.71). Anal. Calcd for $C_{126}H_{96}Cl_6Pd_6S_{12}$: C, 53.26; H, 3.48; S, 13.37. Found: C, 53.17; H, 3.40; S, 13.52.

Synthesis of hexakis{4-(acetatopalladio)-3,5-bis[(pyrazol-1-yl)methyl]phenyl}-benzene (14): A solution of $Pd(OAc)_2$ (0.34 g, 1.53 mmol) and **10** (0.36 g, 0.24 mmol) in AcOH (20 mL) was heated to 120 °C and maintained at this temperature for 15 h. The resulting brown solution was allowed to cool to ambient temperature. Dropwise addition of Et_2O eventually produced a precipitate. The mixture was centrifuged and the solution decanted. Et_2O was added a second time until a precipitate formed and the mixture was again centrifuged and decanted. Et_2O (100 mL) was added to the resulting pale brown solution and the product precipitated as a

tan solid. The solution was decanted and the product immediately washed with Et_2O (2 × 50 mL) and dried *in vacuo*, affording **14** as an off-white solid. Yield: 0.32 g (53%). ^{1}H NMR ($CDCl_3$, 300 MHz): δ 7.86 (br s, 12H, pz*H*), 7.15 (br s, 12H, pz*H*), 6.49 (br s, 12H, pz*H*), 6.12 (s, 12H, Ar*H*), 4.54 (br s, 24H, CH_2), 2.02 (s, 18H, C(O)CH_3). ^{13}C NMR ($CDCl_3$, 75 MHz): δ 142.28, 135.10, 130.92, 129.14, 107.30, 57.81. Anal. Calcd for $C_{102}H_{90}N_{24}O_{12}Pd_6$: C, 49.35; H, 3.65; N, 13.54. Found: C, 49.09; H, 3.75; N, 13.38.

Synthesis of hexakis{4-(chloropalladio)-3,5-bis[(pyrazol-1-yl)methyl]phenyl}-benzene (15): A solution of **14** (0.10 g, 40 μmol) was prepared by dissolution of the complex in acetone (30 mL) and addition of H_2O (3 mL). LiCl (17 mg, 0.4 mmol) was added to this solution and the mixture was left stirring at ambient temperature for 15 h. After this time a brown precipitate had formed, the mixture was centrifuged and the solution decanted. The solid residue was washed with H_2O (50 mL), acetone (50 mL) and Et_2O (50 mL) and then dried *in vacuo*, giving **15** as a brown solid. Yield: 70 mg (74%). Because the product was insoluble in common organic solvents, no NMR data was obtained and the product was derivatized as the corresponding aqua complex **16**.

Synthesis of hexakis{4-(aquapalladio)-3,5-bis[(pyrazol-1-yl)methyl]-phenyl}-benzene hexakis(tetrafluoroborate) (16): A solution of $AgBF_4$ (82 mg, 0.42 mmol) in H_2O (0.5 mL) was added to a stirring suspension of **15** (0.16 g, 70 μmol) in acetone (50 mL). The solution was stirred in the absence of light for 3 h. The solvent was removed *in vacuo* and the residue was extracted with acetone (50 mL) and the product **16** was precipitated as a white/tan powder on addition of Et_2O. Yield: 0.17 g (89%). ^{1}H NMR (acetone-d_6, 300 MHz): δ 8.10 (d, $^3J_{H,H}$ = 2.10 Hz, 12H, pz*H*), 7.53 (s, 12H, pz*H*), 6.81 (s, 12H, Ar*H*), 6.49 (t, 12H, pz*H*), 5.18 (s, 24H, CH_2). ^{13}C NMR (acetone-d_6, 75 MHz): δ 141.34, 137.59, 132.94, 129.19, 107.01, 56.52. Anal. Calcd for $C_{90}H_{84}B_6F_{24}N_{24}O_6Pd_6$: C, 39.21; H, 3.07; N, 12.19. Found: C, 39.06; H, 3.17; N, 12.11.

Synthesis of 1,3,5-tris{4-bromo-3,5-bis[(dimethylamino)methyl]phenyl}benzene (18): A modification of a literature procedure was used.[10] To a stirred solution of 4-bromo-3,5-bis[(dimethylamino)methyl]acetophenone (**17**) (1.3 g, 8.7 mmol) in dry

ethanol (20 mL), tetrachlorosilane (5.0 mL, 43.6 mmol) was added at 0 °C. The reaction mixture was heated to reflux and kept at that temperature for 18 h. The reaction mixture (a white suspension) was cooled to room temperature and aqueous HCl (25 mL, 4 M) was added, resulting in a brown solution. This layer was washed with CH_2Cl_2 (2 × 50 mL) and a NaOH solution (4 M) was added until a pH of 13-14 was reached. Next, the aqueous layer was extracted with CH_2Cl_2 (3 × 50 mL) and the combined organic fractions were dried over $MgSO_4$. All volatiles were evaporated *in vacuo* affording a white sponge. The product was purified by recrystallization from hexane at –30 °C. Yield: 0.79 g (70%). ^{1}H NMR ($CDCl_3$, 200 MHz): δ 7.78 (s, 3H, Ar*H*), 7.67 (s, 6H, Ar*H*), 3.66 (s, 12H, CH_2), 2.35 (s, 26H, CH_3). ^{13}C NMR ($CDCl_3$, 75 MHz): δ 141.9, 140.0, 139.5, 128.7, 126.8, 125.9, 64.4, 46.0. MALDI-TOF-MS *m/z* 884.7 ([M+H]$^+$, calcd 883.2). Anal. Calcd for $C_{42}H_{57}Br_3N_6$: C, 56.96; H, 6.49; N, 9.49. Found: C, 56.82; H, 6.56; N, 9.44.

Synthesis of 1,3,5-tris{4-(bromopalladio)-3,5-bis[(dimethylamino)methyl]-phenyl}benzene (19): Ligand **18** (0.65 g, 0.73 mmol) and $Pd(dba)_2$ (1.39 g, 2.40 mmol) were dissolved in benzene (100 mL) and stirred at room temperature for 18 h. All volatiles were evaporated *in vacuo*, THF (100 mL) was added, and stirring was continued for 1 h, affording a black precipitate. The mixture was filtered through Celite and the filtrate was evaporated to dryness. The remaining solid was dissolved in CH_2Cl_2 (10 mL) and Et_2O (50 mL) was added, yielding a yellow solid. This procedure was repeated three times, resulting in a light yellow solid. Yield: 0.63 g (72%). Analytically pure light-brown crystals of **19** were obtained by slow diffusion of Et_2O into a concentrated solution of the product in CH_2Cl_2. ^{1}H NMR ($CDCl_3$, 200 MHz): δ 7.53 (s, 3H, Ar*H*), 7.06 (s, 6H, Ar*H*), 4.06 (s, 12H, CH_2), 3.01, (s, 36H, CH_3). ^{13}C NMR ($CDCl_3$, 75 MHz): δ 157.4, 145.8, 142.9, 138.4, 124.6, 119.1, 74.8, 54.1. MALDI-TOF-MS *m/z* 1128.6 ([M–Br]$^+$, calcd 1128.0). Anal. Calcd for $C_{42}H_{57}Br_3N_6Pd_3$: C, 41.87; H, 4.77; N, 6.97. Found: C, 42.03; H, 4.72; N, 6.88.

Synthesis of 1,3,5-tris{4-(bromoplatino)-3,5-bis[(dimethylamino)methyl]-phenyl}benzene (20): Ligand **18** (0.60 g, 0.69 mmol) and $[Pt(p\text{-tol})_2SEt_2]_2$ were mixed in benzene (50 mL) and this mixture was refluxed for 3 h, resulting in a yellow precipitate. The reaction mixture was cooled to room temperature and all volatiles were evaporated. Next, the yellow solid was extracted with CH_2Cl_2 (20 mL) and Et_2O was added, yielding a yellow precipitate. This yellow solid was collected and washed

with Et_2O (3 × 20 mL) and dried *in vacuo*. Yield: 0.74 g (73%). ^{1}H NMR ($CDCl_3$, 200 MHz): δ 7.59 (s, 3H, Ar*H*), 7.11 (s, 6H, Ar*H*), 4.09 (s, $^3J_{Pt,H}$ = 22.0 Hz, 12H, CH_2), 3.16 (s, $^3J_{Pt,H}$ = 18.0 Hz, 36H, CH_3). ^{13}C NMR ($CDCl_3$, 50 MHz): δ 146.32, 144.13, 143.56, 137.24, 123.91, 118.79, 77.72, 55.93. Anal. Calcd for $C_{42}H_{57}Br_3N_6Pt_3$: C, 34.29; H, 3.91; N, 5.71. Found: C, 34.38; H, 3.82; N, 5.66.

Synthesis of 1,3,5-tris{4-(aquapalladio)-3,5-bis[(dimethylamino)methyl]phenyl}-benzene tris(tetrafluoroborate) (21): To a solution of **19** in wet acetone (20 mL) was added $AgBF_4$ (0.20 g, 1.0 mmol) in water (1 mL). This mixture was stirred for 30 min at room temperature and then filtered over Celite. The filtrate was concentrated and the product was extracted with acetone (20 mL). Upon slow addition of Et_2O (20 mL) a white precipitate was formed, which was collected and dried *in vacuo*. Yield: 0.26 g (76%). ^{1}H NMR (acetone-d_6, 200 MHz): δ 7.72 (s, 3H, Ar*H*), 7.32 (s, 6H, Ar*H*), 4.23 (s, 12H, CH_2), 2.89 (s, 36H, CH_3). ^{13}C NMR (acetone-d_6, 75 MHz): δ 150.94, 146.28, 142.89, 138.79, 124.26, 119.46, 73.62, 51.78. Anal. Calcd for $C_{42}H_{63}B_3F_{12}N_6O_3Pd_3$: C, 39.42; H, 4.96; N, 6.57. Found: C, 39.64; H, 5.20; N, 6.42.

Synthesis of 9-acetyl-3,5-bis(dimethylaminomethyl)-4-bromobiphenyl (24): A degassed solution of 4-acetophenoneboronic acid (**22**) (1.90 g, 11.6 mmol), 4-bromo-3,5-bis(dimethylaminomethyl)iodobenzene **(23**) (2.42 g, 6.1 mmol) and $Pd(PPh_3)_4$ (176.1 mg, 0.15 mmol) in dimethoxyethane (DME) (50 mL) was mixed with a degassed solution of Na_2CO_3 (aq) (2 M, 15 mL). The resulting mixture was heated to reflux for 15 h. After cooling to room temperature all volatiles were evaporated *in vacuo* and CH_2Cl_2 (100 mL) and H_2O (100 mL) were added. The organic layer was collected and the aqueous layer was extracted with CH_2Cl_2 (3 × 100 mL). The organic layers were combined, concentrated to 100 mL and the product was extracted with 1 M HCl (aq) (3 × 100 mL). The acidic aqueous layers were combined and treated with 6 M K_2CO_3 (aq) until pH 10−11 was reached. The product was extracted with CH_2Cl_2 (3 × 100 mL) and the organic fractions were combined, dried over $MgSO_4$, filtered and concentrated *in vacuo*, leaving an yellow oil which solidified upon standing at room temperature. The product was washed with cold hexanes (−20 ˚C) and dried *in vacuo*. Yield: 1.2 g (53%). ^{1}H NMR (acetone-d_6, 300 MHz): δ 8.12 (d, $^3J_{H,H}$ = 4.2 Hz, 2H, Ar*H*), 7.82 (d, $^3J_{H,H}$ = 4.2 Hz, 2H, Ar*H*), 7.78 (s, 2H, Ar*H*), 3.62 (s, 4H, CH_2), 2.63 (s, 3H, C(O)CH_3), 2.32 (s, 12H, CH_3). ^{13}C NMR (acetone-d_6, 75 MHz): δ 196.8, 144.6, 139.9, 138.5, 136.6, 129.2, 127.9, 127.2, 126.6, 63.2, 45.2, 26.1. Anal. Calcd for $C_{20}H_{26}BrN_2O$: C, 61.70; H, 6.47; N, 7.20. Found: C, 61.58; H, 6.42; N, 7.12.

Synthesis of 1,3,5-tris(4-(4-bromo-3,5-bis(dimethylaminomethyl)phenyl)-phenylene)benzene (25): $SiCl_4$ (5 mL, 43.6 mmol) was added dropwise to a solution of **24** (0.9 g, 2.3 mmol) in dry ethanol (20 mL) at 0 °C. A white precipitate was formed immediately and the solution turned from orange to dark red. The reaction mixture was maintained at reflux for 18 h, whereby the color of the solution changed from dark red to yellow. After cooling to room temperature, HCl (aq) (1 M, 50 mL) was added and stirring was continued for 15 min. The acidic suspension was washed with ether (2 × 50 mL) and treated with 4 M NaOH (aq) until pH 13-14 was reached. The product was extracted with CH_2Cl_2 (4 × 60 ml), dried over $MgSO_4$, filtered and concentrated *in vacuo*, affording a orange/yellow solid. The solid was washed with cold hexane (–20 °C) and dried *in vacuo*. Yield: 0.6 g (70%). ^{1}H NMR (acetone-d_6, 200 MHz): δ 8.06 (s, 3H, Ar*H*), 8.01 (d, $^3J_{H,H}$ = 4.2 Hz, 6H, Ar*H*), 7.85 (d, $^3J_{H,H}$ = 4.2 Hz, 6H, Ar*H*), 7.81 (s, 6H, Ar*H*), 3.63 (s, 12H, CH_2), 2.34 (s, 36H, CH_3). ^{13}C NMR ($CDCl_3$, 75 MHz): δ 142.3, 140.5, 139.7, 139.3, 128.2, 128.0, 127.9, 126.5, 125.3, 64.3, 45.9. Anal. Calcd for $C_{60}H_{69}Br_3N_6$: C, 64.69; H, 6.25; N, 7.54. Found: C, 64.78; H, 6.25; N, 7.46.

Synthesis of 1,3,5-tris(4-(4-(bromopalladio)-3,5-bis(dimethylaminomethyl)-phenyl)phenylene)benzene (26): A solution of **25** (0.25 g, 0.23 mmol) and $Pd(dba)_2$ (0.43 g, 0.74 mmol) in dry benzene (30 mL) was stirred overnight at room temperature. The solvent was removed *in vacuo*, THF (30 mL) was added and stirring was continued for 20 h, affording a black precipitate. The solvent was evaporated and the residue was dissolved in CH_2Cl_2 (15 mL) and filtered through Celite. The filtrate was concentrated and the remaining solid was washed with ether (2 × 15 ml). The crude product was dissolved in CH_2Cl_2 (2 mL) and slow addition of Et_2O (4 mL) resulted in the precipitation of a yellow solid. This last two-step sequence was repeated once. The solid was collected and dried *in vacuo.* Yield: 0.24 g (73%). ^{1}H NMR ($CDCl_3$, 300 MHz): δ 7.87 (s, 3H, Ar*H*), 7.77 (d, $^3J_{H,H}$ = 4.2 Hz, 6H, Ar*H*), 7.63 (d, $^3J_{H,H}$ = 4.2 Hz, 6H, Ar*H*), 7.09 (s, 6H, Ar*H*), 4.10 (s, 12H, CH_2), 3.03 (s, 36H, CH_3). ^{13}C NMR ($CDCl_3$, 75 MHz): δ 157.41, 145.9, 142.2, 141.1, 139.9, 137.9, 127.9, 127.6, 125.1, 118.9, 74.9, 54.1. Anal. Calcd for $C_{60}H_{69}Br_3N_6Pd_3$: C, 50.28; H, 4.86; N, 5.86. Found: C, 50.18; H, 4.74; N, 5.78.

Synthesis of 1,3,5-tris(4-(3,5-bis(dimethylaminomethyl)-4-(bromoplatino)-phenyl)phenylene)benzene (27): Ligand **25** (0.15 g, 0.12 mmol) and $[Pt(p\text{-}tol)_2SEt_2]_2$ (0.18 g, 0.19 mmol) were dissolved in dry benzene (20 mL) and heated at

reflux for 3 h. The reaction mixture was cooled to room temperature and all volatiles were evaporated *in vacuo.* The residue was washed with Et_2O (10 mL) and the remaining solid was dissolved in CH_2Cl_2 (10 mL). The mixture was filtered through Celite and the filtrate was concentrated to 2 mL. Slow addition of Et_2O (3 mL) resulted in the precipitation of a yellow solid. The solid was collected and dried *in vacuo*. Yield: 0.16 g (78%). ^{1}H NMR (CD_2Cl_2, 200 MHz): δ 7.93 (s, Ar*H*), 7.82 and 7.48 (d, AB, $^3J_{H,H}$ = 4.2 Hz, 6H, Ar*H*), 7.17, (s, 6H, Ar*H*), 4.13 (s, $^3J_{Pt,H}$ = 20.6 Hz, 12H, NCH_2), 3.31 (s, $^3J_{Pt,H}$ = 17.2 Hz, 36H, NCH_3). ^{13}C NMR (CD_2Cl_2, 75 MHz): δ 149.6, 144.6, 142.2, 141.8, 139.4, 136.3, 127.9, 127.2, 124.7, 118.4, 77.1, 56.4. Anal. Calcd for $C_{60}H_{69}Br_3N_6Pt_3$: C, 42.41; H, 4.09; N, 4.95. Found: C, 41.99; H, 4.23; N, 4.62.

Synthesis of 1,3,5-tris(4-(4-(aquapalladio)-3,5-bis(dimethylaminomethyl)phenyl)-phenylene)benzene tris(tetrafluoroborate) (28): $AgBF_4$ (45.0 mg, 77.0 μmol) was added to suspension of **26** (0.11 g, 77.2 μmol) in wet acetone (5 mL) and stirred for 30 min. The suspension was filtered through Celite and the solvents were evaporated *in vacuo*. The solid residue was extracted with acetone (5 mL) and the acetone layer was filtered again through Celite. The filtrate was concentrated to 2 mL and slow addition of Et_2O resulted in the precipitation of an off-white solid. The solid was collected and dried *in vacuo.* Yield: 88.5 mg (76%). ^{1}H NMR (acetone-d_6, 200 MHz): δ 8.01 (s, 3H, Ar*H*), 7.97 (d, $^3J_{H,H}$ = 4.4 Hz, 6H, Ar*H*), 7.76 (d, $^3J_{H,H}$ = 4.4 Hz, 6H, Ar*H*), 7.30 (s, 6H, Ar*H*), 4.29 (s, 12H, CH_2), 2.91 (s, 36H, CH_3). ^{13}C NMR (acetone-d_6, 75 MHz): δ 146.3, 142.1, 139.7, 138.2, 127.9, 127.4, 124.6, 119.0, 73.6, 51.8.

Synthesis of 3,5-bis(dimethylaminomethyl)phenylboronic acid (30): To a solution of 3,5-bis(dimethylaminomethyl)bromobenzene (**29**)[13] (2.71 g, 10 mmol) in dry Et_2O (50 ml) at −78 ºC was added *tert*-BuLi (13.0 mL, 19.5 mmol). After stirring for 1 h, B(O*i*Pr)$_3$ (4.48 g, 20 mmol) was added. After complete addition, the temperature was allowed to rise to 25 ºC and stirring was continued overnight. A solution of saturated NH_4OH (aq) (40 mL) was added to the reaction mixture and the organic layer was separated. The aqueous layer was evaporated under reduced pressure to give boronic acid **30** as a white solid. The inorganic salts were removed by column chromatography using silica gel and ethanol/saturated-NH_4OH(aq) (1/1) as the eluent. Yield: 2.10 g (89%). ^{1}H NMR (D_2O, 200 MHz): δ 7.40 (s, 2H, Ar*H*), 7.07 (s, 1H, Ar*H*), 3.52 (s, 4H, CH_2), 2.22 (s, 12H, NCH_3). ^{13}C NMR (CD_3OD, 75 MHz): δ 136.15, 135.95, 132.25, 64.8, 45.05.

Synthesis of 1,4-bis(3,5-(dimethylaminomethyl)phenyl)benzene (31): To a solution of boronic acid derivative **30** (2.48 g, 10.5 mmol) in a degassed mixture of dimethoxyethane (150 ml) and water (80 ml) at room temperature was added 1,4-diiodobenzene (1.65 g, 5 mmol). After 10 min, $Pd(PPh_3)_4$ (0.27 g, 0.5 mmol) and Na_2CO_3 (6.36 g, 60 mmol) were subsequently added. The resulting mixture was stirred at 90 ºC for 48 h. Then, the mixture was cooled to room temperature and HCl (4 M) was added until pH < 2. The aqueous layer was washed with CH_2Cl_2 (3 × 50 mL) and subsequently treated with powdered K_2CO_3 until pH > 12. The basic aqueous layer was extracted with CH_2Cl_2 (2 × 100 ml) and the organic layer was dried over $MgSO_4$, and concentrated to give pure **31** as a yellow solid. Yield: 4.50 g (98%). Mp 112 – 114 ºC. ^{1}H NMR ($CDCl_3$, 200 MHz): δ 7.68 (s, 4H, Ar*H*), 7.49 (s, 4H, Ar*H*), 7.24 (s, 2H, Ar*H*), 3.49 (s, 8H, CH_2), 2.26 (s, 24H, NCH_3). ^{13}C NMR ($CDCl_3$, 75 MHz): δ 140.6, 139.8, 139.2, 128.8, 127.35, 126.4, 64.25, 45.35. Anal. Calcd for $C_{30}H_{42}N_4 \cdot 1/4\ CH_2Cl_2$: C, 75.71; H, 8.93; N, 11.67. Found: C, 75.91; H, 8.46; N, 11.26.

Synthesis of 1,4-bis(3,5-(dimethylaminomethyl)-4-iodophenyl)benzene (32): To a solution of corresponding terphenyl derivative **31** (0.46 g, 1.0 mmol) in dry benzene (10 mL) at room temperature was added a solution of *n*-BuLi (1.63 mL, 2.6 mmol). After stirring this mixture overnight, iodine (0.66 g, 2.6 mmol) in THF (20 mL) was added to the deep pink suspension. After stirring for 1 h, the reaction mixture was quenched with saturated $Na_2S_2O_3$ (aq) (50 mL), and the resulting mixture was extracted with CH_2Cl_2 (2 × 50 ml). The combined organic layer was dried over $MgSO_4$, and concentrated to give **32** as a yellow solid. Elemental analysis pure **32** was obtained by column chromatography using silica and EtOH/saturated-NH_4OH(aq) (9/1) as the eluent. Yield: 0.62 g (87%). Mp 198–200 ºC. ^{1}H NMR ($CDCl_3$, 200 MHz): δ 7.72 (s, 4H, Ar*H*), 7.58 (s, 4H, Ar*H*), 3.59 (s, 8H, CH_2), 2.36 (s, 24H, NCH_3). ^{13}C NMR ($CDCl_3$, 75 MHz): δ 142.2, 139.7, 139.2, 127.4, 127.35, 106.15, 69.0, 45.55. MALDI-TOF-MS (*m/z*): 710.54 (M^+, calcd 710.13). Anal. Calcd for $C_{30}H_{40}I_2N_4$: C, 50.72; H, 5.67; N, 7.89. Found: C, 50.89; H, 5.61; N, 7.76

Synthesis of 1,4-bis(3,5-(dimethylaminomethyl)-4-(iodoplatino)phenyl)benzene (33): A mixture of **32** (0.71 g, 1.0 mmol) and $[Pt(p\text{-tol})_2SEt_2]_2$ (0.93 g, 1.0 mmol) in dry benzene (50 mL) was stirred at 55 ºC for 3 h. The mixture was cooled to room temperature and all volatiles were removed *in vacuo*. The yellow solid was washed with Et_2O (2 × 10 mL) and the very poorly soluble crude diplatinum compound **33**

was suspended in CH_2Cl_2 (20 mL). Subsequently, sulfur dioxide was bubbled trough this mixture, resulting in a clear deep orange solution. Upon addition of Et_2O, an orange solid precipitated. This solid was collected and washed with Et_2O (2 × 15 mL). The orange solid was redissolved in CH_2Cl_2 (20 mL) and this mixture was evaporated to dryness under reduced pressure, in order to liberate the diplatinum complex from sulfur dioxide. This resulted in pure **33** as a yellow solid. Yield: 0.95 g (86%). ^{1}H NMR (CD_2Cl_2, 200 MHz): δ 7.59 (s, 4H, Ar*H*), 7.21 (s, 4H, Ar*H*), 4.11 (s, $^3J_{Pt,H}$ = 49.8 Hz, 8H, CH_2), 3.20 (s, $^3J_{Pt,H}$ = 41.4 Hz, 24H, NCH_3). ^{13}C NMR ($CDCl_3$, 75 MHz): δ 144.2, 140.3, 136.7, 127.3, 126.1, 126.0, 118.4, 77.7, 55.4. MALDI-TOF-MS (*m/z*): 973.98 ([M–I]$^+$, calcd 973.13). Anal. Calcd for $C_{30}H_{40}I_2N_4Pt_2$: C, 32.74; H, 3.66; N, 5.09. Found: C, 32.96; H, 3.78; N, 5.13.

Crystal structure determination of 13. $C_{126}H_{96}Cl_6Pd_6S_{12}$·solvent, M_r = 2845.85, trigonal, R3, a, b = 27.195(3), c = 15.728(4) Å, V = 10074(3) Å^3, Z = 3, ρ_{calcd} = 1.407 g/cm^3, T = 150(2) K, $(\sin \vartheta / \lambda)_{max}$ = 0.649 Å^{-1}, yellow block 0.25 × 0.38 × 0.38 mm^3, measured reflections: 9086, unique reflections: 8113 (R_{int} = 0.051), R-values ($I > 2\sigma(I)$): R1 = 0.0756, wR2 = 0.1709, all data: R1 = 0.1201, wR2 = 0.1942. $-0.52 < \Delta\rho < 1.06$ *e* / Å^3. Diffractometer: Enraf-Nonius CAD4T with rotating anode (l = 0.71073 Å). Absorption correction based on psi-scans (μ = 1.14 mm^{-1}, 0.82–0.97 transmission). Structure solution with direct methods (SHELXS-97).[15] Structure refinement with SHELXL-97[16] against F^2. 415 parameters, 276 restraints. S-Phenyl groups were heavily disordered and refined with isotropic parameters. All other non-hydrogen atoms were refined with anisotropic temperature parameters, hydrogen atoms were refined as rigid groups. Structure graphics, checking for higher symmetry, absorption correction and treatment of disordered solvent (CALC SQUEEZE, 830 e$^-$ / unit cell) were performed with the program PLATON.[17] Crystallographic data (excluding structure factors) for the structure reported in this paper have been deposited with the Cambridge Crystallographic Data Centre as supplementary publication no. CCDC-114913. Copies of the data can be obtained free of charge on application to CCDC, 12 Union Road, Cambridge CB2 1EZ, UK (Fax: (+44)1223-336-033; e-mail: deposit@ccdc.cam.ac.uk).

Crystal Structure Determination of 19: $C_{42}H_{57}Br_3N_6Pd_3$ + solvent, Fw = 1204.87,[18] yellow block, 0.30 × 0.30 × 0.24 mm^3, trigonal, R $\bar{3}$ c (No. 167), a = b = 15.6134(2), c = 35.2061(5) Å, V = 7432.64(17) Å^3, Z = 6, ρ = 1.615 g/cm^3. 32401 reflections were measured on a Nonius Kappa CCD diffractometer with rotating anode (λ =

0.71073 Å) at a temperature of 150(2) K. 1874 reflections were unique (R_{int} = 0.062).[18] The absorption correction was based on multiple measured reflections (program PLATON,[17] routine MULABS, μ = 3.53 mm^{-1},[18] 0.34–0.39 transmission). The structure was solved with Patterson methods (DIRDIF97)[19] and refined with SHELXL97[16] against F^2 of all reflections. Non-hydrogen atoms were refined freely with anisotropic displacement parameters. Hydrogen atoms were refined as rigid groups. The crystal structure contains large isolated voids at the crystallographic origin and its five symmetry related positions (193 $Å^3$/void, 1162 $Å^3$/unit cell) filled with disordered dichloromethane and diethylether molecules. Their contribution to the structure factors was secured by back-Fourier transformation (program PLATON,[17] CALC SQUEEZE, 473 e^-/unit cell). 85 refined parameters, no restraints. R-values [$I > 2\sigma(I)$]: R1= 0.0281, wR2 = 0.0670. R-values [all refl.]: R1= 0.0288, wR2 = 0.0674. GoF = 1.125. Rest electron density between –0.47 and 0.71 e/$Å^3$. Molecular illustration, structure checking and calculations were performed with the PLATON package.[17]

2.5. References and Notes

[1] a) Knapen, J. W. J.; van der Made, A. W.; de Wilde, J. C.; van Leeuwen, P. W. N. M.; Wijkens, P.; Grove, D. M.; van Koten, G. *Nature* **1994**, *372*, 659. b) Kragl, U.; Dreisbach, C. *Angew. Chem. Int. Ed.* **1996**, *35*, 642. c) Reetz, M. T.; Lohmer, G.; Schwickardi, R. *Angew. Chem. Int. Ed.* **1997**, *36*, 1526. d) Giffels, G.; Beliczey, J.; Felder, M.; Kragl, U. *Tetrahedron: Asymm.* **1998**, *9*, 691. e) Brinkmann, N.; Giebel, D.; Lohmer, G.; Reetz, M. T.; Kragl, U. *J. Cat.* **1999**, *183*, 163. f) Hovestad, N. J.; Eggeling, E. B.; Heidbüchel, H. J.; Jastrzebski, J. T. B. H.; Kragl, U.; Keim, W.; Vogt, D.; van Koten, G. *Angew. Chem. Int. Ed.* **1999**, *38*, 1655. g) de Groot, D.; Eggeling, E. B.; de Wilde, J. C.; Kooijman, H.; van Haaren, R. J.; van der Made, A. W.; Spek, A. L.; Vogt, D.; Reek, J. N. H.; Kamer, P. C. J.; van Leeuwen, P. W. N. M. *Chem. Commun.* **1999**, 1623. h) Kleij, A. W.; Gossage, R. A.; Klein Gebbink, R. J. M.; Reyerse, E. J.; Brinkmann, N.; Kragl, U.; Lutz, M.; Spek, A. L.; van Koten, G. *J. Am. Chem. Soc.* **2000**, *122*, 12112. i) Albrecht, M.; Hovestad, N. J.; Boersma, J.; van Koten, G. *Chem. Eur. J.* **2001**, *7*, 1289. j) Rissom, S.; Beliczey, J.; Giffels, G.; Kragl, U.; Wandrey, C. *Tetrahedron: Asymm.* **1999**, *10*, 923. k) Dwars, T.; Haberland, J.; Grassert, I.; Kragl, U. *J. Mol. Cat. A: Chem.* **2001**, *168*, 81.

[2] For a review of the application of metallodendrimers as homogeneous catalysts see: a) Kreiter, R.; Kleij, A. W.; Klein Gebbink, R. J. M.; van Koten, G. *Dendritic Catalysts. Topics in Current Chemistry, Dendrimers IV*; Vögtle, F., Ed.; Springer-Verlag Berlin Heidelberg, **2001**, *217*, 163. b) Kleij, A. W.; Klein Gebbink, R. J. M.; van Koten, G. *Dendritic Polymer Application: Catalysts* in *Dendrimers and*

other Dendritic Polymers; Fréchet, J.; Tomalia, D., Eds.; Wiley, New York, **2002**. c) Oosterom, G. E.; Reek, J. N. H.; Kamer, P. C. J.; van Leeuwen, P. W. N. M. *Angew. Chem. Int. Ed.* **2001**, *40*, 1828.

[3] a) Wooley, K. L.; Klug, C. A.; Tasaki, K.; Schaefer, J. *J. Am. Chem. Soc.* **1997**, *119*, 53. b) Chai, M.; Niu, Y.; Youngs, W. J.; Rinaldi, P. L. *J. Am. Chem. Soc.* **2001**, *123*, 4670.

[4] Albrecht, M.; van Koten, G. *Angew. Chem. Int. Ed.* **2001**, *40*, 3750.

[5] Duchêne, K.–H.; Vögtle, F. *Synth.* **1986**, 659.

[6] Sonogashira, K.; Tohda, Y.; Hagihara, N. *Tetrahedron Lett.* **1975**, 4467.

[7] Grove, D. M.; van Koten, G.; Louwen, J. N.; Noltes, J. G.; Spek, A. L.; Ubbels, H. J. C. J. *J. Am. Chem. Soc.* **1984**, *106*, 6609.

[8] Procedure reported by: a) Loeb, S. J.; Shimizu, G. K. H. *J. Chem. Soc., Chem. Comm.* **1993**, 1396. b) Kickham, J. E.; Loeb, S. J. *Inorg. Chem.* **1994**, *33*, 4351.

[9] van de Kuil, L. A.; Luitjes, H.; Grove, D. M.; Zwikker, J. W.; van der Linden, J. G. M.; Roelofsen, A. M.; Jenneskens, L. W.; Drenth, W.; van Koten, G. *Organometallics* **1994**, *13*, 471.

[10] Modification of a reported method was used: Elmorsy, S. S.; Pelter, A.; Smith, K. *Tetrahedron Lett.* **1991**, *32*, 4175.

[11] Procedure reported by: Canty, A. J.; Patel, J.; Skelton, B. W.; White, A. H. *J. Organomet. Chem.* **2000**, *599*, 195.

[12] Rodríguez, G.; Albrecht, M.; Schoenmaker, J.; Ford, A.; Lutz, M.; Spek, A. L.; van Koten, G. *J. Am. Chem. Soc.* **2002**, *124*, 5127.

[13] Steenwinkel, P.; James, S. L.; Grove, D. M.; Veldman, N.; Spek, A. L.; van Koten, G. *Chem. Eur. J.* **1996**, *2*, 1440.

[14] Rettig, M. F.; Maitlis, P. M.; Cotton, F. A.; Webbs, T. R. *Inorg. Synth.* **1971**, 134.

[15] Sheldrick, G. M. (1997). SHELXS-97. Program for Crystal Structure Solution. University of Göttingen, Germany, **1997**.

[16] Sheldrick, G. M. SHELXL-97. Program for crystal structure refinement. University of Göttingen, Germany, **1997**.

[17] Spek, A. L. PLATON. A multipurpose crystallographic tool. Utrecht University, The Netherlands, **2000**.

[18] Derived values do not contain the contribution of the disordered solvent.

[19] Beurskens, P. T.; Admiraal, G.; Beurskens, G.; Bosman, W. P.; Garcia-Granda, S.; Gould, R. O.; Smits, J. M. M.; Smykalla, C. (1997) The DIRDIF97 program system, Technical Report of the Crystallography Laboratory, University of Nijmegen, The Netherlands.

– *Chapter 3* –

The Use of Organometallic Building Blocks in the Synthesis of Shape-Persistent Multi(NCN-Metal) Complexes

Abstract: Palladated and platinated octakis- and dodecakis(NCN-pincer) complexes based on shape-persistent aromatic backbones were prepared. For the synthesis of these complexes, monometallated NCN-building blocks were coupled to rigid octakis- and dodecakis(benzylic bromide) cores in a one-pot reaction. Following this modular approach, eight or twelve metal centers were selectively introduced under very mild conditions, thereby minimalizing the risk of destroying the individual organometallic moieties, a crucial aspect in the synthesis of multimetallic materials. The octakis(NCN-pincer) complexes have a silicon atom as the central branching point, affording tetrahedral, spherical structures. The dodecakis analogs are based on a persubstituted benzene core, giving the multimetallic complexes more flattened spherical geometries.

H. P. Dijkstra, C. A. Kruithof, N. Ronde, R. van de Coevering, D. J. Ramón, D. Vogt, G. P. M. van Klink, G. van Koten, *J. Org. Chem.,* in press.

3.1. Introduction

In the field of homogeneous catalysis there is currently wide interest in the application of tailored/engineered organic molecules as soluble support materials for anchored catalytically-active metal complexes.[1,2] Such organic materials often have a periphery bearing multidentate ligands or ligand precursors and are usually designed in such a way that the resulting multimetallic catalysts can easily be removed after catalysis from the product-containing solution for reuse.[3]

A crucial aspect in the preparation of multimetallic materials is the sequence in which the metals and appropriate organic functionalities are introduced into the system. Often the organic core bearing the multidentate ligand-sites is prepared as far as possible, prior to the metalation procedures, *i.e.* the metal centers are introduced in the last step to give the multimetallic species (Route A, Scheme 1).[4] This approach has the advantage that a minimal number of steps is performed with the organometallic species itself. A disadvantage of this method is that incomplete metalation can occur, especially when increasing numbers of ligand-sites have to be metalated. An alternative strategy to multimetallic materials is to anchor an appropriately functionalized, monometalated ligand to a support material (Route B, Scheme 1).[5] This approach has the advantage that all ligand-sites in the final multimetallic complex are metalated since the metal is already present in the step in

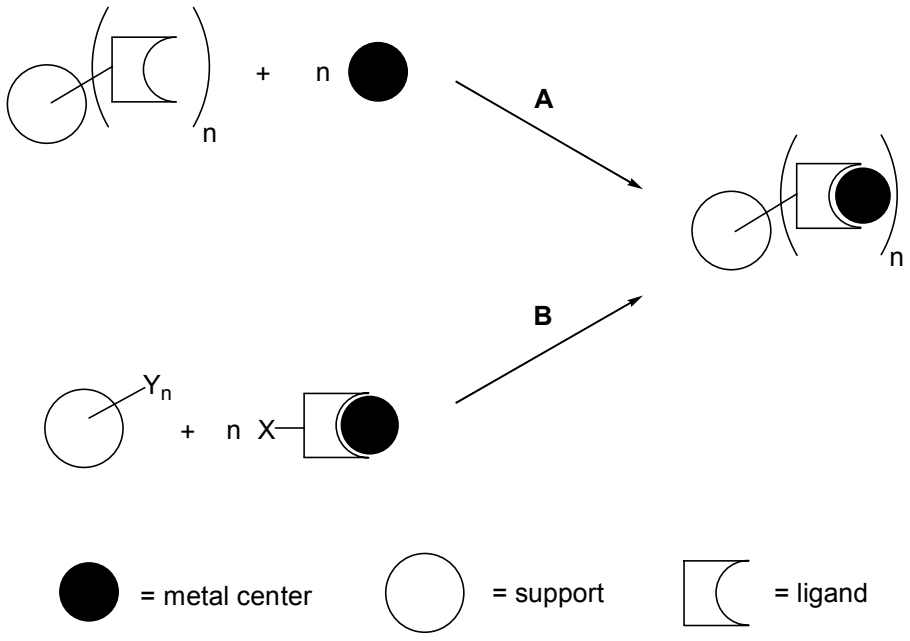

Scheme 1. Two routes to prepare multimetallic materials.

which the multimetallic material is constructed. A prerequisite of this approach is that the organometallic moiety has to be resistent to the reaction conditions used for the coupling of the monometallic building blocks to the support materials.

In this chapter, the use of organometallic mono(NCN-pincer) building blocks in the synthesis of palladated and platinated octakis- and dodecakis(NCN-pincer) complexes is discussed.

3.2. Results and Discussion

Synthesis of Organometallic Building Blocks. For the synthesis of multi(NCN-metal) complexes **7** and **9**, organometallic building blocks **3a** and **3b** were prepared (Scheme 2). The synthesis began with the iodination of **1** using a lithiation/iodination reaction sequence, resulting in ligand precursor **2** in 66% yield. Treatment of **2** with $Pd(dba)_2$ resulted in the formation of palladium(II) pincer **3a** (72%),[6] while the corresponding platinum(II) compound **3b** was prepared in 83% yield by reaction of **2** with $[Pt(p\text{-tol})_2SEt_2]_2$.[7]

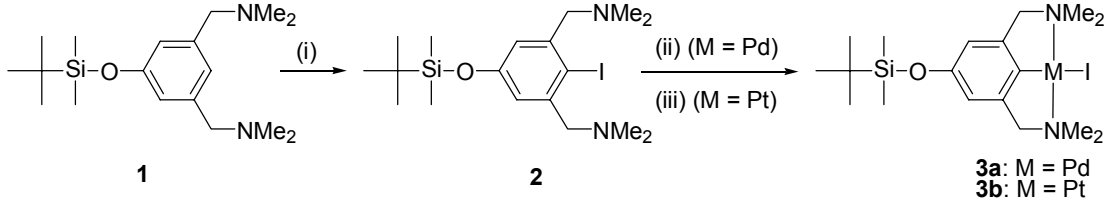

Scheme 2. (i) *n*-BuLi, hexanes, –70 → rt, 4 h, followed by I_2, THF, rt, 3 h; (ii) $Pd(dba)_2$, C_6H_6, rt, 6 h; (iii) $[Pt(p\text{-tol})_2SEt_2]_2$, C_6H_6, reflux, 3 h.

Synthesis of Octakis(NCN-pincer-metal) Complexes. The synthesis of the central organic core for complexes **7a–c** started with the lithiation of iodoarene **4** (Scheme 3). The *in situ* prepared aryllithium compound was reacted with tetrachlorosilane, thereby obtaining tetraarylsilane **5** in 90% yield. Subsequently, the methoxy groups of **5** were converted into bromides by treatment with acetyl bromide and trifluoroborane·etherate, resulting in the formation of octakis(benzylic bromide) **6** in 52% yield. Reaction of this octakis(benzylic bromide) with eight equivalents of palladium(II) building block **3a** in acetone at room temperature in the presence of tetrabutylammonium fluoride, gave the corresponding octakis(NCN-Pd^{II}) complex **7a** (67% yield). Platinum complex **7b** was analogously obtained by reaction of **6** with eight equivalents of platinum(II) building block **3b** in 44% isolated yield. Neutral

octakis(NCN-Pd^{II}) complex **7a** was readily converted into the corresponding ionic complex **7c** by treatment with eight equivalents of silver tetrafluoroborate in wet acetone.

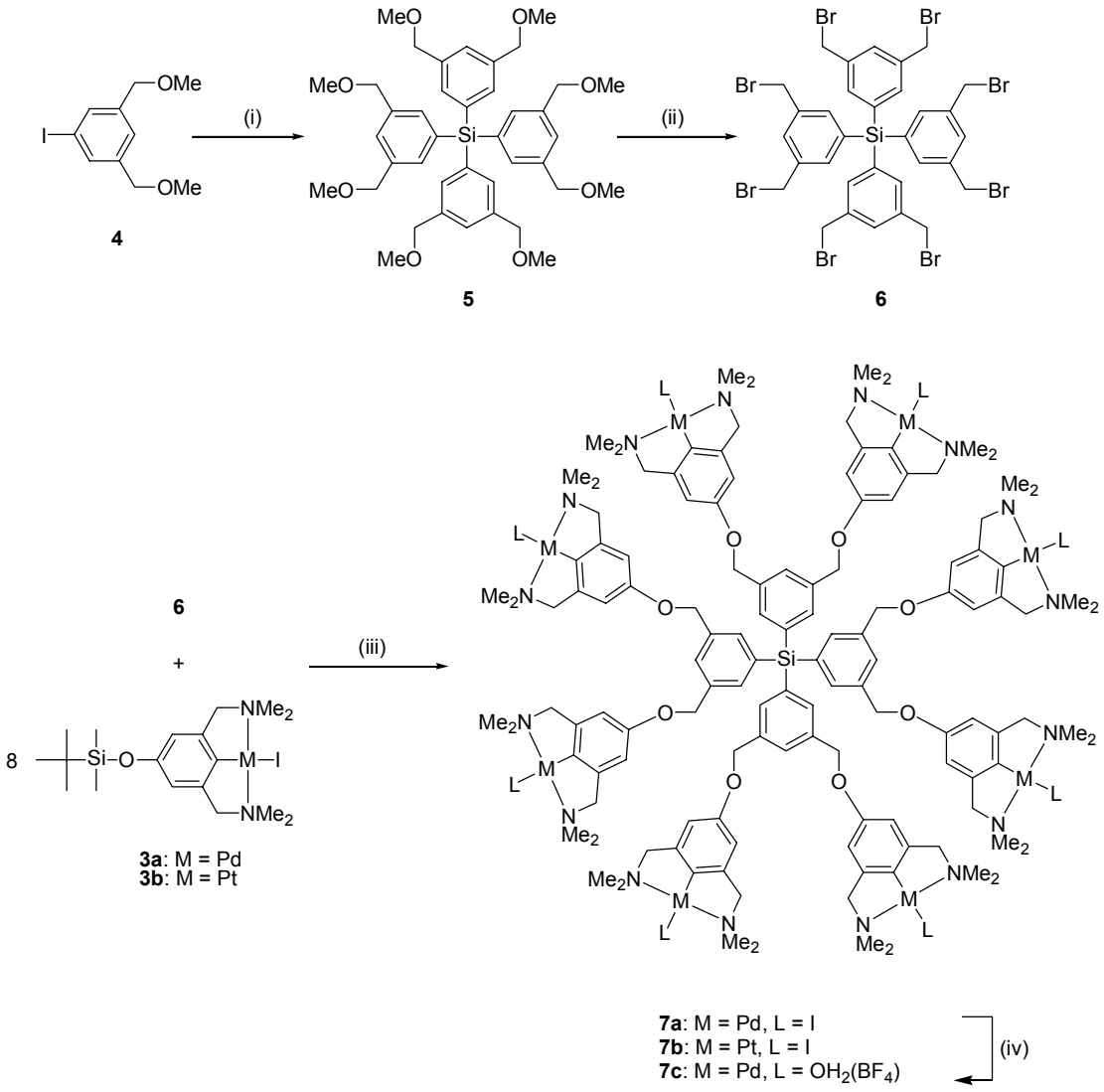

Scheme 3. (i) 2 eq. *t*-BuLi, Et_2O, –90 °C, 15 min followed by 0.25 eq. $SiCl_4$, –90 °C → rt, 20 h; (ii) AcBr, $BF_3{\cdot}OEt_2$, CH_2Cl_2, reflux, 20 h; (iii) Bu_4NF, K_2CO_3, 18-crown-6, acetone, rt, 20 h; (iv) $AgBF_4$, wet acetone, rt, 1 h.

Synthesis of Dodecakis(pincer-metal) Complexes. The synthesis of dodecakis(NCN-pincer) complexes **9a–c** is outlined in Scheme 4. Reaction of twelve equivalents of organometallic building block **3a** with dodecakis(benzylic bromide) **8** in the presence of tetrabutylammonium fluoride, resulted in the formation of

dodecakis(NCN-Pd^{II}) complex **9a**. The corresponding platinum(II) complex **9b** was obtained analogously by reaction of twelve equivalents of **3b** with **8**. The neutral complex **9a** could easily be converted into the corresponding ionic complex **9c** with silver tetrafluoroborate in wet acetone (Scheme 4).

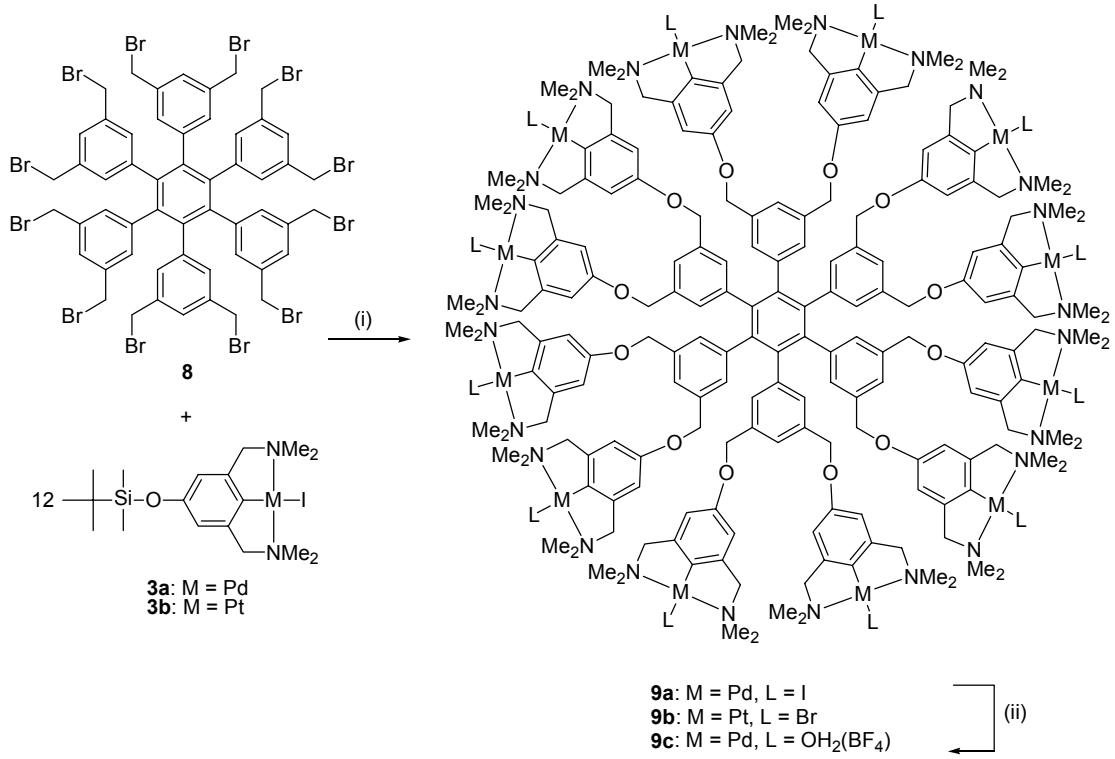

Scheme 4. (i) Bu_4NF, K_2CO_3, 18-crown-6, acetone, rt, 20 h (**9b** was prepared in the presence of LiBr); (ii) $AgBF_4$, wet acetone, rt, 1 h.

Important to note is that in the synthesis of **7** and **9** eight or twelve metal centers, respectively, are introduced into the multimetallic material in a one-pot reaction under very mild reaction conditions. With the metal already present in the pincer moiety in the final construction step of the multimetallic material, this route results in the formation of fully metalated materials. The alternative route - preparation of the octakis- or dodecakis(NCN-pincer) ligands followed by permetalation - is a method which can lead to incomplete metalation (see hexakis(NCN-Pd^{II}) complex **11**, Chapter 2) and enhanced decomposition because more severe reaction conditions are required. Furthermore, in contrast to the shape-persistent macromolecular complexes discussed in Chapter 2, which are rather flat, two-dimensional materials, complexes **7** and **9** possess more three-dimensional

geometries. Complexes **7a**–**c** are based on a tetraaryl substituted silicon center, giving the molecules their spherical, three-dimensional geometries. Complexes **9a**–**c** are based on a hexaaryl substituted benzene core surrounded by a more flexible organometallic core, affording a flattened-spherical geometry. These materials will be further investigated as homogeneous catalysts in organic transformations and will also be used to study the influence of shape-persistence and geometry on the retention rates of macromolecular catalysts by nanofiltration membranes.

3.3. Concluding Remarks

A new modular approach to prepare palladated and platinated octakis- and dodecakis(NCN-M^{II}) complexes **7** and **9**, respectively, was developed. In this approach, functionalized monometallic NCN-pincer building blocks were selectively coupled to multifunctionalized organic supports. These reactions were performed under very mild reaction conditions, *e.g.* in acetone at room temperature, minimalizing the risk of destroying the individual organometallic moieties. Clearly, complexes **7** and **9** possess shape-persistent cores, surrounded by a more flexible organometallic core, affording these structures more spherical geometries. A high degree of shape-persistence together with a three-dimensional geometry is expected to be important to obtain optimal retentions of these molecules by nanofiltration membranes. This can lead to continuous catalytic processes in a nanofiltration membrane reactor in which the homogeneous catalysts are retained very efficiently.

3.4. Experimental Section

General: All reactions were carried out using standard Schlenk techniques under an inert nitrogen atmosphere unless stated otherwise. Et_2O, THF and hexanes were carefully dried and distilled from Na/benzophenone prior to use. CH_2Cl_2 was distilled from CaH_2. All standard reagents were purchased. Compounds **1**,[8] **4**,[9] **8**,[9] $Pd(dba)_2$[10] and $[Pt(p\text{-tol})_2SEt_2]_2$[7] were prepared according to literature procedures. ^1H (200 or 300 MHz) and ^{13}C (50 or 75 MHz) NMR spectra were recorded on a Varian AC200 or Varian 300 spectrometer at 25 °C, chemical shifts are in ppm referenced to residual solvent resonances. MALDI-TOF-MS spectra were acquired using a Voyager-DE Bio-Spectrometry Workstation mass spectrometer equipped with a nitrogen laser emitting at 337 nm. The matrix (3,5-dihydroxybenzoic acid) and the sample were dissolved in THF or CH_2Cl_2 (~30 mg/ml) and 0.2 μl of both solutions were mixed and

placed on a gold MALDI target and analyzed after evaporation of the solvent. Elemental microanalyses were performed by Dornis und Kolbe, Mikroanalytisches Laboratorium, Müllheim a.d. Ruhr, Germany.

Synthesis of 4-*tert*-butyldimethylsiloxyl-2,6-bis[(dimethylamino)methyl]-1-iodobenzene (2): *n*-BuLi (11.3 mL, 18.0 mmol) was added to a solution of **1** (5.0 g, 15.5 mmol) in hexanes (50 mL) at –70 °C. After addition was completed, the temperature was allowed to rise to room temperature and stirring was continued for 4 h. Subsequently, iodine (5.1 g, 20.0 mmol) in THF (15 mL) was added and stirring was continued for 3 h at room temperature. The reaction mixture was poured into $NaHSO_3$ (aq) (2 M, 100 mL) and the organic layer was collected. The aqueous layer was extracted with Et_2O (3 × 50 mL) and the combined organic layer was washed with brine (50 mL), dried over $MgSO_4$ and filtered. After evaporation of all volatiles a brown oil remained, which was flame-distilled to yield a yellow oil. Yield: 4.6 g (66%). This product (**2**) was used without further purification. ^{1}H NMR ($CDCl_3$, 200 MHz): δ 6.86 (s, 2H, Ar*H*), 3.47 (s, 4H, CH_2), 2.30 (s, 12H, NCH_3), 0.97 (s, 9H, CCH_3), 0.19 (s, 6H, CH_3Si).

Synthesis of 4-*tert*-butyldimethylsiloxyl-2,6-bis[(dimethylamino)methyl]-1-(iodopalladio)benzene (3a): A solution of **2** (2.35 g, 5.23 mmol) and $Pd(dba)_2$ (2.85 g, 5.23 mmol) in benzene (30 mL) was stirred at room temperature for 6 h. Subsequently, this mixture was filtered over Celite and all volatiles were evaporated. The residue was extracted with CH_2Cl_2 (10 mL) and pentane was added dropwise to this solution resulting in the formation of a yellowish solid. The procedure was repeated until a white solid was obtained. This solid was collected and dried *in vacuo*. Yield: 2.06 g (72%). ^{1}H NMR ($CDCl_3$, 300 MHz): δ 6.39 (s, 2H, Ar*H*), 3.94 (s, 4H, NCH_2), 3.01 (s, 12H, NCH_3), 0.96 (s, 9H, CCH_3), 0.16 (s, 6H, SiCH_3). ^{13}C NMR ($CDCl_3$, 75 MHz): δ 153.68, 150.57, 145.98, 112.01, 74.21, 55.20, 25.86, 18.30, –4.20. Anal. Calcd for $C_{18}H_{33}IN_2PdOSi$: C, 38.96; H, 6.00; N, 5.05. Found: C, 38.88; H, 5.93; N, 4.95.

Synthesis of 4-*tert*-butyldimethylsiloxyl-2,6-bis[(dimethylamino)methyl]-1-(iodoplatino)benzene (3b): A mixture of **2** (1.03 g, 2.30 mmol) and $[Pt(p\text{-tol})_2SEt_2]_2$ (1.07 g, 1.15 mmol) in benzene (20 mL) was heated at reflux for 3 h. After cooling the solution to room temperature, all volatiles were evaporated. The light-yellow solid was washed with Et_2O (2 × 15 mL) and the remaining white solid was dissolved in

CH_2Cl_2 (5 mL). Upon dropwise addition of hexanes (20 mL) the product precipitated as a white solid. This solid was collected and dried *in vacuo*. Yield: 1.23 g (83%). ^{1}H NMR (C_6D_6, 300 MHz): δ 6.34 (s, 2H, Ar*H*), 3.19 (s, $^3J_{Pt,H}$ = 21.9 Hz, NCH_2), 2.75 (s, $^3J_{Pt,H}$ = 19.2 Hz, NCH_3), 1.06 (s, 9H, CCH_3), 0.19 (s, 6H, SiCH_3). ^{13}C NMR ($CDCl_3$, 75 MHz): δ 152.67, 144.62, 142.94, 111.46, 76.59, 55.93, 25.79, 18.27, –4.36. Anal. Calcd for $C_{18}H_{33}IN_2PtOSi$: C, 33.59; H, 5.17; N, 4.35. Found: C, 33.68; H, 5.08; N, 4.26.

Synthesis of tetra[3,5-bis(methoxymethyl)phenyl]silane (5): To a solution of **4** (4.91 g, 16.8 mmol) in Et_2O (60 mL) was added *t*-BuLi (20 mL, 30 mmol) at –90 °C. After stirring the white suspension for ca. 15 min, $SiCl_4$ (0.4 mL, 3.49 mmol) was added, and the resulting red-brown suspension was allowed to reach room temperature and was stirred for an additional 20 h. An extra amount of *t*-BuLi (5 mL, 7.50 mmol)) was added, followed by H_2O (100 mL) to hydrolyze the excess of *t*-BuLi. The organic layer was separated and the aqueous layer was extracted with Et_2O (2 × 100 mL). The combined organic layers were dried over Na_2SO_4, filtered, and concentrated *in vacuo*. The free 3,5-bis(methoxymethyl)benzene was removed by bulb-to-bulb distillation (140–160 °C, 0.1–0.2 mm Hg) to yield a yellow, viscous oil. Yield: 8.7 g (90 %). ^{1}H NMR (C_6D_6, 200 MHz): δ 7.87 (s, 8H, Ar*H*), 7.55 (s, 4H, Ar*H*), 4.18 (s, 12H, OCH_2), 3.07 (s, 48H, OCH_3). ^{13}C NMR (C_6D_6, 75 MHz): δ 139.0, 135.1, 134.7, 128.9, 74.5, 57.8. ^{29}Si NMR (C_6D_6, 59 MHz): δ –13.2.

Synthesis of tetra[3,5-bis(bromomethyl)phenyl]silane (6): To a solution of **5** (2.16 g, 3.14 mmol) in CH_2Cl_2 (500 mL) was added dropwise a solution of $BF_3{\cdot}Et_2O$ (13 mL, 0.10 mol) and acetyl bromide (8 mL, 0.10 mol) in CH_2Cl_2 (60 mL) at 0 °C. The slightly brown solution was heated to reflux for 20 h, whereupon the reaction mixture was allowed to cool to RT. Aqueous Na_2CO_3 (5%, 450 mL) was added slowly to hydrolyze the excess of $BF_3{\cdot}Et_2O$. Next, the organic layer was separated, washed with water (2 × 200 mL), dried over Na_2SO_4, filtered, and concentrated *in vacuo*. The product was purified by crystallization from a CH_2Cl_2/pentane mixture (v/v 5:1) at –25 °C, to yield a white powder (52%). ^{1}H NMR ($CDCl_3$, 300 MHz): δ 7.56 (s, 4H, Ar*H*), 7.45 (s, 8H, Ar*H*), 4.46 (s, 16H, BrCH_2). ^{13}C NMR ($CDCl_3$, 75 MHz): δ 138.75, 136.86, 134.10, 131.92, 32.88. Anal. Calcd for $C_{32}H_{28}Br_8Si$: C, 35.59; H, 2.61; Si, 2.61. Found: C, 35.74; H, 2.65; Si, 2.64.

Synthesis of 7a: Bu_4NF (1 M in THF, 1.05 mL, 1.05 mmol) was added to a mixture of **6** (0.14 g, 0.13 mmol), **3a** (0.58 g, 1.05 mmol), K_2CO_3 (0.73 g, 5.25 mmol) and 18-crown-6 (20 mg, 76 μmol) in acetone (15 mL) and this mixture was stirred at room temperature for 20 h. Subsequently, all volatiles were evaporated and the residue was extracted with CH_2Cl_2 (10 mL). Upon dropwise addition of Et_2O (20 mL) an off-white solid precipitated, which was collected. This procedure was repeated twice and the product was dried *in vacuo*. Yield: 0.34 g (67%). ^{1}H NMR ($CDCl_3$, 300 MHz): δ 7.65 (s, 4H, Ar*H*), 7.50 (s, 8H, Ar*H*), 6.44 (s, 16H, Ar*H*), 4.92 (s, 16H, OCH_2), 3.92 (s, 32H, NCH_2), 2.95 (s, 96H, NCH_3). ^{13}C NMR (CD_2Cl_2, 75 MHz): δ 156.65, 144.66, 144.38, 137.69, 135.01, 134.22, 128.56, 107.07, 77.44, 70.83, 55.38. Anal. Calcd for $C_{128}H_{172}I_8N_{16}Pd_8O_8Si$: C, 38.85; H, 4.38; N, 5.66. Found: C, 39.03; H, 4.46; N, 5.64.

Synthesis of 7b: Bu_4NF (1 M in THF, 0.75 mL, 0.75 mmol) was added to a mixture of **6** (0.10 g, 93 μmol), **3b** (0.48 g, 0.75 mmol), K_2CO_3 (0.52 g, 3.76 mmol) and 18-crown-6 (20 mg, 76 μmol) in acetone (15 mL) and this mixture was stirred at room temperature for 20 h. Subsequently, all volatiles were evaporated and the residue was extracted with CH_2Cl_2 (10 mL). Upon dropwise addition of Et_2O (20 mL) a white solid precipitated, which was collected. This procedure was repeated twice and the product was dried *in vacuo*. Yield: 0.19 g (44%). ^{1}H NMR (CD_2Cl_2, 300 MHz): δ 7.66 (s, 4H, Ar*H*), 7.61 (s, 8H, Ar*H*), 6.49 (s, 16H, Ar*H*), 4.98 (s, 16H, OCH_2), 3.94 (s, $^3J_{Pt,\ H}$ not resolved, 32H, NCH_2), 3.05 (s, $^3J_{Pt,\ H}$ not resolved, 96H, NCH_3). ^{13}C NMR (CD_2Cl_2, 75 MHz): δ 156.65, 144.69, 144.40, 137.88, 134.92, 134.25, 128.45, 106.98, 77.93, 70.72, 55.13. MALDI-TOF-MS: *m/z* 4542.75 ([M–I]$^+$, calcd 4540.00). Anal. Calcd for $C_{128}H_{172}I_8N_{16}Pt_8O_8Si$: C, 32.94; H, 3.72; N, 4.80. Found: C, 33.16; H, 3.81; N, 4.69.

Synthesis of 7c: A solution of $AgBF_4$ (19.2 mg, 98.8 μmol) in water (0.5 mL) was added to a suspension of **7a** (48.9 mg, 12.4 μmol) in acetone (10 mL) and the resulting mixture was stirred at room temperature in the absence of light for 1 h. The reaction mixture was filtered through Celite and the Celite was washed with acetone (10 mL). The filtrate was concentrated to 3 mL and dropwise addition of Et_2O (10 mL) resulted in an off-white precipitate, which was collected and dried *in vacuo*. Yield: 39.4 mg (84%). ^{1}H NMR (acetone-d_6, 200 MHz): δ 7.73 (m, 12H, Ar*H*), 6.58 (s, 16H, Ar*H*), 5.07 (s, 16H, OCH_2), 4.00 (s, 24H, NCH_2), 2.76 (s, 96H, NCH_3). ^{13}C NMR (acetone-d_6, 75 MHz): δ 158.10, 146.24, 141.23, 137.96, 134.73, 134.24, 128.38, 107.96, 73.49, 70.14, 51.88.

Synthesis of 9a: Bu_4NF (1 M in THF, 0.97 mL, 0.97 mmol) was added to a mixture of **8** (0.12 g, 79 μmol), **3a** (0.53 g, 0.95 mmol), K_2CO_3 (0.66 g, 4.80 mmol) and 18-crown-6 (25 mg, 95 μmol) in acetone (20 mL) and the resulting mixture was stirred at room temperature for 20 h. Subsequently, all volatiles were evaporated and the residue was extracted with CH_2Cl_2 (10 mL). Upon dropwise addition of acetone (20 mL) a white solid precipitated, which was collected. This procedure was repeated twice and the product was dried *in vacuo*. Yield: 0.25 g (53%). ^{1}H NMR (CD_2Cl_2, 300 MHz): δ 6.96 (br s, 18H, Ar*H*), 6.26 (br s, 24H, Ar*H*), 4.69 (br s, 24H, OCH_2), 3.83 (br s, 48H, NCH_2), 2.96 (br s, 144H, NCH_3). ^{13}C NMR (CD_2Cl_2, 75 MHz): δ 157,30, 150.78, 148.99, 146.48, 140.24, 136.79, 129.36, 122.15, 106.89, 74.22, 70.20, 55.16. Anal. Calcd for $C_{198}H_{258}I_{12}N_{24}Pd_{12}O_{12}$: C, 39.86; H, 4.36; N, 5.63. Found: C, 40.08; H, 4.28; N, 5.73.

Synthesis of 9b: Bu_4NF (1 M in THF, 0.97 mL, 0.97 mmol) was added to a mixture of **8** (0.12 g, 79 μmol), **3b** (0.61 g, 0.95 mmol), LiBr (0.83 g, 9.6 mmol), K_2CO_3 (0.66 g, 4.80 mmol) and 18-crown-6 (25 mg, 95 μmol) in acetone (20 mL) and the resulting mixture was stirred at room temperature for 20 h. Subsequently, all volatiles were evaporated and the residue was extracted with CH_2Cl_2 (10 mL) and filtered. Upon dropwise addition of ethyl acetate (20 mL), a white solid precipitated, which was collected. This procedure was repeated twice and the product was dried *in vacuo*. Yield: 0.34 g (67%). ^{1}H NMR (CD_2Cl_2, 300 MHz): δ 7.00 (br s, 18H, Ar*H*), 6.29 (br s, 24H, Ar*H*), 4.69 (br s, 24H, OCH_2), 3.84 (br s, $^3J_{Pt,H}$ not resolved, 48H, NCH_2), 3.03 (br s, $^3J_{Pt,H}$ not resolved, 144H, NCH_3). ^{13}C NMR (CD_2Cl_2, 75 MHz): most relevant peaks δ 143.60, 136.57, 107.92, 76.10, 70.60, 54.64. MALDI-TOF-MS: *m/z* 6381.64 ([M–Br]$^+$, calcd 6386.48). Anal. Calcd for $C_{198}H_{258}Br_{12}N_{24}Pt_{12}O_{12}$: C, 36.78; H, 4.02; N, 5.20. Found: C, 36.94; H, 4.20; N, 5.11.

Synthesis of 9c: A solution of $AgBF_4$ (75 mg, 0.38 mmol) in water (1 mL) was added to a suspension of **9a** (0.19 g, 32.0 μmol) in acetone (10 mL) and the resulting mixture was stirred at room temperature in the absence of light for 1 h. The reaction mixture was filtered through Celite and the Celite was washed with acetone (10 mL). The filtrate was concentrated to 3 mL and dropwise addition of Et_2O (10 mL) resulted in an off-white precipitate, which was collected and dried *in vacuo*. Yield: 0.17 g (91%). ^{1}H NMR (acetone-d_6, 200 MHz): δ 7.07 (s, 12H, Ar*H*), 7.05 (s, 6H, Ar*H*), 6.45 (s, 24H, Ar*H*), 4.75 (s, 24H, OCH_2), 4.00 (s, 48H, NCH_2), 2.80 (s, 144H, NCH_3).

^{13}C NMR (acetone-d_6, 75 MHz): δ 158.30, 146.17, 140.96, 140.36, 136.67, 129.66, 122.54, 107.88, 73.51, 69.90, 52.04.

3.5. References and Notes

[1] a) Knapen, J. W. J.; van der Made, A. W.; de Wilde, J. C.; van Leeuwen, P. W. N. M.; Wijkens, P.; Grove, D. M.; van Koten, G. *Nature* **1994**, *372*, 659. b) Kragl, U.; Dreisbach, C. *Angew. Chem. Int. Ed.* **1996**, *35*, 642. c) Reetz, M. T.; Lohmer, G.; Schwickardi, R. *Angew. Chem. Int. Ed.* **1997**, *36*, 1526. d) Giffels, G.; Beliczey, J.; Felder, M.; Kragl, U. *Tetrahedron: Asymm.* **1998**, *9*, 691. e) Brinkmann, N.; Giebel, D.; Lohmer, G.; Reetz, M. T.; Kragl, U. *J. Cat.* **1999**, *183*, 163. f) Hovestad, N. J.; Eggeling, E. B.; Heidbüchel, H. J.; Jastrzebski, J. T. B. H.; Kragl, U.; Keim, W.; Vogt, D.; van Koten, G. *Angew. Chem. Int. Ed.* **1999**, *38*, 1655. g) de Groot, D.; Eggeling, E. B.; de Wilde, J. C.; Kooijman, H.; van Haaren, R. J.; van der Made, A. W.; Spek, A. L.; Vogt, D.; Reek, J. N. H.; Kamer, P. C. J.; van Leeuwen, P. W. N. M. *Chem. Commun.* **1999**, 1623. h) Kleij, A. W.; Gossage, R. A.; Klein Gebbink, R. J. M.; Reyerse, E. J.; Brinkmann, N.; Kragl, U.; Lutz, M.; Spek, A. L.; van Koten, G. *J. Am. Chem. Soc.* **2000**, *122*, 12112. i) Albrecht, M.; Hovestad, N. J.; Boersma, J.; van Koten, G. *Chem. Eur. J.* **2001**, *7*, 1289. j) Rissom, S.; Beliczey, J.; Giffels, G.; Kragl, U.; Wandrey, C. *Tetrahedron: Asymm.* **1999**, *10*, 923. k) Dwars, T.; Haberland, J.; Grassert, I.; Kragl, U. *J. Mol. Cat. A: Chem.* **2001**, *168*, 81.

[2] For reviews on dendritic catalysts see: a) Kreiter, R.; Kleij, A. W.; Klein Gebbink, R. J. M.; van Koten, G. *Topics in Current Chemistry, Dendrimers IV*; Vögtle, F., Ed.; Springer-Verlag Berlin Heidelberg, **2001**, *217*, 163. b) Kleij, A. W.; Klein Gebbink, R. J. M.; van Koten, G. *Dendrimers and other Dendritic Polymers*; Frechet, J., Tomalia, D., Eds.; Wiley, New York, **2002**. c) Oosterom, G. E.; Reek, J. N. H.; Kamer, P. C. J.; van Leeuwen, P. W. N. M. *Angew. Chem. Int. Ed.* **2001**, *40*, 1828.

[3] For an overview on homogeneous catalyst recycling using ultra- or nanofiltration techniques, see: Dijkstra, H. P.; van klink, G. P. M.; van Koten, G. *Acc. Chem. Res.*, in press, manuscript available on the world wide web: http://pubs3.acs.org/acs/journals.

[4] a) Constable, E. C.; Thompson, A. M. W. *J. Chem. Soc., Dalton Trans.* **1992**, 3467. b) Armspach, D.; Cattalini, C.; Constable, E. C.; Housecroft, C. E.; Phillips, D. *Chem. Commun.* **1996**, 1823. c) Huck, W. T. S.; Snellink-Ruël, B.; van Veggel, F. C. J. M.; Reinhoudt, D. N. *Organometallics* **1997**, *16*, 4287. d) Huck, W. T. S.; Prins, L. J.; Fokkens, R. H.; Nibbering, N. M. M.; van Veggel, F. C. J. M.; Reinhoudt, D. N. *J. Am. Chem. Soc.* **1998**, *120*, 6240. e) Hoare, J. L.; Lorenz, K.; Hovestad, N. J.; Smeets, W. J. J.; Spek, A. L.; Canty, A. J.; Frey, H.; van Koten, G. *Organometallics* **1997**, *16*, 4167. f) Dijkstra, H. P.; Meijer, M. D.; Patel, J.; Kreiter, R.; van Klink, G. P. M.; Lutz, M.; Spek, A. L.; Canty, A. J.; van Koten, G. *Organometallics*, **2001**, *20*, 3159. g) Dijkstra, H. P.; Albrecht, M.; van Koten, G. *Chem. Commun.* **2002**, 126.

[5] a) Albrecht, M.; Gossage, R. A.; Spek, A. L.; van Koten, G. *Chem. Commun.* **1998**, 1003. b) Tzalis, D.; Tor, Y. *Chem. Commun.* **1996**, 1043. c) Albrecht, M.; Schlupp, M.; Bargon, M.; van Koten, G.

Chem. Commun. **2001**, 1874.

[6] Alsters, P. L.; Baesjou, P. J.; Janssen, M. D.; Kooijman, H.; Sicherer-Roetman, A.; Spek, A. L.; van Koten, G. *Organometallics* **1992**, *11*, 4124.

[7] Canty, A. J.; Patel, J.; Skelton, B. W.; White, A. H. *J. Organomet. Chem.* **2000**, *599*, 195.

[8] Davies, P. J.; Veldman, N.; Grove, D. M.; Spek, A. L.; Lutz, B. T. G.; van Koten, G. *Angew. Chem. Int. Ed.* **1996**, *35*, 1959.

[9] See ref. 4f and: Duchêne, K. -H.; Vögtle, F. *Synthesis* **1986**, 659.

[10] Rettig, M. F.; Maitlis, P. M.; Cotton, F. A.; Webbs, T. R. *Inorg. Synth.* **1971**, 134.

– Chapter 4 –

Functionalized Pincer-Palladium(II) Complexes: Synthesis, Catalysis and DFT-Calculations

Abstract: A series of YCY-Pd^{II} complexes (Y = NMe_2, pz, pz*, SPh and PPh_2) and *para*-substituted NCN-Pd^{II} complexes were synthesized in order to investigate the influence of both the donor substituents Y and the *para*-substituents at the Lewis-acidic palladium(II) centers. Therefore, the various cationic pincer-palladium(II) complexes were applied as Lewis-acid catalysts in the double Michael reaction between methyl vinyl ketone and ethyl-α-cyanoactetate. In addition, the electronic influences of the various *para*-substituents at the cationic Pd^{II}-centers of the *para*-functionalized NCN-Pd^{II} complexes were studied by DFT-calculations. The catalytic results revealed that the donor substituent Y has a significant impact on the catalytic activity, while both catalysis and DFT-calculations showed only minor influences from the *para*-substituents on the cationic palladium(II) centers. In addition, several shape-persistent multi(NCN-Pd^{II}) complexes were applied as Lewis-acid catalysts in the double Michael reaction. A similar or even enhanced catalytic activity per Pd^{II}-center was found as compared to the mononuclear analogs.

H. P. Dijkstra, M. D. Meijer, J. Patel, R. Kreiter, G. P. M. van Klink, M. Lutz, A. L. Spek, A. J. Canty, G. van Koten, *Organometallics* **2001**, *20*, 3159.

H. P. Dijkstra, M. Q. Slagt, A. McDonald, C. A. Kruithof, R. Kreiter, A. M. Mills, M. Lutz, A. L. Spek, W. Klopper, G. P. M. van Klink, G. van Koten, submitted.

4.1. Introduction

Metalated pincer complexes (see Figure 1) have been successfully applied as homogeneous catalysts in many organic transformations.[1] Advantageous to the pincer system is the ease of alteration of several functionalities, allowing fine-tuning of these pincer complexes for the desired application.[2] The donor substituents Y can be varied easily, giving acces to NCN- (Y = NR'_2), PCP- (Y = PR'_2) and SCS-type (Y = SR') pincer ligands. As a result, metal centers such as palladium, platinum, nickel, iridium, ruthenium and rhodium can nowadays be introduced into the various pincer ligands thereby allowing application of pincer catalysts in a broad range of catalytic reactions.[2] Furthermore, chirality can be introduced into the pincer catalysts via the benzylic substituent R" and/or the donor group Y, opening the possibility for asymmetric catalysis.[3] In addition, the electronic as well as the steric environment of the metal center can be fine-tuned by variation of the substituent Y and/or the R'-groups attached to Y.[3c] For example, different catalytic activities were found for palladated, cationic PCP-[3b] and bisoxazolinyl-type[3c] pincer ligands, respectivly, in aldol-type reactions. Also the *para*-substituent R (Figure 1) can be used to influence the electron density at the metal center. An illustrative example of the *para*-substituent influence on the reactivity of a pincer-metal catalyst was reported by Van de Kuil *et al.*, in which various *para*-substituted NCN-Ni^{II} catalysts were studied in the Kharasch addition reaction.[1d,4] Electron-donating and withdrawing substituents were found to have a significant effect at the Ni^{II}/Ni^{III} oxidation potential, the crucial step in the catalytic cycle of the Kharasch addition.

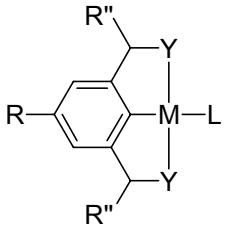

Y = NR'_2, PR'_2, SR'
M = Pd, Pt, Ni, Ru, Rh, Ir, Fe, Au
R" = hydrogen, alkyl
R = hydrogen, halides, alkyl, aryl, dendrimers, fullerenes, peptides

Figure 1. The metalated pincer system.

Immobilization of pincer catalysts on soluble or solid supports in order to prepare recyclable catalysts has been intensively studied in recent years.[1e,5] It was demonstrated that the *para*-position (R, Figure 1) is excellent for anchoring these

pincer complexes to support materials.[1e,5] In the present study, shape-persistent multi(YCY-metal) complexes are investigated as homogeneous catalysts. In particular, their application in a nanofiltration membrane reactor under continuously operating conditions to enhance the total turnover numbers (ttn) per metal center by catalyst recycling is studied.[6,7,8] For the design and synthesis of nanosize homogeneous catalysts based on pincer metal building blocks, knowledge about the influence of the donor substituent Y on the catalytic activity is important. Additionally in this field of research, it is desirable to be able to use diverse functionalities at the *para*-position of the pincer complex for anchoring purposes. Concerning this latter aspect, it is important to estimate beforehand any uncontrolled influences by these *para*-functionalities on the catalytic properties of the pincer-metal moieties. Therefore, we set out a study to investigate the influence of both the donor substituent Y and the *para*-substituents on the catalytic activity of pincer complexes in organic transformations. We decided to use the double Michael reaction between methyl vinyl ketone (MVK) and ethyl-α-cyanoacetate[3c] for our studies, because the conditions nicely meet the requirements for the commercially available nanofiltration membranes.[9] A number of cationic YCY-Pd^{II} complexes (**1**, X = $OH_2(BF_4)$, Figure 2) as well as various *para*-functionalized, cationic NCN-Pd^{II} complexes (**2**, X = $OH_2(BF_4)$, Figure 2) were prepared and applied as Lewis-acidic catalysts in the double Michael reaction. We also performed density functional theory (DFT) calculations on the *para*-functionalized NCN-systems (**2**) to gain insight into the electronic influence of the *para*-substituents at the Pd^{II}-center. Furthermore, palladated shape-persistent multi(NCN-pincer) complexes, in which the pincer-moiety is anchored to the various supports via different *para*-functionalities, were also included in this study.

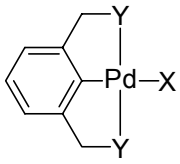

Y = NMe_2 (**1a**), pz (= pyrazol-1-yl, **1b**)
pz* (= 3,5-dimethylpyrazol-1-yl, **1c**)
SPh (**1d**), PPh_2 (**1e**)

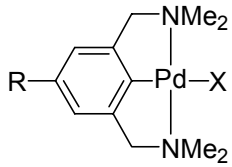

R = NO_2 (**2a**), NMe_2 (**2b**), C(O)Me (**2c**),
OCH_2Ph (**2d**), Ph (**2e**), $SiMe_3$ (**2f**)

Figure 2. A series of YCY-pincer palladium(II) complexes.

4.2. Results and Discussion

Synthesis of YCY-Pd^{II} complexes. YCY-pincer complexes **1a–e** and *para*-functionalized NCN-pincer complexes **2a–f** were selected for this study (Figure 2). Neutral complexes **1a** (X = Br),[10] **1b** (X = Cl),[11] **1d** (X = Cl),[12] **1e** (X = Cl),[13] **2a** (X = Br)[14] and **2f** (X = Cl)[15] were prepared following literature procedures. The palladium complex **1c** (X = Cl) was prepared in a two step sequence (Scheme 1). First bis(3,5-dimethylpyrazol-1-yl) ligand **3** was prepared from 2,6-bis(bromomethyl)benzene and the potassium salt of 3,5-dimethylpyrazole, followed by a direct electrophilic palladation of **3** using $Pd(OAc)_2$ in refluxing acetic acid and subsequent treatment with LiCl.[16]

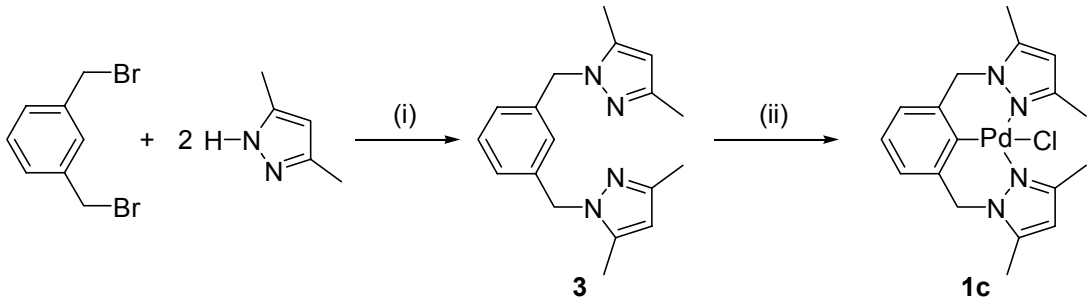

Scheme 1. (i) K, THF, reflux, 18 h; (ii) $Pd(OAc)_2$, AcOH, reflux, 2 h, followed by LiCl, acetone, rt, 18 h.

Palladium(II) complex **2b** (X = Br) was prepared in two steps (Scheme 2). Treatment of *para*-amino pincer derivative **4**[17] with formaldehyde and formic acid, yielded the desired ligand **5b** in 62% yield. Treatment of **5b** with $Pd_2(dba)_3{\cdot}CHCl_3$ in benzene, afforded NCN-palladium(II) complex **2b** (Scheme 2). The *para*-acetyl substituted NCN-pincer complex **2c** (X = Br) was prepared following the same palladation procedure, starting from the previously prepared ligand precursor **5c**[17] (Scheme 2).

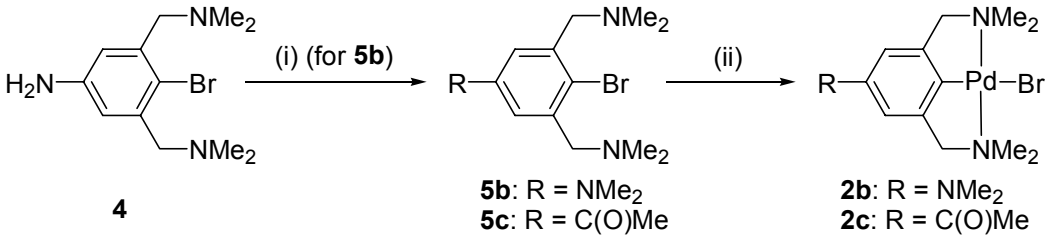

Scheme 2. (i) Formaldehyde, formic acid, rt, 3 h; (ii) $Pd_2(dba)_3{\cdot}CHCl_3$, C_6H_6, rt, 3 h.

para-Benzyloxy pincer complex **2d** (X = I,) was synthesized following a procedure recently developed for the synthesis of nanosize multipincer complexes (Scheme 3, see also Chapter 3).[7b] Treatment of a mixture of the *para*-(*t*-butyldimethylsilyl)-protected phenolic pincer **6**, benzyl bromide, potassium carbonate and 18-crown-6 with tetrabutylammonium fluoride in acetone resulted in the formation of **2d** in 80% yield. Note that the metal is already present during the introduction of the *para*-substituent, showing the versatility and strength of the pincer system.[18]

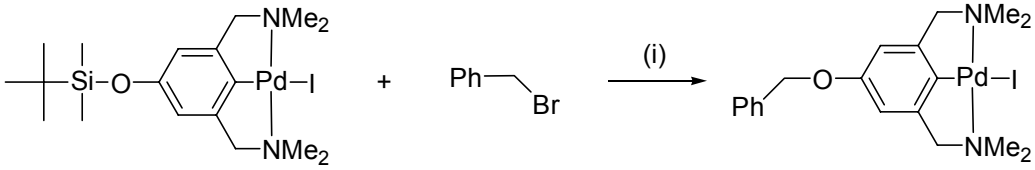

6 **2d**

Scheme 3. (i) Bu_4NF, K_2CO_3, 18-crown-6, acetone, rt, 18 h.

para-Phenyl pincer complex **2e** (X = Cl) was synthesized from *para*-phenyl substituted NCN-ligand precursor **7**[19] via a lithiation/transpalladation procedure in 83% yield (Scheme 4).

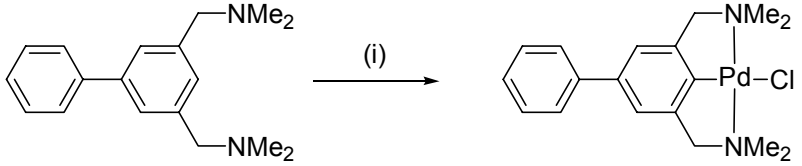

7 **2e**

Scheme 4. (i) *n*-BuLi, hexanes, –80 °C → rt, 4 h, followed by $[PdCl_2(cod)]$, Et_2O, rt, 3 h.

Noteworthy is that four different methods were used to arrive at the various YCY-Pd^{II} complexes: i) a direct cyclometalation (**1b–e**), ii) an oxidative addition reaction (**1a**, **2a–c**), iii) a lithiation/transmetalation reaction (**2e** and **2f**), and iv) the introduction of the *para*-substituent with the metal already present in the pincer ligand (**2d**). These examples illustrate the wide variety of reactions which can be used to prepare functionalized pincer-metal complexes. Especially for the synthesis of

multi(YCY-metal) complexes, having a variety of methods available to construct the multimetallic material is considered to be of great importance.[6,7]

The neutral YCY-Pd^{II} complexes **1a–e** and **2a–f** were readily converted into the corresponding cationic species **8a–k**, the Lewis-acidic catalyst precursors for the double Michael reaction, by treatment with silver tetrafluoroborate in wet acetone (Scheme 5).[20]

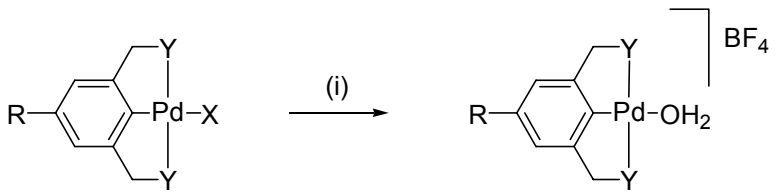

1a - **e**, **2a** - **f**

R = H: **8a** (Y = NMe_2), **8b** (Y = pz), **8c** (Y = pz*), **8d** (Y = SPh), **8e** (Y = PPh_2)

Y = NMe_2: **8f** (R = NO_2), **8g** (R = NMe_2), **8h** (R = C(O)Me) **8i** (R = OCH_2Ph), **8j** (R = Ph), **8k** (R = $SiMe_3$)

Scheme 5. (i) $AgBF_4$, wet acetone, rt, 1 h.

Crystals suitable for X-ray crystal structure determination were obtained for neutral NCN-palladium complexes **2b** and **2c** (Figure 3a and 3b, respectively). The molecular structures comprise square-planar palladium(II) centers ligated by a terdentate η^3-coordinating NCN-ligand and a bromine ligand *trans* to the aryl ring of the pincer ligand. Table 1 summarizes a number of representative interatomic bond

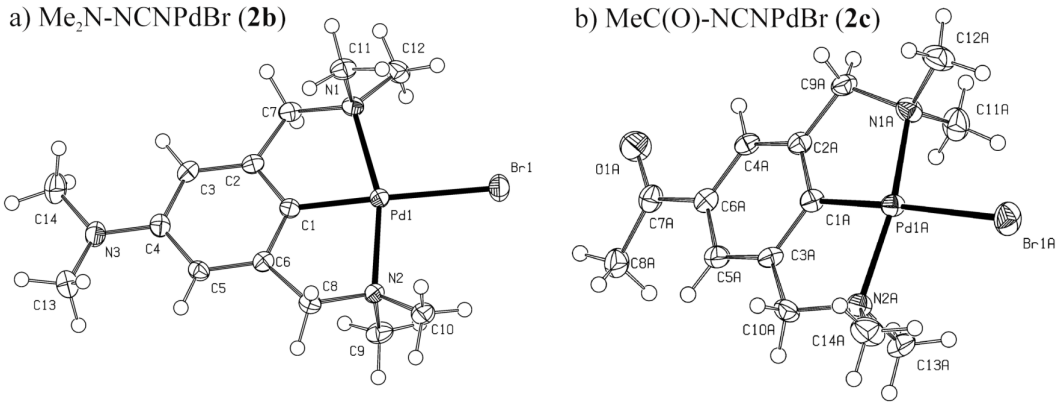

Figure 3. Crystal structures of *para*-substituted NCNPdBr complexes; ORTEP 50% displacement ellipsoids. a) Me_2N-NCNPdBr (**2b**); b) One of the two independent molecules of MeC(O)-NCNPdBr (**2c**).

lengths and angles of **2b** and **2c**. The crystal structure of **2c** contains two independent molecules, of which only one is shown in Figure 3b. The two molecules differ only slightly in the conformation of the acetyl substituent with respect to the pincer-palladium fragment. In both **2b** and **2c**, the *para*-substituents are nearly coplanar with the pincer-aryl ring, as can be concluded from the dihedral angles given in Table 1. This coplanarity is commonly observed in the crystal structures of molecules containing a Me_2N- or MeC(O)-aryl moiety.[21] Furthermore, as indicated by the small differences in the Pd–Br distances (for **2a**, the Pd–Br distance = 2.5516(3) Å),[22] the different *para*-substituents have only minor influences on the electron density at the palladium center.

Table 1. Interatomic bond lengths (Å) and angles (deg) of **2b** and **2c**.

2b		**2c**[a]	
	Bond lengths		
Pd1-C1	1.921(2)	Pd1A-C1A	1.911(5)
Pd1-Br1	2.5565(3)	Pd1A-Br1A	2.5636(7)
Pd1-N1	2.119(2)	Pd1A-N1A	2.121(4)
Pd1-N2	2.1171(19)	Pd1A-N2A	2.120(4)
C4-N3	1.387(3)	C6A-C7A	1.499(7)
	Bond angles		
C1-Pd1-Br1	176.99(7)	C1A-Pd1A-Br1A	172.98(15)
C1-Pd1-N1	80.32(9)	C1A-Pd1A-N1A	82.02(19)
C1-Pd1-N2	81.16(9)	C1A-Pd1A-N2A	81.98(18)
N1-Pd1-N2	161.45(7)	N1A-Pd1A-N2A	161.80(16)
	Dihedral Angles		
C14-N3-C4-C5	179.6(2)	C5A-C6A-C7A-O1A	167.6(5)

a) Only the values for one of the two independent molecules are given.

Density Functional Theory (DFT) Calculations. To further investigate the electronic influences of the *para*-substituents on the Lewis acidity of the palladium(II) center, DFT-calculations were performed on cationic, *para*-functionalized NCN-catalyst precursors **8a**, **8f–k** (see Scheme 5). Recently, similar calculations on substituted NCN-Pt^{II} complexes showed that the calculated structures correlated well with the experimental observations.[14b] In addition, the calculated Mulliken charge at the Pt^{II}-centers showed a linear relationship with the chemical shifts of the Pt-nuclei

in the ^{195}Pt NMR spectra of the various complexes as well as with the σ_p Hammett parameter of the various *para*-substituents.[14b] The DFT-method B3LYP/LANL2DZ[23] as implemented in Gaussian 98[24] was used to calculate the partial charge, by means of Mulliken population analysis, at the palladium(II) centers of *para*-substituted NCN-catalyst precursors **8a**, **8f–k**. Table 2 summarizes a number of selected data which were obtained from these calculations and also displays the Hammett parameters (σ_p) of the various *para*-substituents.

Both from the Mulliken charge at the Pd^{II}-centers and from the Pd–OH_2 and Pd–C_{ipso}(aryl) distances, it becomes clear that the *para*-substituent R has only a minor electronic influence on the palladium(II) centers, and thus on the Lewis acidity. Nevertheless, the complexes with the highest Mulliken charge at the Pd^{II}-center (**8f** and **8h**, most electron withdrawing substituents) have the shortest calculated Pd–OH_2 distances, while complex **8g** (most electron donating substituent) possessing the lowest Mulliken charge at the Pd^{II}-center displays the largest Pd–OH_2 distance (Table 2). In addition, plotting the Hammett parameters (σ_p) against the calculated Mulliken charges at the Pd^{II}-centers of **8a**, **8f–k**, clearly demonstrates the expected trend (Figure 4). Although, the linear fit is rather poor (in particular **8f** shows a significant deviation), this result indicates that DFT-calculations can be used to predict the relative electronic influence of *para*-substituents on catalytically active metal centers.

Table 2: Selected data obtained from DFT-calculation with **8a**, **8f–k**, $[R\text{-}NCNPd(OH_2)]^+$.

***p*-R**	**Compound**	**Charge Pd (e)**[a]	**Pd–OH_2 (Å)**	**Pd–C_{ipso} (Å)**	**σ_p**[b]
H	**8a**	0.187	2.286	1.942	0
NO_2	**8f**	0.217	2.273	1.938	0.778
NMe_2	**8g**	0.171	2.293	1.940	–0.83
C(O)Me	**8h**	0.195	2.281	1.939	0.502
OCH_2Ph	**8i**	0.183	2.286	1.941	–0.42
Ph	**8j**	0.179	2.286	1.940	–0.01
$SiMe_3$	**8k**	0.183	2.285	1.941	–0.07

a) Mulliken population analysis; b) Hammett parameters for the various *para*-substituents were obtained from Exner.[25]

Catalysis using cationic YCY-Pd^{II} catalysts. Cationic YCY-Pd^{II}-aqua complexes **8a–k** were applied as homogeneous Lewis acid catalysts in the double Michael reaction between methyl vinyl ketone (MVK) and ethyl-α-cyanoacetate (Scheme 6).

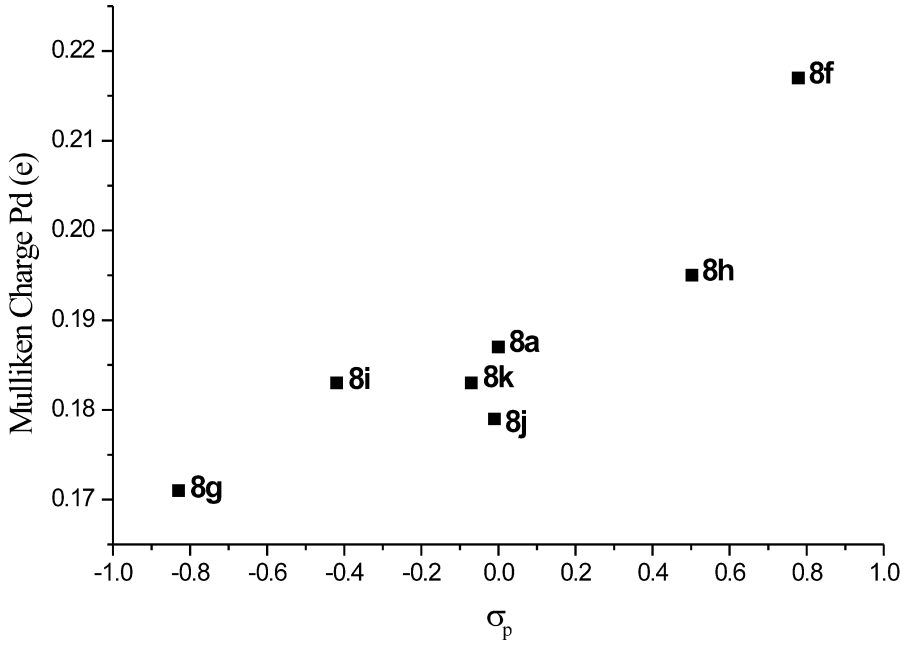

Figure 4. Linear relationship between Hammett parameter (σ_p) of the *para*-substituents and Mulliken charge at Pd-centers.

In all cases, 0.5 mol% [Pd^{II}] centers was used. The results are summarized in Table 3. From these results it becomes clear that pincer complexes based on NCN-type ligands (**8a–c**) are the most active catalysts in this reaction. The PCP-pincer complex **8e** shows rather low activity, while the reaction catalyzed by the SCS-pincer complex **8d** is hardly faster than the blank reaction. Remarkably, the catalytic activity of **8c** is considerably higher than the activity of **8b**. The only difference between the two catalysts is that **8c** contains two electron-donating methyl substituents in the pyrazolyl group (pz*), making **8c** a weaker Lewis acid than **8b**. The effect of the methyl group

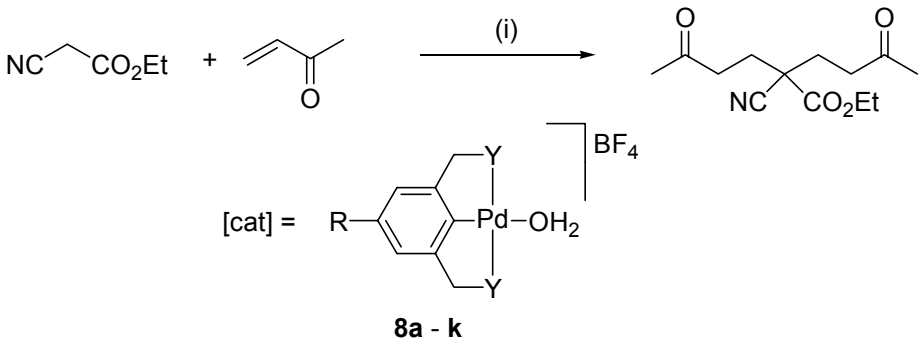

Scheme 6. Double Michael reaction between MVK and ethyl-α-cyanoacetate. (i) *i*Pr_2NEt (10 mol%), [cat] (0.5 mol%), CH_2Cl_2, rt.

substitution can be seen by comparing the pK_a of 1-Mepz (pK_a = 1.19) with that of 1,3,5-Me_3pz (pK_a = 2.90).[26] Thus, although **8c** is a weaker Lewis acid than **8b**, it is the most active catalyst tested in this series and also the most active catalyst of the pincer-type reported in literature so far for this particular reaction.

The k_{obs} and the half-life times ($t_{1/2}$) found for the various *para*-substituted NCN-Pd^{II} catalysts (**8a**, **8f–k**, Table 3), reveal that the *para*-substituents exert only a small influence at the catalytic activity of the Pd^{II}-centers for this particular reaction. Only **8g** (R = Me_2N, Table 3) displays a significantly lower activity in this reaction compared to the other *para*-functionalized NCN-pincer catalysts.

Table 3. Catalytic results of **8a–k** in the double Michael reaction.

Catalyst	Y	*p*-R	k_{obs} ($\times 10^{-6}$ s^{-1})[a]	$t_{1/2}$ (min)[b]
8a	NMe_2	H	280	41
8b	pz	H	130	86
8c	pz*	H	350	33
8d	SPh	H	4.2	2800
8e	PPh_2	H	9.5	1200
8f	NMe_2	NO_2	220	53
8g	NMe_2	NMe_2	130	89
8h	NMe_2	C(O)Me	230	50
8i	NMe_2	OCH_2Ph	240	48
8j	NMe_2	Ph	270	43
8k	NMe_2	$SiMe_3$	260	44
blank			3.8	3056

a) Determined by ^{1}H NMR spectroscopy by comparison of the integration of the α-CH_2 protons of ethyl-α-cyanoacetate to the combined integration of the ethyl ester CH_2 protons of the reactant and product. First-order reactions CN (CN = ethyl-α-cyanoacetate); rate constant k was determined by plotting $-\ln([CN]/[CN]_0)$ *versus* time (in seconds); b) $t_{1/2} = \ln 2 / (k \times 60)$.

Comparison of the experimental catalytic data with the theoretical data, reveals that there is no linear relationship between the observed rate constants (k_{obs}, Table 3) and the calculated Mulliken charges at the Pd^{II}-centers of **8a**, **8f–k** (Table 2). Plotting the Hammett σ_p-parameters of the various *para*-substituents against the $\log(k_{obs})$ of **8a**, **8f–k** resulted in a curved function passing through a maximum (Figure 5). This type of behavior has previously been observed for reactions in which a reversible step is followed by an irreversible step.[27] Apparently, the *para*-substituents alter the relative magnitude of the rate constants of the individual

mechanistic steps and thus change the rate-determining step. In the double Michael reaction, a reversible step – deprotonation of the α-CH_2-group of ethyl-α-cyanoacetate – is followed by an irreversible step – the 1,4-addition of the ethyl-α-cyanoacetate anion to MVK. Thus, changing the *para*-substituent from an electron withdrawing to an electron donating group can shift the rate-determining step from the deprotonation step to the nucleophilic 1,4-addition step. From the catalytic data presented in Table 3, it seems that the *para*-NMe_2 substituent has the largest influence, as the activity of **8g** was found to be considerably lower than that of other *para*-substituted NCN-catalysts. This hypothesis can also explain the difference in catalytic activity found for **8b** and **8c** (Table 3). Thus, for Y = pz or pz*, probably not a deprotonation step but rather a nucleophilic 1,4-addition step or the dissociation of the product or an intermediate from the metal center determines the rate of the reaction, as such a step is expected to be faster for weaker Lewis acids. Further research to elucidate this change in rate-determining step is currently under investigation.

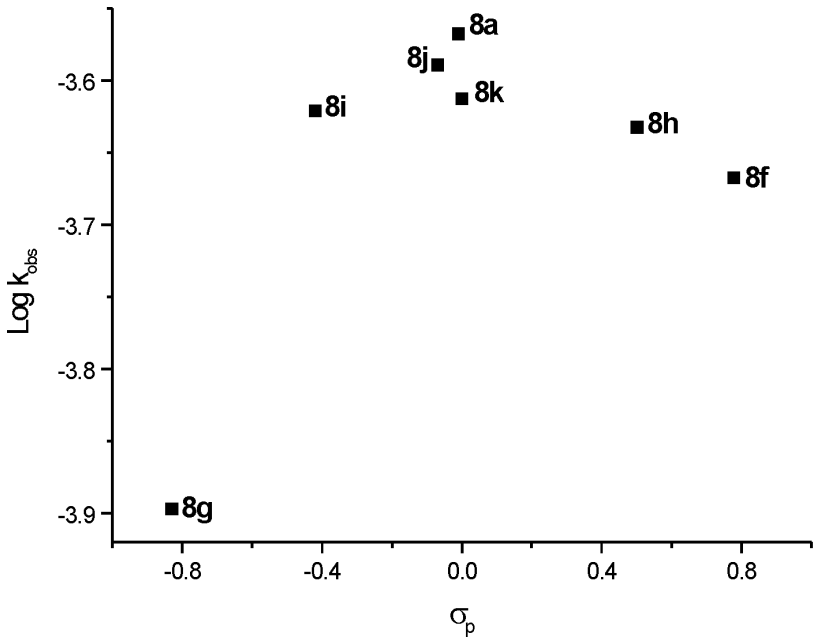

Figure 5. Hammett σ_p-parameter *versus* log(k_{obs}) of **8a**, **8f–k**.

Catalysis using multi(NCN-Pd^{II}) catalysts. Previously, we reported the synthesis of shape-persistent multi(NCN-Pd^{II}) catalyst precursors **9–12** (Figure 6).[28] These complexes were also applied as homogeneous catalysts in the double Michael reaction between MVK and ethyl-α-cyanoacetate (Scheme 6). The catalytic results are

summarized in Table 4. In all cases, 0.5 mol% [Pd^{II}] centers was used and the k_{obs} for the various multimetallic systems were determined per palladium(II) center.

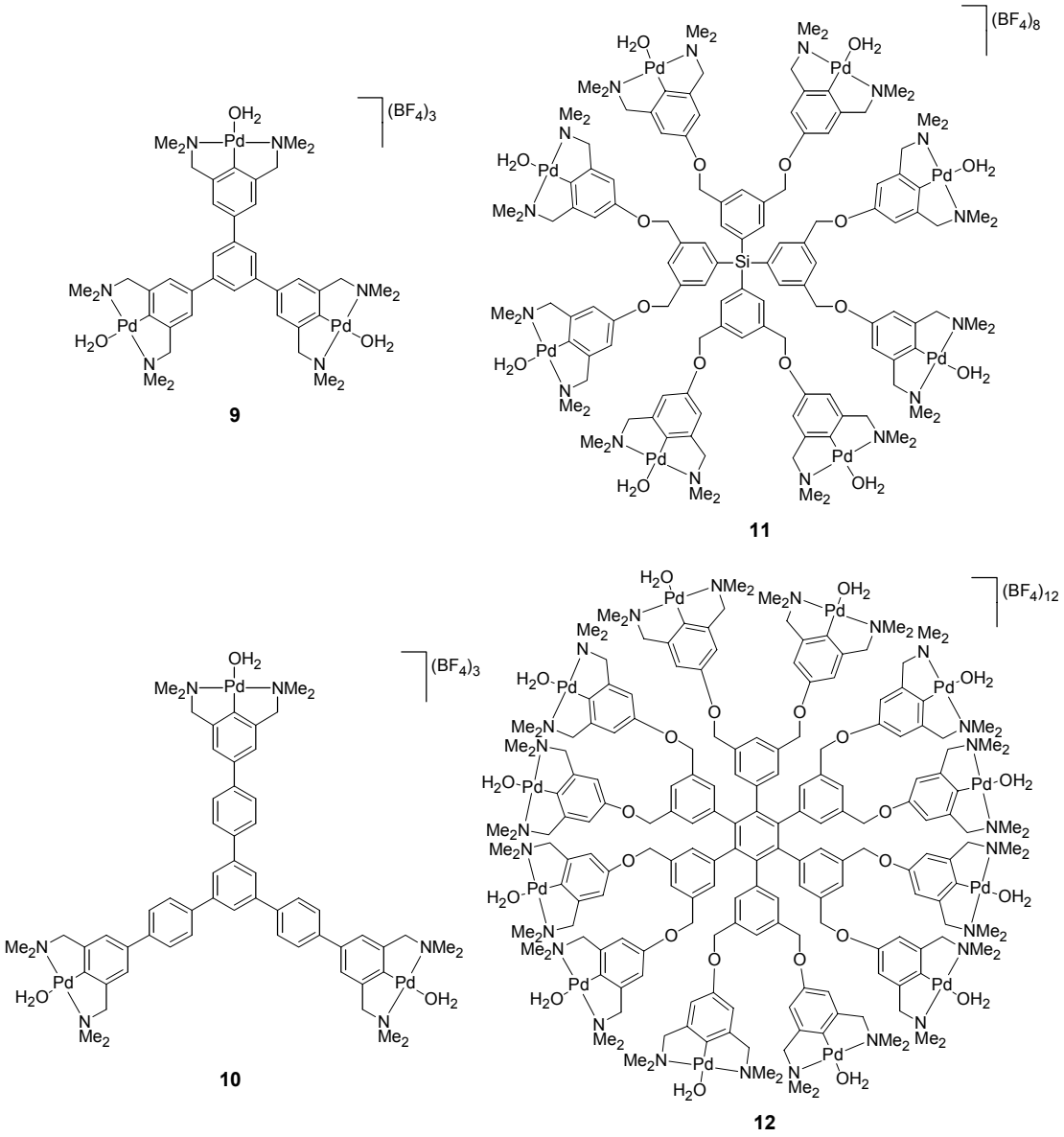

Figure 6. Shape-persistent homogeneous Lewis-acidic catalyst precursors **9–12**.

Compared to the catalytic activity of the reference monometallic catalyst **8a** (R = H, Table 3), it becomes clear that the catalytic activities per palladium(II) center for multi(NCN-Pd^{II}) catalysts **9–11** (Table 4) are similar, indicating that all palladium(II) centers in **9–11** act as independent catalytic sites. This is an important result: it implies an efficient use of all catalytic sites in catalysis. In addition, it once

again underlines that the (Lewis acidic) catalytic activity hardly depends on the *para*-functionality of the pincer moiety, which is in agreement with the results obtained for the monometallic *para*-substituted NCN-Pd^{II} catalysts (**8a**, **8f–k**, Table 3). Interestingly, the dodecakis(NCN-Pd^{II}) catalyst **12** exhibits an almost threefold increase in catalytic activity per Pd^{II}-center (Table 4) as compared to reference **8a** (R = H, Table 3). This increase in catalytic activity does not originate from the influence of the *para*-substituent, since no increase in catalytic activity was observed for **8i** (R = OCH_2Ph, Table 3) and **11** (Table 4), both possessing the same *para*-substituent as **12**. Molecular modeling studies of the isostructural platinum analogs of **11** and **12**,[7b] respectively, already indicated that on average the metal sites are in closer proximity to each other in the case of **12**, suggesting cooperative effects between the Pd^{II}-centers during catalysis. Another possible explanation is that large aggregates of **12**, induced by the polar organometallic periphery, assemble in solution, resulting in the formation of polar micro-environments and thereby enhancing the catalytic transformations. This aggregate formation would be more difficult for **11** due to its spherical geometry.

Table 4. Catalytic activities of **9–12** in the double Michael reaction

Catalyst	k_{obs} ($\times 10^{-6}$ s^{-1})[a]	$t_{1/2}$ (min)[b]
9	230	50
10	260	44
11	210	55
12	810	14

a) Determined by ^1H NMR spectroscopy by comparison of the integration of the α-CH_2 protons of ethyl-α-cyanoacetate to the combined integration of the ethyl ester CH_2 protons of the reactant and product. First-order reactions CN (CN = ethyl-α-cyanoacetate); rate constant k was determined by plotting $-\ln([CN]/[CN]_0)$ *versus* time (in seconds). b) $t_{1/2} = \ln 2 / (k \times 60)$

4.3. Conclusions

A series of YCY-Pd^{II} complexes was synthesized and the influence of both the donor substituents Y and various *para*-substituents at the Lewis-acidic palladium(II) centers was investigated by means of catalysis and/or DFT-calculations. The application of YCY-Pd^{II} complexes as homogeneous Lewis-acid catalysts in the double Michael reaction between MVK and ethyl-α-cyanoacetate, clearly showed that the donor substituent Y has a significantly larger impact on the catalytic activity of the Pd^{II}-centers than the various *para*-substituents. While a large fluctuation was

observed upon changing Y, in the *para*-functionalized NCN-pincer series only the *para*-dimethylamino substituent (**8g**) showed a considerable decrease in catalytic activity. These latter results were confirmed by DFT-calculations, which revealed that the *para*-substituents have only minor influences on the partial charge (expressed by the Mulliken population) and thus on the Lewis acidity of the palladium(II) centers. In addition, several shape-persistent multi(NCN-Pd^{II}) complexes were applied as Lewis-acid catalysts in the double Michael reaction. The catalysis results of **9–11** showed that all catalytic sites act as independent catalysts; the activities per Pd^{II}-center were similar to the activities found for the mononuclear analogs. Surprisingly, the dodecakis(NCN-Pd^{II}) system **12** exhibited a threefold increase in catalytic activity, probably due to cooperativity between metalated pincer groups at the periphery of **12**. Retention measurements with the isostructural platinum analogs of **9–12** in a nanofiltration membrane reactor, revealed that these shape-persistent complexes are very efficiently retained by nanofiltration membranes.[7b] Currently, these shape-persistent nanosize complexes are being further explored as homogeneous catalysts in a nanofiltration membrane reactor under continuously operating conditions.

4.4. Experimental Section

General: Solvents were purified and dried according to standard procedures, stored under a nitrogen atmosphere and freshly distilled prior to use. NMR solvents were purchased and used without further purification. Compounds **1a**,[10] **1b**,[11] **1d**,[12] **1e,**[13] **2a**,[14] **2f**,[15] **4**,[17] **5c**,[17] **6**,[7b] **7**,[19] **8a**,[20] **8b**[11] and $[PdCl_2(cod)]$[29] were prepared according to literature procedures. All other reagents were purchased and used without further purification. NMR spectra were recorded on a Varian 300 spectrometer (^{1}H NMR: 300.1 MHz; ^{13}C NMR: 75.5 MHz; ^{31}P NMR: 121.5 MHz) or a Varian Gemini 200 spectrometer (^{1}H NMR: 200.1 MHz; ^{13}C NMR: 50.3 MHz; ^{31}P NMR: 81.0 MHz). Microanalyses were determined by either Dornis and Kolbe, Mikroanalytisches Laboratorium, Mülheim, Germany, or the Central Science Laboratory, University of Tasmania.

Synthesis of 1,3-bis[(3,5-dimethylpyrazol-1-yl)methyl]benzene (3): To a stirring suspension of finely cut potassium (1.12 g, 29.9 mmol) in THF (60 mL) under an argon atmosphere was added 3,5-dimethylpyrazole (2.88 g, 29.9 mmol). The mixture was heated to reflux and maintained at this temperature until beads of molten potassium were no longer evident (~3 h). The solution was cooled to ambient

temperature and 2,6-bis(bromomethyl)benzene (3.59 g, 13.6 mmol) was added in one portion. The reaction mixture was allowed to stand at reflux overnight, quenched by addition of water (0.1 mL), filtered and the solvent removed *in vacuo*. The product, 1,3-(3,5-$Me_2pzCH_2)_2C_6H_4$ (**3**), was purified by distillation. Yield: 3.27 g (82%). Mp: 68–71 ˚C. ^{1}H NMR ($CDCl_3$, 300 MHz): δ 7.24 (t, $^3J_{H,H}$ = 7.7 Hz, 1H, Ar*H*), 6.94 (d, $^3J_{H,H}$ = 7.8 Hz, 2H, Ar*H*), 6.76 (s, 1H, Ar*H*), 5.85 (s, 2H, H4-3,5-Me_2pz), 5.18 (s, 4H, CH_2), 2.25 (s, 6H, CH_3), 2.12 (s, 6H, CH_3). ^{13}C NMR ($CDCl_3$, 75 MHz): δ 147.5, 139.1, 137.9, 129.0, 125.5, 124.6, 105.5, 52.2, 13.4, 11.0. Anal. Calcd for $C_{18}H_{22}N_4$: C, 73.44; H, 7.53; N, 19.03. Found: C, 73.25; H, 7.39; N, 19.10.

Synthesis of 1-(chloropalladio)-2,6-bis[(3,5-dimethylpyrazol-1-yl)methyl]benzene (1c): A solution of $Pd(OAc)_2$ (0.10 g, 0.45 mmol) and **3** (0.15 g, 0.49 mmol) in acetic acid (10 mL) was heated to 120 ˚C and maintained at this temperature for 2 h. The solvent was removed by rotary evaporation and the residue dissolved in CH_2Cl_2 (50 mL). The resultant solution was washed with water (3 × 50 mL). The solvent was removed by rotary evaporation and the product dissolved in acetone (50 mL) along with LiCl (0.24 g). The mixture was stirred overnight, then centrifuged and the solution decanted to leave a tan solid. The product was washed with water (20 mL), acetone (20 mL) and CH_2Cl_2 (5 mL), and dried *in vacuo*. Yield: 0.18 g (90%). ^{1}H NMR ($CDCl_3$, 300 MHz): δ 6.39 (s, 3H, Ar*H*), 5.82 (s, 2, H4-3,5-Me_2pz), 5.65 (d, $^3J_{H,H}$ = 14.1 Hz, 2H, CH_2), 4.90 (d, $^3J_{H,H}$ = 13.8 Hz, 2H, CH_2), 2.65 (s, 6H, CH_3), 2.34 (s, 6H, CH_3). ^{13}C NMR ($CDCl_3$, 75 MHz): δ 152.3, 145.8, 140.0, 137.0, 125.0, 124.2, 107.0, 54.3, 15.5, 11.7. Anal. Calcd for $C_{18}H_{21}ClN_4Pd$: C, 49.67; H, 4.86; N, 12.87. Found: C, 49.78; H, 4.92; N, 12.80.

Synthesis of 1-bromo-4-(dimethylamino)-2,6-bis[(dimethylamino)methyl]benzene (5b): Arylamine **4** (0.20 g, 0.68 mmol) was dissolved in a mixture of formaldehyde (10 mL) and formic acid (10 mL) and was stirred at room temperature for 3 h. Subsequently, 1 M NaOH (aq) was added to this solution until pH 11 was reached. The aqueous layer was extracted with CH_2Cl_2 (3 × 20 mL) and the combined organic layer was dried over $MgSO_4$. After evaporation of all volatiles, hexanes (20 mL) were added and the resulting mixture was filtered and evaporated to dryness, leaving a slightly brown solid. This product was used without further purification. Yield: 0.13 g (62%). ^{1}H NMR ($CDCl_3$, 200 MHz): δ 6.74 (s, 2H, Ar*H*), 3.50 (s, 4H, CH_2), 2.95 (s,

6H, *p*-NC*H*$_3$), 2.30 (s, 12H, NC*H*$_3$). ^{13}C NMR ($CDCl_3$, 75 MHz): δ 149.59, 138.77, 123.66, 114.15, 64.49, 45.98, 40.95.

Synthesis of 1-(bromopalladio)-4-(dimethylamino)-2,6-bis[(dimethylamino)-methyl]benzene (2b): $Pd_2(dba)_3{\cdot}CHCl_3$ (0.33 g, 0.32 mmol) in benzene (10 mL) was added to a solution of **5b** (0.20 g, 0.64 mmol) in benzene (10 mL) and this solution was stirred at room temperature for 3 h. Subsequently, all volatiles were evaporated, CH_2Cl_2 (15 mL) was added and the resulting solution was filtered over Celite. The Celite layer was washed with CH_2Cl_2 (2 × 5 mL). The combined filtrate was concentrated to ~5 mL and upon addition of Et_2O (10 mL) the product precipitated from the yellow solution. Light-brown crystals suitable for a crystal structure determination were obtained by slow diffusion of pentane into a concentrated solution of **2b** in CH_2Cl_2. Yield: 0.13 g (50%). ^{1}H NMR ($CDCl_3$, 200 MHz): δ 6.26 (s, 2H, Ar*H*), 3.95 (s, 4H, C*H*$_2$), 2.96 (s, 12H, NC*H*$_3$), 2.86 (s, 6H, *p*-NC*H*$_3$). ^{13}C NMR ($CDCl_3$, 75 MHz): δ 149.53, 145.67, 144.53, 105.28, 75.05, 53.96, 41.55. Anal. Calcd for $C_{14}H_{24}BrN_3Pd$: C, 39.97; H, 5.75; N, 9.99. Found: C, 39.78; H, 5.67; N, 9.92.

Synthesis of 4-acetyl-1-(bromopalladio)-2,6-bis[(dimethylamino)methyl]benzene (2c): Synthesis as described for **2b**, using **5c** (0.20 g, 0.64 mmol) and $Pd_2(dba)_3{\cdot}CHCl_3$ (0.33 g, 0.32 mmol) in benzene (10 mL). Orange/brown crystals of **2c** suitable for a crystal structure determination were obtained by slow evaporation in air of a concentrated solution of **2c** in CH_2Cl_2. Yield: 0.18 g (67%). ^{1}H NMR ($CDCl_3$, 200 MHz): δ 7.41 (s, 2H, Ar*H*), 4.05 (s, 4H, NC*H*$_2$), 2.99 (s, 12H, NC*H*$_3$), 2.52 (s, 3H, C(O)C*H*$_3$). ^{13}C NMR ($CDCl_3$, 75 MHz): δ 197.92, 145.45, 134.75, 120.22, 74.66, 54.09, 26.80. Anal. Calcd for $C_{14}H_{21}BrN_2OPd$: C, 40.07; H, 5.04; N, 6.68. Found: C, 40.26; H, 5.11; N, 6.56.

Synthesis of 4-benzyloxy-1-(iodopalladio)-2,6-bis[(dimethylamino)methyl]-benzene (2d): Tetrabutylammonium fluoride (1 M in THF) (0.54 mL, 0.54 mmol) was added to a mixture of **6** (0.30 g, 0.54 mmol), benzylbromide (0.10 mL, 0.83 mmol), K_2CO_3 (0.38 g, 2.7 mmol) and 18-crown-6 (13 mg, 0.05 mmol) in acetone (15 mL). This mixture was stirred at room temperature for 5 h. Subsequently, all volatiles were evaporated, CH_2Cl_2 (15 mL) was added and the resulting mixture was filtered. The filtrate was reduced to 5 mL and upon addition of Et_2O (10 mL) the product precipitated as an off-white solid. Slow diffusion of Et_2O into a concentrated solution of **2d** in CH_2Cl_2, afforded analytically pure **2d** as a white powder. Yield: 0.17 g

(59%). ^{1}H NMR ($CDCl_3$, 300 MHz): δ 7.42–7.30 (m, 5H, Ar*H*), 6.49 (s, 2H, Ar*H*), 4.98 (s, 2H, OCH_2), 3.97 (s, 4H, NCH_2), 2.98 (s, 12H, NCH_3). ^{13}C NMR ($CDCl_3$, 75 MHz): δ 157.48, 145.86, 137.32, 128.84, 128.22, 127.65, 107.25, 74.80, 73.66, 54.01. Anal. Calcd for $C_{19}H_{25}IN_2OPd$: C, 43.00; H, 4.75; N, 5.28. Found: C, 43.15; H, 4.80; N, 5.24.

Synthesis of 1-(chloropalladio)-2,6-bis[(dimethylamino)methyl]-4-phenylbenzene (2e): *n*-BuLi (2.3 mL, 3.7 mmol) was added to a solution of **7** (1.0 g, 3.7 mmol) in dry hexanes (20 mL) at –80 °C. After addition was completed, the temperature was allowed to rise to room temperature and stirring was continued for 4 h. Subsequently, this solution was added to a suspension of [$PdCl_2$(cod)] (1.1 g, 3.7 mmol) in Et_2O at room temperature and the resulting mixture was stirred for an additional 3 h. The mixture was evaporated to dryness and the residue was extracted with CH_2Cl_2 (10 mL). The organic layer was filtered over Celite and the filtrate was reduced to ~3 mL. Addition of Et_2O resulted in the formation of a white precipitate which was collected and dried *in vacuo*. Analytically pure **2e** was obtained by slow diffusion of Et_2O into a concentrated solution of **2e** in CH_2Cl_2, affording colorless needles of **2e**. Yield: 1.2 g (78%). ^{1}H NMR ($CDCl_3$, 200 MHz): δ 7.51–7.30 (m, 5H, Ar*H*), 7.00 (s, 2H, Ar*H*), 4.05 (s, 4H, NCH_2), 2.97 (s, 12H, NCH_3). ^{13}C NMR ($CDCl_3$, 75 MHz): δ 156.09, 145.65, 141.84, 138.51, 128.99, 127.16, 119.00, 75.03, 53.38 (C_{ipso} not observed). Anal. Calcd for $C_{18}H_{23}ClN_2Pd$: C, 52.83; H, 5.66; N, 6.84. Found: C, 52.65; H, 5.75; N, 6.73.

General procedure for the synthesis of 8a–k: $AgBF_4$ (97.3 mg, 0.50 mmol) in wet acetone (1 mL) was added to a solution of **1a–e**, **2a–f** (0.50 mmol) in acetone (10 mL) and the resulting solution was stirred at room temperature for 1 h. The mixture was filtered over Celite and the filtrate was concentrated to ~3 mL. Upon slow addition of Et_2O (5 mL), the product precipitated as an off-white solid. After isolation, the product was analyzed by ^{1}H NMR spectroscopy and immediately used in the catalytic experiments.

8c: Yield: 80 mg (66%). ^{1}H NMR (acetone-d_6, 300 MHz): δ 7.20 (d, $^{3}J_{H,H}$ = 7.5 Hz, 2H, Ar*H*), 7.03 (t, $^{3}J_{H,H}$ = 7.5 Hz, 1H, Ar*H*), 6.08 (s, 2H, H4-3,5-Me_2pz), 5.68 (d, $^{3}J_{H,H}$ = 14.4 Hz, 2H, CH_2), 5.40 (d, $^{3}J_{H,H}$ = 14.7 Hz, 2H, CH_2), 2.50 (s, 6H, CH_3), 2.25 (bs, 6H, CH_3). ^{13}C NMR (acetone-d_6, 75 MHz): δ 150.5, 142.6, 136.8, 126.1, 125.1, 106.8, 53.7, 12.9, 10.7. Anal. Calcd for $C_{18}H_{23}BF_4N_4OPd$: C, 42.84; H, 4.54; N, 11.10. Found: C, 42.71; H, 4.65; N, 10.98.

8d: Yield: 0.55 g (94%). ^{1}H NMR (acetone-d_6, 200 MHz): δ 7.90–7.96 (m, 4H, Ar*H*), 7.52–7.59 (m, 6H, Ar*H*), 7.10–7.13 (m, 3H, Ar*H*), 4.91 (bs, 4H, CH_2).

8e: Yield: 0.69 g (92%). ^{1}H NMR (acetone-d_6, 200 MHz): δ 7.93–7.83 (m, 8H, Ar*H*), 7.72–7.63 (m, 12H, Ar*H*), 7.28–7.17 (3H, Ar*H*), 4,24 (pseudo t, $^{2}J_{P,H}$ and $^{4}J_{P,H}$ = 4.8 Hz, 4H, CH_2). ^{31}P NMR (acetone-d_6): δ 47.9.

8f: Yield: 0.17 g (78%). ^{1}H NMR (acetone-d_6, 300 MHz): δ 7.79 (s, 2H, Ar*H*), 4.34 (s, 4H, NCH_2), 2.92 (s, 12H, NCH_3). ^{13}C NMR (acetone-d_6, 75 MHz): δ 161.97, 146.90, 146.80, 115.81, 73.08, 51.93.

8g: Yield: 0.15 g (67%). ^{1}H NMR (acetone-d_6, 200 MHz): δ 6.38 (s, 2H, Ar*H*), 4.08 (s, 4H, NCH_2), 2.83 (s, 12H, NCH_3), 2.81 (s, 6H, *p*-NCH_3).

8h: Yield: 0.21 g (93%). ^{1}H NMR (acetone-d_6, 300 MHz): δ 7.50 (s, 2H, Ar*H*), 4.22 (s, 4H, NCH_2), 2.94 (s, 12H, NCH_3), 2.49 (s, 3H, C(O)CH_3). ^{13}C NMR (acetone-d_6, 75 MHz): δ 197.02, 162.29, 146.80, 135.78, 120.42, 73.66, 52.42, 26.02.

8i: Yield: 0.24 g (95%). ^{1}H NMR (acetone-d_6, 300 MHz): δ 7.46–7.32 (m, 5H, Ar*H*), 6.63 (s, 2H, Ar*H*), 5.04 (s, 2H, OCH_2), 4.13 (s, 4H, NCH_2), 2.85 (s, 12H, NCH_3). ^{13}C NMR (acetone-d_6, 75 MHz): δ 158.28, 146.11, 137.83, 128.61, 127.95, 127.71, 107.80, 73.49, 70.13, 52.01.

8j: Yield: 0.22 g (93%). ^{1}H NMR (acetone-d_6, 300 MHz): δ 7.60–7.29 (m, 5H, Ar*H*), 7.18 (s, 2H, Ar*H*), 4.25 (s, 4H, NCH_2), 2.89 (s, 12H, NCH_3). ^{13}C NMR (acetone-d_6, 75 MHz): δ 150.31, 146.13, 141.54, 139.08, 129.06, 127.24, 126.94, 119.29, 73.45, 51.93.

8k: Yield: 0.22 g (91%). ^{1}H NMR (acetone-d_6, 200 MHz): δ 7.03 (s, 2H, Ar*H*), 4.16 (s, 4H, NCH_2), 2.85 (s, 12H, NCH_3), 0.21 (s, 9H, SiCH_3). ^{13}C NMR (acetone-d_6, 75 MHz): δ 152.75, 145.30, 136.92, 125.07, 73.45, 51.84, -1.48.

Catalysis in the double Michael reaction between MVK and ethyl-α-cyanoacetate. A typical experiment: Ethyl-α-cyanoacetate (0.17 mL, 1.6 mmol), methyl vinyl ketone (0.40 mL, 4.8 mmol), diisopropyl ethylamine (28 μL, 0.16 mmol) and **8a** (3.2 mg, 8 μmol, 0.5 mol% [Pd]) were mixed in CH_2Cl_2 (5 mL) and stirred at room temperature. The reaction mixture was sampled (100 μL) at regular intervals and the samples worked up by evaporating solvent and methyl vinyl ketone with a gentle stream of nitrogen. The conversions were determined by ^{1}H NMR spectroscopy. Conversions obtained were confirmed by GC analysis of the reaction mixture. In all cases, the product was isolated by bulb-to-bulb distillation. For all reactions, yields were found to be between 85 and 100%.

Crystal structure determinations: Intensities were measured on a Nonius KappaCCD diffractometer with rotating anode (Mo-K_α, λ = 0.71073 Å) at a temperature of 150 K. The structures were solved with automated Patterson methods using the program DIRDIF99,[30] and refined with the program SHELXL97[31] against F^2 of all reflections up to a resolution of $(\sin \vartheta/\lambda)_{max}$ = 0.65 $Å^{-1}$. Non hydrogen atoms were refined freely with anisotropic displacement parameters. Hydrogen atoms were refined as rigid groups. The drawings, structure calculations, and checking for higher symmetry were performed with the program PLATON.[32]

Compound 2b: $C_{14}H_{24}BrN_3Pd$, Fw =420.67, orange plate, 0.24 × 0.24 × 0.09 mm^3, monoclinic, $P2_1/c$ (no. 14), a = 9.1973(1) Å, b = 11.1707(2) Å, c = 16.4736(3) Å, β = 108.3990(8)°, V = 1605.98(4) $Å^3$, Z = 4, ρ = 1.740 g cm^{-3}. The absorption correction was performed with PLATON[32] (routine DELABS, μ = 3.64 mm^{-1}, 0.49–0.72 transmission). 17563 measured reflections, 3671 unique reflections (R_{int} = 0.0508), 2999 observed reflections [$I > 2\sigma(I)$]. 178 refined parameters, 0 restraints. R (obs. refl.): R1 = 0.0254, wR2 = 0.0517. R (all data): R1 = 0.0387, wR2 = 0.0549. S = 1.039. Crystallographic data (excluding structure factors) have been deposited with the Cambridge Crystallographic Data Centre as supplementary publication no. CCDC 187019. Copies of the data can be obtained free of charge on application to CCDC, 12 Union Road, Cambridge CB2 1EZ, UK [fax: (+44) 1223-336-033; e-mail: deposit@ccdc.cam.ac.uk].

Compound 2c: $C_{14}H_{21}BrN_2OPd$, Fw =419.64, yellow plate, 0.12 × 0.12 × 0.05 mm^3, monoclinic, $P2_1/c$ (no. 14), a = 17.1168(3) Å, b = 15.1078(3) Å, c = 12.4777(3) Å, β = 107.1925(12)°, V = 3082.52(11) $Å^3$, Z = 8, ρ = 1.808 g cm^{-3}. The absorption correction was performed with PLATON[32] (routine MULABS, μ = 3.79 mm^{-1}, 0.68–0.82 transmission). 26887 measured reflections, 7047 unique reflections (R_{int} = 0.0729), 5091 observed reflections [$I > 2\sigma(I)$]. 353 refined parameters, 0 restraints. R (obs. refl.): R1 = 0.0456, wR2 = 0.0931. R (all data): R1 = 0.0748, wR2 = 0.1034. S = 1.012. Crystallographic data (excluding structure factors) have been deposited with the Cambridge Crystallographic Data Centre as supplementary publication no. CCDC 187020. Copies of the data can be obtained free of charge on application to CCDC, 12 Union Road, Cambridge CB2 1EZ, UK [fax: (+44) 1223-336-033; e-mail: deposit@ccdc.cam.ac.uk].

4.5. References and Notes

[1] For representative examples see: a) Gupta, M.; Hagen, C.; Flesher, R. J.; Kaska, W. C.; Jensen, C. M. *Chem. Comm.* **1996**, 2083. b) Dani, P.; Karlen, T.; Gossage, R. A.; Gladiali, S.; van Koten, G. *Angew. Chem. Int. Ed.* **2000**, *39*, 743. c) Ohff, M.; Ohff. A.; van der Boom, M. E.; Milstein, D. *J. Am. Chem. Soc.* **1997**, *119*, 11687. d) van de Kuil, L. A.; Grove, D. M.; Gossage, R. A.; Zwikker, J. W.; Jenneskens, L. W.; Drenth, W.; van Koten, G. *Organometallics* **1997**, *16*, 4985. e) Bergbreiter, D. E.; Osburn, P. L.; Liu, Y. -S. *J. Am. Chem. Soc.* **1999**, *121*, 9531. f) Gruber, A. S.; Zim, D.; Ebeling, G.; Monteiro, A. L.; Dupont, J. *Org. Lett.* **2000**, *2*, 1287. g) Granel, C.; Dubois, Ph.; Jérôme, R.; Teyssié, Ph *Macromolecules* **1996**, *29*, 8576.

[2] For a review about pincer-metal-d^8 chemistry see: Albrecht, M.; van Koten, G. *Angew. Chem. Int. Ed.* **2001**, *40*, 3750.

[3] a) Gorla, F.; Togni, A.; Venanzi, L. M.; Albinati, A.; Lianza, F. *Organometallics* **1994**, *13*, 1607. b) Longmire, J. M.; Zhang, X.; Shang, M. *Organometallics* **1998**, *17*, 4374. c) Stark, M. A.; Jones, G.; Richards, C. J. *Organometallics* **2000**, *19*, 1282. d) Motoyama, Y.; Narusawa, H.; Nishiyama, H. *Chem. Commun.* **1999**, 131. e) Denmark, S. E.; Stavenger, R. A.; Faucher, A. -M.; Edwards, J. P. *J. Org. Chem.* **1997**, *62*, 3375. f) van de Kuil, L. A.; Veldhuizen, Y. S. J.; Grove, D. M.; Zwikker, J. W.; Jenneskens, L. W.; Drenth, W.; Smeets, W. J. J.; Spek, A. L.; van Koten, G. *Recl. Trav. Chim. Pays-Bas* **1994**, *113*, 267. g) Albrecht, M.; Kocks, B. M.; Spek, A. L.; van Koten, G. *J. Organomet. Chem.* **2001**, *624*, 271. h) Williams, B. S.; Dani, P.; Lutz, M.; Spek, A. L.; van Koten, G. *Helvetica Chim. Acta* **2001**, *84*, 3519.

[4] van de Kuil, L. A.; Luitjes, H.; Grove, D. M.; Zwikker, J. W.; van der Linden, J. G. M.; Roelofsen, A. M.; Jenneskens, L. W.; Drenth, W.; van Koten, G. *Organometallics* **1994**, *13*, 468.

[5] a) Knapen, J. W. J.; van der Made, A. W.; de Wilde, J. C.; van Leeuwen, P. W. N. M.; Wijkens, P.; Grove, D. M.; van Koten, G. *Nature* **1994**, *372*, 659. b) Kleij, A. W.; Gossage, R. A.; Klein Gebbink, R. J. M.; Reyerse, E. J.; Brinkmann, N.; Kragl, U.; Lutz, M.; Spek, A. L.; van Koten, G. *J. Am. Chem. Soc.* **2000**, *122*, 12112. c) Albrecht, M.; Hovestad, N. J.; Boersma, J.; van Koten, G. *Chem. Eur. J.* **2001**, *7*, 1289. d) Davies, P. J.; Grove, D. M.; van Koten, G. *Organometallics* **1997**, *16*, 800. e) Albrecht, M.; Gossage, R. A.; Lutz, M.; Spek, A. L.; van Koten, G. *Chem. Eur. J.* **2000**, *6*, 1431. f) Meijer, M. D.; Ronde, N.; Vogt, D.; van Klink, G. P. M.; van Koten, G. *Organometallics* **2001**, *20*, 3993. g) van de Kuil, L. A.; Grove, D. M.; Zwikker, J. W.; Jenneskens, L. W.; Drenth, W.; van Koten, G. *Chem. Mater.* **1994**, *6*, 1675. h) Patmamanoharan, C.; Wijkens, P.; Grove, D. M.; Philipse, A. P. *Langmuir* **1996**, *12*, 4372.

[6] Dijkstra, H. P.; Meijer, M. D.; Patel, J.; Kreiter, R.; van Klink, G. P. M.; Lutz, M.; Spek, A. L.; Canty, A. J.; van Koten, G. *Organometallics* **2001**, *20*, 3159.

[7] a) Dijkstra, H. P.; Steenwinkel, P.; Grove, D. M.; Lutz, M.; Spek, A. L.; van Koten, G. *Angew. Chem. Int. Ed.* **1999**, *38*, 2186; b) Dijkstra, H. P.; Kruithof, C. A.; Ronde, N.; van de Coevering, R.; Ramón, D. J.; Vogt, D.; van Klink, G. P. M.; van Koten, G. *J. Org. Chem.,* in press, manuscript available on the world wide web: http://pubs3.acs.org/acs/journals. c) Dijkstra, H. P.; Albrecht, M.; van Koten, G. *Chem. Commun.* **2002**, 126.

[8] Dijkstra, H. P.; van Klink, G. P. M.; van Koten, G. *Acc. Chem. Res.*, in press, manuscript available on the world wide web: http://pubs3.acs.org/acs/journals.

[9] See reference 7b. Commercial nanofiltration membranes (MPF-60: MWCO = 400 Dalton; MPF-50: MWCO = 700 Dalton) were purchased from Koch Membrane Systems Inc., Düsseldorf, Germany; further product information can be found at http://www.kochmembrane.com.

[10] Alsters, P. L.; Baesjou, P. J.; Janssen, M. D.; Kooijman, H.; Sicherer-Roetman, A.; Spek, A. L.; van Koten, G. *Organometallics* **1992**, *11*, 4124

[11] Canty, A. J.; Honeyman, R. T.; Skelton, B. W.; White, A. H. *J. Organomet. Chem.* **1990**, *389*, 277.

[12] Rimml, H.; Venanzi, L. M. *J. Organomet. Chem.* **1983**, *259*, C6.

[13] Lucena, N.; Casabo, J; Escriche, L; Sanchez-Castello, G.; Teixidor, F.; Kivekäs, R.; Sillanpää, R. *Polyhedron* **1996**, *15*, 3009.

[14] a) Slagt, M. Q.; Klein Gebbink, R. J. M.; Lutz, M; Spek, A. L.; van Koten, G. *J. Chem. Soc., Dalton Trans.* **2002**, 2591. b) Slagt, M. Q.; Rodríguez, G.; Klein Gebbink, R. J. M.; Klopper, W.; Lutz, M.; Spek, A. L.; van Koten, G. *manuscript in preparation*.

[15] Kleij, A. W.; Kleijn, H.; Jastrzebski, J. T. B. H.; Spek, A. L.; van Koten, G. *Organometallics* **1999**, *18*, 277.

[16] Hartshorn, C. M.; Steel, P. J. *Organometallics* **1998**, *17*, 3487.

[17] For the synthesis of **4** and **5c**, see references 1d and 4, respectively.

[18] Rodríguez, G.; Albrecht, M.; Schoenmaker, J.; Ford, A.; Lutz, M.; Spek, A. L.; van Koten, G. *J. Am. Chem. Soc.* **2002**, *124*, 5127.

[19] Steenwinkel, P.; James, S. L.; Grove, D. M.; Veldman, N.; Spek, A. L.; van Koten, G. *Chem. Eur. J.* **1996**, *2*, 1440.

[20] Grove, D. M.; van Koten, G.; Louwen, J. N.; Noltes, J. G.; Spek, A. L.; Ubbels, H. J. C. J. *J. Am. Chem. Soc.* **1984**, *104*, 6609.

[21] This information can be obtained from the Cambridge Structural Database.

[22] For the crystal structure of **2a** see: Slagt, M. Q.; Dijkstra, H. P.; McDonald, A.; Klein Gebbink, R. J. M.; Lutz, M.; Spek, A. L.; van Koten, G., *manuscript in preparation.*

[23] The DFT-B3LYP/LANL2DZ method uses density functional theory combined with effective core potentials. The basis set used for palladium is the Los Alamos National Laboratory set (LANL) for effective core potentials (ECP) of double ζ type, consisting of a small core ECP with 3s and 3p orbitals

in the valence space. The functional form used is the B3LYP, and the relativistic correlations for heavy atoms are considered in the ECP.

[24] Frisch, M. J.; Trucks, G. W.; Schlegel, H. B.; Scuseria, G. E.; Robb, M. A.; Cheeseman, J. R.; Zakrzewski, V. G.; Montgomery, J. A., Jr.; Stratmann, R. E.; Burant, J. C.; Dapprich, S.; Millam, J. M.; Daniels, A. D.; Kudin, K. N.; Strain, M. C.; Farkas, O.; Tomasi, J.; Barone, V.; Cossi, M.; Cammi, R.; Mennucci, B.; Pomelli, C.; Adamo, C.; Clifford, S.; Ochterski, J.; Petersson, G. A.; Ayala, P. Y.; Cui, Q.; Morokuma, K.; Malick, D. K.; Rabuck, A. D.; Raghavachari, K.; Foresman, J. B.; Cioslowski, J.; Ortiz, J. V.; Baboul, A. G.; Stefanov, B. B.; Liu, G.; Liashenko, A.; Piskorz, P.; Komaromi, I.; Gomperts, R.; Martin, R. L.; Fox, D. J.; Keith, T.; Al-Laham, M. A.; Peng, C. Y.; Nanayakkara, A.; Gonzalez, C.; Challacombe, M.; Gill, P. M. W.; Johnson, B.; Chen, W.; Wong, M. W.; Andres, J. L.; Gonzalez, C.; Head-Gordon, M.; Replogle, E. S.; Pople, J. A. Gaussian 98, Revision A.7, Gaussian, Inc., Pittsburgh PA, 1998.

[25] Exner, O. in *Correlation Analysis of Chemical Data*, Plenum Press, New York, **1988**.

[26] Canty, A. J.; Lee, C. V. *Organometallics* **1982**, *1*, 1063.

[27] Shorter, J. in *Correlation Analysis in Organic Chemistry: an Introduction to the Linear Free-energy Relationships*, Clarendon Press, Oxford, **1973**.

[28] For the synthesis of **9**, see reference 6. For the synthesis of **10**–**12**, see reference 7b.

[29] Drew, D.; Doyle, J. R.; Shaver, A. G. *Inorg. Synth.* **1972**, *13*, 47.

[30] Beurskens, P. T.; Admiraal, G.; Beurskens, G.; Bosman, W. P.; Garcia-Granda, S.; Gould, R. O.; Smits, J. M. M.; Smykalla, C. (1999) The DIRDIF99 program system, Technical Report of the Crystallography Laboratory, University of Nijmegen, The Netherlands.

[31] Sheldrick, G. M. (1997). SHELXL-97. Program for crystal structure refinement. University of Göttingen, Germany.

[32] Spek, A. L. (2002). PLATON. A multipurpose crystallographic tool. Utrecht University, The Netherlands.

– *Chapter 5* –

The Application of Shape-Persistent Nanosize Pincer Complexes in a Nanofiltration Membrane Reactor

Abstract: The application of linear, flat, and three-dimensional shape-persistent nanosize multi(NCN-metal) complexes (metal = Pd, Pt) in a nanofiltration (NF) membrane reactor was studied to address the important issue of homogeneous catalyst recycling. These complexes were found to be retained more efficiently by NF-membranes than more flexible dendrimers containing similar nanosize dimensions, showing the importance of shape-persistence in the backbone of these materials. In addition, a dodecakis[NCN-Pd^{II}-OH_2]$(BF_4)_{12}$ complex was applied as a homogeneous catalyst in the double Michael reaction between MVK and ethyl-α-cyanoacetate under continuously operating conditions. The total turnover number of this catalyst was increased by a factor greater than 40 as compared to batch experiments.

H. P. Dijkstra, C. A. Kruithof, N. Ronde, R. van de Coevering, D. J. Ramón, D. Vogt, G. P. M. van Klink, G. van Koten, *J. Org. Chem.*, in press.
H. P. Dijkstra, N. Ronde, G. P. M. van Klink, D. Vogt, G. van Koten, submitted.

Nanofiltration Process to Recycle Shape-Persistent Homogeneous Catalysts

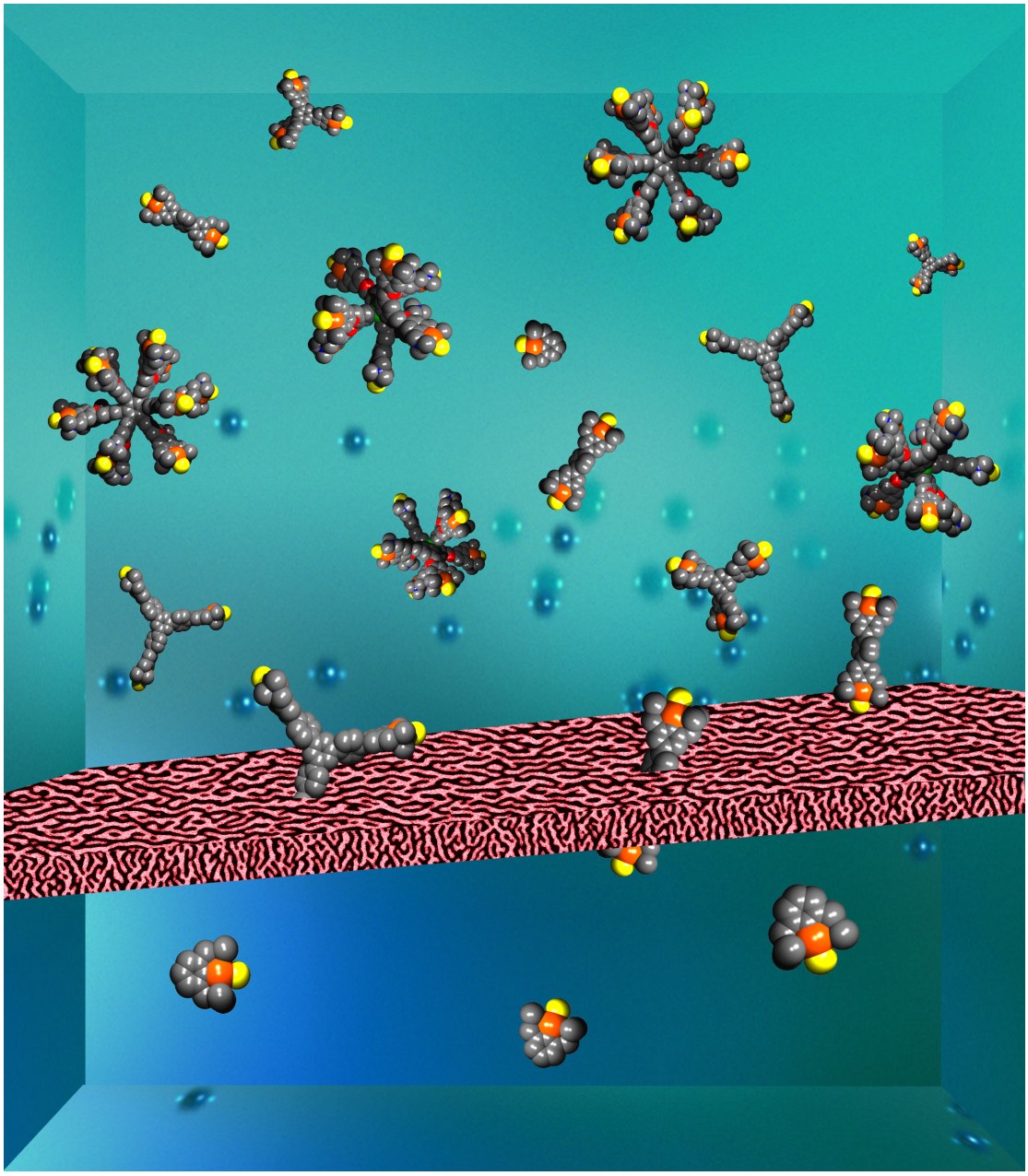

5.1. Introduction

Homogeneous catalysts are increasingly used for selective organic transformations. Especially in asymmetric syntheses, the contribution of homogeneous catalysts is significant.[1] Nevertheless, in industry most processes are still catalyzed by heterogeneous catalysts because of their facile separation from the product stream, rendering these processes more efficient and cheaper. In the field of homogeneous catalysis, separation of the catalyst from the product mixture is rather complicated, making these catalysts often inefficient and too expensive, preventing large scale industrial applications.[2] In addition, the often toxic metal is still present in the product mixture, making an extra purification step necessary.

A recent, promising development in the area of homogeneous catalyst recovery and reuse (recycling) is the incorporation of catalysts on large organic frameworks. In this way, macromolecular catalysts are created which can be separated from the product-containing solution by ultra- or nanofiltration techniques, also allowing the application of homogeneous catalysts under continuously operating conditions.[3,4] By applying this technology, several advantages of homogeneous (high selectivity / activity, good catalyst description and reproducibility) and heterogeneous catalysis (easy catalyst recovery, high turnover numbers and small amounts of catalyst needed) can be combined. For this purpose, dendrimer-bound homogeneous catalysts have been investigated extensively in recent years.[5]

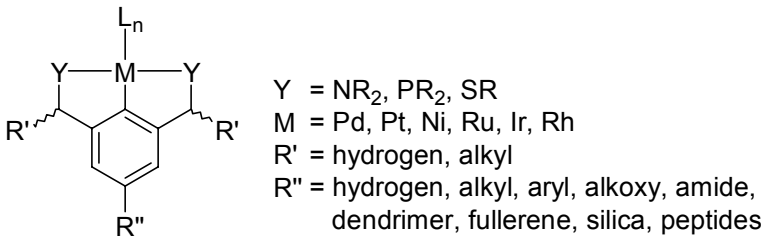

Figure 1. Metalated pincer complexes; a versatile catalyst.

The prevention of rapid wash-out of the catalyst and/or loss of activity are absolute prerequisites for any possible industrial application of nanosize homogeneous catalysts in a continuous catalytic process.[6] However, a good understanding of how macromolecular catalysts can be designed to avoid these pitfalls is still lacking. In recent studies, it was shown that the combination of a monoanionic, terdentate coordinating YCY-pincer ligand system (Figure 1) and an

appropriate metal resulted in catalytic systems[7] that do not suffer from catalyst deactivation or decomposition.[8] The strong, covalent metal-carbon bond is maintained during catalysis. Furthermore, it was demonstrated that the aryl-C4 position (R") is an excellent branching point for anchoring these pincer complexes to support materials such as dendrimers,[9] fullerenes,[10] polymers,[11] solid supports,[12] and peptides.[13] These features make the pincer moiety suitable for attachment to a soluble nanosize support in order to create a homogeneous catalyst which can be retained by nano- or even ultrafiltration membranes and is also stable under continuous reaction conditions.

Very efficient retentions (> 99%) of the homogeneous macromolecular catalysts by nanofiltration membranes are required in order to prevent a fast wash-out of the catalysts (R = 99.9% means a wash-out of 10% after 100 reactor volume exchanges). From previous explorative homogeneous catalysis studies in nanofiltration membrane reactors, it was concluded that predominantly the higher generation metallodendrimers (G2 or higher, M_w > 2000 Dalton) are applicable in continuous processes.[3] This is rather surprising since the reported cut-off masses of the nanofiltration membranes are normally lower than 1000 Dalton. This contradiction is due to a number of features: i) the imperfect structure of the membranes used (*vide infra*), ii) the solvent used, since the structure of the membrane alters upon changing solvents, iii) the flexibility of the dendrimer backbones, and iv) the nature of the *surface* groups of the macromolecular catalysts.

Since the first two features are determined by the membrane and the reaction conditions, we concentrated mainly on the third issue; the construction of more rigid (*i.e.* shape-persistent) catalyst structures. So far, mainly metallodendrimers have been used in this research field because of their well-defined structure, which allows easy comparison with the monometallic analogs in terms of selectivity and activity. However, dendritic materials often possess flexible backbones and are thus able to undergo shape-changes in solution.[14] This behavior can affect their retention rates by nanofiltration membranes. A detailed investigation on the influences of flexibility, size and geometry of nanosize catalysts on their retention rates by a given type of nanofiltration membrane has never been performed. This important aspect of nanomembrane filtration is investigated in this chapter. In the future, this will enable predictions of the minimal size and optimal geometry needed for the macromolecular catalysts. In addition, knowledge about the influence of these features on retention rates is likewise important to design nanosize catalytic materials which can be synthesized in a minimal number of synthetic steps.

Nanosize shape-persistent molecules of types **1**, **2**, **3**, **4** and the rod-like bispincer complex **5** (Figure 2)[15] were selected in order to investigate the influence of size and geometry on the retention rates of these macromolecules by the MPF-60 and MPF-50 nanofiltration membranes.[16] As reference we also decided to test the mononuclear NCN-Pt-Br complex **6**[17] in a nanofiltration membrane reactor. All of these molecules do not undergo significant shape-changes in solution due to their rigid backbones. While in complexes **1**, **2**, and **5** the organometallic sites are part of

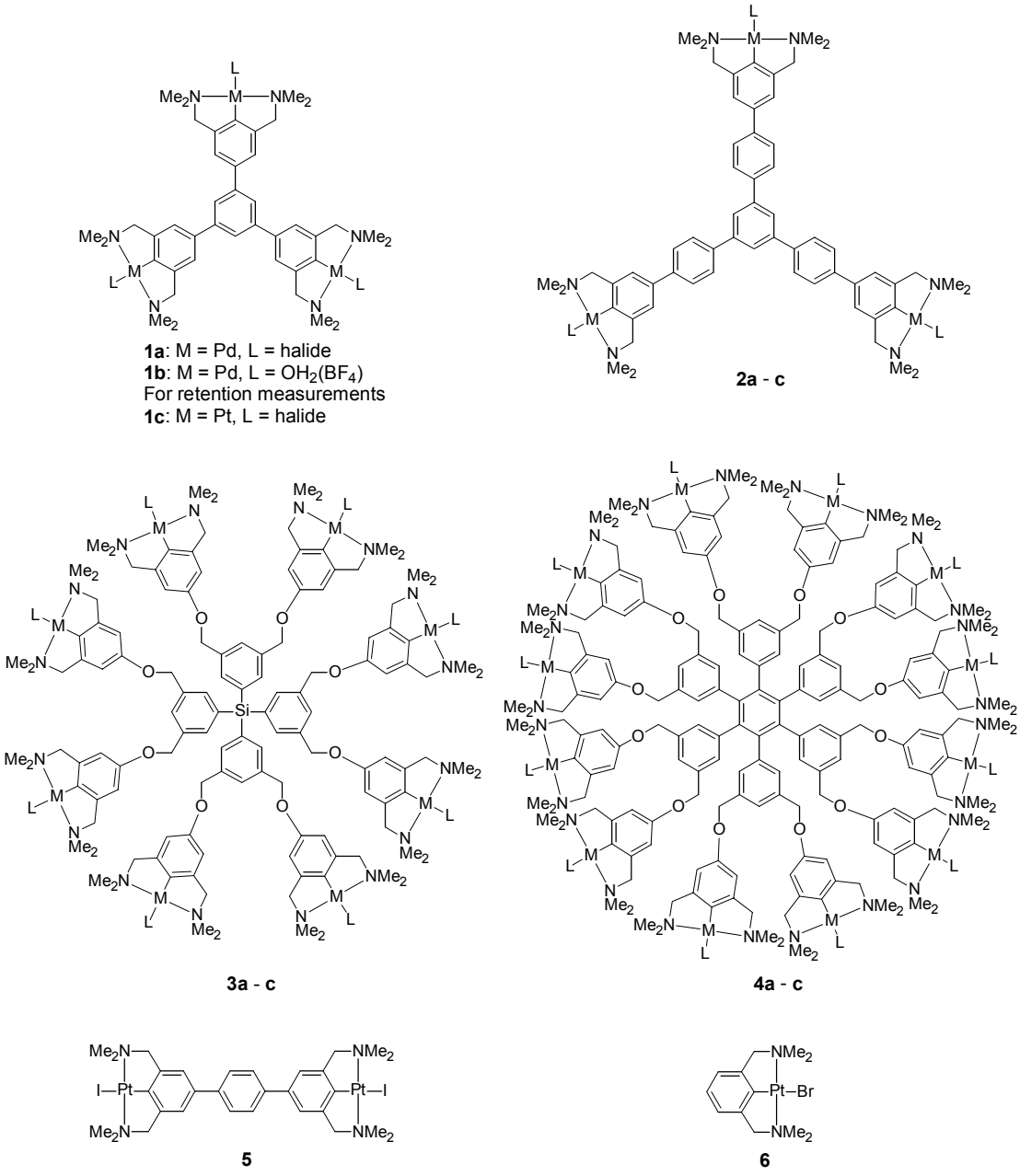

Figure 2. Shape-persistent nanosize complexes.

the shape-persistent cores, **3** and **4** possess a more flexible organometallic shell around a rigid core. Compounds **1**, **2**, **5** and **6** are rather flat, two-dimensional structures, while **3** possesses a spherically-shaped, three-dimensional geometry. In spite of the rigid two-dimensional core, **4** exerts a three-dimensional structure due to the more flexible organometallic shell at its periphery, affording this molecule its flattened-spherical geometry. The use of complexes **1**–**6** in a nanofiltration membrane reactor should provide direct information about the influence of size and geometry on the retention rates of these molecules by the organic polymeric nanofiltration membranes. Finally, also the application of complex **4b** (M = Pd, L = $OH_2(BF_4)$) as a homogeneous catalysts in a continuous double Michael reaction in a nanofiltration membrane reactor will be discussed.

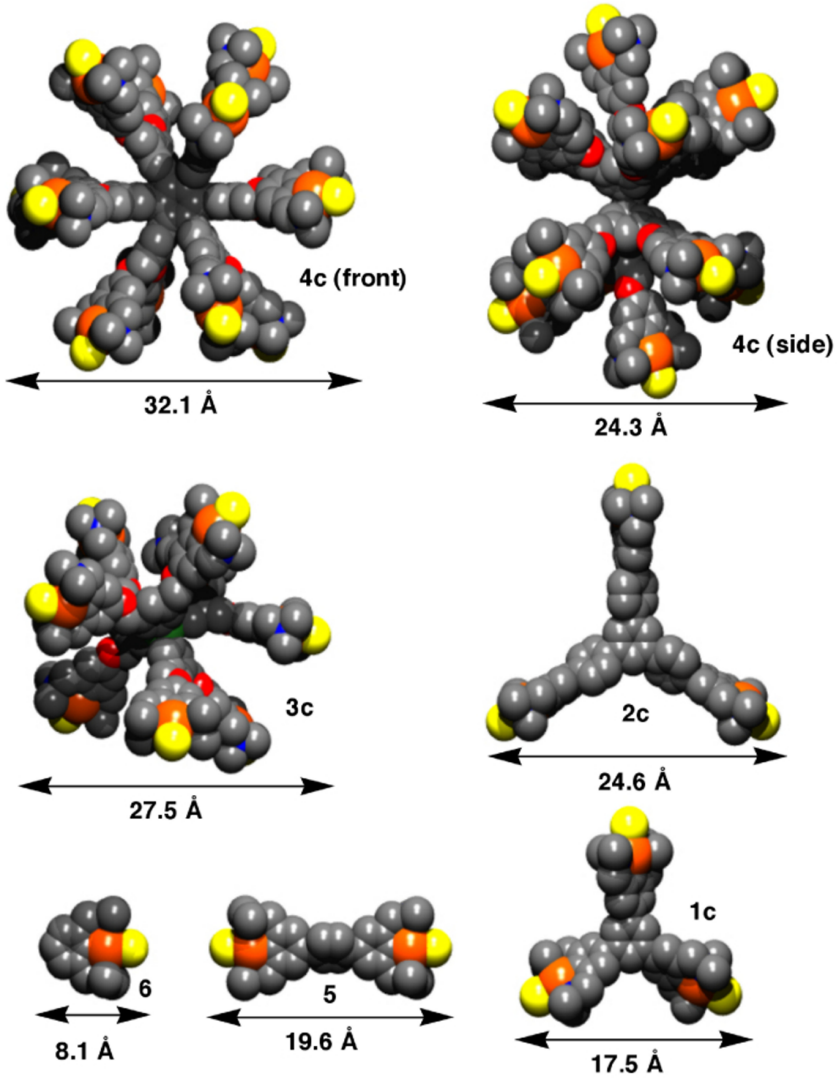

Figure 3. Space-filling molecular structures of **1**–**6**.

5.2. Results and discussion

To obtain an impression of the size and molecular structure of complexes **1–6** we have performed molecular modeling[18] studies on the platinum complexes **1c–4c**, **5** and **6** (Figure 3). In addition, the X-ray crystal structure of **1a** (L = Br, see Chapter 2)[15b] was determined and was compared to the structure of **1a** obtained by molecular modeling. The modeled shape and geometry of **1a** are in good agreement with the structure found for **1a**. Furthermore, changing the metal from palladium to platinum (**1a** *vs.* **1c**) and/or changing the metal-bound halide (L) did not influence the molecular geometry and size of **1**. This means that molecular modeling gives an accurate representation of the molecular structures of **1**–**6**, and allows a direct comparison between the palladium complexes (**1a–4a**) and their platinum analogs (**1c–4c**). The molecular modeling structure of **1c** (L = Br) shows a disk-like molecule with a bromide-bromide distance of 17.5 Å, and a disk-thickness of ~ 6 Å, which emphasizes the two-dimensional form of **1c**. The molecular modeling structure of **2c** (L = Br) also shows a two-dimensional structure with a bromide-bromide distance of 24.6 Å and a thickness of ~ 6 Å. The calculated structures of **3c** (L = I) and **4c** (L = Br), on the other hand, display three-dimensional structures, with **3** having a tetrahedral sphere-like structure with a diameter of 27.5 Å, while **4** has a structure which resembles a flattened sphere with a diametrically opposed bromide-bromide distance of 32.1 Å and a thickness of 24.3 Å. Bispincer **5** (L = I) shows a rather one-dimensional, rod-like structure with an iodide-iodide distance of 19.6 Å, while monopincer **6** possesses a maximum diameter of 8.1 Å.

Nanofiltration studies. Nanofiltration is a relatively new method to address the separation problems of metal-containing homogeneous catalysts from product-containing solutions.[3] Therefore, the question is raised whether the MPF-membranes, the most widely used nanofiltration membranes in this research area, only discriminate on size or also on the flexibility and the molecular shape (geometry) of the molecules. To obtain more insight on this issue, we performed nanofiltration membrane filtration experiments with complexes **1**–**6**.

A prerequisite to accurately determine the retention rates of the nanosize materials by nanofiltration membranes is having a sensitive analysis technique. Very small variations in the retention rates can already have large influences on the performance of these catalysts in continuous catalytic processes.[3] Therefore, we decided to use the neutral multi(NCN-Pt^{II}-X) complexes **1c,**[15b] **2c**, **3c**, **4c**, **5** and **6** (X =

halide) for the retention rate determinations. Previously, it was found that square-planar neutral [$Pt^{II}X(NCN)$] complexes reversibly bind sulfur dioxide (Scheme 1), leading to five-coordinate SO_2 adducts which are deep orange in color and thus have strong absorptions in the UV/Vis region (300–450 nm).[19] These absorptions originate from two Pt→S metal-to-ligand charge transfer bands.[20] Extinction coefficients (ε) were found to be between 6000 and 16000 $M^{-1}cm^{-1}$ (depending on R, Scheme 1),[9f] indicating that even concentrations of approximately 10^{-7}–10^{-6} M can be determined, allowing a precise determination of the retention rates. In addition, since molecular modeling studies indicated that the dimensions of the multipincer systems are independent of the metal, the retention rates determined for **1c–4c**, **5** and **6** can be directly translated to the catalytically active derivatives (*i.e.* palladium analog) of **1–6**.

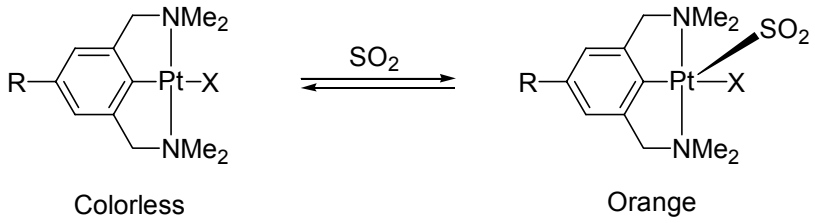

Scheme 1. [$Pt^{II}X(NCN)$] as SO_2 sensor.

Treatment of **1c–4c**, **5** and **6** in methylene chloride with sulfur dioxide afforded the corresponding SO_2 adducts **1d–4d**, **7** and **8**, respectively (Equation 1). The observed maxima of **1d–4d**, **7** and **8** in the UV/Vis spectrum are positioned at approximately 359 nm with a broad shoulder at longer wavelengths. The extinction coefficients (ε) per platinum center at 359 nm are summarized in Table 1. The sometimes large differences in the extinction coefficients of the various complexes can be ascribed to the variable absorptive abilities of the aromatic systems of these materials in the UV/Vis region. Complexes **2c** and **5** in particular are already strongly colored without subjection to sulfur dioxide.

$$\textbf{1c - 4c, 5, 6} \underset{}{\overset{SO_2}{\rightleftharpoons}} \textbf{1d - 4d, 7, 8} \qquad (1)$$

The nanofiltration experiments were performed in a continuously operating high-pressure membrane reactor equipped with the MPF-60 or MPF-50 nanofiltration membrane. The concentrations of **1d–4d**, **7** and **8** in the permeate and in the retentate were determined by UV/Vis spectroscopy and the obtained retention rates of the

complexes **1–6** are summarized in Table 1. With the MPF-60 membrane, the concentration of **4d** in the permeate was below the detection limit of UV/Vis spectroscopy, *i.e.* a retention rate higher than 99.9%. Surprisingly, the one-dimensional, rod-like pincer **5** is retained in 99.6% by the MPF-60 membrane, which is considerably higher than the retention rates obtained for the two-dimensional tris(pincer) systems **1c** and **2c** (93.9 and 98.7%, respectively). For the membrane filtration tests, however, **5** was first converted into **7** in order to obtain a sufficiently soluble bis(pincer) complex for retention rate determination. Since the sulfur dioxide coordination is a reversible process, it is likely that at elongated residence times **7** is completely converted into **5** which subsequently can precipitate and clog the membrane. As a result higher retention rates will be observed. A second possibility is the formation of aggregates in solution at higher concentrations, preventing leaching of the uni-molecular complexes. With the filtration set-up (dead-end filtration) used, it is known that molecules can accumulate at the membrane surface, possibly inducing aggregate formation. These aspects are currently under investigation. With the mononuclear NCN-pincer **6** a retention rate of 82.4% was found, which is already rather efficient for such a small molecule. It has to be noted, however, that 82.4% retention means that the catalyst is completely washed out of the reactor within 30 cycles, which is far from being sufficient for continuous catalysis.

Table 1: Extinction coefficients and retention rates of the various platinated NCN-pincer complexes

Compound	**Ext. Coeff. (ε)**[a] **(x 10^3 M^{-1} cm^{-1})**	**R (%)**[b] **(MPF-60)**[c]	**R (%)**[b] **(MPF-50)**[c]
1c	9.8	93.9	n.d
2c	11.7	98.7	97.6
3c	8.1	99.5	n.d.
4c	7.7	> 99.9	99.9
5	10.8	99.6	n.d.
6	9.2	82.4	n.d.

a) The extinction coefficients were determined for the SO_2-adducts **1d**–**4d**, **7** and **8**; b) The following formula was used for determining the retention rates: $R = 1 + (V_t/V_r)\ln(C_f/C_0)$, V_t = total volume flushed through membrane, V_r = reactorvolume, C_f = concentration in filtrate, C_0 = initial concentration in reactor. For the nanofiltration experiments, complexes **1c–4c**, **7** and **6** were dissolved in CH_2Cl_2 and injected into the reactor. The corresponding SO_2-adducts **1d–4d**, **7** and **8** were used for analysis with UV/Vis spectroscopy; c) MPF-60: MWCO = 400 Dalton; MPF-50: MWCO = 700 Dalton.

Complexes **2c** and **4c** were also tested in combination with the MPF-50 membrane; the observed retention rates were only slightly lower than with the MPF-60 membranes (Table 1). Thus, although the MWCO (defined as the molecular weight at which 90% of the solutes are retained by the membrane) of the MPF-50 membrane is considerably higher as compared to the MPF-60 membrane (700 *vs.* 400 Dalton), no significant influence on the retention rates of these macromolecular materials was found.

To further investigate the concept of shape-persistence in the core of the macromolecular catalysts for attaining optimal retentions, we related the retention rates of **2c** and **4c** to the calculated molecular volumes of these complexes. The same procedure was performed with recently prepared flexible G0-Ni_4, **9**, and G1-Ni_{12}, **10**, carbosilane dendrimers (Figure 4).[4h] For **2c** and **4c**, molecular modeling gave molecular volumes of 1.2×10^3 and 4.4×10^3 Å^3, respectively, while the G0-Ni_4 and the G1-Ni_{12} dendrimers **9** and **10** possess volumes of 1.7×10^3 and 5.3×10^3 Å^3, respectively. Earlier studies with the MPF-50 membrane revealed a retention rate of 97.4% for **9** and 99.8% for **10**.[4h] Thus, although **2c** (R = 97.7%) and **4c** (R = 99.9%) possess smaller molecular volumes as compared to G0- **9** and G1-dendrimer **10**, respectively, the shape-persistent materials **2c** and **4c** are retained more efficiently by the nanofiltration membranes than the more flexible dendritic systems. Although these differences in retention seem rather small, under continuously operating reaction conditions, such small differences (between 0.1 and 0.5%) can already have a significant impact.[3]

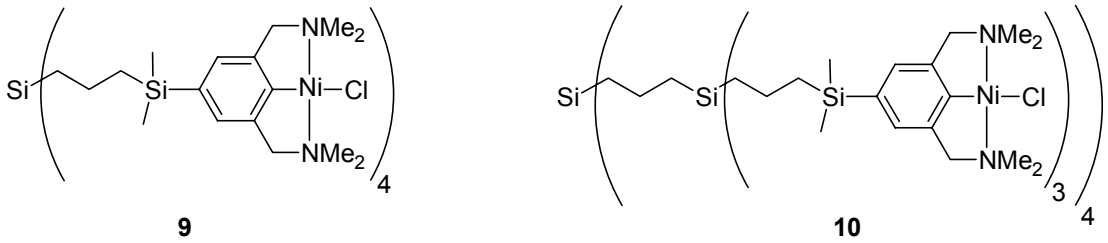

9 **10**

Figure 4. Nickelated G0- and G1-carbosilane dendrimers.

Continuous Catalysis. Since dodecakis(NCN-Pt^{II}) complex **4c** was found to be retained very efficiently by the commercially available MPF-60 (R > 99.9%) and MPF-50 (R = 99.9%) nanofiltration membranes,[15c,16] we decided to use the iso-structural dodecakis[NCN-Pd^{II}-OH_2]$(BF_4)_{12}$ complex **4b** as a homogeneous catalyst in the continuous double Michael reaction between methyl vinyl ketone (MVK) and

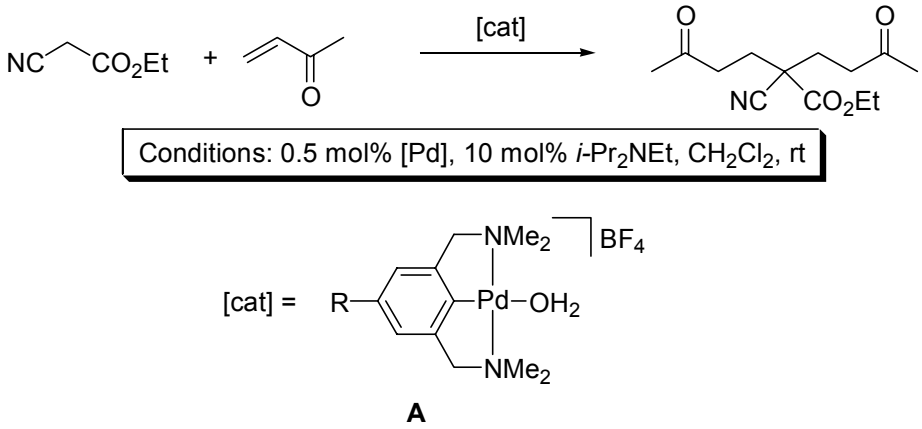

Scheme 2. Double Michael reaction using cationic NCN-Pd^{II}-catalysts.

ethyl-α-cyanoacetate (Scheme 2) in a nanofiltration membrane reactor. Previously, it was found that palladated cationic NCN-pincer complexes of type **A** are very active as Lewis acid catalysts in this reaction.[15b,21] Dodecakis(NCN-Pd^{II}) catalyst **4b**, in particular, was found to possess a remarkable high catalytic activity per Pd^{II}-center; an almost three-times higher activity was found compared to the mononuclear analog **A** (R = OCH_2Ph, Scheme 2).[21] Furthermore, the mild reaction conditions, *i.e.* CH_2Cl_2, Hünigs base, room temperature, are ideal for application under continuously operating conditions using this type of organic polymeric NF membranes. Important to note is that the solvent used for the retention rate determinations,[15c] *i.e.* CH_2Cl_2, is the same as the solvent in which catalysis is performed, making direct comparison feasible.

For the continuous catalytic experiments in a high-pressure membrane reactor (volume = 12 mL), the MPF-50 NF membrane was used.[16] The concentration of the substrates in solution was kept equal to the batch process.[15b,21] Furthermore, the flow-rate was chosen such that the conversion never exceeded 85%. In this way, we were able to study the behavior of the catalyst in time.

Figure 5 shows the space-time yield Y (g L^{-1} h^{-1}) *versus* time for two different continuous catalytic runs. For Run I, a palladium concentration of 1.6 mM (= 0.13 mM of **4b**) and a flow-rate of 12 mL h^{-1} (= one reactor volume per hour) was used. In Run II, the palladium concentration and the flow-rate were increased by a factor 2.5 to 4.2 mM (= 0.35 mM of **4b**) and 30 mL h^{-1} (= 2.5 reactor volumes per hour), respectively, allowing to investigate the influence of these parameters on the catalytic process. In both experiments, the space-time yield shows first a large increase, followed by a slow decrease in time until a more or less constant level is reached. For

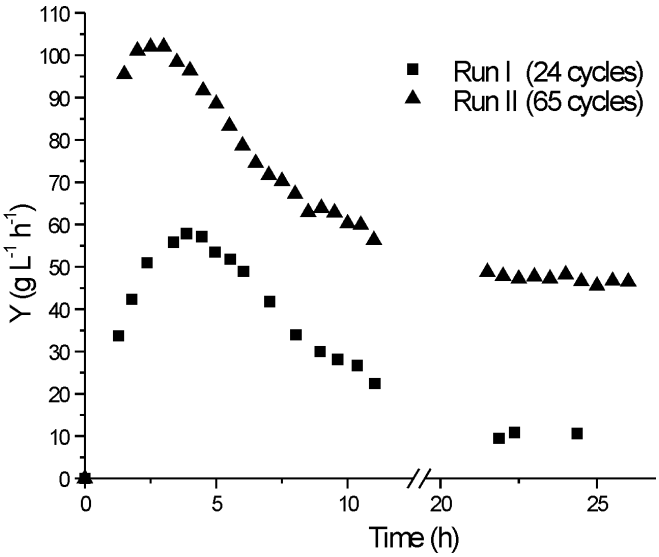

Figure 5. Two different continuous experiments; MPF-50 NF membrane, 1 M MVK, 0.32 M ethyl-α-cyanoacetate and 0.032 M *N*-ethyldiisopropylamine ; Run I: 1.6 mM [Pd], flow-rate = 12 mL h^{-1}, τ = 1 (residence time in h), p = 20 bar; Run II: 4.2 mM [Pd], flow-rate = 30 mL h^{-1}, τ = 0.4, p = 20 bar.

prolonged reaction times, no apparent decrease of the space-time yield was observed anymore, pointing to a constant activity of the catalyst. Remarkable is the difference in the average space-time yield between Run I and II, indicating a more efficient catalytic process when higher catalyst concentrations and flow-rates are applied. In addition, these results show the ease of tuning of such a continuous catalytic setup. The high initial activity of the system can be explained by a higher concentration of ethyl-α-cyanoacetate, necessary to completely solubilize **4b**, at the start of the experiment. Apparently under the chosen continuous conditions, a constant conversion level is only obtained after a considerable number of cycles. In both runs, no Pd-black formation or precipitation, suggesting decomposition or deactivation processes, was observed during the reaction as was established by inspection of the reactor content after completion of the experiment.

These examples nicely illustrate that it is relatively easy to obtain higher space time yields for prolonged time by simply adjusting the continuous reaction conditions, such as catalyst loading, residence times and substrate concentrations. By applying nanofiltration techniques, the total turnover number per palladium center of **4b** is increased by a factor greater than 40 from 80 (batch, Run II) to over 3000 Pd^{-1}. Even after more than 65 residence times (Run II) the system still shows a good activity for product formation. This is not so easy to obtain by other homogeneous catalysts

recycling methods. For example, biphasic systems are often used for this purpose in which the catalyst dissolves in one phase and the substrates and products in the other phase, *e.g.* aqueous biphasic systems,[22] fluorous biphasic systems[23] or non-conventional solvents such as ionic liquids.[24] In most of these systems a continuous operating process is not possible since the catalyst has to be separated in an additional step, *e.g.* separation of the two phases in biphasic systems. Another method is anchoring of the homogeneous catalyst to a solid support,[25] creating a hybrid catalytic system possessing the catalytic properties of a homogeneous catalyst and the recycling properties of a heterogeneous catalyst. Such a system, however, suffers from mass-transfer limitations and often possesses a lower activity than the corresponding homogeneous catalyst due to diffusional limitations caused by the narrow channels in the heterogeneous supports. Furthermore, the distribution of the catalytic centers is often not known, making direct comparison with the corresponding homogeneous catalyst not possible. Applying nanofiltration membranes in homogeneous catalyst recycling overcomes these limitations, since the catalysts are homogeneously dissolved and thus do not suffer from mass-transfer and diffusional limitations, while the separation takes place in the same phase as the catalytic reaction, making it ideal for continuous processes.

5.3. Concluding Remarks

From the nanofiltration studies, it can be concluded that for future development and application in the area of homogeneous catalyst recycling by means of nanofiltration membranes, it is advisable to use macromolecular catalysts with a high degree of shape-persistence in the backbone. UV/Vis spectroscopy was found to be an excellent tool to accurately determine the retention rates of the various shape-persistent complexes, making use of the sensor properties of the [PtX(NCN)] unit for sulfur dioxide. Retention rates varying from 82.4 to >99.9% were obtained using the MPF-60 and MPF-50 nanofiltration membranes. Furthermore, it was shown that the dodecakis[NCN-Pd^{II}-OH_2]$(BF_4)_{12}$ complex **4b** can be used efficiently as a homogeneous catalyst in a continuous double Michael reaction in a nanofiltration membrane reactor. The TTN was increased by a factor >40, showing the high potential of this technique for large scale applications.

In future, it is desirable to develop homogeneous catalysts based on a variety of different catalytic units which show an efficient retention by nanofiltration membranes, a high catalyst efficiency and a high durability of the catalyst during

catalysis. Especially, the latter aspect needs more attention, since the endurance of many homogeneous catalysts, in contrast to heterogeneous catalysts, does not meet the requirements needed for long running continuous catalytic processes. Developing such catalytic systems will allow the application of a variety of homogeneous catalysts in a broad range of selective organic transformations in a nanofiltration membrane reactor. Eventually, this can lead to an increased number of industrial processes involving homogeneous catalysis.

5.4. Experimental Section

General: CH_2Cl_2 was distilled from CaH_2. All standard reagents were carefully distilled prior to use. Complexes **1–5** were prepared as described in Chapters 2 and 3.[15] Complex **6** was prepared according to a literature procedure.[17] The nanofiltration and continuous catalysis experiments were carried out in a stainless steel membrane reactor under elevated pressures.

Retention measurements: The retention measurements were performed in CH_2Cl_2 at room temperature in a nanofiltration membrane cell with a flow-rate of 20 mL h^{-1} using a Koch MPF-60 or MPF-50 flat-membrane.[16] Prior to the filtration experiments, the membranes were first stored overnight in a methanol bath, followed by 1 hour in a CH_2Cl_2-bath and finally CH_2Cl_2 was flushed through the membrane in the membrane reactor in order to remove residual traces of methanol. Typically, 70 μmol of **1c–4c** and **6** was dissolved in 3 mL of CH_2Cl_2 and injected into the reactor. For solubility reasons, **5** was first converted into **7** by treating a suspension of **5** in CH_2Cl_2 (3 mL) with sulfur dioxide, resulting in a bright orange solution which was injected into the reactor. After the filtration experiments the concentration of the macromolecular materials **1–6** in the permeate and the retentate were determined by UV/Vis spectroscopy: an exact volume of the retentate/permeate was mixed with an exact volume of a saturated solution of sulfur dioxide in CH_2Cl_2 and the resulting solution was analyzed with UV/Vis spectroscopy.

Continuous catalysis experiments: The continuous catalytic experiments were performed in CH_2Cl_2 in a nanofiltration membrane cell (12 mL) using the Koch MPF-50 flat-membrane.[16] Prior to the continuous experiments, the membranes were first stored overnight in a methanol bath, followed by 1 h in a CH_2Cl_2-bath. Finally CH_2Cl_2 was flushed through the membrane in the membrane reactor in order to

remove residual traces of methanol. In a typical experiment (Run II), catalyst **4b** (MW = 5701.2; 24.1 mg, 4.2 μmol) was suspended in 3 mL of CH_2Cl_2 and ethyl-α-cyanoacetate (0.5 mL) was added, affording a clear solution. This solution was transferred into the reactor. Subsequently, a solution of MVK (2 M) and diisopropylethylamine (0.064 M) in CH_2Cl_2 (500 mL), as well as a solution of ethyl-α-cyanoactetate (0.64 M) and *n*-decane (0.4 M, internal standard) in CH_2Cl_2 (500 mL) were pumped simultaneously with equal flow-rates (15 mL h^{-1}) into the reactor. Resulting flow-rate = 30 mL h^{-1}, τ = 0.4 h, T = 23 °C, p = 20 bar. Samples of the solution leaving the reactor were taken continuously, quenched with Et_2O and analyzed by GC spectroscopy

5.5. References and Notes

[1] Noyori, R. *Asymmetric Catalysis in Organic Synthesis*, Wiley, New York, **1994**.

[2] For industrial processes catalyzed by homogeneous catalysts see: a) Parshall, G. W.; Ittel, S. D. *The Applications and Chemistry of Catalysis by Soluble Transition Metal Complexes*, Wiley, New York, **1992**. b) Cornils, B.; Herrmann, W. A. *Applied Homogeneous Catalysis with Organometallic Compounds*, VCH, Weinheim, Germany, **1996**.

[3] For an overview on homogeneous catalyst recycling using ultra- or nanofiltration techniques, see: Dijkstra, H. P.; van Klink, G. P. M.; van Koten, G. *Acc. Chem. Res.* **2002**, in press, manuscript available on the world wide web: http://pubs3.acs.org/acs/journals.

[4] a) Knapen, J. W. J.; van der Made, A. W.; de Wilde, J. C.; van Leeuwen, P. W. N. M.; Wijkens, P.; Grove, D. M.; van Koten, G. *Nature* **1994**, *372*, 659. b) Kragl, U.; Dreisbach, C. *Angew. Chem. Int. Ed.* **1996**, *35*, 642. c) Reetz, M. T.; Lohmer, G.; Schwickardi, R. *Angew. Chem. Int. Ed.* **1997**, *36*, 1526. d) Giffels, G.; Beliczey, J.; Felder, M.; Kragl, U. *Tetrahedron: Asymm.* **1998**, *9*, 691. e) Brinkmann, N.; Giebel, D.; Lohmer, G.; Reetz, M. T.; Kragl, U. *J. Cat.* **1999**, *183*, 163. f) Hovestad, N. J.; Eggeling, E. B.; Heidbüchel, H. J.; Jastrzebski, J. T. B. H.; Kragl, U.; Keim, W.; Vogt, D.; van Koten, G. *Angew. Chem. Int. Ed.* **1999**, *38*, 1655. g) de Groot, D.; Eggeling, E. B.; de Wilde, J. C.; Kooijman, H.; van Haaren, R. J.; van der Made, A. W.; Spek, A. L.; Vogt, D.; Reek, J. N. H.; Kamer, P. C. J.; van Leeuwen, P. W. N. M. *Chem. Commun.* **1999**, 1623. h) Kleij, A. W.; Gossage, R. A.; Klein Gebbink, R. J. M.; Reyerse, E. J.; Brinkmann, N.; Kragl, U.; Lutz, M.; Spek, A. L.; van Koten, G. *J. Am. Chem. Soc.* **2000**, *122*, 12112. i) Albrecht, M.; Hovestad, N. J.; Boersma, J.; van Koten, G. *Chem. Eur. J.* **2001**, *7*, 1289. j) Rissom, S.; Beliczey, J.; Giffels, G.; Kragl, U.; Wandrey, C. *Tetrahedron: Asymm.* **1999**, *10*, 923. k) Dwars, T.; Haberland, J.; Grassert, I.; Kragl, U. *J. Mol. Cat. A: Chem.* **2001**, *168*, 81.

[5] For a review on dendritic catalysts see: a) Kreiter, R.; Kleij, A. W.; Klein Gebbink, R. J. M.; van Koten, G. *Dendritic Catalysts. Topics in Current Chemistry, Dendrimers IV*; Vögtle, F., Ed.; Springer-

Verlag Berlin Heidelberg, **2001**, *217*, 163. b) Kleij, A. W.; Klein Gebbink, R. J. M.; van Koten, G. *Dendrimers and other Dendritic Polymers*; Frechet, J., Tomalia, D., Eds.; Wiley, New York, **2002**. c) Oosterom, G. E.; Reek, J. N. H.; Kamer, P. C. J.; van Leeuwen, P. W. N. M. *Angew. Chem. Int. Ed.* **2001**, *40*, 1828.

[6] de Smet, K.; Aerts, S.; Ceulemans, E.; Vankelecom, I. F. J.; Jacobs, P. A. *Chem. Comm.* **2001**, 597.

[7] For leading references see: a) van Koten, G. *Pure Appl. Chem.* **1989**, *61*, 1681. b) Rietveld, M. H. P.; Grove, D. M.; van Koten, G. *New J. Chem.* **1997**, *21*, 751. c) Rybtchinski, B.; Milstein, D. *Angew. Chem. Int. Ed*. **1999**, *38*, 870. d) Steenwinkel, P.; Gossage, R. A.; van Koten, G. *Chem. Eur. J.* **1998**, *4*, 759.

[8] For a review about pincer-metal-d^8-chemistry see: Albrecht, M.; van Koten G. *Angew. Chem. Int. Ed.* **2001**, *40*, 3750.

[9] See 4a, h, i and: a) Huck, W. T. S.; van Veggel, F. C. J. M.; Reinhoudt, D. N. *Angew. Chem. Int. Ed.* **1996**, *35*, 1213. b) Huck, W. T. S.; Hulst, R.; Timmerman, P.; van Veggel, F. C. J. M.; Reinhoudt, D. N. *Angew. Chem. Int. Ed.* **1997**, *36*, 1006. c) Huck, W. T. S.; van Veggel, F. C. J. M.; Reinhoudt, D. N. *New J. Chem.* **1998**, *22*, 165. d) Huck, W. T. S.; Snellinck-Ruël, B.; van Veggel, F. C. J. M.; Reinhoudt, D. N. *Organometallics* **1997**, *16*, 4286. e) Davies, P. J.; Grove, D. M.; van Koten, G. *Organometallics* **1997**, *16*, 800; f) Albrecht, M.; Gossage, R. A.; Lutz, M.; Spek, A. L.; van Koten, G. *Chem. Eur. J.* **2000**, *6*, 1431.

[10] a) Meijer, M. D.; Rump, M.; Gossage, R. A.; Jastrzebski, J. T. B. H.; van Koten, G. *Tetrahedron Lett.* **1998**, *39*, 6773. b) Meijer, M. D.; de Wolf, E.; Lutz, M.; Spek, A. L.; van Klink, G. P. M.; van Koten, G. *Organometallics* **2001**, *20*, 4198. c) Meijer, M. D.; Ronde, N.; Vogt, D.; van Klink, G. P. M.; van Koten, G. *Organometallics* **2001**, *20*, 3993.

[11] a) van de Kuil, L. A.; Grove, D. M.; Zwikker, J. W.; Jenneskens, L. W.; Drenth, W.; van Koten, G. *Chem. Mater.* **1994**, *6*, 1675. b) Bergbreiter, D. E.; Osborn, P. L.; Liu, Y. -S. *J. Am. Chem. Soc.* **1999**, *121*, 9531.

[12] a) Patmamanoharan, C.; Wijkens, P.; Grove, D. M.; Philipse, A. P. *Langmuir* **1996**, *12*, 4372. b) Mehendale, N.; Bezemer, C; Klein Gebbink, R. J. M.; van Koten, G. manuscript in preparation. c) Ford, A.; van Klink, G. P. M.; van Koten, G. manuscript in preparation.

[13] Albrecht, M.; Rodríguez, G.; Schoenmaker, J.; van Koten, G. *Org. Lett.* **2000**, *22*, 3461.

[14] a) Wooley, K.; Klug, C. A.; Tasaki, K.; Schaefer, J. *J. Am. Chem. Soc.* **1997**, *119*, 53. b) Chai, M.; Niu, Y.; Youngs, W. J.; Rinaldi, P. L. *J. Am. Chem. Soc.* **2001**, *123*, 4670.

[15] For the synthesis of **1**–**5** see Chapters 2 and 3 and: a) Dijkstra, H. P.; Steenwinkel, P.; Grove, D. M.; Lutz, M.; Spek, A. L.; van Koten, G. *Angew. Chem. Int. Ed.* **1999**, *38*, 2186. b) Dijkstra, H. P.; Meijer, M. D.; Patel, J.; Kreiter, R.; van Klink, G. P. M.; Lutz, M.; Spek, A. L.; Canty, A. J.; van Koten, G. *Organometallics* **2001**, *20*, 3159. c) Dijkstra, H. P.; Kruithof, C. A.; Ronde, N.; van de Coevering, R.;

Ramón, D. J.; Vogt, D.; van Klink, G. P. M.; van Koten, G. *J. Org. Chem.*, in press, manuscript available on the world wide web: http://pubs3.acs.org/acs/journals.

[16] MPF-nanofiltration membranes (MPF-60: MWCO = 400 Dalton; MPF-50: MWCO = 700 Dalton) were purchased from Koch Membrane Systems Inc., Düsseldorf, Germany; further product information can be found at http://www.kochmembrane.com.

[17] Grove, D. M.; van Koten, G.; Louwen, J. N.; Noltes, J. G.; Spek, A. L.; Ubbels, H. J. C. *J. Am. Chem. Soc.* **1982**, *104*, 6609.

[18] For molecular modeling the Spartan 5.1.1 (SGI) program was used with MMFF94 as the force field.

[19] See 9f and a) Terheijden, J.; Mul, P. W.; van Koten, G.; Muller, F.; Stam, H. C. *Organometallics* **1986**, *5*, 519. b) Albrecht, M.; Gossage, R. A.; Spek, A. L.; van Koten, G. *Chem. Comm.* **1998**, 1003. c) Albrecht, M; van Koten, G. *Adv. Mater.* **1999**, *11*, 171. c) Albrecht, M.; Lutz, M.; Spek, A. L.; van Koten, G. *Nature* **2000**, *406*, 970.

[20] Albrecht, M; Gossage, R. A.; Frey, U.; Ehlers, A. W.; Baerends, E. J.; Merbach, A. E.; van Koten, G. *Inorg. Chem.* **2001**, *40*, 850.

[21] See Chapter 4 and: Dijkstra, H. P.; Slagt, M. Q.; McDonald, A.; Kruithof, C. A.; Kreiter, R.; Mills, A. M.; Lutz, M.; Spek, A. L.; Klopper, W.; van Klink, G. P. M.; van Koten, G., submitted.

[22] For a review on aqueous biphasic systems see: Herrmann, W. A.; Kohlpaintner, C. W. *Angew. Chem. Int. Ed. Engl.* **1993**, *32*, 1524.

[23] For reviews on fluorous biphasic systems see: a) de Wolf, E.; van Koten, G.; Deelman, B. –J. *Chem. Soc. Rev.* **1999**, *28*, 37. b) Horváth, I. T. *Acc. Chem. Res.* **1998**, *31*, 641.

[24] For reviews on ionic liquids see: a) Welton, T. *Chem. Rev.* **1999**, *99*, 2071. b) Wasserscheid, P.; Keim, W. *Angew. Chem, Int. Ed.* **2000**, *39*, 3772.

[25] For reviews on supported catalysts see: a) Clark, J. H.; Macquarrie, D. J. *Chem. Commun.* **1998**, 853. b) de Miguel, Y. R. *J. Chem. Soc., Pekin Trans. 1* **2000**, 4213.

– Chapter 6 –

Hexakis(PCP-Platinum and -Ruthenium) Complexes by the Transcyclometalation (TCM) Reaction and Their Use in Catalysis

Abstract: Hexakis(PCP-pincer) complexes $[C_6\{PtBr(PCP)\}_6]$ and $[C_6\{RuCl(PCP)(PPh_3)\}_6]$ were synthesized via the transcyclometalation (TCM) procedure. Mixing the hexakis(PCHP-arene) ligand with six equivalents of [PtBr(NCN)] or $[RuCl(NCN)(PPh_3)]$, respectively, resulted in the selective metalation of all PCP-ligand sites and the concomitant formation of six equivalents of the NCHN-arene ligand. This procedure was found to be superior over existing metalation procedures. In addition, the hexaruthenium complex was applied as a homogeneous catalyst in the hydrogen transfer reactions of cyclohexanone, acetophenone and benzophenone to the corresponding alcohols. In these reactions, the activity per ruthenium center was found to be of the same order of magnitude as that of the mononuclear analog $[RuCl(PCP)(PPh_3)]$, indicating that all ruthenium centers act as independent catalytic sites.

H. P. Dijkstra, M. Albrecht, G. van Koten, *Chem. Commun.* **2002**, 126.
H. P. Dijkstra, M. Albrecht, S. Medici, G. P. M. van Klink, G. van Koten, submitted.

6.1. Introduction

In the last decade, organometallic complexes containing the monoanionic, terdentate coordinating PCP-pincer ligand (PCP = $[C_6H_3(CH_2PR_2)_2\text{-}2,6]^-$) have been intensively studied as homogeneous catalysts in organic transformations, *e.g.* aldol reactions,[1] asymmetric allylic alkylations,[2] dehydrogenation of alkanes,[3] Heck reactions[4] and hydrogen transfer reactions.[5] The preparation of these PCP-metal complexes often proceeds by C–H bond activation using suitable transition metal precursors.[6] Recently, we reported the synthesis of ruthenated and platinated PCP-ligands applying the *transcyclometalation* (TCM) procedure (Scheme 1).[7] In close relation to (organic) transesterification reactions, TCM reactions comprise the substitution of one cyclometalated ligand by another. For example, the reaction of [M(NCN)] **1** with PCHP **2** affords quantitatively complex [M(PCP)] **3** and the free arene NCHN **4** for both ML = PtBr (**1a**) or RuCl(PPh_3) (**1b**) (Scheme 1). A crucial aspect of the TCM reactions is the difference in bond strengths of the various metal-heteroatom bonds, which have to be stronger in the products than in the starting material (viz. M–P stronger than M–N bond). The reaction pathway followed is similar to that of the electrophilic aromatic substitution reaction.[7b] In addition, the reactions take place under mild conditions (in terms of temperature, pressure and reagents), are very selective for *ortho,ortho*–metalation and proceed in quantitative yields with the NCHN-arene ligand as the only co-product.

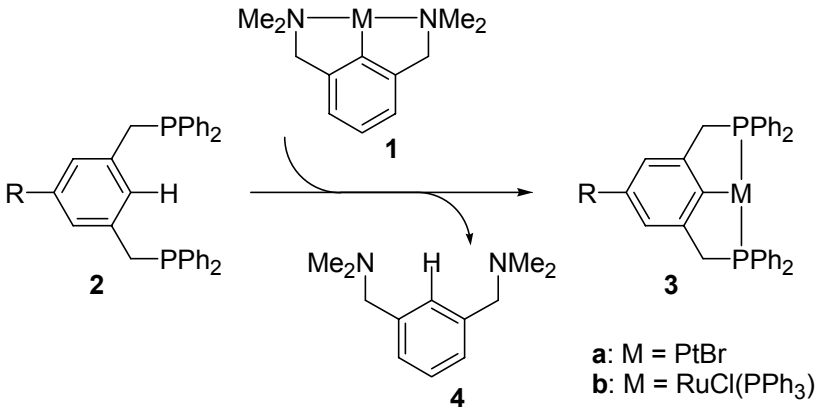

Scheme 1. Synthesis of PCP(ruthenium and platinum) complexes using the TCM procedure.

Recently, we started to develop shape-persistent nanosize multi(pincer-metal) complexes and explore their application in a nanofiltration membrane reactor.[8] Due to

their shape-persistence, these soluble complexes were found to be retained very efficiently by nanofiltration membranes,[8c] allowing their use as homogeneous catalysts in organic transformations under continuously operating reaction conditions.[8d,9] In addition, highly symmetric tris- and hexakismetallic complexes of type **5** and **6** (Figure 1) were used as templates in the synthesis of large heterocycles (ringsize: 69 – 75 atoms) using olefin metathesis for the ring closing reaction.[10] Until now, however, mainly palladium and in some cases platinum (only in combination with NCN-type ligands) complexes were used for these purposes.[8,10] For a broad application of these multimetallic complexes in the field of homogeneous catalysis and template-directed synthesis, it is desirable to synthesize such systems containing different metals. Since monometallic PCP-complexes can be applied in a broader and complementary range of organic transformations, gaining access to shape-persistent nanosize multi(PCP-metal) complexes containing various metals also would allow the application of these catalytic reactions under continuously operating conditions in a nanofiltration membrane reactor.

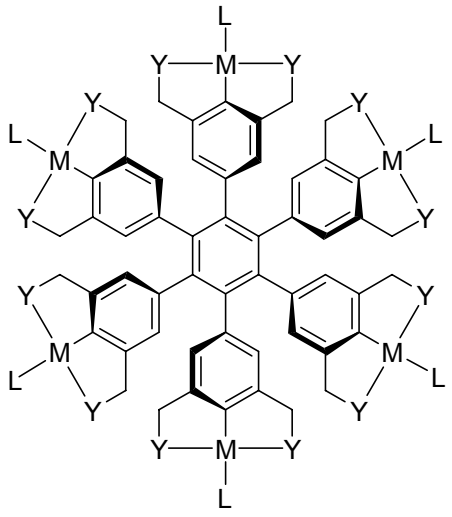

5a: M = Pd, Y = SPh
5b: M = Pd, Y = PPh_2
5c: M = Pd, Y = pyrazol-1-yl

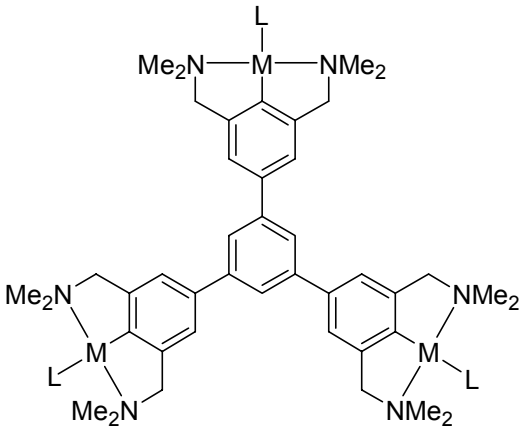

6a: M = Pd
6b: M = Pt

Figure 1. Shape-persistent multi(YCY-pincer-metal) complexes.

In this chapter, the synthesis of hexakis(PCP-platinum and -ruthenium) complexes (**5**, Y = PPh_2, ML = PtBr or $RuCl(PPh_3)$, Figure 1) using the TCM reaction is presented.[11] In addition the application of the hexakis(PCP-Ru)-complex as a homogeneous catalyst in three different hydrogen transfer reactions will be discussed.

6.2. Results and Discussion

Recently, we reported the synthesis of hexakis(PCHP-arene) ligand **7** (Figure 2) and its palladation procedure.[8b] However, various attempts to directly cycloplatinate ligand **7** six times failed in spite of using different metal precursors that previously were successfully applied for the cycloplatination of analogous single site PCP ligands.[12] Treatment of **7** with six equivalents of $[PtCl_2(cod)]$ in mesitylene at reflux conditions, resulted in the formation of intractable mixtures. Reaction of six equivalents of *cis*-$[PtCl_2(PPh_3)_2]$ with **7** in CH_2Cl_2 at room temperature also failed. Most likely, the local phosphine concentration, which is exceptionally high in **7**, leads to the formation of η^2*–P,P–*coordinated platinum centers which do not undergo subsequent C–H bond activation. This activation process is anticipated to require transient decoordination of one phosphine ligand in order to generate the electronically and coordinatively unsaturated reactive intermediate.[13] An alternative method is to introduce six platinum centers via a multiple lithiation/transmetalation procedure, a method developed to metalate NCN-pincer ligands.[14] Only one example is known in which a PCP ligand is used in a transmetalation procedure.[15] Various attempts, however, to lithiate **7** with six equivalents of *n*-BuLi or *tert*-BuLi in hexanes at various temperatures, followed by a transplatination with $[PtCl_2(cod)]$ or $[PtCl_2(SEt_2)]$ failed. Probably, bis(ortho)-lithiation of **7** suffered from low selectivity because of the relatively high acidity of the neighboring benzylic protons. Thus, both direct cyclometalation and lithiation/transmetalation did not lead to full and selective platination of **7**.

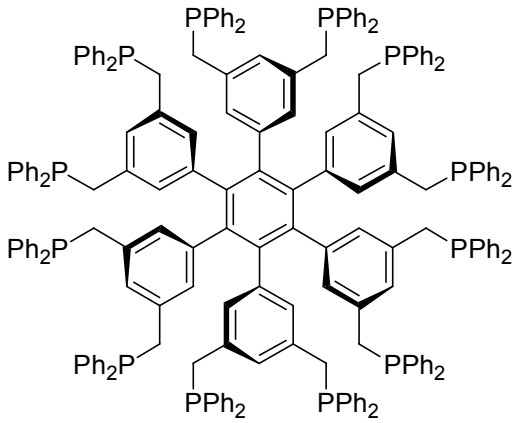

7

Figure 2. Hexakis(PCP) ligand **7**.

As reported earlier, in the TCM reaction the precursor [PtBr(NCN)] (**1a**, Scheme 1) has (thermodynamically and kinetically) a rigid *trans-N,N*-configuration and, therefore, forces eventual formed bisaryl platinum intermediates, *i.e.* [Pt(PCP)(NCN)] type structures (Figure 3), in a *trans-C,C*-configuration.[7b] Most of the metal precursors used in cyclometalation reactions, however, do not ultimately exclude the formation of alternative species with the heteroatom donors in a mutual *cis*-configuration. This prevents cyclometalation and is likely to promote rigid η^2-*P,P*-bidentate *cis*-coordination of adjacent phosphine sites.[16] Particularly with multisite ligands such as **7**, possessing a high concentration of coordination sites at the periphery, this is likely to take place. Since the TCM reaction proceeds via a *trans*-configuration, competitive undesired coordination modes are prevented, making the TCM reaction very promising for metalation of ligands such as **7**. In addition, the TCM reaction proceeds in quantative yield, which is a crucial aspect when applying such a metalation procedure for preparing multimetallic complexes.

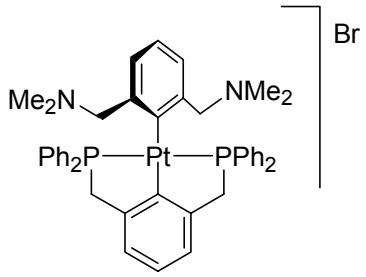

Figure 3. *trans-C,C*-Bisarylplatinum intermediate in the TCM reaction.[7b]

Treatment of hexakis(PCHP-arene) ligand **7** with six equivalents of [PtBr(NCN)] (**1a**), led to the formation of hexakis(PCP-Pt-Br) **8** in 70% isolated yield (Scheme 2) (equal to a 94% yield per single ligand site). Separation of **8** from NCHN, the only other formed product, was achieved by a double extraction and precipitation procedure using CH_2Cl_2 and Et_2O, respectively. Complete transcyclometalation was unequivocally assessed by multinuclear NMR spectroscopy, elemental analysis and by MALDI-TOF mass spectrometry (m/z 4557.74 (M^+); calcd 4557.11). In the ^{1}H NMR spectrum, the resonances due to the benzylic protons of **8** are characteristically shifted toward lower field upon metal insertion (δ_H = 2.88 in **7** and 3.07 in **8**). No signals due to traces of metal-free PCHP units or residual [PtBr(NCN)] (**1a**) were detected. The ^{31}P NMR spectrum displays a diagnostic single resonance at 36.1 ppm ($^1J_{Pt,P}$ = 2864 Hz)[7b] due to the *trans*-phosphorus nuclei of the PCP ligand sites that are

coordinated to platinum. No signals were observed which could point to only partial metalation, which is remarkable and emphasizes once again the scope of the TCM reaction.

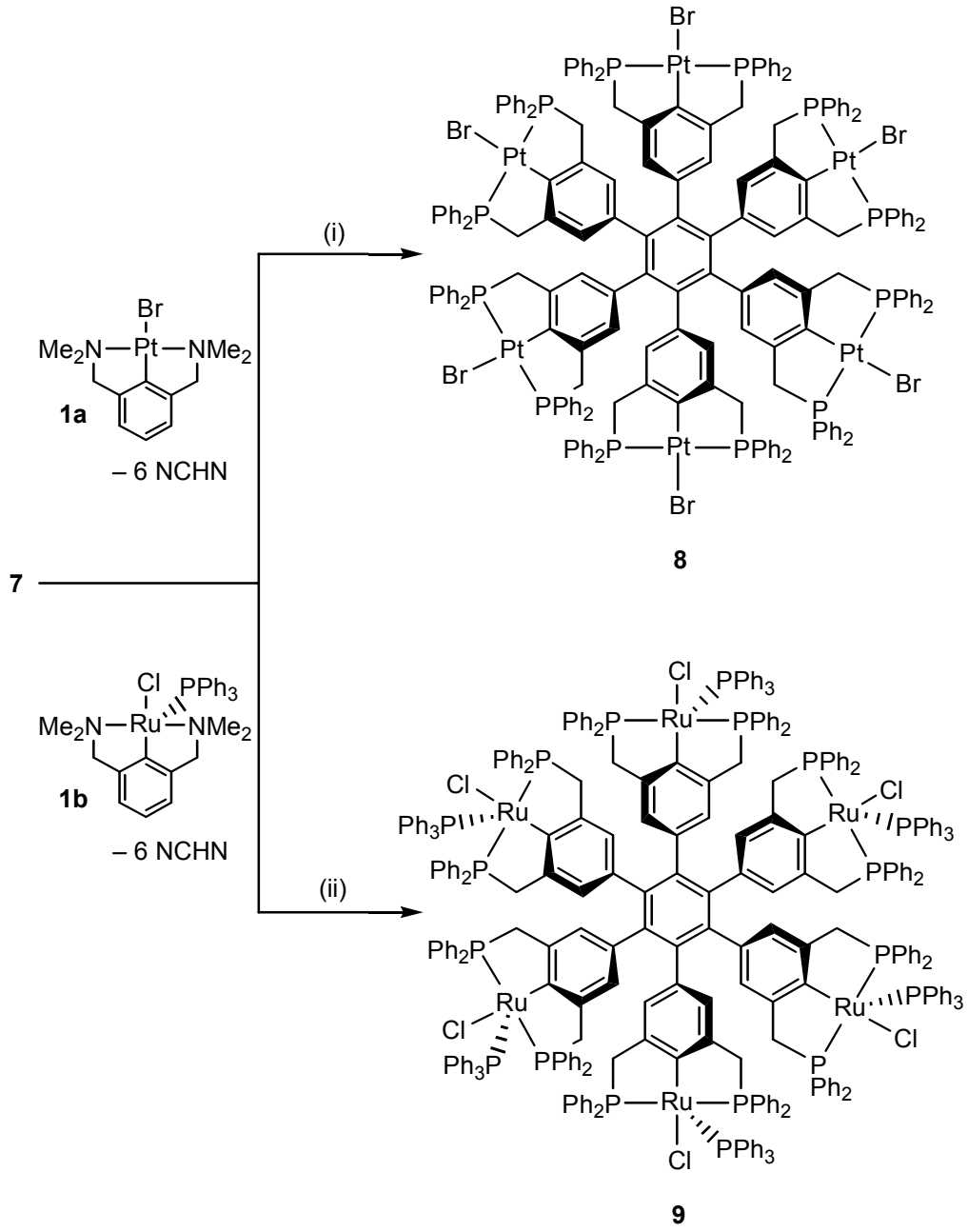

Scheme 2. Synthesis of hexakis(PCP-platinum and -ruthenium) complexes applying the TCM reaction: (i) six equiv of **1a**, toluene, reflux, 3 d; (ii) six equiv of **1b**, benzene, reflux, 18 h.

The same procedure is followed to prepare hexakis(PCP-Ru) complex **9** (Scheme 2). Treatment of **7** with six equivalents of [RuCl(NCN)(PPh_3)] (**1b**), resulted in the formation of dark green, air sensitive hexaruthenium complex **9** in 79% yield (equal to a 96% yield per single ligand site). The NMR spectra of this multimetallic species are uniformly broad, which most likely is due to dynamic processes involving a change in mutual orientation of the PCP aryl planes (note that each ruthenium center has a square-pyramidal configuration); Scheme 2 shows only one of the several possible conformations of **9**. The ^{31}P NMR spectrum (CD_2Cl_2) of **9** shows two peaks (δ_P 80.8 (m) and 40.7 (m), the multiplicity of the peaks is due to different conformers of **9**). These chemical shift values are in agreement with those found for the monometallic analog [RuCl(PCP)(PPh_3)] (δ_P 81.3 (t) and 36.5 (d)). Due to the extreme air sensitivity, a correct elemental analysis pointing to the isolation of pure **9** could not be obtained. Therefore for further analysis, **9** was converted into [hexakis(PCP-Ru-terpy)]$(X)_6$ complex **10a** (X = Cl) containing cationic hexacoordinate ruthenium centers (Scheme 3). This was achieved by prolonged reaction (2 d) of a solution of **9** with six equivalents of 2,2':6',2"-terpyridine (terpy) in methanol at reflux conditions.[6e] This reaction was accompanied by a characteristic color change from dark green to dark red. The changed geometry around the metal

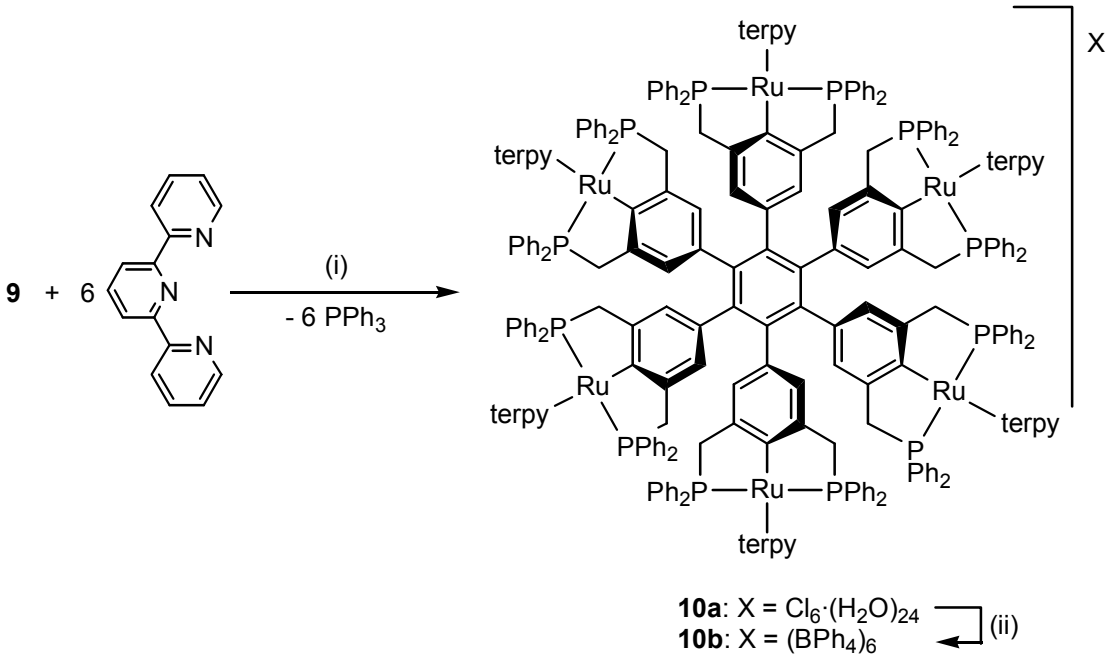

Scheme 3. Synthesis of [hexakis(PCP-Ru-terpy)]$(X)_6$ complexes **10a** and **10b**: (i) 6 equiv of 2,2':6',2"-terpyridine (terpy), MeOH, reflux, 2 d; (ii) $NaBPh_4$, acetone, rt, 2 h.

centers in **10a**, from distorted square-pyramidal into octahedral, has two advantageous consequences; i) the complex is stable toward air and water, and ii) the coordination geometry around ruthenium has a markedly higher symmetry, thereby reducing the number of potential conformers of **10a**. The ^{31}P NMR spectrum now shows a single resonance at δ_P 41.5, with a value characteristic for a phosphorous-center in a [Ru(PCP)(terpy)]Cl complex.[6e] The elemental analysis of **10a** revealed a structure with a bruto formula of $C_{288}H_{270}Cl_6N_{18}O_{24}P_{12}Ru_6$, indicating that for each molecule of **10a** 24 water molecules are included. This observation was confirmed by ^1H NMR spectroscopy, which showed a large peak at δ_H 3.5, which could not be ascribed solely to small amounts of water present in the deuterated solvents. Replacing the chloride counterions by tetraphenylborate anions, by treating **10a** with six equivalents of sodium tetraphenylborate in acetone, resulted in the disappearance of the water molecules as was shown by ^1H NMR spectroscopy of a solution of **10b** in CD_2Cl_2. Interestingly this observation suggests that the water molecules in **10a** have a distinct orientation, *e.g.* four water molecules could be bound to each chloride anion. Regrettably, no crystals of **10a** suitable for X-ray single crystal structure determination could be obtained and thus also the exact binding mode of the co-crystallized water molecules could not be elucidated.

Catalysis. An important new application for multimetallic complexes is their use as homogeneous catalysts in a nanofiltration membrane reactor in order to address the important issue of catalyst recycling.[9] Applying this technique in catalyst recycling results in significantly higher total turnover numbers as well as in preventing the presence of toxic metals in the product stream. It was already shown that a high degree of shape-persistence in the organic backbone of such materials is important to acquire optimal retentions of these catalysts by nanofiltration membranes.[8c] So far, only the use of shape-persistent multi(NCN-Pd^{II}) complexes as homogeneous catalysts was explored.[8b,e] It is known that monometallic PCP-Ru^{II} complexes are very active as homogeneous hydrogen-transfer catalysts in the conversion of ketones to alcohols.[5] Encouraged by these results, hexakis(PCP-Ru^{II}) complex **9** was tested as a homogeneous catalyst in the hydrogen-transfer reaction of several ketones to the corresponding alcohols (Scheme 4). In order to make a direct comparison possible with the monoruthenated species, we also tested [RuCl(PCP)(PPh_3)] **3b** (Scheme 4) under the same conditions. Cyclohexanone, acetophenone and benzophenone were selected as reagents. In all reactions, 0.1 mol% [Ru], 2 mol% potassium hydroxide and 0.67 M ketone in *i*-propanol was used.

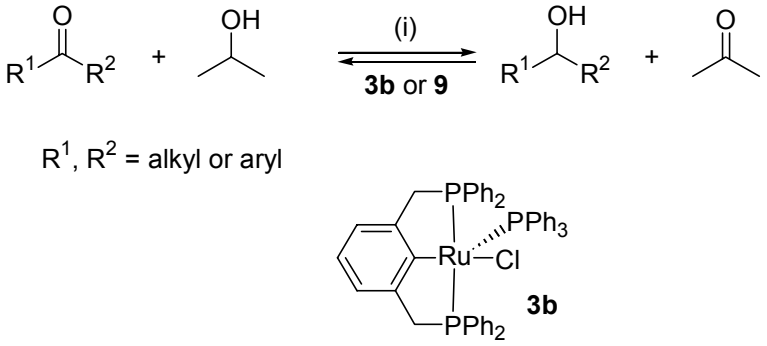

Scheme 4. PCP-Ruthenium complexes **3b** and **9** as hydrogen-transfer catalysts. (i) 0.1 mol% [Ru], [KOH]/[Ru] = 20, 20 mmol ketone, 30 mL *i*-PrOH, reflux.

Table 1. Hydrogen-transfer reaction of ketones using **3b** and **9** as catalysts.

Entry	Substrate	Product	Catalyst	TOF (h^{-1}) [a]
1	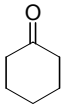	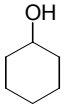	**9**	4300
2			**3b**	9300
3			**9**	2200
4			**3b**	2300
5			**9**	320
6			**3b**	350

a) Turnover frequency (moles of ketone converted to alcohol per mole of [Ru] per hour), determined in the first 50% conversion.

The turnover frequencies (TOF) obtained with catalysts **3b** and **9** in the hydrogen-transfer reactions are summarized in Table 1. In the reduction of cyclohexanone to cyclohexanol (entries 1 and 2, Table 1), the catalytic activity of **3b** was found to be twice as high as that of hexametallic catalyst **9** (per ruthenium center). Nevertheless, a TOF of 4300 means complete conversion within 30 minutes under the given reaction conditions. In the hydrogen-transfer reaction of acetophenone and benzophenone to 1-phenylethanol (entries 3 and 4) and benzhydrol (entries 5 and 6), respectively, the activity of **9** (per ruthenium center) was found to be equal to that of the mononuclear analog **3b** (entry 3 *vs.* 4 and 5 *vs.* 6). These latter

results, clearly indicate that all six ruthenium centers in **9** act as independent catalytic sites for this type of reaction.

In the research area of homogeneous catalyst recycling using nanofiltration membranes, not only an efficient retention of the catalyst by the membranes is important, but also efficient use of all catalytic sites and catalyst stability is a prerequisite. To investigate the stability of the catalyst in hydrogen-transfer reactions, **9** was tested again in the reduction of cyclohexanone to cyclohexanol using the same reaction conditions as described before. This time, however, after complete conversion, heating of the reaction mixture under reflux conditions was continued for an additional 20 h. Subsequent addition of cyclohexanone and monitoring this reaction in time, revealed that the catalyst (**9**) still possessed the same catalytic activity, as a similar TOF was found (TOF = 4000; compare with entry 1, Table 1). Thus, **9** shows both an efficient use of all catalytic ruthenium centers and a high catalyst stability in hydrogen transfer reactions, ensuring application of **9** in hydrogen-transfer reactions for prolonged reaction times. Since it was already found that shape-persistent complexes such as **9** possess high retention rates by nanofiltration membranes,[8] hexanuclear complex **9** is an attractive candidate as a homogeneous catalyst in a nanofiltration membrane reaction. This research is currently in progress.

6.3. Concluding Remarks

Nowadays, an increasing number of macromolecular homogeneous catalysts are reported that show high retentions by nanofiltration membranes and an efficient use of all catalytic sites during catalysis.[9] In future, for nanofiltration membrane technology to be applicable on large industrial scale, research should be focussed on the durability of the catalyst during catalysis. The endurance of many homogeneous catalysts, in contrast to heterogeneous catalysts, does not yet meet the requirements needed for long running continuous catalytic processes. Furthermore, developing recyclable homogeneous catalysts based on a variety of different catalytic units is also desirable, since it allows the application of a broad range of selective organic transformations in a nanofiltration membrane reactor, the first step toward large scale continuous processes.

6.4. Experimental Section

General: All reactions were carried out using standard Schlenk techniques under an inert nitrogen atmosphere unless stated otherwise. Et_2O, THF and hexanes were carefully dried and distilled from Na/benzophenone prior to use. CH_2Cl_2 was distilled from CaH_2. All standard reagents were purchased. Compounds **1a**[8b], **1b**,[17] **3b**[18] and **7**[8b] were prepared according to literature procedures. ^1H and ^{13}C NMR spectra were recorded at 25 °C, chemical shifts are in ppm referenced to residual solvent resonances. MALDI-TOF-MS spectra (nitrogen laser emitting at 337 nm) were acquired using a Voyager-DE Bio-Spectrometry Workstation mass spectrometer using (3,5-dihydroxybenzoic acid) as the matrix. The samples were dissolved in THF or CH_2Cl_2 (~30 mg/ml) and 0.2 µl of both solutions were mixed and placed on a gold MALDI target and analyzed after evaporation of the solvent. Elemental microanalyses were performed by Dornis und Kolbe, Mikroanalytisches Laboratorium, Müllheim a.d. Ruhr, Germany.

Synthesis of 8: A solution of hexakis(PCHP) **7** (0.20 g, 68.7 µmol) and [PtBr(NCN)] **1a** (0.19 g, 0.42 mmol) in toluene (50 mL) was heated to reflux for 3 d. The reaction mixture was allowed to cool to room temperature, filtered and the filtrate was evaporated to dryness. The resulting yellow solid was dissolved in CH_2Cl_2 (20 mL) and the product was precipitated from this solution by slow diffusion of Et_2O. This procedure was repeated twice, affording an off-white solid. Yield: 0.22 g (70%). ^1H NMR ($CDCl_3$, 200 MHz): δ 7.84–6.47 (m, 132H, Ar*H*), 3.07 (br, $^3J_{Pt,H}$ = 28 Hz, 24H, ArC*H*$_2$P). ^{13}C NMR ($CDCl_3$, 75 MHz): δ 161–105 (C_{aryl}), 38.4 ($^3J_{C,Pt}$ not resolved, *C*H$_2$P). ^{31}P NMR ($CDCl_3$, 81 MHz): δ 36.1 ($^1J_{Pt,P}$ = 2864 Hz). MALDI–TOF (m/z): 4557.74 (calcd M^+ : 4557.11), 4478.12 (calcd [M^+–Br]: 4477.20), 4315.55 (calcd [M^+–3Br]: 4317.38). Anal. calcd for $C_{198}H_{156}Br_6P_{12}Pt_{12}$: C, 52.19; H, 3.45; P, 8.11. Found: C, 52.06; H, 3.54; P, 8.11.

Synthesis of 9: A solution of hexakis(PCHP) **7** (0.21 g, 70.6 µmol) and [RuCl(NCN)(PPh_3)] **1b** (0.25 g, 0.42 mmol) in benzene (40 mL) was heated to reflux for 18 h. Upon heating, a slow color change from dark purple to dark green was observed. The reaction mixture was allowed to cool to room temperature, filtered and the filtrate was evaporated to dryness. The resulting dark green solid was dissolved in degassed CH_2Cl_2 (20 mL) and the product was precipitated from this solution by slow diffusion of pentane. This procedure was repeated twice, affording a dark-green solid.

Yield: 0.30 g (79%). ^{1}H NMR (CD_2Cl_2, 200 MHz): δ 8.1–6.4 (br m, 222H, Ar*H*), 3.67 (br, 12 H, ArCH_2P), 3.19 (br, 12H, ArCH_2P). ^{13}C NMR (CD_2Cl_2, 75 MHz): δ 165–114 (C_{aryl}), 43.3 (br, *C*H_2P). ^{31}P NMR (CD_2Cl_2, 81 MHz): δ 80.8 (m, PPh_3), 40.7 (app. m, PPh_2).

Synthesis of 10: A solution of **9** (0.30 g, 56.6 μmol) and 2,2':6',2''-terpyridine (79 mg, 0.34 mmol) in MeOH (15 mL) was heated to reflux for 2 d. In this period, a color change from dark green to brown red was observed. After cooling the mixture to room temperature, THF (15 mL) was added, affording a brown red precipitate. This precipitate was collected, washed with THF (2 × 10 mL) and dried *in vacuo*, affording **10a** as a brown red powder. Yield: 0.31 g (97%). In order to replace the chloride anion for a tetraphenylborate anion, **10a** (20 mg, 3.6 μmol) was suspended in dry acetone (2 mL) and a solution of sodium tetraphenylborate (7.4 mg, 21.6 μmol) in dry acetone (0.5 mL) was added. Immediately, a clear solution was obtained and this mixture was stirred at room temperature for 2 h. All volatiles were evaporated, the residue was extracted with CH_2Cl_2 (2 mL) and slow addition of pentane to the CH_2Cl_2 solution resulted in the precipitation of a brown solid. This precipitate was collected and dried *in vacuo*, to give [hexakis(PCP-Ru-terpy)]$(BPh_4)_6$ (**10b**) as a brown solid. Yield: 22 mg (90%).

10a: ^{1}H NMR (DMSO-d_6, 300 MHz): δ 9.2–6.0 (br m, 198H, Ar*H*), 3.52–4.40 (br m, 24H, ArCH_2P). ^{13}C NMR (DMSO-d_6, 75 MHz): δ 158–156, 154–152, 146–144, 139–126, 125–122 (all br, Ar*C*), 44.9 (*C*H_2P). ^{31}P NMR (DMSO-d_6, 81 MHz): δ 45.9 (CH_2*P*). Anal. Calcd for $C_{288}H_{222}Cl_6N_{18}P_{12}Ru_6 \cdot (H_2O)_{24}$: C, 62.23; H, 4.90; N, 4.54; P, 6.69. Found: C, 62.84; H, 4.56; N, 4.45; P, 6.79.

10b: ^{1}H NMR (CD_2Cl_2, 300 MHz): δ 8.2–6.0 (br m, 318H, Ar*H*), 4.3–2.8 (br m, 24 H, ArCH_2P). ^{31}P NMR (CD_2Cl_2, 81 MHz): δ 46.6 (br s, CH_2*P*).

General procedure for the catalytic hydrogen transfer reaction: Complex **9** (17.7 mg, 3.3 μmol = 20 μmol [Ru]) or [RuCl(PCP)(PPh_3)] **3b** (17.4 mg, 20 μmol) was mixed with potassium hydroxide (22 mg, 0.4 mmol) in *i*-PrOH (10 mL) and the resulting mixture was heated to reflux for 1 h, resulting in a brown solution. Subsequently, a solution of the appropriate ketone (20 mmol) in *i*-PrOH (20 mL) was added and the resulting solution was heated to reflux for several hours. The reaction was monitored by GC analysis with either *n*-decane (for cyclohexanone and acetophenone) or *n*-pentadecane (for benzophenone) as internal standard.

6.5. References and Notes

[1] a) Gorla, F.; Togni, A.; Venanzi, L. M.; Albinati, A.; Lianza, F. *Organometallics* **1994**, *13*, 1607. b) Longmire, J. M.; Zhang, X.; Shang, M. *Organometallics* **1998**, *17*, 4374.

[2] a) Zhu, G.; Terry, M.; Zhang, X. *Tetrahedron Lett.* **1996**, *37*, 4475. b) Longmire, J. M.; Zhang, X. *Tetrahedron Lett.* **1997**, *38*, 1725.

[3] a) Gupta, M.; Hagen, C.; Flesher, R. J.; Kaska, W. C.; Jensen, C. M. *Chem. Commun.* **1996**, 2083. b) Gupta, M.; Kaska, W. C.; Jensen, C. M. *Chem. Commun.* **1997**, 461. c) Gupta, M.; Hagen. C.; Kaska, W. C.; Cramer, R. E.; Jensen, C. M. *J. Am. Chem. Soc.* **1997**, *119*, 840. d) Jensen, C. M. *Chem. Commun.* **1999**, 2443.

[4] Ohff, M.; Ohff, A.; van der Boom, M. E.; Milstein, D. *J. Am. Chem. Soc.* **1997**, *119*, 11687.

[5] a) Dani, P.; Karlen, T.; Gossage, R. A.; Gladiali, S.; van Koten, G. *Angew. Chem. Int. Ed.* **2000**, *39*, 743. b) Dani, P.; Karlen, T.; Gossage, R. A.; Smeets, W. J. J.; Spek, A. L.; van Koten, G. *J. Am. Chem. Soc.* **1997**, *119*, 11317.

[6] See reference 1a and: a) Perera, S. D.; Shaw, B. L. *J. Chem. Soc., Dalton Trans.* **1995**, 3861. b) Moulton, C. J.; Shaw, B. L. *J. Chem Soc., Dalton Trans.* **1976**, 1020. c) Nemeh, S.; Jensen, C. M.; Binamira-Soriaga, E.; Kaska, W. C. *Organometallics* **1983**, *2*, 1442. d) van der Boom, M. E.; Liou, S. –Y.; Ben-David, Y.; Gozin, M.; Milstein, D. *J. Am. Chem. Soc.* **1998**, *120*, 13415. e) Karlen, T.; Dani. P.; Grove, D. M.; Steenwinkel, P.; van Koten, G. *Organometallics* **1996**, *15*, 5687.

[7] See reference 5 and: a) Dani, P.; Albrecht, M.; van Klink, G. P. M.; van Koten, G. *Organometallics* **2000**, *19*, 4468. b) Albrecht, M.; Dani, P.; Lutz, M.; Spek, A. L.; van Koten, G. *J. Am. Chem. Soc.* **2000**, *122*, 11833.

[8] a) Dijkstra, H. P.; Steenwinkel, P.; Grove, D. M.; Lutz, M.; Spek, A. L.; van Koten, G. *Angew. Chem. Int. Ed.* **1999**, *38*, 2186. b) Dijkstra, H. P.; Meijer, M. D.; Patel, J.; Kreiter, R.; van Klink, G. P. M.; Lutz, M.; Spek, A. L.; Canty, A. J.; van Koten G. *Organometallics* **2001**, *20*, 3159. c) Dijkstra, H. P.; Kruithof, C. A.; Ronde, N.; van de Coevering, R.; Ramón, D. J.; Vogt, D.; van Klink, G. P. M.; van Koten, G. *J. Org. Chem*., in press, manuscript available on the world wide web: http://pubs3.acs.org/acs/journals. d) Dijkstra, H. P.; Ronde, N.; van Klink, G. P. M.; Vogt, D.; van Koten, G., submitted. e) Dijkstra, H. P.; Slagt, M. Q.; McDonald, A.; Kruithof, C. A.; Kreiter, R.; Mills, A. M.; Lutz, M.; Spek, A. L.; van Klink, G. P. M.; van Koten, G., submitted.

[9] For an overview on homogeneous catalyst recycling using ultra- and nanofiltration membranes see: Dijkstra, H. P.; van Klink, G. P. M.; van Koten, G. *Acc. Chem. Res.*, in press, manuscript available on the world wide web: http://pubs3.acs.org/acs/journals.

[10] a) Dijkstra, H. P.; Chuchuryukin, A.; Suijkerbuijk, B. M. J. M.; van Klink, G. P. M.; Mills, A. M.; Spek, A. L.; van Koten, G. *Adv. Synth. Catal.*, in press. b) Chuchuryukin, A.; Dijkstra, H. P.; van Klink, G. P. M.; Klein Gebbink, R. J. M.; van Koten, G., submitted.

[11] Dijkstra, H. P.; Albrecht, M.; van Koten, G. *Chem. Commun.* **2002**, 126.

[12] a) Gorla, F.; Venanzi, L. M.; Albinati, A. *Organometallics* **1994**, *13*, 43. b) Bennett, M. A.; Jin, H.; Willis, A. C. *J. Organomet. Chem.* **1993**, *451*, 249. c) van der Boom, M. E.; Kraatz, H. –B.; Hassner, L.; Ben-David, Y.; Milstein, D. *Organometallics* **1999**, *18*, 3873.

[13] Huang, D.; Streib, W. E.; Bollinger, J. C.; Caulton, K. G.; Winter, R. F.; Scheiring, T. *J. Am. Chem. Soc.* **1999**, *121*, 8087.

[14] a) Grove, D. M.; van Koten, G.; Louwen, J. N.; Noltes, J. G.; Spek, A. L.; Ubbels, H. J. C. J. *J. Am. Chem. Soc.* **1984**, *104*, 6609. b) Kleij, A. W.; Kleijn, H.; Jastrzebski, J. T. B. H.; Smeets, W. J. J.; Spek, A. L.; van Koten, G. *Organometallics* **1999**, *18*, 268. c) Kleij, A. W.; Gossage, R. A.; Klein Gebbink, R. J. M.; Brinkmann, N.; Reyerse, E. J.; Kragl, U.; Lutz, M.; Spek, A. L.; van Koten, G. *J. Am. Chem. Soc.* **2000**, *122*, 12112.

[15] Br-4-$C_6H_3(CH_2PMe_2)_2$-2,6 was lithiated with *n*-BuLi (bromo-lithium exchange) and transmetalated with MgX_2 to give a PCP-magnesium complex: Pape, A.; Lutz, M.; Müller, G. *Angew. Chem. Int. Ed.* **1994**, *33*, 2281.

[16] Steenwinkel, P.; Kolmschot, S.; Gossage, R. A.; Dani, P.; Veldman, N.; Spek, A. L.; van Koten, G. *Eur. J. Inorg. Chem.* **1998**, 477.

[17] Terheijden, J.; van Koten, G.; Muller, F.; Grove, D. M.; Vrieze, K.; Nielsen, E.; Stam, C. A. *J. Organomet. Chem.* **1986**, *315*, 401.

[18] a) Sutter, J. –P.; James, S. L.; Steenwinkel, P.; Grove, D. M.; Veldman, N.; Spek, A. L.; van Koten, G. *Organometallics* **1996**, *15*, 941. b) Steenwinkel, P.; James, S. L.; Grove, D. M.; Veldman, N.; Spek, A. L.; van Koten, G. *Chem. Eur. J.* **1996**, *2*, 1440.

– Chapter 7 –

Metathesis of Olefin-Substituted Pyridines: The Metalated YCY-Pincer Complex in a Dual Role as Protecting Group and Scaffold

Abstract: Pincer-palladium(II) and -platinum(II) cations, $[YCY\text{-}M]^+$ (YCY = $[C_6H_3(CH_2Y)_2\text{-}2,6]^-$; Y = NMe_2, SPh; M = Pd, Pt), bound to diolefin-substituted pyridines (3,5- or 2,6-substitution) were successfully synthesized, and subsequently used in ring-closing olefin metathesis (RCM). In this study the organometallic pincer moiety acts as a protecting group for the pyridyl functionality, normally a non-tolerated substituent in RCM, by coordinating to the Lewis basic pyridine-nitrogen. Furthermore, this research was used as a model study for the template-directed synthesis of macrocycles applying highly symmetric multimetallic pincer complexes as templates.

H. P. Dijkstra, A. Chuchuryukin, B. M. J. M. Suijkerbuijk, G. P. M. van Klink, A. M. Mills, A. L. Spek, G. van Koten, *Adv. Synth. Catal.*, in press.

7.1. Introduction

The number of applications of olefin metathesis in organic synthesis has increased rapidly during the last decade.[1] Especially with the introduction of the well-defined metal-alkylidene catalysts, metathesis chemistry is increasingly being used in organic transformations.[2] In particular, Grubbs' ruthenium catalyst [$(Cy_3P)_2Cl_2Ru$=CHPh] has attracted wide-spread attention due to its ease of handling and tolerance toward many functional groups.[3] Unfortunately, Lewis-basic functional groups, such as nitriles, amines and pyridines, are not tolerated in the olefin metathesis reaction using this ruthenium catalyst.[4]

The use of olefin-substituted metal complexes in olefin metathesis has not been investigated in great detail yet. Grubbs, Sauvage and coworkers reported the use of phenanthroline-containing olefins assembled with copper(II) ions in ring-closing metathesis (RCM) to form catenanes.[5] Furthermore, Gladysz and coworkers reported olefin metathesis in the metal coordination sphere using olefin-substituted phosphine- and sulfur-ligands coordinated to platinum(II), rhenium(II) and tungsten(0) centers.[6] The application of a 2,6-diolefin-substituted pyridine coordinated to a palladium(II) center in olefin metathesis has also been reported.[7] In all of these cases the metal ion serves as the template to preorganize the ligands prior to metathesis in order to construct heterocyclic structures.

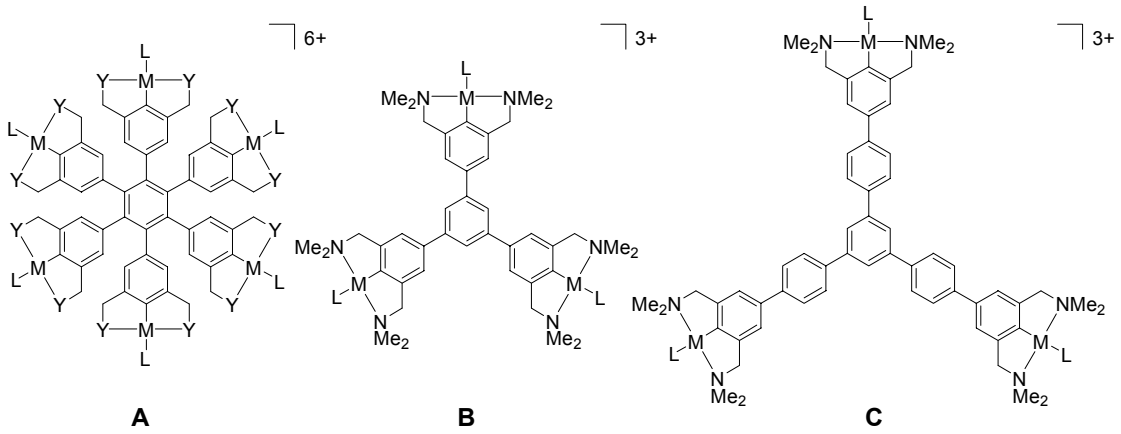

Figure 1. Highly ordered shape-persistent multimetallic materials.

Recently, we started to explore the application of shape-persistent nanosize multimetallic materials (**A–C**, Figure 1) as recyclable homogeneous catalysts by applying nanofiltration techniques,[8] as well as the use of these supramolecular

scaffolds for the controlled synthesis of macromolecular structures. These multimetallic complexes possess a high symmetry, making them promising candidates as templates in the synthesis of macromolecular heterocyclic structures. By coordinating bifunctionalized ligands to the metal centers of **A**–**C**, a pre-organization of the functional groups is attained (Scheme 1). The functional groups can now selectively react with each other, which should lead to the formation of large heterocyclic structures (as exemplified in Scheme 1 for **A** as template). The challenging step in this process is the final ring-closing reaction, since various side-reactions are anticipated, such as small intraligand ring formation, intermolecular couplings and metal-ligand dissociation. Also, the nature of the metal-to-ligand coordination bond is of crucial importance for the success of this ring-closure process. It has to be sufficiently strong under the reaction conditions in order to prevent ligand dissociation from the template. However, afterward dissociation of the macrocycle by

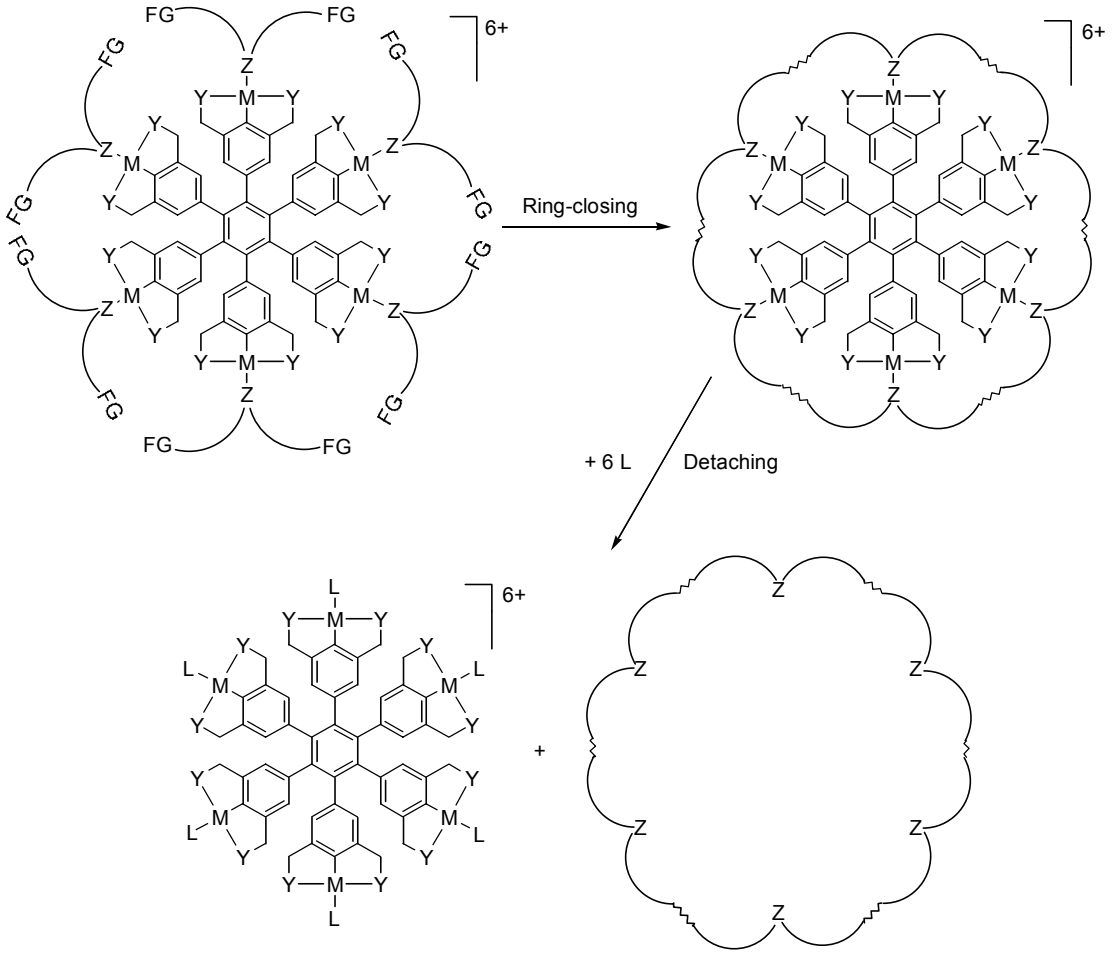

Scheme 1. Symmetrical cationic hexa(pincer-metal) complex as template for the formation of large heterocyclic structures (FG = functional group).

cleavage of the metal-to-ligand interactions has to be facile as well. Regarding these aspects, olefin metathesis seems to be very promising for the crucial ring-closing step, since it tolerates many functional groups and can be performed under rather mild reaction conditions. However, the use of coordination complexes in RCM has hardly been the subject of investigation. Therefore, we performed a model study with monometallic pincer systems in order to determine the ideal conditions for this approach. In this study, diolefin-substituted pyridines were selected as the ligands because of the suitable stability of the pyridine palladium and -platinum bonds. Here, we report the synthesis of various diolefin-substituted pyridines and the corresponding coordination pincer-palladium and -platinum complexes. Furthermore, we will discuss the behavior of these monometallic diolefin-substituted pyridine-pincer complexes in RCM.

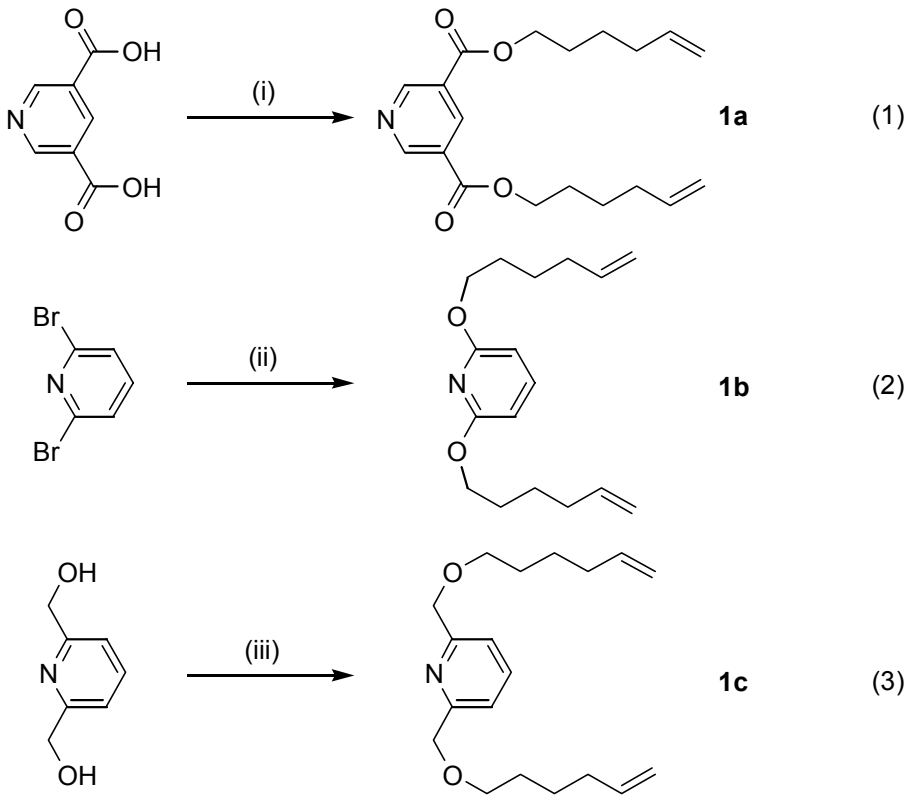

Scheme 2. (i) $SOCl_2$, reflux, 20 h followed by 5-hexenol in CH_2Cl_2, 0 °C → reflux, 3h; (ii) Sodium 5-hexenolate, DMF, 95 °C, 16 h; (iii) $SOCl_2$, CH_2Cl_2, rt, 20 h, followed by sodium 5-hexenolate, THF, reflux, 18 h.

7.2. Results and Discussion

Synthesis of diolefin-substituted pyridines. A number of diolefin-substituted pyridines were selected for this study and their syntheses are summarized in Scheme 2. We chose these symmetric pyridines because the olefinic tails are then directed in such a way that the formation of macrocycles using template-directed synthesis should be facilitated (Scheme 1). Furthermore, it enabled us to study the influence of the positioning of the olefinic tails on the pyridine rings (3,5- or 2,6-substitution) in RCM as well as the influence of a slightly longer olefinic tail (**1b** *vs.* **1c**). Treatment of 3,5-pyridinedicarboxylic acid with thionyl chloride and subsequent reaction of *in situ* generated diacid chloride with 5-hexenol resulted, after a basic work-up, in the formation of **1a** (Scheme 2, eqn. 1). Treatment of 2,6-dibromopyridine with *in situ* prepared sodium salt of 5-hexenol in dry DMF, gave 2,6-disubstituted pyridine **1b** in 90% yield (Scheme 2, eqn. 2). Finally, pyridine **1c** was obtained in a two-step sequence; 2,6-pyridinedimethanol was first reacted with thionyl chloride and subsequent treatment of *in situ* formed 2,6-bis(chloromethyl)pyridine with the sodium salt of 5-hexenol yielded **1c** in 91% yield (Scheme 2, eqn. 3).

Preparation of monometallic pyridine complexes. Metalated *pincer* complexes (pincer ligand: monoanionic, terdentate coordinating ligand: YCY = $[2,6\text{-}(CH_2Y)_2C_6H_3]^-$) were chosen as the organometallic moieties for coordination of the difunctionalized pyridines. Various functionalities of the pincer moiety can be altered rather easily, thus allowing fine-tuning of the material for various applications.[9] In this investigation, we decided to use the monoanionic NCN-pincer ligand (NCN = $[2,6\text{-}(CH_2NMe_2)_2C_6H_3]^-$) in combination with palladium(II) and platinum(II) centers. In Scheme 3, the general synthetic pathway to NCN-metal-pyridine complexes is shown. Treatment of NCN-M-Br (**2**, M = Pd; **3**, M = Pt) with $AgBF_4$ in CH_2Cl_2 in the presence of the appropriate diolefin-substituted pyridine, resulted in the formation of the various pincer-metal-pyridine tetrafluoroborate complexes **4a-b** and **5a-c** all in high yields.

The ^{1}H NMR spectra of complexes **4a-b** and **5a-b** showed the expected chemical shifts upon coordination of the pyridine moiety to the organometallic pincer complexes. For **5c**, ^{1}H NMR spectroscopy showed an unusual large downfield shift of $\Delta\delta = 1.0$ ppm for the py-C*H*$_2$O-protons of the 2,6-disubstituted pyridine **1c** upon coordination, indicating the existence of a rather strong interaction between these

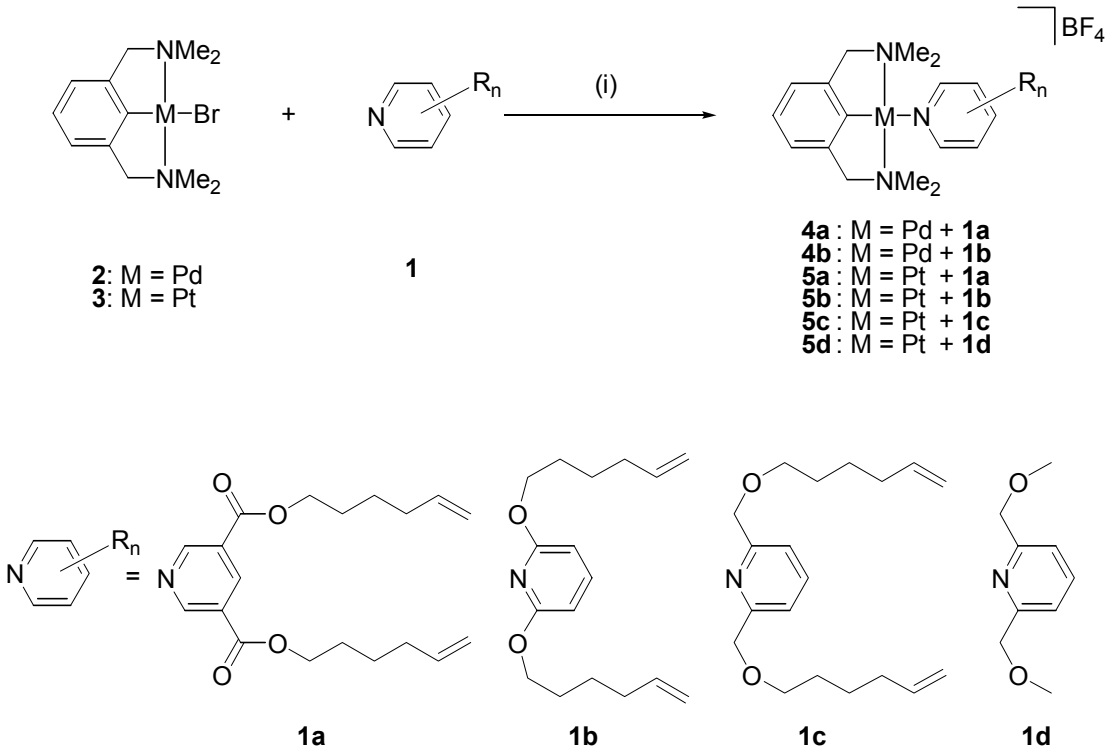

Scheme 3. (i) $AgBF_4$, CH_2Cl_2, rt, 1 h.

protons and the platinum center. Unfortunately, crystals of **5c** suitable for an X-ray single crystal structure determination could not be obtained. In order to study the influence of the *ortho*-methylalkoxy substituents on the pyridine orientation with respect to the pincer moiety, **5d**[10] (see Scheme 3) was prepared as a model compound for **5c** and analyzed by ^{1}H NMR spectroscopy and X-ray single crystal structure determination (Figure 2). ^{1}H NMR analysis of **5d** showed the same large downfield shift of the py-C*H*$_2$O-protons of **1d** upon coordination to the platinum center. In the crystal structure of **5d**, the unit cell contains two independent cationic platinum complexes. Since the geometry of both are similar, the structural features of only one of the complexes will be discussed here. Table 1 summarizes a number of selected distances and angles for one of the independent complexes of **5d** in the solid state. As shown in Figure 2, the square-planar platinum(II) center is ligated by a terdentate η^3-coordinated NCN-ligand and a η^1-*N*-coordinated pyridine ligand. As a result of the η^3-*N,C,N*-coordination, C_{ipso} and N(py) are mutually *trans* orientated. The pincer aryl ring is tilted 13.21(15)° with respect to the N1-C1-N2-N3 coordination-plane, while the pyridine is fixed in a conformation that is almost perpendicular (87.47(16)°) to

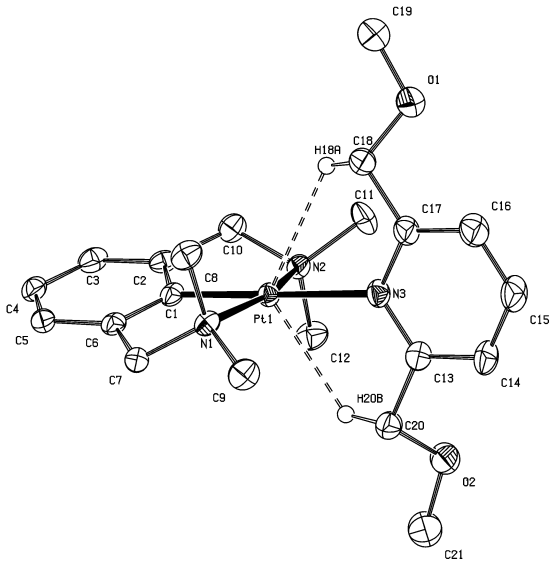

Figure 2. Crystal structure of one of the two independent **5d** cations; ORTEP 50% displacement ellipsoids; only the relevant hydrogens are shown, the tetrafluoroborate anion and co-crystallized CH_2Cl_2 are omitted for clarity.

Table 1. Interatomic bond lengths (Å) and angles (deg.) of **5d**.

Bond lengths		**Bond angles**	
Pt1-C1	1.935(3)	C1-Pt1-N3	179.26(13)
Pt1-N1	2.099(3)	C1-Pt1-N1	81.12(13)
Pt1-N2	2.107(3)	C1-Pt1-N2	81.31(13)
Pt1-N3	2.192(3)	N1-Pt1-N2	162.42(11)
Pt1-H18A	2.6385	N1-Pt1-N3	98.91(11)
Pt1-H20B	2.5934	N2-Pt1-N3	98.67(11)
		C18-H18A-Pt1	119.96
		C20-H20B-Pt1	124.23

this plane. The stereochemistry, bond lengths and bond angles are normal for a square-planar platinum(II) center containing the NCN ligand.[11] An interesting feature of the structure is the positioning of H18A and H20B near the virtual *z*-axis of the platinum center. The distances H18A–Pt1 (2.639 Å) and H20B–Pt1 (2.593 Å) are significantly shorter than the sum of the van der Waals radii of both nuclei (3.50 Å), indicating an additional interaction with the filled d_{z2} orbital of the platinum center, providing extra stability to this structure. The earlier mentioned large down-field shift of the py-CH_2O-protons in the ^{1}H NMR spectrum of **5d** in acetone-d_6 also suggests a

similar interaction of these protons with the platinum center in solution, leading to hindered rotation of the pyridine ligand about the Pt1-N3 axis as well as to restricted rotation about the C17-C18 and C13-C20 axes. Consequently, these hydrogen nuclei undergo a down-field shift. Such behavior has been observed previously for a neutral [Pt(η^3-NCN)(η^1-NCN)] complex.[12]

An important aspect of this research is the strength of the pyridine-metal coordination bond in the various NCN-M-N(py) cationic complexes. First of all, for template-directed synthesis of macromolecular heterocycles using **A** – **C** (Figure 1) as templates, it is of crucial importance that the M-N(py) bond is maintained during the formation of the large ring and thus has sufficient kinetic stability under the reaction conditions. Furthermore, for RCM (as the crucial ring-closing reaction) it is important that the Lewis-basic pyridine ligands remain coordinated to the pincer-metal centers in order to prevent fast deactivation of the metathesis catalyst due to competitive coordination of free pyridine in solution to the active site of the catalyst. Therefore, we performed a number of independent ^{1}H NMR spectroscopy experiments with cationic NCN-M-(4-picoline) complexes (prepared similarly to the complexes shown in Scheme 3). In the first experiment, cationic NCN-Pt-aqua complex **6** was mixed in CD_2Cl_2 with the cationic NCN-Pd-(4-picoline) complex **7** at room temperature (Scheme 4). ^{1}H NMR spectroscopy clearly indicated the disappearance of palladium-(4-picoline) complex **7** and the quantitative formation of the platinum-(4-picoline) complex **8**, *i.e.* a $\Delta\delta$ of 0.15 ppm of the *ortho*-picoline protons together with the appearance of platinum-couplings on the *ortho*-protons ($^3J_{Pt,H}$ = not resolved) were observed.[13] In a second set of experiments, both NCN-Pd-(4-picoline) complex **7** and the platinum analog **8** were separately dissolved in CD_2Cl_2 in the presence of a 10-fold excess of 4-picoline. In the case of platinum-complex **8**, ^{1}H NMR spectroscopy showed two sharp resonances for coordinated and non-coordinated picoline in a 1:10 ratio, as indicated by a characteristic downfield shift of $\Delta\delta_H$ = 0.5 ppm for the *ortho*-aromatic protons of 4-picoline upon coordination. This observation points to a slow

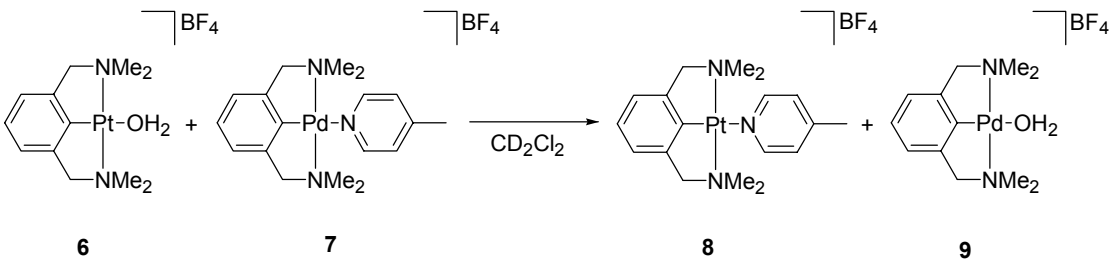

Scheme 4. 4-Picoline exchange experiment.

exchange reaction for the 4-picolyl complex in solution on the NMR time-scale. As expected the corresponding palladium complex **7** undergoes a fast 4-picolyl exchange reaction, as ^{1}H NMR spectra showed a single resonance pattern for coordinated and free 4-picoline.

Metathesis with diolefin-substituted pyridines bound to mononuclear pincer-palladium and -platinum complexes. Pyridine complexes **4a**,**b** and **5a–c** were subjected to RCM reaction conditions using the first-generation Grubbs' catalyst, $[(Cy_3P)_2Cl_2Ru{=}CHPh]$. The results are summarized in Scheme 5. All metathesis reactions were performed under the same reaction conditions: 0.016 M [olefin end groups], 5 mol% [Ru] per pyridine in CH_2Cl_2 at reflux temperatures. The reaction progress was monitored by ^{1}H NMR spectroscopy and GC-MS. Applying these RCM reaction conditions to pyridine-complexes **4a** and **5a**, resulted in the formation of the metathesized products **10a** (50%, cis/trans mixture) and **11a** (100%, cis/trans mixture) (eqn. 4, Scheme 5), respectively. Remarkably, the time needed for complete

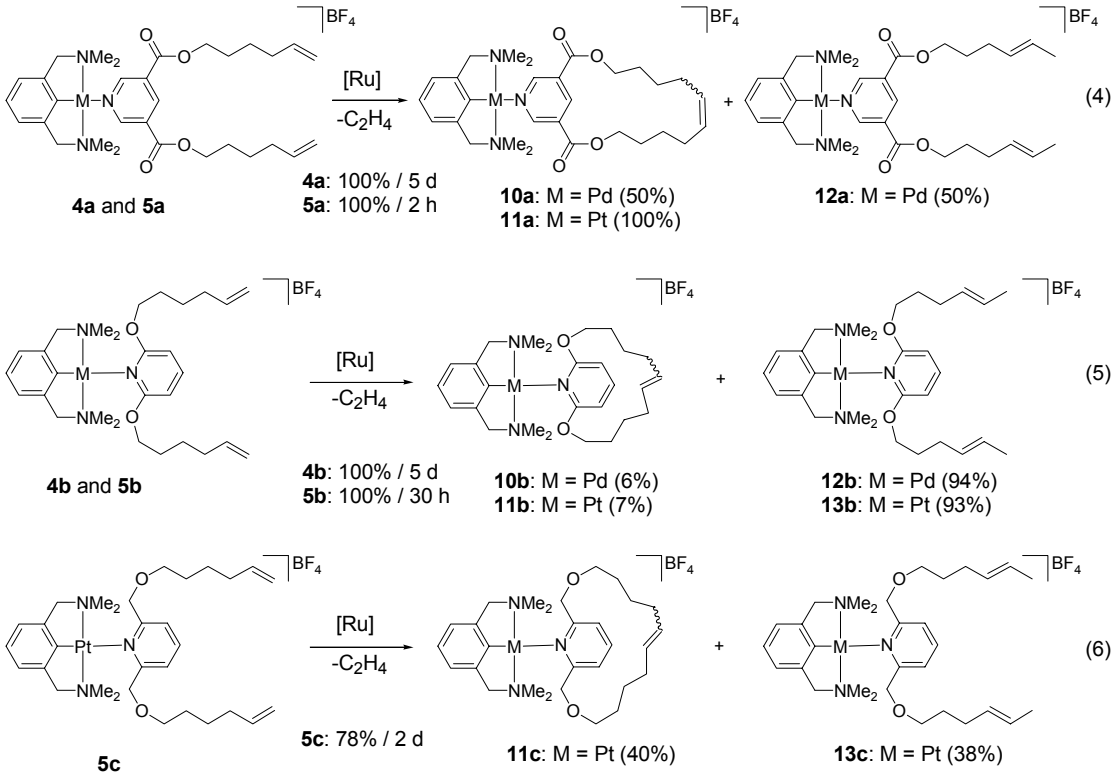

Scheme 5. Metathesis with diolefin-substituted pyridines coordinated to palladium and platinum centers. Percent values under the arrows refer to the specific conversions.

conversion of **4a** was found to be considerably longer (5 d) than for **5a** (2 h). Furthermore, with **4a** the isomerized product **12a** (50%) was formed in addition to the metathesis product **10a**. The formation of **12a** is due to a prototropic isomerization of the double bond, which is known to be catalyzed by transition metal complexes.[14] The origin of the large differences observed between palladium and platinum (**4a** and **5a**, respectively) probably lies in the much higher kinetic stability of the M-N(py) coordination bond in **5a** as compared to **4a** (*vide supra*). As a consequence, in the case of palladium complex **4a**, the pyridine ligand dissociates partially from the palladium-center, leading to free pyridine in solution, which can compete for the active site of the ruthenium metathesis catalyst. This leads to a decreased catalyst activity and thus to longer metathesis reaction times. Apparently, under these conditions isomerization (usually a slow reaction), which leads to the formation of internal olefinic ligands, becomes relatively more important and competitive as the RCM becomes slower.

Subjecting complexes **4b** and **5b** to metathesis reaction conditions, resulted mainly in the formation of isomerized products **12b** and **13b** (>90%; eqn. 5, Scheme 5), while minor amounts of metathesis products **10b** (6%) and **11b** (7%) were present. These results point to the importance of the position as well as the conformational stability of the group linking the olefinic substituents to the pyridine ring; the carbonyl linkage in **4a** and **5a**, which is coplanar with the pyridine ring and provides a 17-membered ring on ring-closing, *vs.* the ether-linkage in **4b** and **5b**, which directs the olefinic substituents less and gives a smaller ring of 15 atoms. Furthermore, **4b** and **5b** possess 2,6-diolefin-substituted pyridines, resulting in increased steric hindrance (by the pincer moiety and the pyridine ring) for the olefinic tails during RCM, forcing the ring-closing reaction to take place via a back-flip conformation. This will lead to a slower metathesis reaction and thus shifting the selectivity of the reaction toward the competing isomerization process. Remarkably, the reaction time needed for complete conversion of **4b** is considerably longer than for **5b** (5 days *vs.* 30 hours, respectively). Apparently, under the reaction conditions the pincer-metal moiety plays a significant role in the isomerization reaction as indicated by the large difference in isomerization rates between platinum (**5b**) and palladium (**4b**). Most likely dissociation of the pyridine ligand from the pincer-metal center has to occur before the pincer moiety can take part in the isomerization process, however the exact role of the pincer moiety is not understood yet and is subject to further investigation. These results once again demonstrate that isomerization becomes a competing reaction when the reaction times for complete conversion increase.

In the final example, complex **5c** is applied in the RCM (eqn. 6, Scheme 5). In this case, both metathesis (**11c**) and isomerization (**13c**) take place in approximately equal ratios. The slightly longer olefin-tails (one CH_2-group) in **5c**, as compared to **5b**, result in less ring-strain (17-membered ring), allowing metathesis to take place to a greater extent. For **5c**, both metathesis (as compared to **5a**, eqn. 4, Scheme 5) and isomerization (as compared to **5b**, eqn. 5, Scheme 5) are rather slow (78% total conversion of **5c** in 2 days). The slow metathesis reaction can be attributed to steric hindrance involved in the formation of the cyclic compound because of the positioning of the olefinic tails at the 2- and 6-positions (in **5c**) of the pyridine ligand rather than at the 3- and 5-positions (in **5a**). The slow isomerization reaction is probably caused by stronger binding of the pyridine to the NCN-Pt^{II} moiety due to the additional interaction of the py-CH_2O-protons with the platinum center (also discussed for model compound **5d**, *vide supra*). This latter behavior results in a lower concentration of active Pt^{II} isomerization species in solution (assuming that a pyridine-free ionic NCN-Pt^{II} center takes part in the isomerization process) and thus in a slower isomerization process. In addition, a lower concentration of free pyridine in solution also results in less metathesis catalyst poisoning, which can be an additional explanation for the observed differences in metathesis between **5b** and **5c**.

Monometallic pincer complexes as protecting groups for Lewis-basic substituents in olefin-metathesis. An interesting aspect of this approach is that olefins containing Lewis-basic substituents (such as nitriles, amines and pyridines) can in principle now be applied in metathesis reactions. Here, we have shown that olefin-substituted pyridines can now be applied in RCM by coordinating the Lewis-basic nitrogen-atom of the pyridine to a Lewis-acidic pincer-metal center prior to metathesis. The protecting organometallic pincer moiety has the advantage that it can be very easily cleaved off by addition of NaX (X = Cl, Br, I) to a solution of the pincer-metal-pyridine complex, affording the free pyridine and the neutral NCN-M-X complex (Scheme 6). The neutral pincer complex can subsequently be isolated and reused (cf. Scheme 3). We believe that this approach can generally be applied to metathesize various olefinic compounds containing Lewis-basic substituents. In addition, since basic substituents are often not tolerated in many other catalytic reactions as well, this approach of using transition-metal complexes, *e.g.* the cationic NCN-Pt-moiety, as protecting groups during catalysis can be of general interest. Currently, we are investigating the scope of this approach.

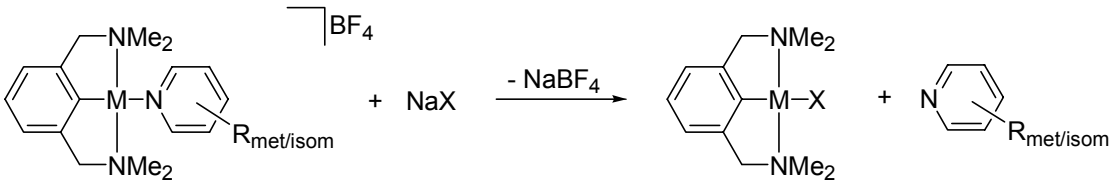

Scheme 6. Decomplexation of the pyridine-product by NaCl, NaBr or NaI.

Metathesis with a diolefin-substituted pyridine bound to a hexakis(SCS-Pd^{II}) template. Preliminary experiments with 3,5-diolefin-substituted pyridine **1a** connected to hexa-cationic hexakis(SCS-Pd^{II}) template **14** (Scheme 7) in RCM (using 5 mol% [Ru] per pyridine), did not result in the formation of the desired macrocycle **15**. Instead mainly isomerized product **17** was obtained, while only minor amounts of intrapyridyl metathesis product **16** were observed (**16** : **17** = 1 : 9, complete conversion of **14** in 36 h). When these results are compared to the results obtained with NCN-Pd-pyridine complex **4a** (eqn. 4, Scheme 5), it is clear that the isomerization reaction is considerably faster in the case of **14** (5 d *vs.* 36 h for complete conversion). Metathesis, on the other hand, is almost completely suppressed with **14** under the reaction conditions. Apparently, the palladium-pyridine bond in **14**, *i.e.* in each of the six cationic SCS-Pd-pyridine units, is weaker than in **4a**. Consequently, it can be assumed that the high concentration of free diolefinic-pyridine ligand **1a** in solution results in more effective metathesis-catalyst poisoning and thus in almost no RCM product formation. Moreover, the free SCS-Pd cationic sites are apparently effective catalytic sites for the olefin isomerization process (*vide supra*). These assumptions were confirmed by independent experiments in which **4a** and its mononuclear SCS-Pd-pyridine analog (SCS = $[C_6H_3(CH_2SPh)_2\text{-}2,6]^-$) were dissolved in CH_2Cl_2 and stirred at *room temperature* for 20 hours (without [Ru] metathesis catalyst). The SCS-complex gave 75% isomerization of **1a** to the internal olefin in 20 hours, whereas **4a** showed no conversion at all under the same conditions. Furthermore, independent ^{1}H NMR spectroscopic experiments (acetone-d_6, 200 MHz) showed a smaller downfield shift for the *ortho*-protons of the 3,5-disubstituted pyridine in **14** (δ_H = 9.08 ppm) as compared to **4a** (δ_H = 9.67 ppm), pointing to a stronger Pd-N(py) coordination bond in the case of **4a**. These results clearly suggest that the relatively weak SCS-Pd-pyridine bond is responsible for the almost exclusive formation of **17** in the attempted synthesis of macrocycle **15** (Scheme 7). Furthermore, the fact that in metathesis no **15** but rather **16**, albeit in small amounts,

was found, reveals that with **16** intraligand RCM occurs rather than interligand RCM which would result in the formation of **15**.

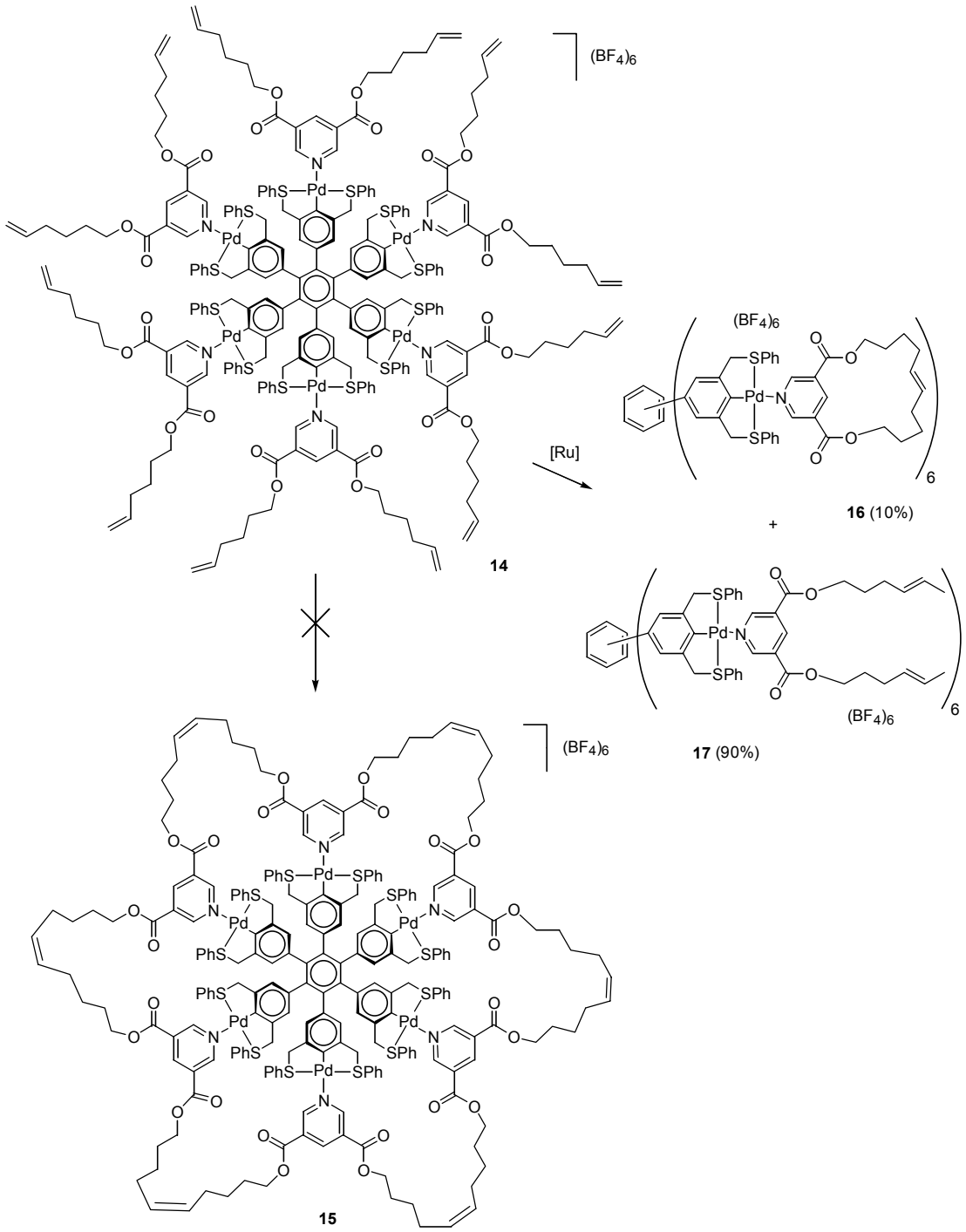

Scheme 7. Preliminary test toward macrocyclic structures.

7.3. Concluding Remarks

It is obvious from the results of this study that in order to selectively form macromolecular heterocycles, such as **15**, by RCM, the fast intraligand metathesis and the isomerization reaction of the olefinic substituents have to be competed for by fast interligand metathesis and slow M-N(diolefinic-pyridine) dissociation. The most promising candidate to achieve this goal using multipincer templates should comprise 2,6-diolefin-substituted pyridines bound to a multi(NCN-Pt^{II}) template, which can subsequently undergo RCM. The latter complexes likely match low Pt-N(py) dissociation rates with low intraligand RCM reactivity of 2,6-diolefin-substituted pyridines. As an effect, interligand RCM along the periphery of the template can be successful. The preparation of the required multi(NCN-Pt^{II}) templates and their use in the synthesis of large heterocyclic compounds is currently under investigation.

7.4. Experimental Section

All reactions were carried out using standard Schlenk techniques under an inert atmosphere of dry, oxygen-free nitrogen unless stated otherwise. All solvents were carefully dried and distilled over appropriate drying agents prior to use. All standard reagents were purchased. $C_6H_3\{PdBr\}$-1-$(CH_2NMe_2)_2$-3,5 (**2**),[15] $C_6H_3\{PtBr\}$-1-$(CH_2NMe_2)_2$-3,5 (**3**)[15] and 2,6-bis(methoxy-methyl)pyridine (**1d**)[10] were prepared according to literature procedures. ^1H (200 or 300 MHz) and ^{13}C (50 or 75 MHz) NMR spectra were recorded on a Varian AC200 or Varian 300 MHz spectrometer at 25 °C, chemical shifts are in ppm referenced to residual solvent resonances. GC-MS analysis was performed using the following conditions: column: PE-17; 30 m × 0.32 mm^2 = 50 μm film thickness; gas chromatograph: Perkin-Elmer Autosystem XL; mass spectrometer: Perkin Elmer Turbomass.

Synthesis of 3,5-pyridinedicarboxylic acid bis(5-hexenyl) ester (1a): 3,5-Pyridinedicarboxylic acid (1.0 g, 6.0 mmol) was suspended in $SOCl_2$ (4.4 mL, 60.0 mmol) and this mixture was heated to reflux for 20 h. Subsequently, excess $SOCl_2$ was evaporated *in vacuo* and the remaining white solid was dissolved in CH_2Cl_2 (20 mL). Next, 5-hexenol (1.16 mL, 18.0 mmol) was added to this solution at 0 °C, the solution was allowed to warm to room temperature and was subsequently heated to reflux for 3 h. After removal of all volatiles *in vacuo*, the off-white residue was washed several times with hexanes until a white solid was obtained. This solid was

dissolved in CH_2Cl_2 (20 mL) and washed with aqueous NaOH (1 M, 50 mL). The organic layer was collected and dried ($MgSO_4$). After filtration and evaporation of the solvent, the crude product was flame-distilled, resulting in a yellow viscous oil. Yield: 1.3 g (65%). ^{1}H NMR (C_6D_6, 300 MHz): δ 9.43 (d, $^4J_{H,H}$ = 3.3 Hz, 2H, Ar*H*), 8.87 (t, $^4J_{H,H}$ = 3.3 Hz, 1H, Ar*H*), 5.61 (m, 2H, CH_2=C*H*), 4.94 (m, 4H, CH=CH_2), 4.01 (t, $^3J_{H,H}$ = 9.6 Hz, 4H, OCH_2), 1.80 (m, 4H, CH_2), 1.36 (m, 4H, CH_2), 1.15 (m, 4H, CH_2). ^{13}C NMR (acetone-d_6, 50 MHz): δ 164.80, 154.47, 139.19, 137.85, 127.09, 115.17, 66.19, 33.96, 28.75, 25.95. Anal. Calcd for $C_{19}H_{25}NO_4$: C, 68.86; H, 7.60; N, 4.23. Found: C, 68.72; H, 7.68; N, 4.35.

Synthesis of 2,6-bis(5-hexenoxy)pyridine (1b): 5-Hexenol (3.7 mL, 30.0 mmol) was dissolved in THF (40 mL) and sodium (0.72 g, 30 mmol) was added in small portions. The reaction mixture was stirred until all sodium was dissolved. Subsequently all volatiles were evaporated, yielding a white solid. 2,6-Dibromopyridine (2.4 g, 8.7 mmol) dissolved in dry degassed DMF (20 mL) was added to the solid and the resulting reaction mixture was stirred overnight at 95 °C. The mixture was subsequently hydrolyzed by addition of H_2O (5 mL) and the resulting mixture was evaporated to dryness. The solid residue was dissolved in H_2O (20 mL) and the aqueous layer was extracted with Et_2O (3 × 20 mL). The combined organic layers were dried ($MgSO_4$), filtered and evaporated to dryness, affording a yellow oil. This oil was flame-distilled under reduced pressure, giving a colorless oil. Yield: 2.5 g (90%). ^{1}H NMR (acetone-d_6, 200 MHz): δ 7.54 (t, $^3J_{H,H}$ = 8.0 Hz, 1H, Ar*H*), 6.27 (d, $^3J_{H,H}$ = 8.0 Hz, 2H, Ar*H*), 5.84 (m, 2H, CH_2=C*H*), 4.98 (m, 4H, CH=CH_2), 4.29 (t, $^3J_{H,H}$ = 6.2 Hz, 4H, OCH_2), 2.11 (m, 4H, CH_2), 1.76 (m, 4H, CH_2), 1.55 (m, 4H, CH_2). ^{13}C NMR (acetone-d_6, 50 MHz): δ 163.65, 141.82, 139.42, 114.97, 101.91, 66.11, 34.16, 29.34, 26.17. Anal. Calcd for $C_{18}H_{26}NO_2$: C, 74.14; H, 9.15; N, 5.09. Found: C, 73.97; H, 9.04; N, 5.14.

Synthesis of 2,6-bis(5-hexenoxymethyl)pyridine (1c): 2,6-Pyridinedimethanol (1.2 g, 8.9 mmol) was suspended in CH_2Cl_2 (20 mL) and $SOCl_2$ (1.6 mL, 21.6 mmol) was added dropwise at room temperature. The reaction mixture was stirred overnight and subsequently all volatiles were evaporated *in vacuo*, leaving a white solid. This solid was added to a freshly prepared solution of the sodium salt of 5-hexenol (from Na (0.65 g, 28 mmol) and 5-hexenol (3.5 mL, 28 mmol) in THF, *vide supra*) in THF (50 mL) and this mixture was heated to reflux overnight. Next, the mixture was allowed to cool to room temperature and H_2O (1.0 mL) was added. Subsequently, the reaction

mixture was evaporated to dryness, the residue was dissolved in H_2O (50 mL) and the aqueous layer was extracted with Et_2O (3 × 50 mL). The combined organic layers were dried ($MgSO_4$) and evaporated to dryness, leaving an yellow oil. This oil was flame-distilled under reduced pressure, giving a light yellow oil. Yield: 2.46 g (91%); ^{1}H NMR (acetone-d_6, 200 MHz): δ 7.78 (d, $^3J_{H,H}$ = 7.8 Hz, 1H, Ar*H*), 7.35 (d, $^3J_{H,H}$ = 7.8 Hz, 2H, Ar*H*), 5.85 (m, 2H, CH_2=C*H*), 4.98 (m, 4H, CH=CH_2), 4.54 (s, 4H, py-CH_2), 3.57 (t, $^3J_{H,H}$ = 3.0 Hz, 4H, OCH_2), 2.07 (m, 4H, CH_2), 1.56 (m, 8H, CH_2). ^{13}C NMR (acetone-d_6, 50 MHz): δ 159.17, 139.52, 137.64, 120.00, 114.84, 74.26, 71.23, 34.20, 29.93, 26.25. Anal. Calcd for $C_{20}H_{30}NO_2$: C, 75.21; H, 9.63; N, 4.62. Found: C, 75.06; H, 9.55; N, 4.71.

Synthesis of 4 and 5, a typical procedure: The appropriate combination of NCN-metal complex (0.37 mmol) and diolefin-substituted pyridine (0.75 mmol) were dissolved in CH_2Cl_2 (10 mL). A solution of $AgBF_4$ (72.0 mg, 0.37 mmol) in H_2O (0.2 mL) was added and the resulting suspension was stirrred at room temperature for 1 h. Subsequently, the reaction mixture was filtered over Celite and the filtrate was evaporated to dryness. The obtained sticky solid was washed with hexanes to remove residual non-coordinated pyridine. After drying *in vacuo*, the desired products were isolated as yellowish/white solids or as a sticky residue (**5c**) and immediately used without further purification.

4a: Yield: 0.24 g (89%); ^{1}H NMR (acetone-d_6, 200 MHz): δ 9.67 (s, 2H, Ar*H*), 8.91 (s, 1H, Ar*H*), 7.07 (t, $^3J_{H,H}$ = 7.2 Hz, 1H, Ar*H*), 6.91 (d, $^3J_{H,H}$ = 7.2 Hz, 2H, Ar*H*), 5.85 (m, 2H, CH_2=C*H*), 4.98 (m, 4H, CH=CH_2), 4.44 (t, $^3J_{H,H}$ = 6.6 Hz, 4H, OCH_2), 4.22 (s, 4H, NCH_2), 2.83 (s, 12H, NCH_3), 2.13 (m, 4H, CH_2), 1.83 (m, 4H, CH_2), 1.60 (m, 4H, CH_2).

4b: Yield: 0.17 g (80%); 1H NMR (acetone-d_6, 200 MHz): δ 8.06 (t, $^3J_{H,H}$ = 8.0 Hz, 1H, Ar*H*), 7.06 (t, $^3J_{H,H}$ = 6.6 Hz, 1H, Ar*H*), 6.88 (m, 4H, Ar*H*), 5.76 (m, 2H, CH_2=C*H*), 4.88 (m, 4H, CH=CH_2), 4.41 (t, $^3J_{H,H}$ = 6.2 Hz, 4H, OCH_2), 4.14 (s, 4H, NCH_2), 2.85 (s, 12H, CH_3N), 2.10 (m, 8H, CH_2), 1.88 (m, 4H, *CH*$_2$), 1.51 (m, 4H, CH_2).

5a: Yield: 0.27 g (92%); ^{1}H NMR (acetone-d_6, 300 MHz): δ 9.82 (d, $^4J_{H,H}$ = 1.4 Hz, 2H, Ar*H*), 9.00 (t, $^4J_{H,H}$ = 1.4 Hz, 1H, Ar*H*), 7.07 (t, $^3J_{H,H}$ = 5.4 Hz, 1H, Ar*H*), 6.96 (d, $^3J_{H,H}$ = 5.4 Hz, 2H, Ar*H*), 5.84 (m, 2H, CH_2=C*H*), 4.98 (m, 4H, CH=CH_2), 4.47 (t, $^3J_{H,H}$ = 6.9 Hz, 4H, OCH_2), 4.33 (s, $^3J_{Pt,H}$ = 24.9 Hz, 4H, NCH_2), 2.94 (s, $^3J_{Pt,H}$ = 19.5 Hz, 12H, NCH_3), 2.15 (m, 4H, CH_2), 1.86 (m, 4H, CH_2), 1.58 (m, 4H, CH_2).

5b: Yield: 0.23 g (93%). ^{1}H NMR (acetone-d_6, 200 MHz): δ 8.12 (t, $^3J_{H,H}$ = 8.4 Hz, 1H, Ar*H*), 6.97 (m, 5H, Ar*H*), 5.75 (m, 2H, CH_2=C*H*), 4.86 (m, 4H, CH=CH_2), 4.39 (t, $^3J_{H,H}$ = 6.2 Hz, 4H, OCH_2), 4.21 (s, $^3J_{Pt,\ H}$ = 26.0 Hz, 4H, NCH_2), 2.89 (s, $^3J_{Pt,H}$ = 19.0 Hz, 12H, NCH_3), 2.11 (m, 4H, CH_2), 2.04 (m, 4H, CH_2), 1.84 (m, 4H, CH_2)
5c: Yield: quantitative; ^{1}H NMR (acetone-d_6, 200 MHz): δ 8.27 (t, $^3J_{H,H}$ = 8.0 Hz, 1H, Ar*H*), 7.91 (d, $^3J_{H,H}$ = 8.0 Hz, 2H, Ar*H*), 7.02 (m, 3H, Ar*H*), 5.80 (s, 4H, py-CH_2), 5.78 (m, 2H, CH_2=C*H*), 4.94 (m, 4H, CH=CH_2), 4.32 (s, $^3J_{Pt,H}$ = 26.4 Hz, 4H, NCH_2), 3.79 (t, $^3J_{H,H}$ = 6.2 Hz, 4H, OCH_2), 2.88 (s, $^3J_{Pt,H}$ = 20.0 Hz, 12H, NCH_3), 2.07 (m, 4H, CH_2), 1.70 (m, 4H, CH_2), 1.48 (m, 4H, CH_2).
5d: Crystals suitable for X-ray single crystal structure determination were obtained by slow diffusion of hexane into a concentrated solution of **5d** in CH_2Cl_2. Yield: 92%; ^{1}H NMR (acetone-d_6, 200 MHz): δ 8.27 (t, $^3J_{H,H}$ = 8.0 Hz, 1H, Ar*H*), 7.90 (d, $^3J_{H,H}$ = 8.0 Hz, 2H, Ar*H*), 7.00 (m, 3H, Ar*H*), 5.74 (s, 4H, OCH_2), 4.33 (s, $^3J_{Pt,H}$ = 27.0 Hz, 4H, NCH_2), 3.60 (s, 6H, OCH_3), 2.87 (s, $^3J_{Pt,H}$ = 20.3 Hz, 12H, NCH_3). Anal. Calcd for $C_{21}H_{32}BF_4N_3O_2Pt\cdot(CH_2Cl_2)_{1/2}$: C, 37.82; H, 4.87; N, 6.15. Found: C, 37.95; H, 4.80; N, 6.14.

Synthesis of 14: Hexakis(SCS-Pd-Cl)[8b] **A** (Y = SPh, M = Pd, L = Cl; 0.10 g, 35 μmol) and **1a** (139 mg, 0.42 mmol) were dissolved in CH_2Cl_2 (5 mL). A solution of $AgBF_4$ (41 mg, 0.21 mmol) in H_2O (0.1 mL) was added and the resulting suspension was stirrred at room temperature for 1 h. Subsequently, the reaction mixture was filtered over Celite and the filtrate was evaporated to dryness. The obtained sticky solid was washed with hexanes to remove residual non-coordinated pyridine. After drying *in vacuo*, **14** was obtained as yellowish solid and immediately used without further purification.Yield: 87%; ^{1}H NMR (acetone-d_6, 200 MHz): δ 9.22 (br s, 12H, Ar*H*), 8.91 (m, 6H, Ar*H*), 7.76 (m, 24H, Ar*H*), 7.47 (m, 36H, Ar*H*), 6.78 (br s, 12H, Ar*H*), 5.85 (m, 12H, CH_2=C*H*), 5.0 (m, 24H, CH=CH_2), 4.69 (br s, 24H, SCH_2), 4.40 (t, $^3J_{H,H}$ = 6.7 Hz, 24H, OCH_2), 2.19 (m, 24H, CH_2), 1.83 (m, 24H, CH_2), 1.58 (m, 24H, CH_2).

Typical procedure for the metathesis reactions: A solution of $[(Cy_3P)_2Cl_2Ru$=CHPh] (3.2 mg, 3.9 μmol) and the appropriate olefin precursor (80 μmol of olefin end groups) were dissolved in dry, degassed CH_2Cl_2 (5.0 mL). This mixture was heated to reflux for 12 h. The reaction was followed by ^{1}H NMR spectroscopy in order to determine the full conversion times. After complete conversion, excess NaBr in H_2O (1 mL) was added and all volatiles were evaporated.

The liberated pyridine products were extracted with hexanes (2 × 5 mL) and the combined organic layers were filtered and concentrated to dryness. The product mixture was analyzed by ^{1}H NMR spectroscopy (by monitoring the disappearance of the characteristic CH_2=C*H* resonance (at 5.70–5.85 pm) and appearance of internal double bonds (at 5.40–5.70 ppm)) and by GC-MS (for the determination of the ratio between isomerized products and metathesis products).

Crystal Structure Determination of 5d: Colorless plates of **5d** were obtained after recrystallization in hexane/dichloromethane. Intensity data were collected for a single crystal (0.24 × 0.18 × 0.06 mm) on a Nonius KappaCCD diffractometer with rotating anode at 150 K in the range 3° ≤ 2θ(Mo *K*α) ≤ 55°. Of the 37923 reflections measured, 11509 were unique (R_{int} = 0.044). An empirical absorption correction was applied using DELABS in PLATON (μ = 5.683 mm^{-1}, 0.275–0.725 transmission).[16] The structure was solved by automated Patterson methods using DIRDIF99,[17] and refined on F^2 by least-squares procedures using SHELXL97.[18] Structure validation and molecular graphics preparation were performed with the PLATON package.[16] 2($C_{21}H_{32}N_3O_2Pt$) · 2(BF_4) · CH_2Cl_2, FW = 1365.70 amu, triclinic, *P*1bar (No. 2), *a* = 9.1923(1) Å, *b* = 13.8349(2) Å, *c* = 21.0198(3) Å, α = 77.1163(5)°, β = 79.2591(5)°, γ = 80.6366(7)°, *V* = 2539.67(6) Å^3, *Z* = 2, ρ_{calc} = 1.786 g cm^{-3}; 676 refined parameters, 389 restraints, *R*(*F*) [*I* > 2σ(*I*)] = 0.0268, *wR*(F^2) = 0.0557, GooF = 1.036, $\Delta\rho_{max}$ = 1.06 e Å^{-3}, $\Delta\rho_{min}$ = –0.74 e Å^{-3}. Crystallographic data (excluding structure factors) have been deposited with the Cambridge Crystallographic Data Centre as supplementary publication no. CCDC-179385. Copies of the data can be obtained free of charge on application to CCDC, 12 Union Road, Cambridge CB2 1EZ, UK [fax: (+44) 1223-336-033; e-mail: deposit@ccdc.cam.ac.uk].

The unit cell of **5d** contains two independent cationic platinum complexes, their respective tetrafluoroborate anions and one molecule of dichloromethane. In one of the independent cations, one ether side chain is disordered over two sets of atomic positions. One of the two independent anions is also disordered. All non-hydrogen atoms were refined with anisotropic displacement parameters, but the displacement parameters of the disordered atoms were restrained to be approximately isotropic. Hydrogen atoms were constrained to idealized geometries and allowed to ride on their carrier atoms with an isotropic displacement parameter related to the equivalent displacement parameter of their carrier atoms. The tetrafluoroborate anions were restrained to approximately tetrahedral geometries.

7.5. References and Notes

[1] a) Ivin, K. J.; Mol, J. C. *Olefin Metathesis and Metathesis Polymerisation*, Academic Press, New York **1997**. b) *Topics in Organomet. Chem*., Ed. A. Fürstner, Springer, Berlin **1998**, vol. I.

[2] a) Schrock, R. R.; Murdzek, J. S.; Bazan, G. C.; Robbins, J.; DiMare, M.; O'Regan, M. *J. Am. Chem. Soc.* **1990**, *112*, 3875. b) Schwab, P.; France, M. B.; Ziller, J. W.; Grubbs, R. H. *Angew. Chem. Int. Ed.* **1995**, *34*, 2039.

[3] Blackwell, H. E.; O'Leary, D. J.; Chatterjee, A. K.; Washenfelder, R. A.; Bussmann, D. A.; Grubbs, R. H. *J. Am. Chem. Soc.* **2000**, *122*, 58.

[4] Trnka, T. M.; Grubbs, R. H. *Acc. Chem. Res.* **2001**, *34*, 18.

[5] Mohr, B.; Weck, M.; Sauvage, J. –P.; Grubbs, R. H. *Angew. Chem. Int. Ed.* **1997**, *36*, 1308.

[6] a) Martín-Alvarez, J. M.; Hampel, F.; Arif, A. M.; Gladysz, J. A. *Organometallics* **1999**, *18*, 955. b) Bauer, E. B.; Ruwwe, J.; Martín-Alvarez, J. M.; Peters, T. B.; Bohling, J. C.; Hampel, F. A.; Szafert, S.; Lis, T.; Gladysz, J. A. *Chem. Commun.* **2000**, 2261. c) Ruwwe, J.; Martín-Alvarez, J. M.; Horn, C. R.; Bauer, E. B.; Szafert, S.; Lis, T.; Hampel, F.; Cagle, P. C.; Gladysz, J. A. *Chem. Eur. J.* **2001**, *7*, 3931.

[7] Ng, P. L.; Lambert, J. *Synlett* **1999**, *11*, 1749.

[8] a) Dijkstra, H. P.; Steenwinkel, P.; Grove, D. M.; Lutz, M.; Spek, A. L.; van Koten, G. *Angew. Chem. Int. Ed.* **1999**, *38*, 2185. b) Dijkstra, H. P.; Meijer, M. D.; Patel, J.; Kreiter, R.; van Klink, G. P. M.; Lutz, M.; Spek, A. L.; Canty, A. J.; van Koten, G. *Organometallics* **2001**, *20*, 3159. c) Dijkstra, H. P.; Albrecht, M.; van Koten, G. *Chem. Commun.* **2002**, 126.

[9] Albrecht, M.; van Koten, G. *Angew. Chem. Int. Ed.* **2001**, *40*, 3750.

[10] For the synthesis of **1d** see: Bradshaw, J. S.; Jones, B. A.; Gebhard, J. S. *J. Org. Chem.* **1983**, *48,* 1127.

[11] a) Wehman, E.; Jastrzebski, J. T. B. H.; Ernsting, J. –M.; Grove, D. M.; van Koten, G. *J. Organomet. Chem.* **1988**, *353*, 145. b) Jastrzebski, J. T. B. H.; van Koten, G.; Konijn, M.; Stam, C. H. *J. Am. Chem. Soc.* **1982**, *104*, 5490.

[12] Albrecht, M.; James, S. L.; Veldman, N.; Spek, A. L.; van Koten, G. *Can. J. Chem.* **2001**, *79*, 709.

[13] For this particular reaction, no changes in the chemical shifts of the protons of the pincer moieties in the ^{1}H NMR spectrum are observed.

[14] Bird, *Transition Metal Intermediates in Organic Synthesis*, Academic Press: New York **1967**, 69.

[15] a) For **2** see: Alsters, P. L.; Baesjou, P. J.; Janssen, M. D.; Kooijman, H.; Sicherer-Roetman, A.; Spek, A. L.; van Koten, G. *Organometallics* **1992**, *11*, 4124. b) for **3** see: Grove, D. M.; van Koten, G.; Louwen, J. N.; Noltes, J. G.; Spek, A. L.; Ubbels, H. J. C. J. *J. Am. Chem. Soc.* **1984**, *106*, 6609.

[16] A. L. Spek, PLATON, A multipurpose crystallographic tool, Utrecht University (The Netherlands), **2002**.

[17] Beurskens, P. T.; Admiraal, G.; Beurskens, G.; Bosman, W. P.; García-Granda, S.; Gould, R. O.; Smits, J. M. M.; Smykalla, C. The DIRDIF99 Program System, Technical Report of the Crystallography Laboratory, University of Nijmegen (The Netherlands), **1999**.

[18] G. M. Sheldrick, SHELXL97, University of Göttingen (Germany), **1997**.

– *Summary* –

An important new research area in the field of homogeneous catalysis is the development of catalytic processes which combine the advantages of homogeneous (high activity/selectivity, mild conditions, reproducibility, good catalyst description) and heterogeneous catalysis (easy catalyst recycling, low catalyst quantities, high total turnover number (ttn)). A promising approach to achieve this, is by applying nanofiltration technology: adjusted homogeneous catalysts are applied in a membrane reactor and recycled *in situ*, even allowing catalytic reactions under continuously operating conditions. This leads to a significant increase in the total turnover number of the catalyst. Due to the very small pore-sizes in the membranes, macromolecules with sizes between 0.5 and 8 nanometers can be retained in solution by applying nanofiltration technology. To create homogeneous catalysts which possess the dimensions needed for efficient retainment by nanofiltration membranes, it is necessary to anchor catalytically active transition-metal complexes to soluble macromolecular supports.

This thesis describes the design and synthesis of shape-persistent nanosize multi(pincer-metal) complexes (for a general description of the pincer ligand, see Chapter 4) containing linear, flat or three-dimensional geometries. In particular, these complexes were studied in a nanofiltration membrane reactor in order to investigate the influences of shape-persistence, dimension and geometry on the retention of these compounds by nanofiltration membranes. Furthermore, these macromolecular complexes were tested as homogeneous catalysts in different organic transformations. One example is given in which a shape-persistent nanosize complex is applied as a homogeneous catalyst in a nanofiltration membrane reactor under continuous reaction conditions.

In this research, aromatic supports were chosen for the macromolecular complexes since it assures a high rigidity (shape-persistence) as well as a high inertness toward many reagents, allowing a versatile use as homogeneous catalyst for diverse organic reactions. A further objective of this work was to investigate whether these highly symmetric (C_3- or D_3-symmetry, as a result of the aromatic backbone and the substitution pattern) macromolecular materials could be used as supramolecular templates in the selective construction of large heterocycles, using olefin metathesis as the ring-closing reaction.

The application of nano- and ultrafiltration techniques in the field of homogeneous catalyst recycling is reviewed in Chapter 1. In Chapters 2 and 3, novel synthetic pathways for the synthesis of shape-persistent bis-, tris-, hexakis-, octakis- and dodecakis(pincer-palladium(II) and/or platinum(II)) complexes are presented, involving the construction of the multimetallic material via four different procedures (Scheme 1): i) direct cyclometalation (Chapter 2), ii) lithiation followed by transmetalation (Chapter 2), iii) oxidative addition (Chapter 2), and iv) construction of the multimetallic material using mono(pincer-metal) building blocks (Chapter 3). Bis-, tris- and hexakis(pincer) ligands were metalated using the first three methods (Scheme 1), thus the multisite ligand is prepared prior to the metalation step. For the hexakis(NCN-pincer) ligand (NCN = $C_6H_3(CH_2NMe_2)_2$-3,5) using a lithiation/trans-palladation procedure (method ii, Scheme 1), incomplete metalation (up to 70% metal incorporation) was obtained. From dendritic systems, it was already known that incomplete metalation of multisite ligands does occur, especially with an increasing number of ligand sites to be metalated. This leads to less well-defined products.

Scheme 1

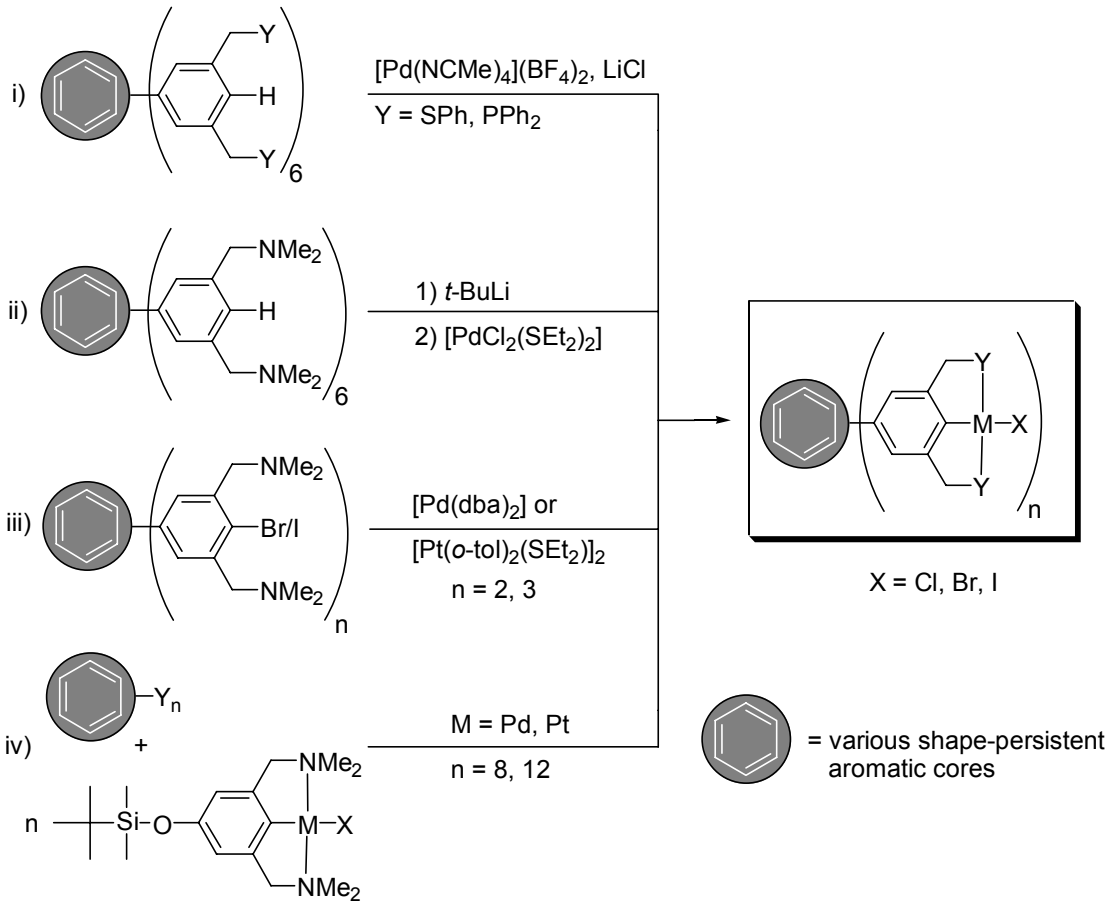

Therefore, for the construction of octakis- and dodecakis(NCN-metal) complexes (Chapter 3), a modular approach was developed: a monometalated pincer building block (M = Pd, Pt) was coupled to an octakis- or dodecakis-functionalized shape-persistent core (method iv, n = 8 or 12, Scheme 1). With the metal already present in the ligand-site during the construction of the multimetallic material, this approach leads to fully metalated materials. The multiple coupling of monometallic building blocks to support materials was performed under mild reaction conditions (acetone, room temperature), which is a prerequisite in order to prevent destruction of the individual organometallic moieties in the final multimetallic material synthesis step.

Chapter 4 describes the use of various YCY-palladium(II) complexes (Y = NMe_2, SPh, PPh_2, pz (pyrazol-1-yl) and pz* (3,5-dimethylpyrazol-1-yl)) as homogeneous catalysts in the double Michael reaction between methyl vinyl ketone and ethyl-α-cyanoacetate (Scheme 2). In particular, the influence of the donor substituent Y on the catalytic activity was investigated as well as the catalytic behavior of various *para*-functionalized cationic NCN-palladium(II) complexes (Y = NMe_2, Scheme 2). Furthermore, the electronic influence of the *para*-substituents on the electron density of the catalytically active palladium(II) centers was studied by Density-Functional Theory (DFT) calculations. From the experimental catalysis results it was concluded that NCN-type (N = NMe_2, pz, pz*, Scheme 2) catalysts are superior over SCS- and PCP-type catalysts for this particular reaction. The SCS- and PCP-catalysts showed only slightly higher activities than the blank reaction. In contrast, the various *para*-functionalized NCN-Pd^{II} complexes only showed small variations in catalytic activity (except for the *para*-Me_2N-substituent which showed a significant

Scheme 2

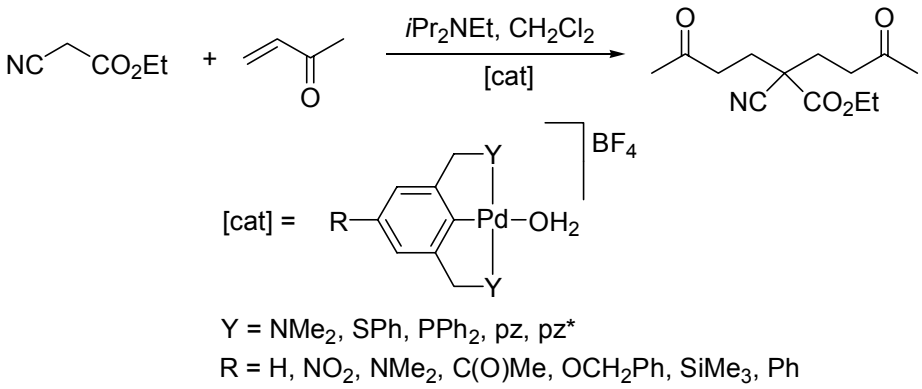

decrease in activity), indicating an only small electronic influence of the *para*-substituent on the Lewis acidic palladium(II) center. These latter results were confirmed by DFT-calculations (Gaussian 98), which showed small differences in the calculated Mulliken charges on the cationic palladium(II) centers. In particular in the field of immobilized homogeneous catalysts, knowledge about the influence of the *para*-functionality on the catalytic activity of the metal center is important. It allows the selection of a suitable functionality for anchoring of the catalyst to a support without affecting the catalytic activity of the individual sites.

The results found with the *para*-functionalized mono(NCN-Pd^{II}) complexes were supported by catalytic experiments performed with various nanosize multi(NCN-pincer) complexes in the double Michael reaction: tris- and octakis(NCN-Pd^{II}) complexes containing different *para*-functionalities were found to possess the same activity per catalytic unit as the mononuclear analogs. The complex with the highest catalyst loading, twelve NCN-Pd^{II} units connected to an aromatic backbone, showed an unexpected threefold increase in catalytic activity per catalytic unit as compared to the mononuclear analog. This increase is probably due to cooperation between (cationic) catalytic sites which are in close proximity to each other, thereby enhancing catalysis. An alternative explanation can be the formation of larger aggregates in solution, leading to the formation of polar micro-environments in which catalytic rates are considerably faster.

The application of shape-persistent nanosize multi(NCN-metal) complexes (metal = Pt, Pd) having different dimensions and geometries (Figure 1) in a nanofiltration membrane reactor is studied in Chapter 5. It was found that a high degree of rigidity in the backbone of these macromolecular complexes indeed results in more efficient retentions of these materials by the (commercially available) MPF-60 and MPF-50 nanofiltration membranes. Comparison between shape-persistent complexes and flexible dendrimers of similar nanosize dimensions (according to molecular modeling), revealed higher retentions for the shape-persistent complexes. Especially, in relating the molecular volumes (calculated with molecular modeling) of the various complexes to the retention rates, it becomes clear that shape-persistence is advantageous for obtaining optimal retentions by nanofiltration membranes.

For the retention determinations, we made use of the ability of the NCN-Pt^{II}-X (X = halide) unit to absorb SO_2, a process which is accompanied by a strong, characteristic color change from colorless to bright orange. Submillimolar amounts of

the SO_2-complexes in the retentate and permeate can be detected by UV/Vis-spectroscopy, allowing an accurate determination of the retention rates of the various complexes.

Figure 1

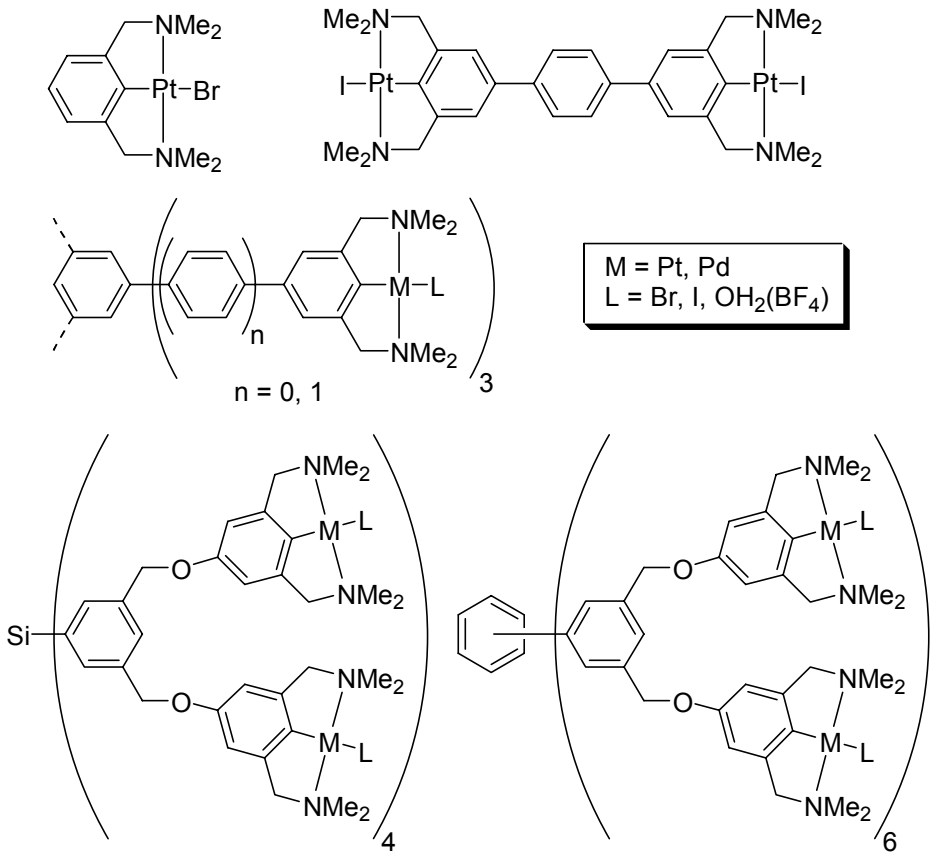

Finally, a dodecakis(NCN-palladium(II)) complex (L = $OH_2(BF_4)$, Figure 1) was applied as a homogeneous catalyst in the double Michael reaction under continuously operating conditions. This catalyst showed a constant activity for prolonged reaction times, resulting in an increase of the total turnover number by a factor of over 40. For the retention measurements, the NCN-Pt^{II} unit was used instead of the catalytically active NCN-Pd^{II} unit. According to molecular modeling studies, this exchange of metals has no marked influence on the size and geometry of the dodecakis(NCN-metal) complexes. The overall properties for retaining the macromolecular catalyst by nanofiltration membranes are thus very similar, making direct comparison between the two dodecakis(NCN-metal) complexes legitimate.

In Chapter 6, a new methodology, *i.e.* the transcyclometalation (TCM) procedure, to prepare hexakis(PCP-platinum(II) and ruthenium(II)) complexes (PCP = $[C_6H_2(CH_2PPh_2)_2\text{-}3,5]^-$) is reported (Scheme 3). The TCM procedure was found to be superior over classical metalation procedures developed previously for mono(PCP-metal) complexes. Whereas the classical procedures led only to the formation of intractable product mixtures (probably due to the high phosphine concentration at the periphery of the hexakis(PCP-pincer) ligand), applying the TCM reaction gave selectively the fully hexametalated materials in high yields. This large difference in selectivity is proposed to be due to the unique reaction pathway of the TCM reaction, in which the formation of *trans*-*C,C*-bisaryl-metal intermediates plays a significant role.

In addition, the hexakis(PCP-ruthenium(II)) complex was applied as a homogeneous catalyst in the hydrogen transfer reactions of various ketones to the corresponding alcohols (Scheme 3). In the reduction of cyclohexanone to cyclohexanol, the hexakis(pincer-ruthenium) species showed a lower activity (twofold) per ruthenium center compared to the mononuclear analog, while in the reduction of acetophenone and benzophenone to the corresponding alcohols, the activity per PCP-Ru^{II} unit was equal to that of the mono(ruthenium) analog. The latter results show an efficient use of all six ruthenium centers in catalysis, meaning that they act as independent catalytic sites, an important aspect when applying multimetallic complexes as homogeneous catalysts in organic transformations.

Scheme 3

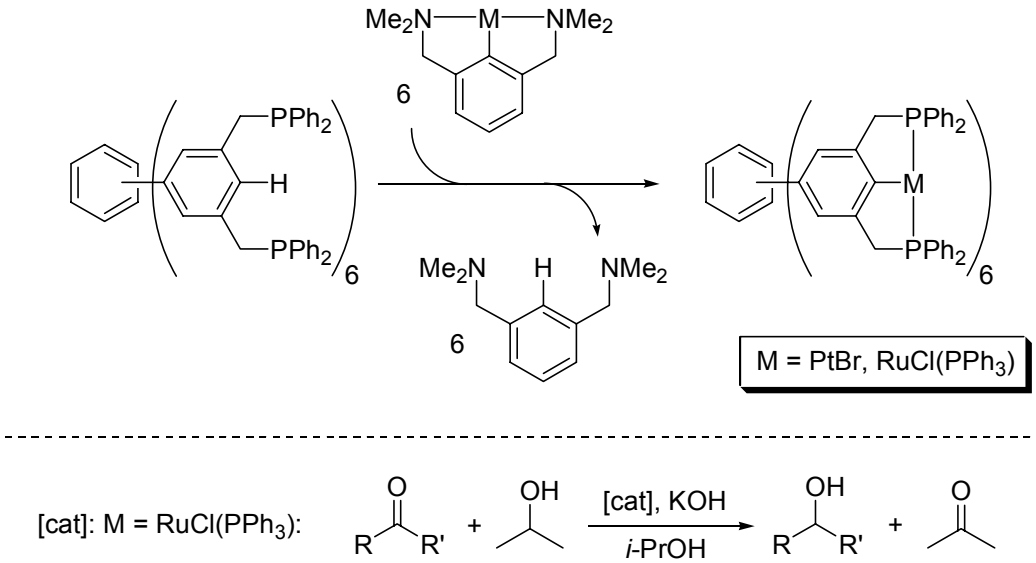

Chapter 7 describes the use of pincer-metal complexes as protecting groups for the Lewis basic nitrogen atom of diolefin-substituted pyridines (normally a forbidden functionality) in olefin metathesis reactions (see example in Scheme 4). The cationic NCN-Pt^{II} complex appeared to be the best protecting agent, as it forms the most stable coordination complex with the olefin-substituted pyridines. With the palladium analog, the weaker Pd–N(py) bond resulted in a relatively high concentration of free pyridine in solution, leading to deactivation of the ruthenium metathesis catalyst (first generation Grubb's catalyst). Furthermore, the use of YCY-palladium(II) complexes (Y = NMe_2, SPh) as protecting agents led to a relatively fast side-reaction: isomerization of the olefinic bonds from external to internal double bonds. The positioning of the olefin chains on the pyridine ring (2,6- or 3,5-functionalization) also greatly influenced the rate of the olefin metathesis reaction. In all reactions where long reaction times were needed for complete conversions, isomerization of the double bonds of the olefin tails occurred. In addition, a new strategy for the use of highly symmetric multi(pincer-metal) complexes as supramolecular templates for the construction of large heterocycles, using olefin metathesis, was discussed.

Scheme 4

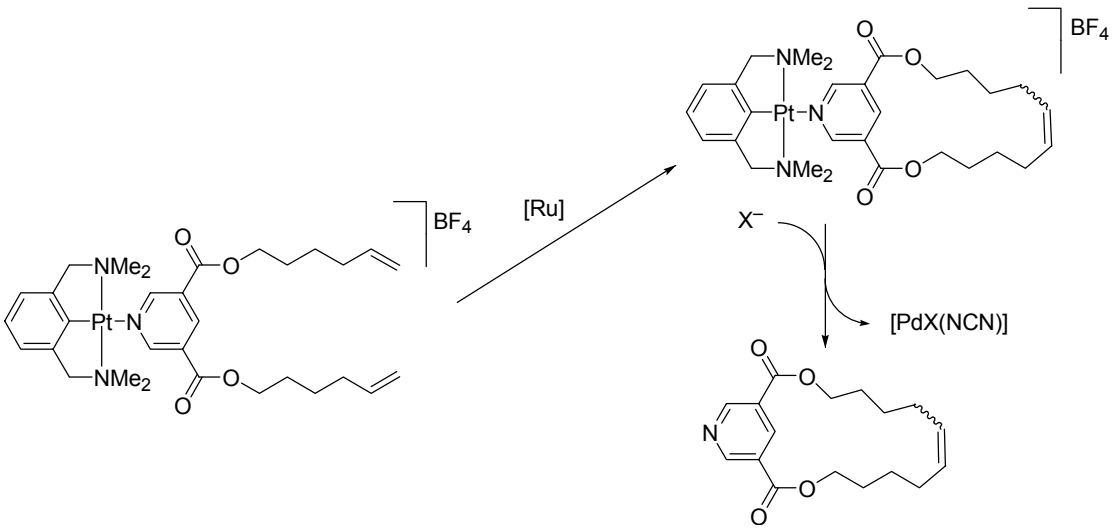

General Conclusions

In conclusion, new synthetic pathways to synthesize shape-persistent nanosize multi(pincer-metal) complexes were developed. Applying these multimetallic

complexes as homogeneous catalysts in different catalytic reactions, revealed that all metal centers were able to act as independent catalytic units. In one particular case, it was even shown that a threefold increase in catalytic activity per metal center was obtained as compared to the mononuclear analog, which must be a direct result of the macromolecular material design.

In addition, nanofiltration experiments revealed that a high degree of rigidity in the backbone of macromolecular complexes is advantageous for obtaining optimal retentions by nanofiltration membranes. Furthermore, for a dodecametalated complex, it was shown that such shape-persistent macromolecular complexes are well-suited for application as homogeneous catalysts in a nanofiltration membrane reactor under continuously operating conditions for prolonged reaction times. A large increase of the total turnover number of the catalyst was found, showing the high potential of this technology in homogeneous catalyst recycling, which eventually can lead to enhanced applications of homogeneous catalysts in large scale industrial processes. An important condition that should be fulfilled for a broader future application of membrane technology in homogeneous catalyst recycling, is a high stability of the homogeneous catalyst toward decomposition during catalysis. Additionally, developing more resistant membranes and improving the reactor technology is desirable, since these factors, together with catalyst stability, largely determine the applicability of membrane technology in homogeneous catalyst recycling.

Based on the successful use of pincer-metal complexes as protecting groups for olefin-substituted pyridines in olefin metathesis reactions, future research should be focused on a general application of organometallic complexes as protecting groups for Lewis-basic substituents (normally forbidden) in olefin metathesis. In addition, since basic substituents are often not tolerated in many other catalytic reactions as well, this approach of using transition-metal complexes as protecting groups during catalysis can be of general interest. Eventually this will lead to a high functional group tolerance in a broad range of catalytic reactions.

Finally, based on the foregoing and making use of the high symmetry of the shape-persistent multi(pincer-metal) complexes as discussed in this thesis, applying these multimetallic complexes as supramolecular templates to construct large heterocycles by olefin metathesis is very interesting. For future research, this particular application of multimetallic compounds needs to be further developed, which eventually can lead to an efficient and selective synthesis of large crown-ether type heterocycles.

– *Samenvatting* –

Een belangrijke nieuwe ontwikkeling in de katalyse van organisch chemische reacties is er op gericht de voordelen van de homogene katalyse (hoge activiteit en selectiviteit, milde reactiecondities, reproduceerbaarheid, een goede definitie van de katalysator) en die van de heterogene katalyse (efficiënte katalysator recycling, lage katalysatorconcentratie, hoge totaal aantal omzettingen (ttn)) in één katalytisch proces te combineren. Een interessante mogelijkheid om dat te bereiken is door gebruik te maken van (nano)filtratietechnologie: in een membraanreactor kunnen daarvoor geschikt gemaakte homogene katalysatoren *in situ* herwonnen worden (recycling) waardoor reacties onder continue homogene reactiecondities kunnen worden uitgevoerd. Dat leidt tot een aanzienlijke toename van het totaal aantal omzettingen (ttn) per katalysatordeeltje. Vanwege de extreem kleine poriegrootte in de membranen is het mogelijk om met behulp van deze technologie macromoleculen met afmetingen tussen de 0,5 en 8 nanometer in oplossing te filtreren. Om dit voor homogene katalysatoren te realiseren is het nodig om katalytisch actieve overgangsmetaal-complexen te binden aan oplosbare macromoleculen (als dragermateriaal) om zodoende katalysatoren te verkrijgen met de gewenste afmetingen.

Dit proefschrift beschrijft de synthese van starre multi(tang-metaal)-complexen (voor een algemene beschrijving van het tang-ligand zie Hoofdstuk 4) waarvan de dimensies in het nanometergebied vallen en die een lineaire, vlakke of driedimensionale geometrie bezitten. Met name is onderzocht wat de invloeden van starheid, grootte en geometrie van deze complexen zijn op hun filtreerbaarheid door nanofiltratiemembranen. Vervolgens zijn deze complexen getest als homogene katalysatoren in een aantal organisch chemische reacties. Tevens is één van deze macromoleculaire complexen toegepast als homogene katalysator in een nanofiltratiemembraanreactor onder continue reactiecondities.

In dit onderzoek is gekozen voor een aromatisch ringsysteem om de verschillende organometaalcomplexen te binden: aromatische groepen bezitten een grote starheid en zijn tevens inert ten opzichte van veel reagentia waardoor ze in een verscheidenheid aan reacties kunnen worden toegepast. De hoge symmetrie (als gevolg van het aromatische skelet) van deze multi(tang-metaal)-complexen maakt het in principe mogelijk om deze moleculen ook te gebruiken als een supramoleculaire

mal ("template") in de selectieve synthese van grote heterocyclische structuren door middel van olefine-metathese. Deze mogelijkheid is eveneens onderzocht.

In Hoofdstuk 1 wordt een overzicht gegeven van de toepasbaarheid van nano- en ultrafiltratiemembranen in de recycling van homogene katalysatoren. Nieuwe methoden voor de synthese van di-, tri-, hexa-, octa- en dodeca(tang-palladium(II) en -platina(II))-complexen staan beschreven in Hoofdstukken 2 en 3. Vier verschillende manieren om deze multimetaal-materialen te maken worden behandeld (Schema 1): 1) directe cyclometallering (Hoofdstuk 2), ii) lithiëring gevolgd door transmetallering (Hoofdstuk 2), iii) oxidatieve additie (Hoofdstuk 2) en iv) opbouw uit monometaal bouwstenen (Hoofdstuk 3). Di-, tri-, en hexa(tang) liganden werden gemetalleerd door gebruik te maken van de eerste drie methoden; het multi-gefunctionaliseerd ligand wordt daarbij eerst gesynthetiseerd en dan volledig gemetalleerd. Enkel de palladering van het hexa(NCN-tang)-ligand (NCN = $C_6H_3(CH_2NMe_2)_2$-3,5) via een

Schema 1

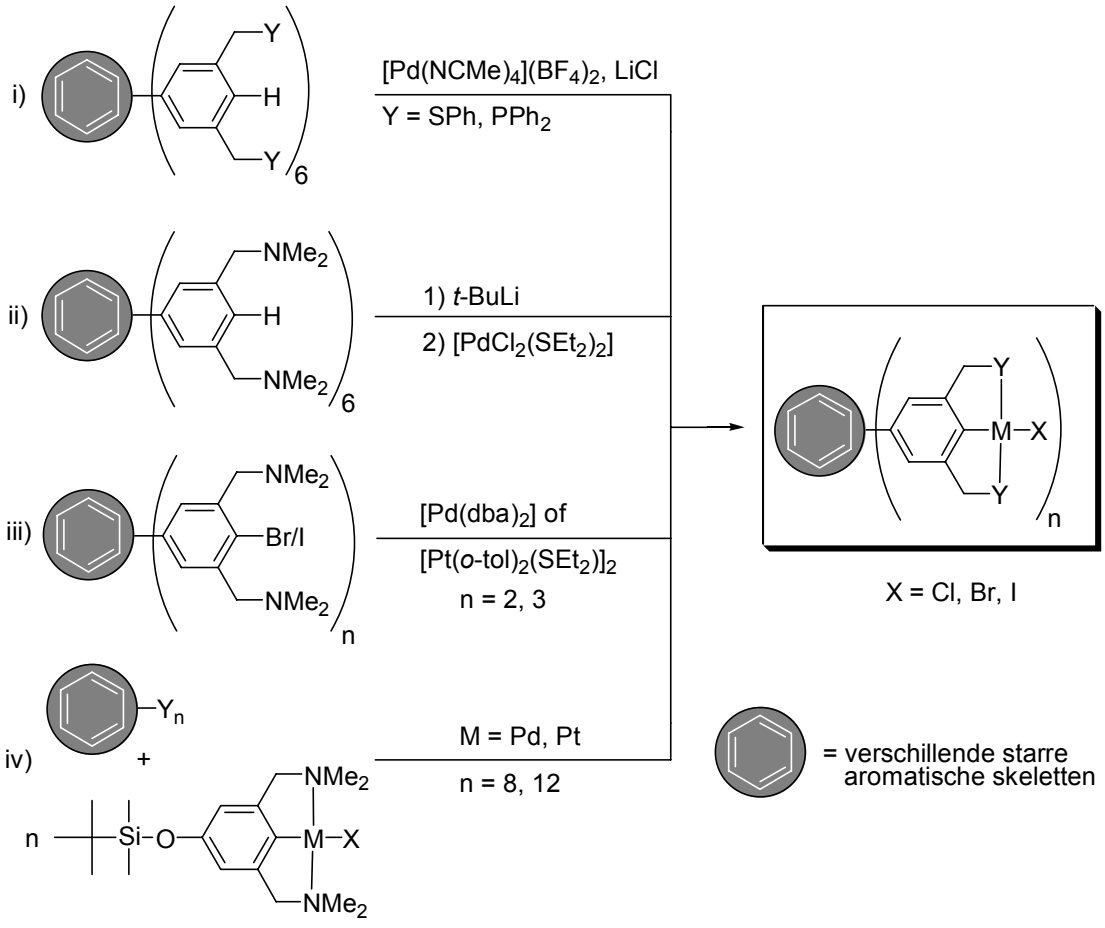

lithiëring/transmetallering procedure (methode ii, Schema 1) resulteerde in een niet-volledig gemetalleerd product (70% metaalinbouw). Dit verschijnsel was al bekend uit de synthese van multimetaal-dendrimeren. Bij een aanzienlijke toename van het aantal te metalleren liganden in één molecuul wordt de kans op onvolledige metallering groter, waardoor een minder goed gedefinieerd product wordt verkregen. Daarom werd voor de synthese van octa- en dodeca(NCN-metaal)-complexen een modulaire benadering ontwikkeld. Hierbij wordt een monometaal-bouwsteen (metaal = Pd, Pt) gekoppeld aan een acht- of twaalfvoudig gefunctionaliseerd star aromatisch skelet (methode iv, Schema 1). Met het metaal reeds in het tangligand aanwezig in de synthesestap is volledige metallering van het complex gegarandeerd. Deze veelvoudige koppeling van een aantal monometaal bouwstenen aan een dragermateriaal kan worden uitgevoerd onder milde reactiecondities (in aceton bij kamertemperatuur). Dit is een absoluut vereiste voor deze reactie omdat ontleding van de individuele organometaaleenheden in de uiteindelijke synthesestap van het multimetaal-materiaal moet worden voorkomen.

In Hoofdstuk 4 worden diverse YCY-palladium(II)-complexen (Y = NMe_2, SPh, PPh_2, pz (= pyrazol-1-yl) en pz* (= 3,5-dimethylpyrazol-1-yl)) getest als homogene katalysator in de dubbele Michael reactie van methylvinylketon met ethyl-α-cyanoacetaat (Schema 2). In het bijzonder werd de invloed van de donorsubstituent Y op de katalytische activiteit onderzocht, alsmede het gedrag van een aantal *para*-gesubstitueerde NCN-palladium(II)-complexen (N = NMe_2, Schema 2). Tevens werd met behulp van ab initio berekeningen de elektronische invloed van de *para*-substituenten op de Mullikenlading van het katalytisch actieve palladium(II)-centrum onderzocht. Uit de experimenteel bepaalde katalyseresultaten kon worden

Schema 2

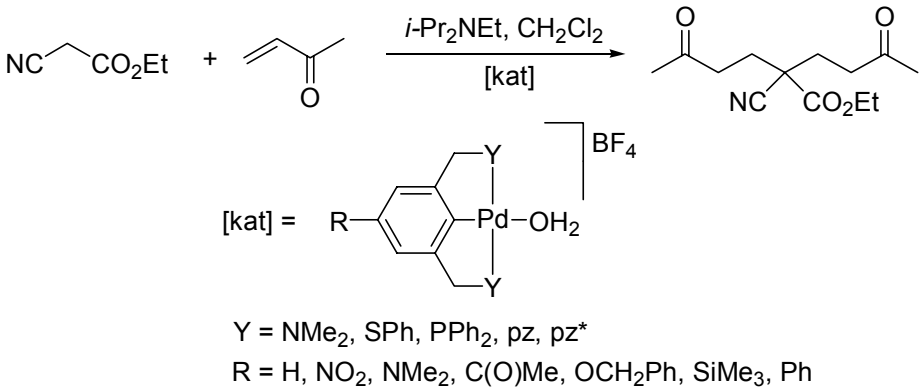

Y = NMe_2, SPh, PPh_2, pz, pz*

R = H, NO_2, NMe_2, C(O)Me, OCH_2Ph, $SiMe_3$, Ph

geconcludeerd dat NCN-type katalysatoren (N = NMe_2, pz en pz*, Schema 2) superieur zijn in de Michael reactie ten opzichte van SCS- en PCP-type katalysatoren. De SCS- en PCP-type katalysatoren vertonen nauwelijks activiteit. De resultaten verkregen met de verschillende *para*-gesubstitueerde NCN-Pd^{II}-katalysatoren vertonen slechts een kleine spreiding in activiteit (alleen de *para*-NMe_2 heeft een duidelijk lagere activiteit); dit geeft aan dat de elektronische invloed van de *para*-substituent op het Lewis-zure palladium(II)-centrum gering is. Deze conclusie werd bevestigd door DFT-berekeningen (Gaussian 98) waarbij slechts kleine verschillen in de berekende Mullikenlading op de kationische palladium(II)-centra werden gevonden. Deze kennis van de invloed van *para*-substituenten is van groot belang bij de toepassing van geïmmobiliseerde homogene katalysatoren in organisch chemische reacties. Hierdoor kan de juiste *para*-functionaliteit geselecteerd worden waarmee de katalysator aan het dragermateriaal gebonden kan worden zonder dat hierdoor de katalytische activiteit van de individuele metaalcentra wordt beïnvloed.

De gevonden resultaten met de *para*-gesubstitueerde mono(NCN-Pd^{II})-complexen werden bevestigd door de (experimentele) resultaten verkregen met een aantal multi(NCN-tang)-katalysatoren in de dubbele Michael reactie: tri- en octa(NCN-Pd^{II})-complexen, waarvan de tang-eenheden verschillende *para*-functionaliteiten bezitten, hebben vergelijkbare activiteiten per palladium(II)-centrum als de analoge monopalladium(II)-verbindingen. Het multimetaal-complex met de hoogste katalysatorbelading, twaalf NCN-Pd^{II}-tangeenheden gebonden aan een star aromatisch skelet, vertoonde echter een verdrievoudigde katalytische activiteit per palladium(II)-centrum. Een mogelijke verklaring voor dit gedrag is samenwerking tussen ruimtelijk dicht bijelkaar gelegen (kationische) katalytische groepen, resulterend in een aanmerkelijke versnelling van de reactie. Een andere mogelijke verklaring is de vorming van grotere aggregaten in oplossing waarbij polaire microdomeinen ontstaan met als gevolg een versnelling van de katalysereactie.

Het gebruik van verschillende starre multi(NCN-metaal) complexen (metaal = Pt, Pd) met verschillende nanodimensies en geometriën (Figuur 1) in een nanofiltratiemembraanreactor wordt beschreven in Hoofdstuk 5. Gevonden werd dat een hoge mate van starheid in het centrale deel van de macromoleculaire complexen inderdaad resulteert in efficiëntere retenties van deze verbindingen door de (commercieel verkrijgbare) MPF-60 en MPF-50 nanofiltratiemembranen. Vergelijking van starre complexen met flexibele dendrimeren met vergelijkbare nanoschaal afmetingen (bepaald met “molecular modeling”) gaf iets hogere retenties

te zien voor de starre complexen. Vooral het relateren van de moleculaire volumes van de verschillende complexen aan de gevonden retentiewaarden maakte duidelijk dat een hoge mate van starheid inderdaad voordelig is voor het bereiken van een optimale retentie van macromoleculen door nanofiltratiemembranen.

Figuur 1

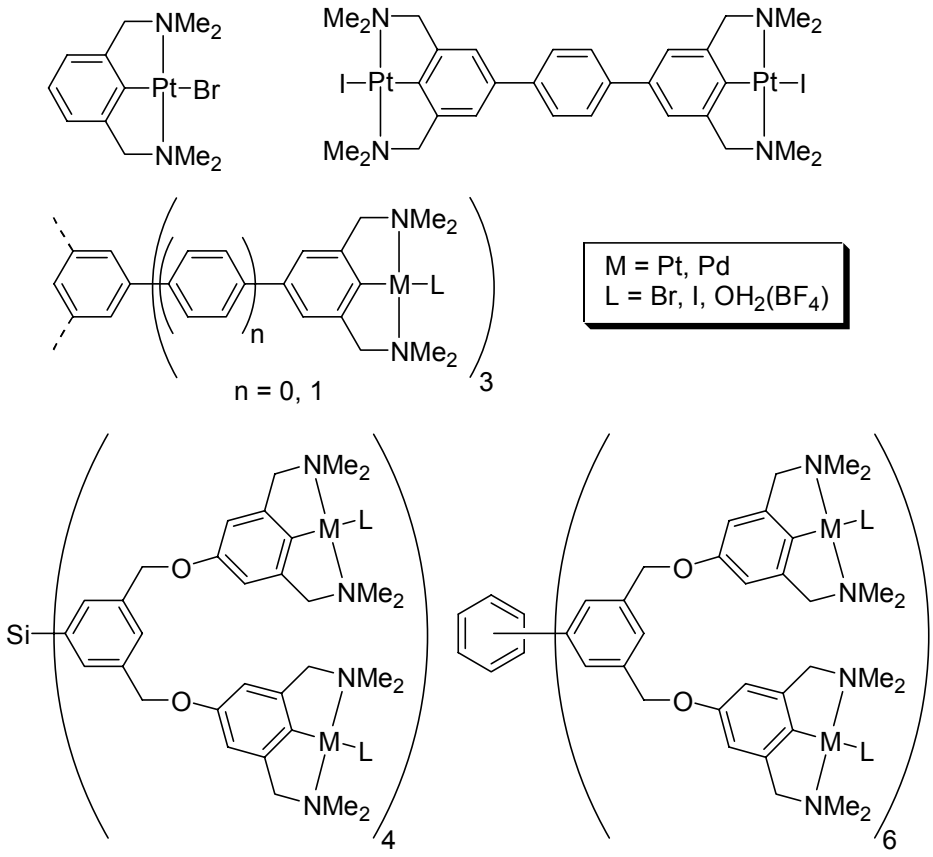

Voor de retentiebepalingen werd gebruik gemaakt van het vermogen van de NCN-Pt^{II}-X-eenheid (X = halide) om SO_2 te binden hetgeen gepaard gaat met een karakteristieke kleuromslag van kleurloos naar oranje. Met behulp van UV/Vis spectroscopie kunnen al submillimolaire hoeveelheden van deze SO_2-complexen in oplossing worden aangetoond waardoor de retenties van de verschillende complexen zeer nauwkeurig kunnen worden bepaald.

Tenslotte werd een dodeca(NCN-palladium(II))-complex (L = $OH_2(BF_4)$, Figuur 1) toegepast als homogene katalysator in de dubbele Michael reactie onder continue reactiecondities in een nanofiltratiemembraanreactor. De katalysator vertoonde een constante activiteit over langere reactietijden. Dit resulteert in een

toename van het totaal aantal omzettingen (ttn) per palladium(II)-centrum met een factor groter dan 40. Bij de retentiebepalingen werd gebruik gemaakt van het dodeca(NCN-platina(II))-complex in plaats van het katalytisch actieve dodeca(NCN-palladium(II))-complex. Met behulp van "molecular modeling" werd aangetoond dat deze verwisseling van metaal geen verandering in molecuulgrootte tot gevolg heeft. De eigenschappen die bepalend zijn voor de retentie van de katalysator door nanofiltratiemembranen blijven dus nagenoeg gelijk waardoor een vergelijking tussen de twee dodeca(NCN-metaal)-complexen gerechtvaardigd is.

In Hoofdstuk 6 wordt een nieuwe methode, de zogenaamde transcyclometallering (TCM), om hexa(PCP-platina(II) en ruthenium(II))-complexen (PCP = $[C_6H_2(CH_2PPh_2)_2\text{-}3,5]^-$) te synthetiseren behandeld (Schema 3). De TCM-reactie is superieur ten opzichte van de klassieke metalleringsmethoden die reeds ontwikkelt waren voor de synthese van mono(PCP-metaal)-complexen. Terwijl het gebruik van de klassieke methoden leidde tot niet te analyseren productmengsels (waarschijnlijk door de hoge concentratie aan fosfinegroepen op het oppervlak van het hexa(PCP-pincer)-ligand), werd met behulp van de TCM reactie selectief en in hoge opbrengst volledig gemetalleerde producten verkregen. Dit grote verschil in selectiviteit wordt toegeschreven aan het unieke reactiepad van de TCM reactie, waarbij *trans*-*C,C*-bisarylmetaal-intermediairen een belangrijke rol spelen.

Schema 3

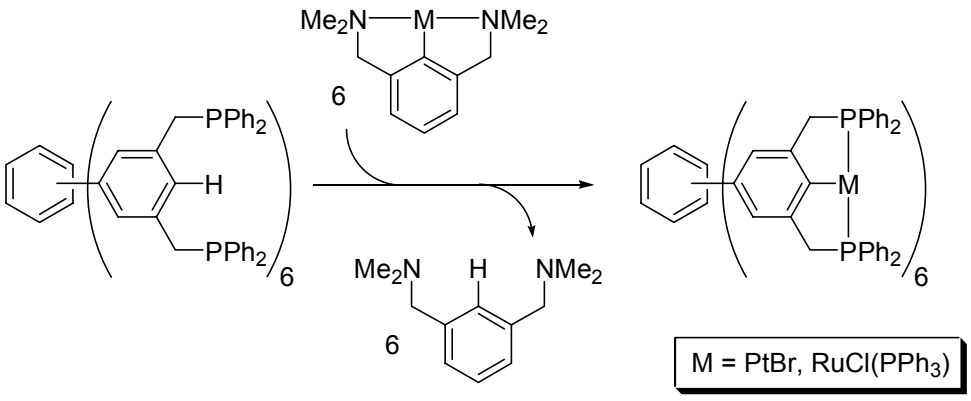

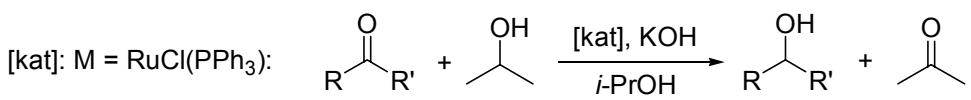

De hexa(PCP-ruthenium(II))-verbinding werd tevens als homogene katalysator getest in de reductie van een aantal ketonen tot de overeenkomstige alcoholen met behulp van de waterstofoverdrachtsreactie (Schema 3). De hexakis(pincer-ruthenium(II))-verbinding vertoonde in de reductie van cyclohexanon tot cyclohexanol een lagere activiteit ten opzichte van de mono(PCP-Ru^{II})-katalysator terwijl in de reductie van acetofenon en benzofenon de katalytische activiteit per PCP-Ru^{II}-eenheid gelijk was aan die van de mono(PCP-Ru^{II})-katalysator. In de laatste twee katalytische reacties wordt dus efficiënt gebruik gemaakt van alle zes ruthenium-centra, hetgeen inhoudt dat ze als onafhankelijke katalytische eenheden optreden. Voor de toepassing van multimetaal-complexen als homogene katalysatoren in organische reacties is dit een uitermate belangrijk aspect.

In Hoofdstuk 7 worden tang-metaal-complexen toegepast als beschermende groepen voor de stikstofatomen van diolefine-gesubstitueerde pyridines om olefine-metathese reacties mogelijk te maken (normaal zijn pyridines daarin niet-toegestane substituenten) (zie voorbeeld in Schema 4). Het blijkt dat het kationische NCN-Pt^{II}-complex een uitstekende beschermende groep is vanwege de stabiele coördinatiebinding met het olefine-gesubstitueerde pyridine. Toepassing van de analoge palladium(II)-verbinding met een zwakkere Pd-N(py)-binding resulteerde in een hogere concentratie aan vrij pyridine in oplossing hetgeen zich uitte in een deactivering van de metathese-katalysator. Tevens trad bij het toepassen van YCY-palladium(II)-complexen (Y = NMe_2, SPh) als beschermende groepen een relatief snelle isomerisering van externe naar interne dubbele bindingen op. Deze ongewenste

Schema 4

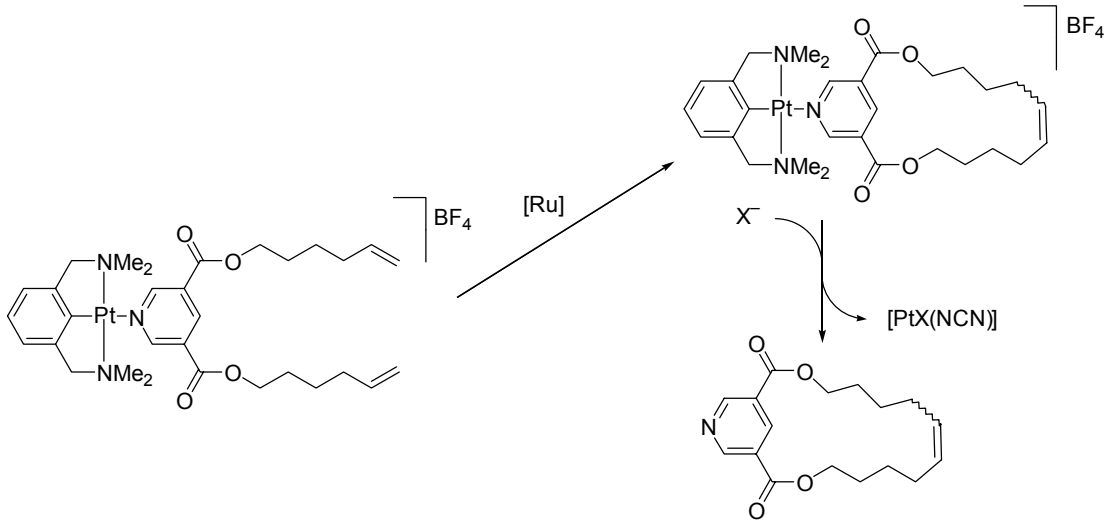

nevenreactie (interne dubbele bindingen zijn minder actief in olefine-metathese) is een bekend fenomeen in reacties waarin overgangsmetaalcomplexen worden toegepast. Ook de positie van de onverzadigde substituenten aan de pyridinering (2,6- of 3,5-substitutie) bleek een grote invloed te hebben op de snelheid van de olefine-metathese reactie. Tenslotte wordt in dit hoofdstuk een nieuwe strategie besproken waarin symmetrische starre multi(tang-metaal)-complexen worden gebruikt als supramoleculaire mal ("template") voor de synthese van grote heterocyclische verbindingen via olefine-metathese.

Algemene Conclusies

Kort samengevat beschrijft dit proefschrift nieuwe syntheseroutes voor starre multi(tang-metaal)-complexen met nanoschaalafmetingen. De toepassing van deze complexen in een aantal katalytische reacties toont aan dat alle metaalcentra als onafhankelijke katalytische eenheden actief zijn. In één specifiek voorbeeld werd zelfs een drievoudige toename in katalytische activiteit per metaalcentrum gevonden vergeleken met een analoge monometaalverbinding. Dit gedrag is het resultaat van de speciale structuur van de macromoleculaire katalysator.

Nanofiltratie-experimenten toonden aan dat een hoge mate van starheid in het skelet van macromoleculaire complexen voordelig is voor het verkrijgen van optimale retenties van deze verbindingen door nanofiltratiemembranen. Voor een dodeca(tang-palladium(II))-complex werd aangetoond dat dit type starre macromoleculaire complexen bij uitstek geschikt is als homogene katalysator onder continue reactiecondities in een nanofiltratiemembraanreactor. Een grote toename in het totaal aantal omzettingen (ttn) per metaalcentrum kon worden bewerkstelligd waarmee de potentie van deze techniek in de recycling van homogene katalysatoren wordt geïllustreerd. Deze technologie kan uiteindelijk leiden tot meer toepassingen van homogene katalysatoren op grotere industriële schaal. Voor een bredere toepassing van de membraantechnologie op het gebied van homogene katalysator recycling is een grote katalysatorstabiliteit, ter voorkoming van ontleding tijdens de katalytische reactie, een belangrijke voorwaarde. Tevens is het ontwikkelen van meer resistente membranen en het verbeteren van de reactortechnologie wenselijk, omdat deze factoren, tezamen met de katalysatorstabiliteit, grotendeels de toepasbaarheid van de membraantechnologie in homogene katalysator recycling bepalen.

Het hier vermelde succesvolle gebruik van tang-metaal-complexen als beschermende groepen voor pyridine-gesubstitueerde olefines in olefine-metathese

reacties suggereert dat organometaalverbindingen in veel meer gevallen een nuttige toepassing zouden kunnen vinden als beschermende groepen voor normaal niet getolereerde Lewis-basische substituenten in de olefine-metathese. Aangezien basische substituenten in veel katalytische reacties niet getolereerd worden, kan het gebruik van organometaal-complexen als beschermende groep tijdens katalyse zelfs van algemeen belang zijn. Dit kan uiteindelijk resulteren in een hogere tolerantie voor verschillende functionele groepen in een breed scala aan katalytische reacties.

Tenslotte, gebaseerd op het voorgaande en gebruikmakend van de hoge mate van symmetrie van de starre multi(tang-metaal)-complexen (zoals beschreven in dit proefschrift) is het toepassen van deze complexen als supramoleculaire mal voor de synthese van grote heterocyclische verbindingen, door middel van olefine-metathese, uitermate interessant. In de toekomst zal deze toepassing van symmetrische multimetaalverbindingen verder ontwikkeld moeten worden om uiteindelijk te kunnen resulteren in een efficiënte en selectieve synthesemethode voor grote kroonether-achtige verbindingen.

Graphical Abstract

***Synthesis of Shape-Persistent Multi(pincer-metal) Complexes**, Chapters 2, 3 and 6*

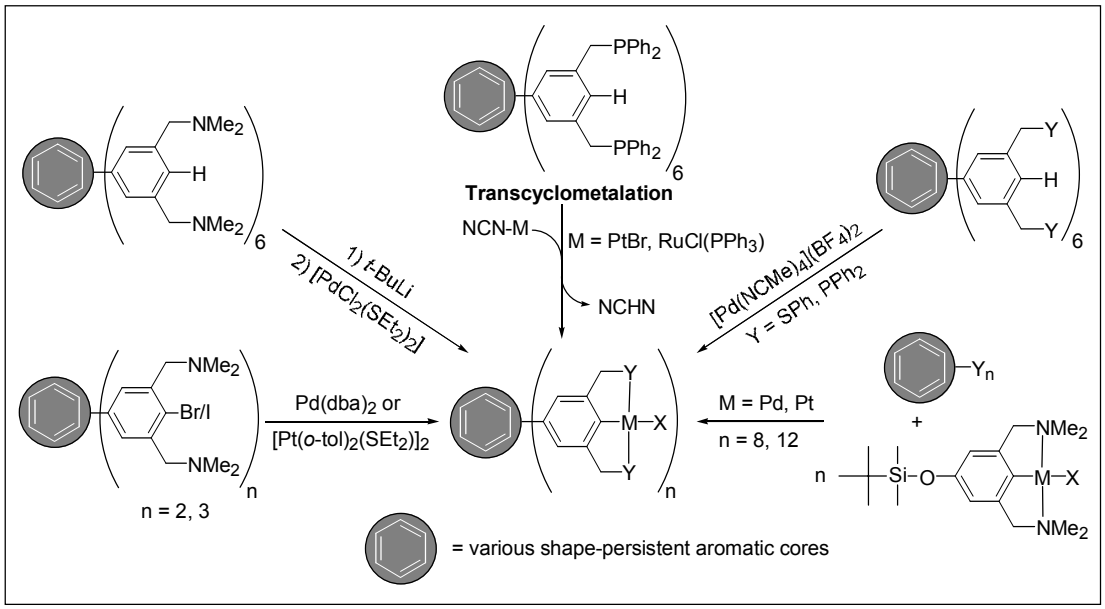

***Homogeneous Catalysis**, Chapters 4 and 6*

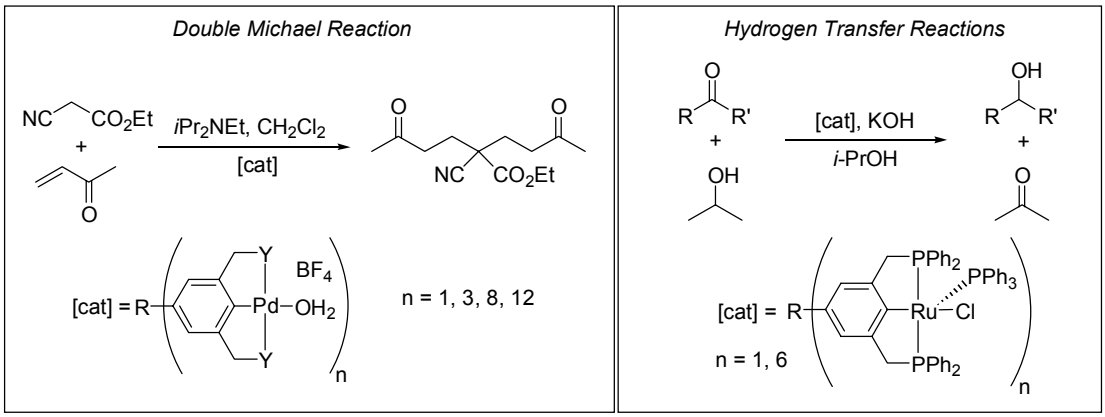

***Nanofiltration/Continuous Catalysis**, Chapter 5*

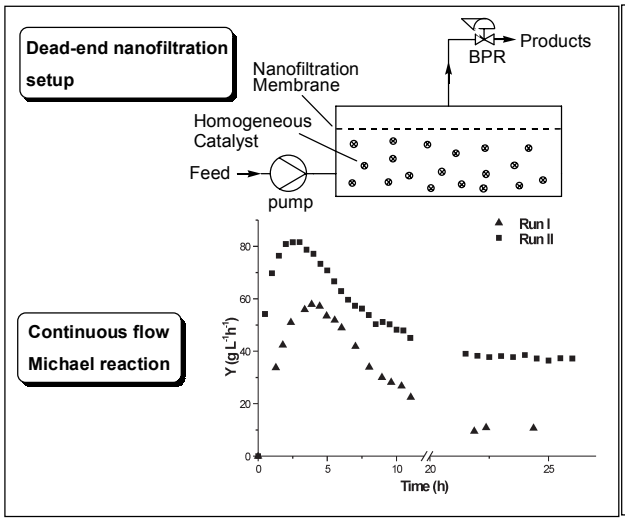

***Metathesis**, Chapter 7*

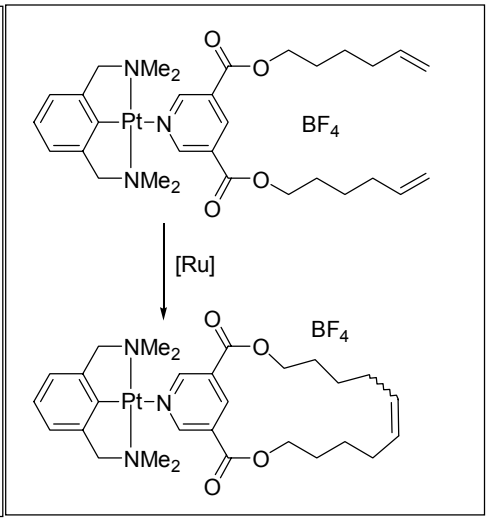

Dankwoord

Aangezien ik nu ben aanbeland bij het schrijven van de laatste paar bladzijden van mijn proefschrift wordt het de hoogste tijd om eens terug te blikken op de afgelopen jaren. Ongeveer viereneenhalf jaar geleden besloot ik om als *oprjochte Frys* (of, zoals sommige mensen steevast bleven zeggen, Groninger) de Rijksuniversiteit van Groningen vaarwel te zeggen en een promotieonderzoek te gaan doen in 'het westen', in Utrecht. Achteraf gezien kan ik alleen maar concluderen dat het de beste keus is geweest die ik mogelijkerwijs kon maken. Ik heb in Utrecht ontzettend leuke jaren gehad, zowel persoonlijk als wetenschappelijk, en dat is te danken aan een groot aantal mensen die ik hier graag bij name wil noemen.

Graag wil ik beginnen met alle mensen die deel hebben uitgemaakt van de Sectie Organische Synthese in de afgelopen jaren hartelijk te bedanken voor de goede sfeer en gezelligheid in en rondom het lab. De labstaps, borrels, kerstdiners, pannenkoeken eten etc. waren altijd erg gezellig en dragen mijns inziens voor een belangrijk gedeelte bij aan de goede sfeer in de groep.

Uiteraard wil ik hier ook een aantal mensen in het bijzonder noemen. In de eerste plaats mijn hooggeleerde promotor Prof. dr. Gerard van Koten. Beste Gerard, ik ben je heel dankbaar voor het feit dat je mij zo'n viereneenhalf jaar geleden de kans hebt geboden om een promotieonderzoek in jouw groep te beginnen. Ik heb grote waardering voor de manier waarop jij de groep leidt en voor de manier waarop jij promovendi en postdocs altijd weer weet te motiveren. Ik heb ontzettend veel van je geleerd in de afgelopen jaren en vooral de gesprekken aan het eind van de dag als je na zessen nog even binnen kwam wippen heb ik als erg prettig ervaren. Tevens heb jij me alle mogelijkheden en vrijheden gegeven om mezelf verder te ontwikkelen. Daarvoor grote dank.

Veel dank ben ik ook verschuldigd aan mijn co-promotor Dr. Gerard van Klink. Beste Gerard, jij was altijd bereid om te luisteren en advies te geven als ik daarom vroeg. Tevens was je een onmisbare schakel in het hele schrijf- en corrigeerproces en het is dan ook voor een groot gedeelte aan jou te danken dat alles op het einde zo soepel is verlopen. Ik heb grote waardering voor jouw vermogen om zelfs de kleinste foutjes uit de experimentals en de referenties te plukken. Eventuele foutjes die er nu nog in staan komen dan ook geheel voor mijn rekening, omdat ik waarschijnlijk weer te koppig was om ze te veranderen. We schijnen op elkaar te lijken.

Verder wil ik ook alle andere leden van de vaste staf bedanken voor al het werk dat zo noodzakelijk is om alles in een vakgroep gesmeerd te laten verlopen. In het bijzonder wil ik Margo noemen. Margo, bedankt voor al je hulp in de afgelopen jaren. Geen moeite was voor jou te veel. Jij hebt de gave om zelfs in de meest stressvolle situaties (uiterlijk) kalm te blijven. Tevens wil ik Dr. Jaap Boersma bedanken voor het zeer kritisch nakijken van mijn posters (de posterprijzen waren anders absoluut niet gewonnen) en de Nederlandse samenvatting van dit proefschrift.

Mijn eerste inleidingen in de tang- en organometaalchemie heb ik genoten van Dr. Pablo Steenwinkel. Pablo, ik ben je erg dankbaar voor de vliegende start die jij me hebt bezorgd en waar ik prima op voort heb kunnen bouwen. Dit proefschrift zou ook een stuk minder volledig zijn geweest zonder de hoofd- en bijvakstudenten met wie ik heb mogen samenwerken. Leslie, als mijn eerste hoofdvakker heb jij te lijden gehad van mijn onervarenheid. Toch heb jij problemen goed het hoofd weten te bieden en is een gedeelte van je werk (wat je misschien niet had verwacht) toch nog in het proefschrift verwerkt. Rob, vanwege mijn uitstapje naar Tasmanië was jij gedwongen om al in een vroeg stadium zelfstandig te werken, iets wat je erg goed hebt gedaan. Het bleek dat jij een meester bent in het eerst denken en dan het juiste experiment doen. Kees, jij was de juiste man op de juiste plaats. Met veel doorzettingsvermogen (soms hebben we jou zelfs moeten dwingen om naar huis te gaan) heb je een lastig project tot een zeer goed einde gebracht. Bart, wat mij het meest aan jou bij zal blijven is je nimmer aflatende enthousiasme voor chemie, wat wel tot gevolg had dat jij niet met één maar met wel drie verschillende projecten bezig was die je onmogelijk allemaal tot een goed einde kon brengen. Ik weet zeker dat je hier veel van geleerd hebt. Kees en Bart, ik voel me ook zeer vereerd dat jullie erin hebben toegestemd om op *de grote dag* als mijn paranimfen op te treden. Rob, Kees en Bart, jullie wil ik zeer veel succes wensen met het vervolgen en afronden van jullie respectievelijke promotieonderzoeken. Finally, Aidan, you are not only a noisy Irish bloke, but also a talented chemist. I am very grateful for the important work you did in the final stage of my PhD project. To all of you, thank you for all the hard work and fruitful discussions.

Iedereen met wie ik de afgelopen jaren de tweede zuidzaal heb gedeeld, Arjan, Michel (natuurlijk ook voor het tripincer werk), Martijn, Chris, Joep, Sander, Rob K., Alexey, Kees en natuurlijk vele studenten en gasten, wil ik bedanken voor de goede (soms luidruchtige, Michel) werksfeer. Furthermore, I would like to mention Dr. Alexey Chuchuryukin (is this the preferred spelling, Alex?), Dr. Serenella Medici, Dr. Martin Albrecht, Dr. Diego Ramón and Dr. Scott Williams, whom I would like to thank for their collaborations and their (non)scientific discussions. Sander, jou wil ik ook bedanken voor de vele uurtjes waarin we ons hebben uitgeleefd op de squashbaan, blauwe plekken op de meest vreemde plaatsen voor lief nemende. Martijn, zonder jouw hulp had ik waarschijnlijk de DFT-berekeningen die in dit proefschrift beschreven staan niet kunnen doen.

Onmisbaar voor het werk beschreven in dit proefschrift is de perfecte samenwerking met de groep van Prof. dr. Dieter Vogt aan de Technische Universiteit van Eindhoven geweest. Beste Dieter, heel veel dank voor alle nanofiltratie experimenten die ik in jouw groep heb mogen uitvoeren. Niek, jouw hulp daarbij was onontbeerlijk en ik ben me terdege bewust van het feit dat dit proefschrift er heel anders had uitgezien zonder jouw belangrijke bijdrage, dus daarvoor dank.

I would like to express my gratitude to all people who kindly welcomed me and helped me during my stay in Hobart, Tasmania, Australia. In particular, Prof. dr. Allan Canty, dear Allan, thank you for your hospitality and the perfect working atmosphere in the lab and all the fruitful discussions

we had. A special thanks goes to Dr. Jim Patel (and of course his wife Michaela). Jim, it was an honor working with you, both in Utrecht and in Hobart. I will never forget the way you and your family and friends welcomed me in Tasmania. Thanks for "entertaining" me during my visit, especially the weekend bush walks and the *winter challenge* were incredible.

Binnen de Universiteit Utrecht wil ik Prof. dr. Ton Spek, Dr. Allison Mills en Dr. Martin Lutz hartelijk danken voor het snel meten van de kristalstructuren, wat veel mooie plaatjes voor publicaties, lezingen en posters heeft opgeleverd. Tevens ben ik dank verschuldigd aan Dr. Wim Klopper van de Theoretische Chemie groep voor de vruchtbare samenwerking die we hebben op het gebied van DFT-berekeningen. Jan den Boesterd, Ingrid van Rooijen and Aloys Lurvink van de AV-dienst ben ik zeer erkentelijk voor de altijd snelle en professionele service betreffende posters en sheets. In het bijzonder wil ik Jan bedanken voor het maken van de omslag van dit proefschrift en voor de prachtige coverpicture die binnenkort op de voorkant van het JOC te bewonderen is en nu al op pagina 96 van dit boekje. Vakwerk.

I am also very grateful to Prof. dr. Bill Kaska, from whom I learned a lot about phosphorous and PCP-type chemistry. Furthermore, Prof. dr. A. E. Merbach and Dr. Robert Ruloff from the University of Lausanne are kindly acknowledged for their interest in our shape-persistent multi(pincer) systems and I hope this collaboration will be continued in the future.

Uiteraard wil ik mijn familie, schoonfamilie, vrienden en kennissen bedanken voor de noodzakelijke ontspanning en gezelligheid buiten de chemie. Met name wil ik hier mijn ouders noemen. Heit en mem, ik ben jullie heel erg dankbaar voor alle steun die ik (en natuurlijk later ook Froukje) in al die jaren van jullie heb gekregen. Jullie stonden altijd klaar als er weer eens verhuisd (volgens mij zeker 5x in 5 jaar) of geklust moest worden. Zonder jullie prettige stimulans om toch weer dat stapje hoger te proberen was dit boekje waarschijnlijk nooit geschreven. Het is een erg prettig gevoel om te weten dat er een gezellig 'thús' is waar je altijd terechtkunt.

En tenslotte blijft er natuurlijk nog één persoon over. Froukje, aan jou heb ik heel veel te danken. Je hebt me altijd gesteund en alle ruimte gegeven om mezelf te ontdekken en te ontwikkelen, ook al is dat voor jou niet altijd even gemakkelijk geweest. Mijn eeuwige dank voor al je liefde en geduld en ik hoop in de toekomst nog veel dingen met jou te mogen delen.

Curriculum Vitae

De schrijver van dit proefschrift, Harmen Pieter Dijkstra, werd geboren op 26 oktober 1973 te Nes. In juni 1992 behaalde hij het Atheneum diploma aan het Ichthus College te Drachten. In september van datzelfde jaar werd begonnen met de studie Scheikunde aan de Rijksuniversiteit van Groningen. In augustus 1993 werd het propedeutisch examen afgelegd. Het doctoraal examen, met als hoofdvak Organische Chemie in de vakgroep Organische en Moleculair Anorganische Chemie (Prof. dr. A. M. van Leusen) en als bijvak een stage bij DSM Research (Dr. P. L. Alsters) te Geleen, werd afgesloten in augustus 1997. Van september tot december 1997 was hij werkzaam bij Syncom BV te Groningen. Van januari 1998 tot januari 2002 verrichte de schrijver het in dit proefschrift beschreven onderzoek als onderzoeker in opleiding (OIO) in de Sectie Organische Synthese (Prof. dr. G. van Koten) aan de Universiteit Utrecht. In deze periode werden starre macromoleculaire multimetaal-complexen ontwikkeld en toegepast in homogene katalyse, nanofiltratie en supramoleculaire chemie. Vanaf augustus tot november 1999 werd een werkbezoek gebracht aan de groep van Prof. dr. A. J. Canty (University of Tasmania, Hobart, Australia) om te werken aan een gezamenlijk onderzoeksproject. Het werk beschreven in dit proefschrift werd gedeeltelijk gepresenteerd tijdens nationale en internationale symposia, zoals The Chemistry of the Platinum Group Metals (Nottingham, England) en The International Symposium on Metathesis (Boston, USA). Tevens werd Harm Dijkstra uitgenodigd om deel te nemen aan het "Roche Symposium for Leading Chemists of the Next Decade" (October 2001, Basel, Switzerland).

The author of this thesis, Harmen Pieter Dijkstra, was born on October 26, 1973, in Nes (The Netherlands). After graduating from high school in 1992 at the Ichthus College in Drachten, he started his Chemistry studies at the University of Groningen in September 1992. The MS degree, with a major in Organic Chemistry in the Department of Organic and Molecular Inorganic Chemistry (Prof. dr. A. M. van Leusen) and a traineeship at DSM Research (Dr. P. L. Alsters) in Geleen, was obtained in August 1997. From September until December 1997 he worked at Syncom BV, Groningen. In January 1998 he started as a Ph.D. student in the Department of Metal-Mediated Synthesis (Prof. dr. G. van Koten) at the Utrecht University. During this period, he worked on the development of macromolecular shape-persistent multimetallic complexes and their application in the fields of homogeneous catalysis, nanofiltration and supramolecular chemistry. From August until November 1999, the author visited the group of Prof. dr. A. J. Canty (University of Tasmania, Hobart) to work on a collaborative project. Parts of the work described in this thesis were presented at national and international symposia, including The Chemistry of the Platinum Group Metals (Nottingham, England) and The International Symposium on Metathesis (Boston, USA). Furthermore, Harm Dijkstra was invited to participate at the "Roche Symposium for Leading Chemists of the Next Decade" (October 2001, Basel, Switzerland).

List of Publications

An Unexpected Trimethylstannylpyrrole from a Stannylated Derivative of Tosylmethyl Isocyanide (TocMIC) and Chalcone

A. Meetsma, H. P. Dijkstra, R. ten Have, A. M. van Leusen, Acta Crystallogr. C **1996**, *C52*, 2747.

A Direct Synthesis of 2-(Trimethylstannyl)pyrroles from Michael Acceptors and Stannylated Tosylmethyl Isocyanide

H. P. Dijkstra, R. Ten Have, A. M. van Leusen, *J. Org. Chem.* **1998**, *63*, 5332.

Design of Novel Hexametallic Cartwheel Complexes from Persubstituted Benzene Compounds

H. P. Dijkstra, P. Steenwinkel, D. M. Grove, M. Lutz, A. L. Spek, G. van Koten, *Angew. Chem. Int. Ed.* **1999**, *38*, 2186-2188.

Conjugated G0 Metallodendrimers, Functionalized with Tridentate Pincer type Ligands

I. P. Beletskaya, A. V. Chuchurjukin, H. P. Dijkstra, G. P. M. van Klink, G. van Koten, *Tetrahedron Lett.* **2000**, *41*, 1081-1085.

Acetylene bridged PCP Ligands and corresponding Cyclopalladated Compounds

I. P. Beletskaya, A. V. Chuchurjukin, H. P. Dijkstra, G. P. M. van Klink, G. van Koten, *Tetrahedron Lett.* **2000**, *41*, 1075-1079.

Design and Performance of Rigid Nanosize Multimetallic Cartwheel Pincer Compounds as Lewis Acid Catalysts

H. P. Dijkstra, M. D. Meijer, J. Patel, R. Kreiter, G. P. M. van Klink, M. Lutz, A. L. Spek, A. J. Canty, G. van Koten, *Organometallics*, **2001**, *20*, 3159-3168.

Transcyclometalation, a versatile Methodology for Muliple Metal-carbon Bond Formation with Multisite Ligands

H. P. Dijkstra, M. Albrecht, G. van Koten, *Chem. Commun.* **2002**, 126-127.

Shape-Persistent Nanosize Organometallic Complexes: Synthesis and Application in a Nanofiltration Membrane Reactor

H. P. Dijkstra, C. A. Kruithof, N. Ronde, R. van de Coevering, D. J. Ramón, D. Vogt, G. P. M. van Klink, G. van Koten, *J. Org. Chem.,* in press, manuscript available on the world wide web: http://pubs3.acs.org/acs/journals.

The Use of Ultra- and Nanofiltration Techniques in Homogeneous Catalyst Recycling
H. P. Dijkstra, G. P. M. van Klink, G. van Koten, *Acc. Chem. Res.*, in press, manuscript available on the world wide web: http://pubs3.acs.org/acs/journals.

Metathesis of Olefin-substituted Pyridines: The Metalated NCN-Pincer Complex in a Dual Role as Protecting Group and Scaffold
H. P. Dijkstra, A. Chuchuryukin, B. M. J. M. Suijkerbuijk, G. P. M. van Klink, A. M. Mills, A. L. Spek, G. van Koten, *Adv. Synth. Catal.*, in press.

para-Functionalized NCN-pincer Palladium(II) Complexes; Synthesis, Catalysis and DFT-calculations
H. P. Dijkstra, M. Q. Slagt, A. McDonald, C. A. Kruithof, R. Kreiter, A. M. Mills, M. Lutz, A. L. Spek, W. Klopper, G. P. M. van Klink, G. van Koten, submitted.

Application of a Homogeneous Dodecakis[NCN-pincer-Pd^{II}] Catalyst in a Nanofiltration Membrane Reactor under Continuous Reaction Conditions
H. P. Dijkstra, N. Ronde, G. P. M. van Klink, D. Vogt, G. van Koten, submitted.

Hexakis(PCP–Platinum and –Ruthenium) Complexes by the Transcyclometalation Reaction and Their Use in Catalysis
H. P. Dijkstra, M. Albrecht, S. Medici, G. P. M. van Klink, G. van Koten, submitted.